

Analysis of the membrane binding mechanism
of Remorins and their role in beneficial
endosymbioses



Dissertation zur Erlangung des Doktorgrades
der Fakultät für Biologie
der Ludwig-Maximilians-Universität München

vorgelegt von

Claudia Popp

aus Emmendingen

München, Mai 2017

Die vorliegende Arbeit wurde im Bereich der Genetik in der Arbeitsgruppe von Herrn Prof. Dr. Thomas Ott angefertigt.

1. Gutachter: Prof. Dr. Thomas Ott (Albert-Ludwigs Universität Freiburg)
2. Gutachter: Prof. Dr. Wolfgang Frank (Ludwig-Maximilians-Universität München)

Tag der Abgabe: 08.05.2017

Tag der mündlichen Prüfung: 11.07.2017

Eidesstattliche Erklärung

Hiermit versichere ich an Eides statt, dass die vorgelegte Dissertation von mir selbständig und ohne unerlaubte Hilfe angefertigt ist.

München, den

Claudia Popp

Erklärung

Ich habe weder anderweitig versucht eine Dissertation einzureichen oder mich einer Doktorprüfung zu unterziehen, noch habe ich diese Dissertation oder Teile derselben einer anderen Prüfungskommission vorgelegt.

München, den

Claudia Popp

Table of Content

I.	Frequently used Abbreviations.....	6
II.	List of Publications and Manuscripts.....	8
III.	Contributions to Publications and Manuscripts.....	10
IV.	Summary.....	12
V.	Zusammenfassung.....	14
A)	Introduction.....	16
1.	Beneficial Plant – Microbe Interactions.....	16
1.1.	Morphological Development of Arbuscular Mycorrhiza.....	17
1.2.	Morphological Development of Root Nodule Symbiosis.....	18
<i>1.2.1.</i>	<i>Root Nodule Infection Process</i>	<i>20</i>
<i>1.2.2.</i>	<i>Root Nodule Organogenesis Process.....</i>	<i>21</i>
1.3.	Signaling Pathway.....	23
<i>1.3.1.</i>	<i>Common Symbiosis Pathway.....</i>	<i>23</i>
<i>1.3.2.</i>	<i>RNS Specific Signaling Components.....</i>	<i>27</i>
<i>1.3.2.1</i>	<i>Infection Process.....</i>	<i>27</i>
<i>1.3.2.2</i>	<i>Root Nodule Organogenesis.....</i>	<i>28</i>
<i>1.3.3</i>	<i>AM-Specific Signaling Components.....</i>	<i>29</i>
1.4	The Evolution of AM and RNS.....	30
2.	Remorins – A Plant-Specific Multi-Gene Family	32
1.5	Symbiotic Remorins.....	33
1.6	Remorins as Membrane Domain Marker.....	33
<i>1.6.2</i>	<i>The Compartmentalized Plasma Membrane</i>	<i>33</i>
<i>1.6.2.1</i>	<i>Membrane Compartmentalization.....</i>	<i>34</i>
<i>1.6.3</i>	<i>Membrane Domain Marker.....</i>	<i>35</i>
1.7	Membrane Anchoring Mechanism of Remorins.....	36
<i>1.7.2</i>	<i>Current Anchoring Model Hypotheses.....</i>	<i>37</i>
3.	Aims Of This Study.....	38
3.1.	SYMREM1.....	38
3.2.	MYCREM (formerly REMORIN-LIKE 1).....	39

B) Publications and Manuscripts.....	40
1. Overview Publications and Manuscripts.....	40
1.1. Publication 1: S-acylation anchors remorin proteins to the plasma membrane but does not primarily determine their localization in membrane microdomains.....	41
1.2. Publication 2: Functional Domain Analysis of the Remorin Protein LjSYMREM1 in <i>Lotus japonicas</i>.....	62
1.3. Manuscript 1: A remorin protein controls symbiotic dualism in the legume <i>Medicago truncatula</i>.....	82
1.4. Manuscript 2: The formation of an infection-related membrane domain is controlled by the sequential recruitment of scaffold and receptor proteins.....	124
C) Discussion.....	162
1. SYMREM1 - SYMbiotic REMorin 1.....	162
1.1. SYMREM1 anchors to the PM via S-acylation in the RemCa region.....	162
1.2. S-acylation of SYMREM1 is not required for MD localization.....	164
1.3. SYMREM1 is necessary for a successful Infection Thread formatio.....	168
2. MYCREM - MYCorrhiza-induced REMorin.....	170
2.1. MYCREM: A putative component of a “new” regulatory pathway.....	170
2.1.1. <i>A “New” regulatory circuit and prerequisites for a putative negative component.....</i>	<i>171</i>
2.1.2. <i>MYCREM - a regulatory component of root nodule organogenesis under tripartite co-inoculation conditions.....</i>	<i>173</i>
2.1.3. <i>Symbioses-related Remorins are inducible by the Common Symbiosis Pathway.....</i>	<i>178</i>
2.1.4. <i>MYCREM - potentially adapted from a lateral root organogenesis program?.....</i>	<i>182</i>
2.1.5. <i>Outlook.....</i>	<i>183</i>
D) References.....	185
VI. Curriculum Vitae.....	209
VII. Danksagung.....	211

I. Frequently used Abbreviations

AM	Arbuscular Mycorrhiza
AMF	Arbuscular Mycorrhiza fungus
AON	Autoregulation of Nodulation
AOM	Autoregulation of Mycorrhization
<i>At</i>	<i>Arabidopsis thaliana</i>
C1	Cortex layer adjacent to epidermis
C5	Cortex layer adjacent to endodermis
CCaMK	CALCIUM- AND CALMODULIN-DEPENDENT PROTEIN KINASE
CERK1	CHITIN ELICITOR RECEPTOR KINASE 1
CK	Cytokinin
CLE	CLAVATA3/endosperm-surrounding region-related peptide
CLV1	CLAVATA1
CRE1	CYTOKININ RECEPTOR 1
CSP	Common Symbiosis Pathway
DIM	Detergent Insoluble Membrane
DMI	DOESN'T MAKE INFECTION
D	Aspartic Acid
ED	Endodermis
EP	Epidermis
ERN	ETHYLENE RESPONSE FACTOR REQUIRED FOR NODULATION
FaFaCuRo	Fabales, Fagales, Cucurbitales and Rosales
FLOT	FLOTILLIN
<i>Gm</i>	<i>Glycine max</i>
GPI	Glycosylphosphatidylinositol
IPD3	INTERACTING PROTEIN OF DMI3
IT	Infection Thread
<i>Lj</i>	<i>Lotus japonicus</i>
LHK1	LOTUS HISTIDINE KINASE 1
LYK3	LysM RECEPTOR KINASE 3
<i>Mt</i>	<i>Medicago truncatula</i>
MD	Membrane Domain

Frequently used Abbreviations

NIN	NODULE INCEPTION
NFP	NOD FACTOR PERCEPTION
NFR	NOD FACTOR RECEPTOR
NSP	NODULATION SIGNALING PATHWAY
<i>Os</i>	<i>Oriza sativa</i>
P	Pericycle
PIT	Pre-Infection Thread
PM	Plasma Membrane
PPA	Prepenetration Apparatus
RAM	REQUIRED FOR ARBUSCULAR MYCORRHIZA
RemCA	Remorin C-terminal Anchor
RNS	Root Nodule Symbiosis
SDI	Shoot-derived inhibitor
SPN	Spontaneous Nodules
<i>St</i>	<i>Solanum tuberosum</i>
SYMRK	SYMBIOSIS RECEPTOR KINASE
T	Threonine
TF	Transcription factor
TMD	Transmembrane domain
TML	TOO MUCH LOVE

II. List of Publications and Manuscripts

Publication 1

Konrad, S.S.A.*, Popp, C.*, Stratil, T.F., Jarsch, I.K., Thallmair, V., Folgmann, J., Marin, M., and Ott, T.

S-acylation anchors remorin proteins to the plasma membrane but does not primarily determine their localization in membrane microdomains. *The New Phytologist* **203**, 758-769

Status: published | Year: 2014 | DOI: 10.1111/nph.12867

* These authors contributed equally to this study.

Publication 2

Tóth, K., Stratil, T.F., Madsen, E.B., Ye, J., Popp, C. Antolín-Llovera, M., Grossmann, C., Jensen, O.N., Schüßler, A., Parniske, M. and Ott, T.

Functional Domain Analysis of the Remorin Protein LjSYMREM1 in *Lotus japonicas*. *PLoS ONE*, **7**, e30817

Status: published | Year: 2012 | DOI: 10.1371/journal.pone.003081

Publication 3

Binder A, Lambert J, Morbitzer R, Popp C. Ott T, Lahaye T, Parniske M.

A modular plasmid assembly kit for multigene expression, gene silencing and silencing rescue in plants. *PLoS ONE*, **9**, e88218

Status: published | Year: 2014 | DOI: 10.1371/journal.pone.008821

Manuscript 1

Popp, C., Bittencourt-Silvestre J., Thallmair, V., Mysore, K.S., Wen, J., Delaux, PM., and Ott, T.

A remorin protein controls symbiotic dualism in the legume *Medicago truncatula*, *Proceedings of the National Academy of Sciences*, USA

Status: Invited for resubmission | Year: NN | DOI: NN

Manuscript 2

Stratil. T.F., Popp, C., Konrad, S.S.A., Marín, M., Folgmann, J., and Ott, T.

The formation of an infection-related membrane domain is controlled by the sequential recruitment of scaffold and receptor proteins. *Proceedings of the National Academy of Sciences*, USA

Status: Invited for resubmission | Year: NN | DOI: NN

III. Contributions to Publications and Manuscripts

Publication 1:

Sebastian S.A. Konrad (S.S.A.K.) designed the research, analyzed the data and was involved in writing the manuscript.

S.S.A.K. cloned constructs for expression in *N. benthamiana* and *S. cerevisiae*. S.S.A.K performed localization studies in *N. benthamiana* and *S. cerevisiae*, and the corresponding WB analysis (Fig. 3, 4 and 6; Fig. S2, S4 and S6).

S.S.A.K conducted the biotin switch experiments and performed in silico prediction (Fig. 5. and S5; Table 1).

Claudia Popp (C.P.) and Thomas Ott initiated the study. C.P. performed initial unpublished experiments for this study. C.P. analyzed the data and was involved in writing the manuscript. C.P. established the *M. truncatula* expression system and the sterol depletion assay in the laboratory.

C.P. cloned full-length and mutant variants constructs of SYMREM1 for expression studies in *N. benthamiana* and *M. truncatula*. C.P. performed localization studies in *M. truncatula* and corresponding WB analysis (Fig. 2 and 6).

C.P. conducted viability experiment of sterol depletion assay (Fig. 1).

C.P. performed analysis indicating band shift (Fig. S3).

I hereby confirm the above statements:

Claudia Popp

Sebastian S. A. Konrad

Prof. Thomas Ott

Hereby I confirm that the above-mentioned work was the significant part of the first half of my PhD thesis.

Claudia Popp

Publication 2:

C.P. cloned genomic sequence of MtSYMREM1 and the expression vectors of MtSYMREM1 for BiFC experiments.

Publication 3:

A.B., J.L., R.M., C.P. designed the research and initiated the study. C.P. cloned several LI expression constructs.

I hereby confirm the above statements:

Claudia Popp

Prof. Thomas Ott

Manuscript 1:

C.P. and T.O. initiated and designed the research. J.B.S. propagated *Tnt1* insertion lines, cloned ProMYCREM:GUS vector and conducted initial AM phenotyping. PM. D. analyzed MYCREM evolution. C.P. performed all phenotyping assays, promoter studies and transcript analysis. C.P., PM. D. and T.O. analyzed data and wrote the paper.

Manuscript 2:

C.P. performed phenotyping and complementation experiment of *symrem1*.

I hereby confirm the above statements:

Claudia Popp

Prof. Thomas Ott

IV. Summary

The plasma membrane is highly organized and within the plasma membrane proteins cluster into so-called membrane domains. Remorins are well-established membrane domain marker proteins. However, the general plasma membrane anchoring mechanism of these proteins was so far unknown. Biochemical approaches and localization studies investigating different remorins from *Medicago truncatula* and *Arabidopsis thaliana* enabled us to demonstrate that S-acylation (palmitoylation) within a C-terminal plasma membrane anchoring motif mediates tight plasma membrane attachment of these proteins. However, we could show that S-acylation is not the sole driving force for remorin immobilization in membrane nanodomains.

The focus of the second part of this thesis was on the beneficial interaction between plants and symbionts. More than 80% of today's land plants can undergo an interaction with endosymbiotic fungi that is known as Arbuscular Mycorrhiza (AM). In addition, legume plants have gained the ability to establish a second type of endosymbiosis by interacting with nitrogen-fixing rhizobia: the Root Nodule Symbiosis (RNS). Both interactions are partly controlled by the same pathway, the so-called Common Symbiosis Pathway (CSP) that has evolved through recruitment of signaling components from the evolutionary older AM to the more recently evolved RNS signaling pathway. Depending on the recognition of either fungi or rhizobia downstream of this pathway two morphologically different symbiotic structures are formed within the inner root cortex, either arbuscules or root nodules, respectively.

In parallel to the evolution of RNS a local negative regulatory circuit must have evolved to suppress root nodule organogenesis when both interacting symbionts are present and arbuscule formation takes place. In this study first evidence for such a postulated regulatory pathway is presented based on the characterization of the legume-specific remorin MYCREM, which co-evolved with RNS. Phenotypic studies of mutant plants revealed that in the presence of both symbionts MYCREM functions as a negative regulator with respect to root nodule organogenesis events in a CSP-dependent manner. Analyzing the effect of overexpression of auto-active CSP-signaling components, which are known to spontaneously induce root nodule organogenesis, demonstrated a negative regulatory function of MCYREM as well. In

summary, this work could serve as basis for further studies to understand the tripartite interaction of legume plants, fungi and rhizobia, as it is found in nature.

V. Zusammenfassung

Die Plasmamembran einer Zelle ist ein hochgradig strukturiertes Kontinuum, in dem Membranproteine in Membrandomänen (MD) organisiert sind. Sehr häufig in MD anzutreffende Proteine stellen die sog. “Remorin” Proteine dar, die mittlerweile als breit akzeptierte Marker für MD gelten. Allerdings ist der generelle Mechanismus nach wie vor unklar, der zu einer Plasmamembranlokalisierung dieser Proteine führt. Mittels biochemischer Methoden und Lokalisierungsstudien verschiedener *Medicago* und *Arabidopsis* Remorine, konnte im Rahmen diese Arbeit gezeigt werden, dass die stabile Plasmamembranverankerung auf der S-Acylierung (Palmitylierung) eines Cysteins im C-terminalen Plasmamembranankermotiv beruht. Zusätzlich konnte nachgewiesen werden, dass diese Modifizierung jedoch nicht als der alleinige Grund für eine Membrandomänenlokalisierung fungieren kann.

Im zweiten Teil dieser Arbeit lag der Fokus auf der vorteilhaften Verbindung zwischen Pflanzen und Symbionten. Mehr als 80 % der heutigen Landpflanzen können eine Verbindung mit endosymbiontischen Pilzen eingehen, die auch als “Arbuskuläre Mykorrhiza” bekannt ist. Zusätzlich sind Leguminosen in der Lage eine zweite Symbiose, die sog. Wurzelknöllchensymbiose, einzugehen, die auf der Interaktion mit Stickstoff fixierenden Bakterien beruht. Beide Symbiosen werden teilweise durch den selben Signalweg kontrolliert. Dieser gemeinsame Signalweg wird auch “Common Symbiosis Pathway” (CSP) genannt und entstand höchstwahrscheinlich während der Evolution der evolutionär jüngeren Wurzelknöllchensymbiose durch die Adaption von Signalwegskomponenten, die benötigt werden um die evolutionär älteren Arbuskulären Mykorrhiza zu regulieren. Abhängig von dem interagierenden Symbiont, Pilz oder Bakterium, resultiert dieser Signalweg in der Bildung zweier morphologisch sehr verschiedenen symbiontischen Strukturen in den inneren Zellschichten der Wurzel, dem Arbuskel oder dem Wurzelknöllchen.

Parallel zur Evolution des gemeinsamen Signalwegs und der Wurzelknöllchensymbiose musste sich ein weiterer Signalweg entwickeln, um während der Bildung von Arbuskeln die gleichzeitige Bildung von Wurzelknöllchen zu unterdrücken. Die im Rahmen dieser Arbeit erfolgte Charakterisierung des Leguminosen-spezifischen Remorins MYCREM konnte erste Hinweise für einen

derartigen postulierten negative Signalweg liefern. *MYCREM* entstand im Zuge der Evolution der Wurzelknöllchensymbiose. Durch die Auswertung der sich entwickelnden Wurzelknöllchenanzahl in der Gegenwart von beiden Symbionten und anhand von Transkriptanalysen konnte gezeigt werden, dass *MYCREM* durch den CSP Signalweg induzierbar ist und als eine negativ regulierende Komponente auf die Entwicklung von Wurzelknöllchen einwirkt. Dieser negative Effekt von *MYCREM* konnte ebenfalls durch die Überexpression von autoaktiven Komponenten des CSP-Signalwegs bestätigt werden, die die Knöllchenorganogenese spontan induzieren können, zudem ist dieser Effekt in der *mycrem* Mutante noch verstärkt. Diese Arbeit kann als Basis für zukünftige Studien angesehen werden, um die dreiseitige Interaktion von Pilz, Bakterium und Leguminose zu verstehen, wie sie auch in der Natur vorkommt.

A) Introduction

1. Beneficial Plant – Microbe Interactions

Plants are sessile; therefore, they have to cope with the environmental conditions at the place of growth, for example low water supply and restricted nutrient or nitrogen availability. To overcome these limitations approximately 80% of today's land plants can undergo a beneficial interaction with fungi of the phylum *Glomeromycota*, called Arbuscular Mycorrhiza (AM) (Heijden *et al.*, 1998; Smith & Read, 2008; Harrison, 2012). Due to this symbiotic interaction plants can enhance their water and nutrient acquisition (Javot *et al.*, 2007; Smith & Smith, 2011). In addition, plants from a clade within the Eurosid I, including the orders Fabales, Fagales, Cucurbitales and Rosales (FaFaCuRo) have gained the ability to establish a second type of symbiosis with nitrogen-fixing soil rhizobia, called Root Nodule Symbiosis (RNS) (Soltis *et al.*, 2000; Kistner & Parniske, 2002). In the newly formed nodule the rhizobia reduce atmospheric dinitrogen to ammonia, which can be taken up by the plant. In exchange the rhizobia receive carbon in the form of dicarboxylic acids (Schubert, 1986; Vasse *et al.*, 1990; Den Herder & Parniske, 2009; Desbrosses & Stougaard, 2011). Since many of today's crop plants like soybean (*Glycine max*), pea (*Pisum sativum*) or common bean (*Phaseolus vulgaris*) belong to the FaFaCuRo clade, it is of general interest to gain a better understanding of these two plant-microbe endosymbioses (Sprent, 2007).

The diploid and autogamous legume species *Lotus japonicus* and *Medicago truncatula* have become the main model plants for studying RNS and AM, due to their small genomes, the susceptibility to transformation by *Agrobacteria*, their self-pollination ability, small seeds and short generation times (Barker *et al.*, 1990; Handberg & Stougaard, 1992; Perry, 2003; Tadege *et al.*, 2005, 2008; Sato *et al.*, 2008; Young *et al.*, 2011; Urbański *et al.*, 2012).

In the following section the morphological changes during AM and RNS will be described focusing on *Medicago truncatula*, since the studies for this work have been carried out using this model organism.

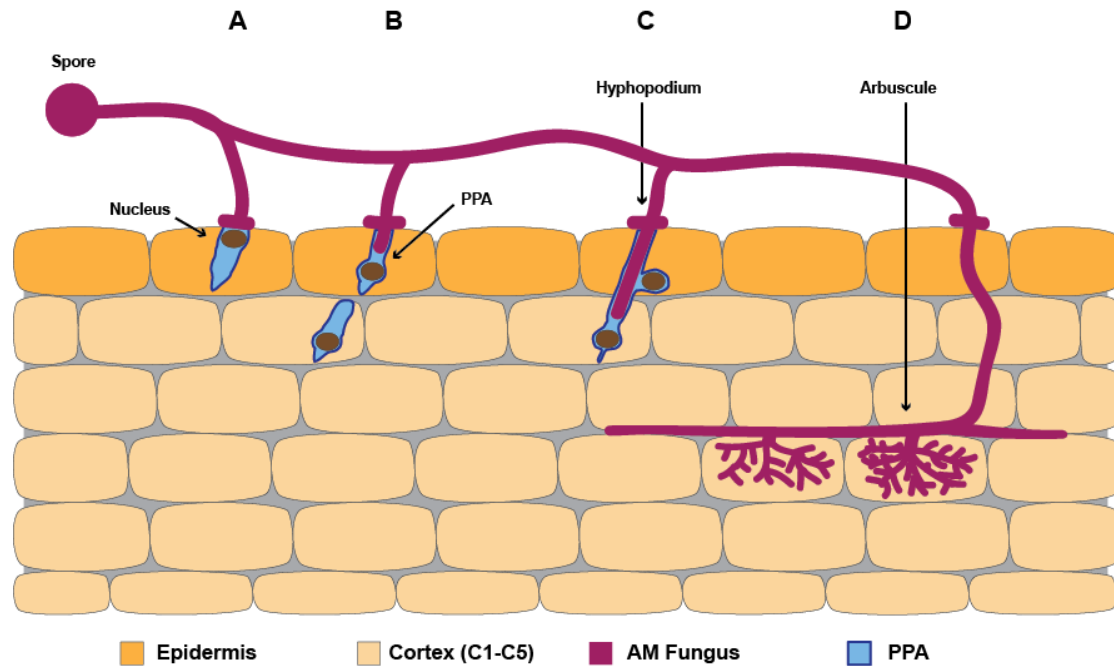


Figure 1: AM development stages.

A) Hyphopodium formation by the fungus and re-localization of the nucleus. B) First intracellular growth phase of the fungus. A pre-penetration apparatus (PPA), which guides the fungal hyphae through the cell, is formed. C) Progression of fungal hyphae to the inner root cortex. D) In the inner root cortex fungal hyphae spread along the longitudinal root axis in the apoplast and the colonization of the root cortex by the formation of arbuscules takes place. For simplicity reasons the periarbuscular membrane around the arbuscule is not depicted. (C1-C5= Cortex layer with C1 being the outermost and C5 the inner most layer.)

1.1. Morphological Development of Arbuscular Mycorrhiza

The plant–fungus interaction is initiated by the perception of plant-released strigolactones by the fungus, which induces spore germination and hyphal branching of the fungus (Akiyama *et al.*, 2005; Besserer *et al.*, 2006). In turn, the fungus secretes tetra- or pentachitooligosaccharides, and sulphated and non-sulphated lipochitooligosaccharides (Myc factors) (Maillet *et al.*, 2011; Genre *et al.*, 2013). The perception of these molecules by the plant, by a so far unknown receptor, induces Ca^{2+} -spiking and activates the Common Symbiosis Pathway (CSP) (discussed in detail in section A 1.3) (Maillet *et al.*, 2011; Genre *et al.*, 2013). This leads to the secretion of cutin monomers by the plant, which supports the development of a hyphopodium at the root epidermis by the AM fungus (AMF) (Fig. 1A) (Wang *et al.*, 2012). To establish the first intraradical growth phase of the AMF, it forms a penetration peg to enter the root (between two epidermal cells in *Lotus* or intracellular via one epidermal cell in *Medicago*) (Bonfante *et al.*, 2000; Genre *et al.*, 2005). The

plant cell responds by a re-localization of the nucleus underneath the peg (Fig. 1A). The nucleus transverses the plant cell vacuole and the formation of the pre-penetration apparatus (PPA) takes place. The PPA is a tubular-like subcellular structure, formed by microtubules, microfilaments and endoplasmic reticulum, that guides the fungus through the plant cell (Genre *et al.*, 2005, 2008) (Fig. 1B and C). When the fungus reaches the cortex an intercellular growth phase within the apoplast starts and the fungus spread along the longitudinal root axis. In a final third intracellular growth phase the fungus invades again the plant cell by an initial PPA that ends in the formation of the arbuscule (Demchenko *et al.*, 2004; Genre *et al.*, 2008) (Fig. 1D).

The resulting arbuscule is a tree-shaped fungal structure within the cortical root cell that is surrounded by a plant-derived membrane called periarbuscular membrane (Genre *et al.*, 2012; Ivanov *et al.*, 2012). This highly branched structure formed by the plant and the fungus is the site of nutrient exchange between the two symbiotic partners (Bonfante-Fasolo, 1984; Harrison *et al.*, 2002; Harrison, 2005).

1.2. Morphological Development of Root Nodule Symbiosis

The establishment of a fully working root nodule symbiosis is achieved by the formation of the root nodule organ and a successful infection by rhizobia. These two processes have to be very tightly controlled and synchronized (Madsen *et al.*, 2010; Rival *et al.*, 2012; Hayashi *et al.*, 2014; Xiao *et al.*, 2014; Saha *et al.*, 2016). The interaction between legume plants and their bacterial symbionts is initially induced by a molecular dialog between the two partners. The plant releases flavonoids into the soil to attract rhizobia (Coronado *et al.*, 1995; Juszczuk *et al.*, 2004; reviewed in Liu & Murray, 2016). In turn, these compounds induce the production and secretion of so-called Nod factors by the rhizobia (Lerouge *et al.*, 1990). Nod factors are acylated lipochitooligosaccharides, that are decorated by strain-specific substituents like methyl, fucosyl, acetyl and sulphate groups (Dénarié & Cullimore, 1993; reviewed in Dénarié *et al.*, 1996; D'Haese & Holsters, 2002). The perception of rhizobia by the plant induces many morphological changes that lead to the formation of an entire new organ to host the symbiont, the root nodule. At the same time the rhizobia invade the plant by a plant-derived tubular structure, the infection thread (IT), which guides the rhizobia to the developing nodule. The rhizobia infect the nodule by an endocytotic

release from the IT. After this endocytosis-like event the rhizobia will be surrounded by a plant-derived membrane and are now called bacteroids. Further differentiation finally enables these bacteroids to perform nitrogen fixation (Vasse *et al.*, 1990; Murray, 2011; Oldroyd *et al.*, 2011; Popp & Ott, 2011).

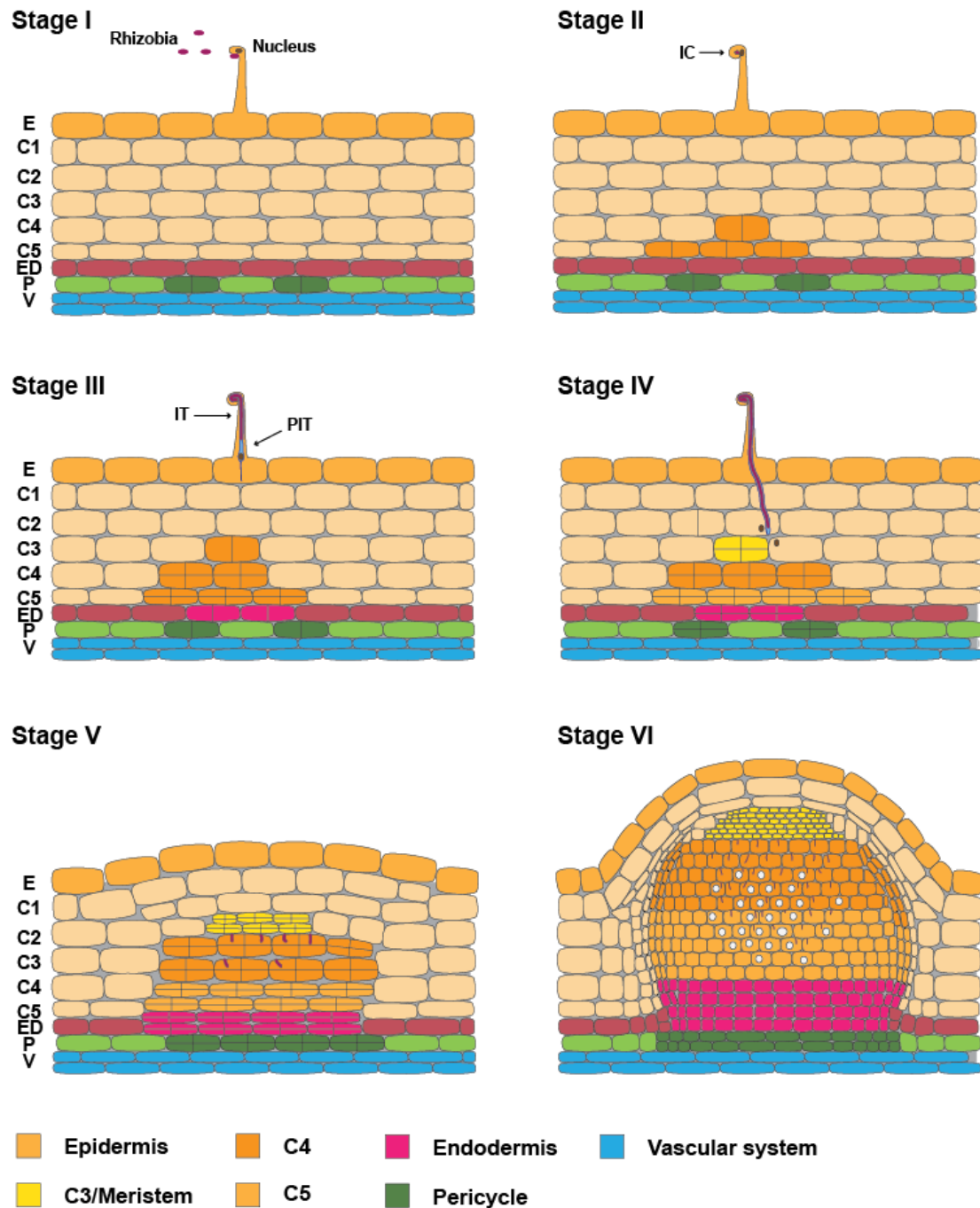


Figure 2: Developmental stages of a root nodule primordium.

For detailed description of each developmental stage compare section A 1.2.2. For simplicity reasons ramification of the IT and symbiosomes are not depicted. E=Epidermis, C=Cortex, ED=Endodermis, P=Pericycle, V=Vasculature, IT=Infection thread, PIT=Pre-infection thread

1.2.1. Root Nodule Infection Process

Following the above described molecular dialog the rhizobia attach to the root hairs (Gage, 2004). This adhesion is mediated by a first weak Ca^{2+} -dependent adhesin binding and second tight binding due to cellulose fibrils synthesized by rhizobia (Smit *et al.*, 1987, 1989). A high Nod factor concentration at the adhesion spot of the rhizobia induces Ca^{2+} influx at the plasma membrane (PM) on the root hair tip (Fig. 2A stage I). This leads to swelling and to the formation of a tightly curled root hair, which is called Shepard's crook (Callaham & Torrey, 1981; Heidstra *et al.*, 1997; De Ruijter *et al.*, 1998; Sieberer & Emons, 2000; Esseling *et al.*, 2003; Miwa *et al.*, 2006). The newly formed space with the entrapped micro-colony of rhizobia is called infection pocket or infection chamber (Fig. 2A stage II) (Esseling *et al.*, 2003; Gage, 2004; Fournier *et al.*, 2015). A recent work by Fournier and co-workers (2015) postulated a new model on how the IT initiation takes place. First, the infection chamber enlarges radially by the transport of exocytotic vesicles to the surrounding membrane. By the end of this enlargement the infection chamber reorganizes into a globular IT-like compartment. At this stage, a few rhizobial cell divisions have taken place. After this infection chamber remodeling a switch from radial expansion to tip elongation growth occurs, which is the initiation of IT development (Fournier *et al.*, 2015). At the same time a change in the orientation of the microtubule arrays can be observed from helical, cortical orientation to a orientation parallel to the long root hair axis (Timmers *et al.*, 1999). At the initiation of the IT growth the nucleus has moved close to the tip of the growing IT. The IT then grows along the aligned cytoskeleton and the nucleus guides the IT through the epidermal cell (van Brussel *et al.*, 1992; Timmers *et al.*, 1999). During this growth the IT tip is connected with the nucleus by a cytoplasmic bridge, which consists of bundles of endoplasmic microtubules (also called pre-infection thread, PIT) and a thin cytoplasmic strand connects the nucleus to the side, where the rhizobia are released into the apoplast (Fig. 2A stage III) (van Brussel *et al.*, 1992; Timmers *et al.*, 1999; Gage, 2004; Fournier *et al.*, 2008). When the IT has fused with the opposite cell side, the underlying two cortical cell layers have already started to form PITs. The next IT forms in the adjacent cortex layer (C1) at the spot of the PIT (Fig. 2A). However, the precise mechanism of this cell-to-cell transition still needs to be finally clarified. At the end of the invading process rhizobia reach the newly formed cells of the cortex in layer C4/C5 (Fig. 2A Stage IV). Within

these cells the IT ramifies and the rhizobia are released into the cytosol (Vasse *et al.*, 1990; Brewin, 2004; Fournier *et al.*, 2008, 2015; Xie *et al.*, 2012). The further development of a nitrogen-fixing nodule will be described in the following section.

1.2.2. Root Nodule Organogenesis Process

Root nodules formed by different legume species can either be of determinate or indeterminate nature. *Lotus* plants develop determinate nodules with a defined lifespan due to the loss of an initial meristem. *Medicago* plants, in contrast, are able to form nodules with a persistent meristem at the nodule apex, which allows the continuous cell division and consequently further growth of the nodule (Guinel, 2009; Łotocka *et al.*, 2012). The root cell layers which are involved in the formation of the nodule differ between these two types (Timmers *et al.*, 1999; Suzaki *et al.*, 2012; Xiao *et al.*, 2014). For reasons of simplicity this section will focus on the development of indeterminate *Medicago* nodules.

The *Medicago* root is composed of one epidermal (EP), 5 cortical (C1-C5), one endodermal (ED) and one pericycle (P) cell layer, which surround the central vasculature (Fig. 2) (Dolan *et al.*, 1993; Timmers *et al.*, 1999; Herrbach *et al.*, 2014; Xiao *et al.*, 2014). After rhizobia perception the first visible response by the plant is an anticlinal cell division in the pericycle (stage I) opposite of a protoxylem pole (Fig. 2A stage I) (Timmers *et al.*, 1999), followed by anticlinal cell divisions in C5 and C4 (stage II) (Fig. 2A stage II). Next anticlinal cell divisions can be observed in C3 and ED, while already periclinal cell divisions occur in C5 and C4 (stage III). At this stage the approaching infection threads have to reach the C4/C5 derived cell layers for infection, otherwise the future meristem cannot be properly formed (Fig. 2A stage III/IV). Stage IV is marked by periclinal divisions in C3, P and ED, while in C4 and C5 the cell division activity persists. The stage V is marked by the six to eight layers formed by P and ED, the eight layers formed by C4 and C5 and a multi-layered meristem formed by C3. At stage VI vascular bundles start to form and the meristem starts to add cell to all nodule tissues of the growing nodule (Fig. 2) (Xiao *et al.*, 2014).

The mature indeterminate nodule consists of a central zone that can be divided into zone I to IV (Fig. 3) (Vasse *et al.*, 1990; Łotocka *et al.*, 2012). Zone I encompasses the meristematic tissue of a nodule and is rhizobia-free. Zone II is also called

‘infection zone’, where cells get infected with rhizobia by an endocytotic event. The bacteria are still surrounded by a host-derived membrane (symbiosome membrane) and within this membrane the bacteria differentiate into bacteroids (Brewin, 1991; Gage, 2004; Mergaert *et al.*, 2006). This zone is followed by an interzone II/III, which serves as a transition zone for the bacteroids to fully differentiate. Zone III, which is also known as nitrogen fixation zone, is the actual place of the reduction of N_2 to NH_4^+ . The adjacent tissue is called senescence zone (zone IV), where bacteroids, which stopped fixing nitrogen get degraded and the plant cells get degraded as well (Fig. 3) (Vasse *et al.*, 1990; Timmers *et al.*, 2000).

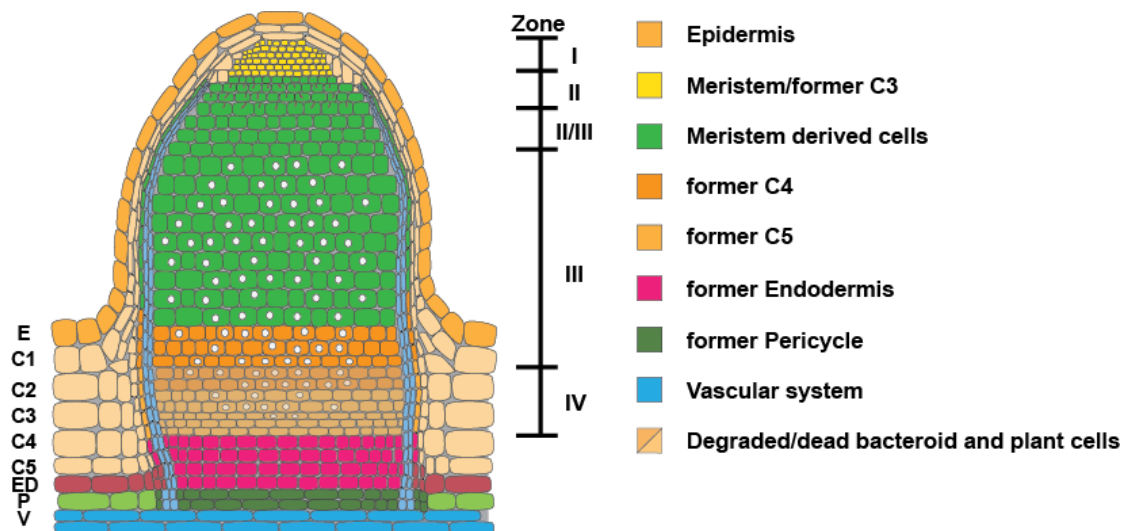


Figure 3: Zonation of an indeterminate nodule.

Zone I (nodule meristem) consists of small, rhizobia-free mitotic cells. Within Zone II (infection zone) bacteria get released from the IT. Interzone II/III serves as transition zone for the bacteria to fully differentiate for nitrogen fixation. In Zone III (nitrogen fixation zone) the fixation of the atmospheric nitrogen takes place. Zone IV (senescence zone) describes the plant cells containing bacteroids, which stopped fixing nitrogen and get degraded. Symbiosomes are not illustrated. E=Epidermis, C=Cortex, ED=Endodermis, P=Pericycle, V=Vasculature

During AM and RNS different morphological changes take place within the root cortex. On the one hand arbuscules are formed and on the other hand cortical cells become mitotic active again. However, both symbioses share common characteristics. (1) Tubular structures (PIT and PPA) are formed by the plant during the initial phase to guide the symbionts through the cell. (2) Plant-derived membranes enclose the fungus and the bacteroids (PAM and symbiosome membrane).

1.3. Signaling Pathway

The specific recognition of beneficial symbionts begins with the molecular dialog between the host and the symbiont (for details see section A1.1 and A1.2). The bacterial Nod factor is perceived by two LysM receptor-like kinases, NOD FACTOR RECEPTOR (NFR) 1 and NFR5 in *Lotus japonicus* or LysM RECEPTOR KINASE 3 (LYK3) and NOD FACTOR PERCEPTION (NFP) of *Medicago truncatula* (Fig. 4) (Amor *et al.*, 2003; Limpens *et al.*, 2003; Madsen *et al.*, 2003; Radutoiu *et al.*, 2003; Arrighi *et al.*, 2006; Broghammer *et al.*, 2012). Recently, it was shown that the CHITIN ELICITOR RECEPTOR KINASE 1 (CERK1) of rice (*Oriza sativa*), also a LysM receptor, is involved in establishing AM in rice (Miyata *et al.*, 2014; Zhang *et al.*, 2015). In addition, it could be shown that the closest homologs of OsCERK1 in *Medicago truncatula* and *Lotus japonicus*, LYK3 and NFR1, respectively, are also required for the AM development (Zhang *et al.*, 2015). Due to these findings the receptor LYK3/NFR1 should also be considered as a part of the CSP, which will be described in more detail in the next section.

1.3.1. Common Symbiosis Pathway

Besides the similarities in morphological structures, the findings of legume mutants that are impaired in establishing both endosymbioses supported the idea of a partially shared genetic program (Hirsch, 2001; Stougaard, 2001; Marsh & Schultze, 2001). Further characterization led to the identification of a core set of genes that are required for both interactions. These genes are called ‘Common Symbiosis Genes’ and the corresponding signaling pathway CSP (Kistner & Parniske, 2002; Parniske, 2008; Oldroyd *et al.*, 2011; Gutjahr & Parniske, 2013). The CSP is initiated by a specific recognition of the symbiont at the PM (see section above). The major events of the CSP are signal transduction, Ca²⁺ spiking in the nucleus, decoding of this pattern and downstream transcriptional induction (Fig. 3).

After the perception of the specific signaling components, the Leucine Rich Repeat-receptor kinase SYMBIOSIS RECEPTOR KINASE (SYMRK) in *L. japonicus* and DOESN'T MAKE INFECTION (DMI) 2 in *M. truncatula* are involved in the activation of the CSP for further signal transduction at the PM (Stracke *et al.*, 2002; Endre *et al.*, 2002; Kosuta *et al.*, 2011; Ried *et al.*, 2014).

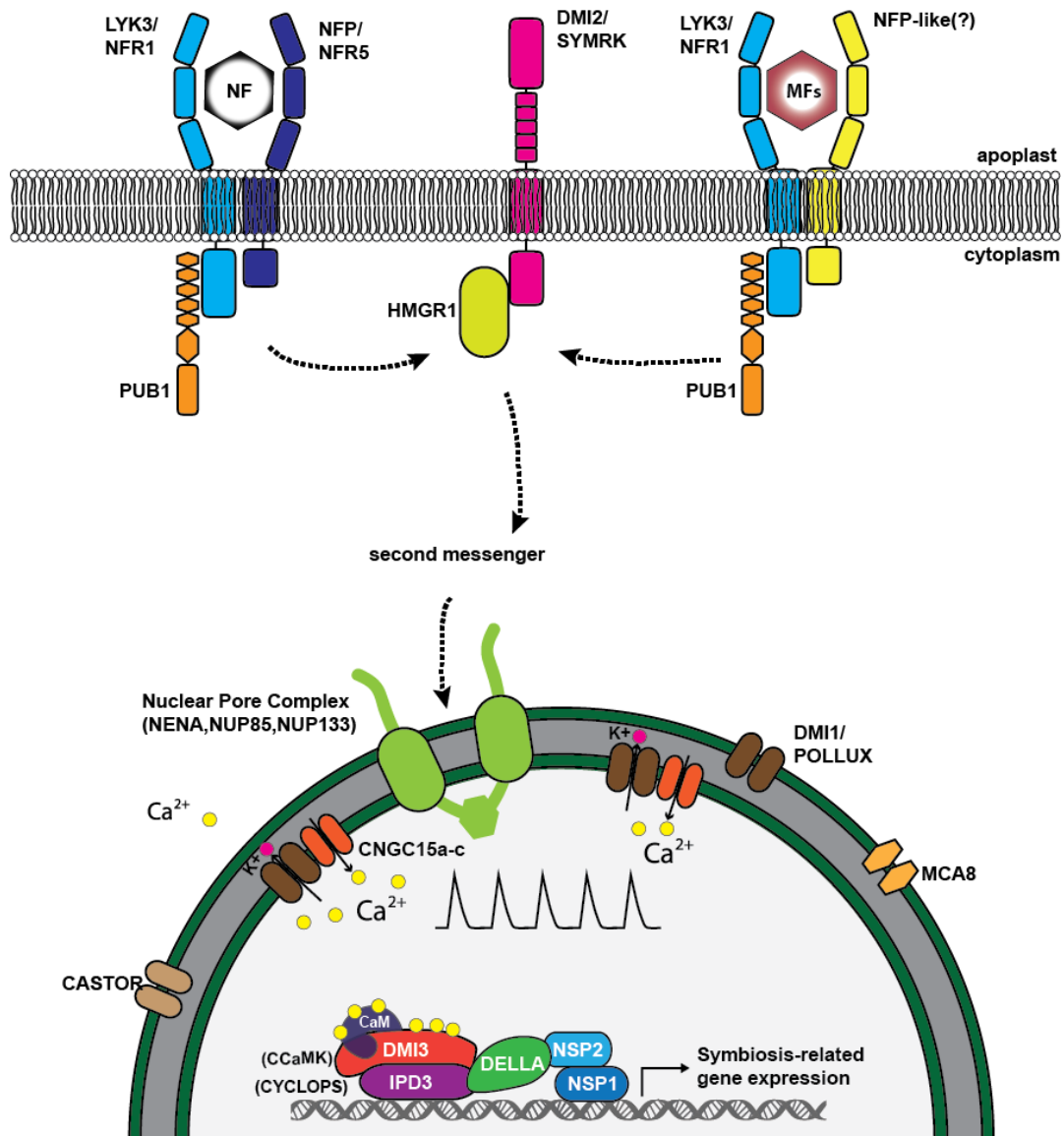


Figure 3: Common Symbiosis Pathway.

Specific Nod or Myc factors are perceived either via a LYK3/NFP complex or LYK3 and a putative NFP-like receptor. Signal transduction is further mediated by the action of the receptor DMI2, the E3-ligase PLANT U-BOX PROTEIN 1 (PUB1) and the 3-HYDROXY-3-METHYLGLUTARYL CoA REDUCTASE 1 (HMGR1). This leads to Ca²⁺ spiking in the nucleus dependent on the function of nuclear pore proteins (NENA, NUP85, NUP133), potassium channels (DMI1/POLLUX and CASTOR), calcium channel (CNGC15a-c) and calcium pump (MCA8). By the combined action of DMI3 and IPD3 in a complex with DELLA, NSP1 and NSP2 the spiking is decoded into transcriptional activation of downstream targets.

Recently, it was shown that SYMRK can interact with NFR5 and associates with NFR5 and NFR1 (Antolín-Llovera *et al.*, 2014; Ried *et al.*, 2014). Therefore, it is most likely that the three receptors act in a complex for signal transduction. DMI2 interacts also with the CSP protein 3-HYDROXY-3-METHYLGLUTARYL CoA REDUCTASE 1 at the PM (Kevei *et al.*, 2007). This reductase produces the second messenger molecule mevalonate, which is involved in the induction of Ca²⁺ spiking in the nucleus (Venkateshwaran *et al.*, 2015).

Another CSP-member that is proposed to modulate the signal transduction at the PM is the E3 Ubiquitin ligase PLANT U-BOX PROTEIN 1. This ubiquitin ligase is a phosphorylation target of LYK3 and DMI2 and acts as a negative regulator of infection stages during RNS and AM (Mbengue *et al.*, 2010; Vernié *et al.*, 2016).

The described perception and signal transduction lead to the formation of Ca²⁺ spiking in the nucleus (Ehrhardt *et al.*, 1996; Sieberer *et al.*, 2012). To establish this spiking three nucleoporins have been shown to be necessary: NUP133, NUP85 and NENA. However, their precise role is still unclear (e.g. transporting a so far unknown CSP signaling component) (Kanamori *et al.*, 2006; Saito *et al.*, 2007; Groth *et al.*, 2010). In addition potassium channels (CASTOR and POLLUX/DMI1) and the ATP-powered MEMBRANE CALCIUM PUMP 8 have been shown to be necessary for establishing Ca²⁺ oscillation (Ané *et al.*, 2004; Imaizumi-Anraku *et al.*, 2005; Charpentier *et al.*, 2008; Kosuta *et al.*, 2008; Capoen *et al.*, 2011; Sieberer *et al.*, 2012). In 2016, Charpentier and co-workers could identify the Ca²⁺ channel, which is proposed to be responsible for the release of Ca²⁺ into the nucleus from the nuclear envelope. This channel consists of three cyclic nucleotide-gated channels, CNGC15a-c, and can interact with the potassium channel DMI1. The authors postulate that this interaction is important for the synchronized action of these channels to create the Ca²⁺ signal (Charpentier *et al.*, 2016).

The decoding of Ca²⁺ spiking in the nucleus is performed by the CALCIUM- AND CALMODULIN-DEPENDENT PROTEIN KINASE (CCaMK)/ DOESN'T MAKE INDECTION 3 (DMI3) (Gleason *et al.*, 2006a; Tirichine *et al.*, 2006a; reviewed in Singh & Parniske, 2012). CCaMK consists of a kinase domain, a Calmodulin-binding domain and three Ca²⁺ binding EF-hand motifs by which it is able to sense different Ca²⁺ concentrations within the nucleus (Levy *et al.*, 2004; Mitra *et al.*, 2004; Gleason *et al.*, 2006; Shimoda *et al.*, 2012; Miller *et al.*, 2013; Routray *et al.*, 2013).

In an inactive state, the phosphorylation site T265 (*Lj*) or T271 (*Mt*) cannot be auto-phosphorylated, since it is engaged in a hydrogen-bond network (Shimoda *et al.*, 2012). As soon as the EF-hands bind Ca^{2+} this T265/T271 site is available for auto-phosphorylation, which causes the Calmodulin binding site to become accessible for interaction with Calmodulin (Gleason *et al.*, 2006; Shimoda *et al.*, 2012; Miller *et al.*, 2013). In this fully active state CCaMK can phosphorylate its targets (Sathyanarayanan *et al.*, 2000; Hudmon & Schulman, 2002; Chao *et al.*, 2011). Further auto-phosphorylation in the Calmodulin binding site induces the release of Calmodulin and with this the auto-regulatory inactivation of CCaMK (Liao *et al.*, 2012; Miller *et al.*, 2013; Routray *et al.*, 2013). Being the decoder of the Ca^{2+} signal, CCaMK is playing a central role in establishing the symbiotic interaction. This was supported by the findings that auto-active versions CCaMK-T265D/DMI3-T271D could induce the formation of spontaneous nodules (SPN) in the absence of rhizobia (Gleason *et al.*, 2006; Tirichine *et al.*, 2006). Furthermore, overexpressing the kinase domain alone was sufficient to induce nodule organogenesis and PPA formation (Gleason *et al.*, 2006; Shimoda *et al.*, 2012; Takeda *et al.*, 2012; Hayashi *et al.*, 2014). The transcriptional activation of target genes downstream of CCaMK is mediated by its phosphorylation target CYCLOPS/INTERACTING PROTEIN OF DMI3 (IPD3) (Messinese *et al.*, 2007; Yano *et al.*, 2008; Horváth *et al.*, 2011; Ovchinnikova *et al.*, 2011; Singh *et al.*, 2014). IPD3 is necessary for the induction of SPN induced by overexpressing kinase domain of DMI3 (Ovchinnikova *et al.*, 2011). Singh *et al.* (2014) could also show that an auto-active version of CYCLOPS (CYCLOPS-S50D-S154D) can induce root nodule organogenesis. These results support the view of CYCLOPS playing a central role in transcriptional induction. Furthermore, the promoter of the transcription factor NODULE INCEPTION (NIN) could be shown to be target of CYCLOPS (Marsh *et al.*, 2007; Soyano *et al.*, 2013; Singh *et al.*, 2014; Vernié *et al.*, 2015). So far, NIN is thought to be the first nodule specific transcription factor to be activated for the nodulation signaling pathway downstream of the CSP (Oldroyd *et al.*, 2011; Soyano & Hayashi, 2014).

The recent work of two groups showed that DELLA proteins, an unique type of GRAS (GA3 insensitive, Repressor of GAI, and Scarecrow) transcription factors (TFs), work in a complex with CCaMK-CYCLOPS to activate downstream targets (Jin *et al.*, 2016; Pimprikar *et al.*, 2016). In the work of Pimprikar *et al.* (2016) it was

demonstrated that this activation complex can activate the AM-specific REQUIRED FOR ARBUSCULAR MYCORRHIZA (RAM) 1 promoter. In the second work Jin *et al.* (2016) could show that IPD3 and NODULATION SIGNALING PATHWAY (NSP) 2 can form a complex by the linker DELLA. Jin *et al.* postulate that CCaMK-CYCLOPS and NSP1 and NSP2 form an activation complex, with DELLA as a bridging protein to induce downstream gene expression (Jin *et al.*, 2016).

The already mentioned GRAS transcription factors NSP1 and NSP2 act in a complex to induce the nodulation specific gene ETHYLENE RESPONSE FACTOR REQUIRED FOR NODULATION (ERN) 1 and are involved in AM development as well (Hirsch *et al.*, 2009; Maillet *et al.*, 2011; Cerri *et al.*, 2012; Laressergues *et al.*, 2012; Delaux *et al.*, 2013; Takeda *et al.*, 2013).

A next challenging step will be to find the precise mechanism of how the signal for the specific AM- or RNS-pathway bifurcates after sharing the same components of the CSP. One possibility could be that the CCaMK or the CCaMK-CYCLOPS complex can interact with different partners depending on their phosphorylation status (Singh & Parniske, 2012; Limpens & Bisseling, 2014; Singh *et al.*, 2014). Another mechanism might be that perception of the Myc or Nod factor induces not only the CSP but also additional parallel pathways to modulate the CSP (Bonfante & Requena, 2011; Genre & Russo, 2016).

1.3.2. RNS-Specific Signaling Components

1.3.2.1. Infection Process

Different types of infection process-relevant signaling components downstream of the CSP have been discovered like scaffold proteins, E3-ligases and TFs. Two members of the FLOTILLIN gene family, FLOT2 and FLOT4, have been shown to be upregulated upon rhizobia infection and the RNAi lines of these genes display a reduced number of ITs and nodules (Haney & Long, 2010). Flotillins are scaffold proteins and localize to PM domains (Schulte *et al.*, 1997; Glebov *et al.*, 2006; Frick *et al.*, 2007). Furthermore, FLOT4 co-localizes with LYK3 in a Nod factor-dependent manner in membrane domains (MDs) and most likely modulate downstream signaling by mediating interaction with further interaction partners of LYK3 (see also section A 2.2.1.1) (Haney *et al.*, 2011).

As for the CSP, E3-ligases have been shown to be involved in IT signaling as well. For example, SEVEN IN ABSENTIA 4 from *L. japonicus* has been shown to interact with SYMRK and is proposed to be involved in the turn over of this kinase in an RNS-specific manner (Den Herder *et al.*, 2012).

To establish again specificity downstream of the CSP one way is to induce RNS-specific TFs. Indeed, several TFs have been already identified downstream of the CSP and to be involved in IT formation/progression, like the negative regulator ETHYLENE RESPONSE FACTOR REQUIRED FOR NODULE DIFFERENTIATION (Vernié *et al.*, 2008; Moreau *et al.*, 2014) or the two TFs ERN1 and ERN2 (Middleton *et al.*, 2007; Andriankaja *et al.*, 2007; Cerri *et al.*, 2012, 2016). ERN1 and ERN2 function as transcriptional activator and have been shown to be functionally redundant (Andriankaja *et al.*, 2007; Cerri *et al.*, 2012, 2016).

However, of the above described proteins only ERN1 was shown to be directly activated by the CSP-component NSP1 (Cerri *et al.*, 2012). For the other RNS-specific proteins the precise induction mechanism needs to be elucidated.

The above mentioned CSP-dependent TF NIN plays a central role in regulating IT initiation and progression, nodule organogenesis and control of nodule number (see also section A 1.3.2.2) (Schauser *et al.*, 1999; Marsh *et al.*, 2007; Hirsch *et al.*, 2009; Soyano *et al.*, 2013, 2014, 2015; Singh *et al.*, 2014; Yoro *et al.*, 2014; Vernié *et al.*, 2015). NIN negatively regulates infection by restricting the infection zone in the epidermis via competitive inhibition of ERN1 (Marsh *et al.*, 2007; Vernié *et al.*, 2015). The involvement of NIN in the nodule organogenesis process will be discussed in the following section.

1.3.2.2. Root Nodule Organogenesis

Simultaneous to the IT formation a second pathway in the inner root cortex cells is activated to initiate cell division to form the root nodule (Fig. 2). The CSP pathway induces the organogenesis program as well, which demonstrates the formation of SPN induced by the auto-active versions of CCaMK/DMI3.

However, this program can also be triggered by an auto-active version of a Cytokinin receptor LOTUS HISTIDINE KINASE 1 (LHK1)/CYTOKININ RECEPTOR 1 (CRE1), which acts downstream of the CSP (Gleason *et al.*, 2006; Tirichine *et al.*, 2006, 2007; Gonzalez-Rizzo *et al.*, 2006; Ovchinnikova *et al.*, 2011). Heckmann *et al.*

(2011) showed that exogenous application of Cytokinin induces the formation of root nodules. The mutants of LHK1 and CRE1 are impaired in initiating cortical cell division and fail to activate NIN expression in the cortex (Murray *et al.*, 2006; Plet *et al.*, 2011). The LHK1/CRE1 dependent Cytokinin signaling pathway initiates nodule formation by an alteration of the acro- and basipetal auxin transport to form a local auxin maximum (Plet *et al.*, 2011; Ng *et al.*, 2015).

Interestingly, NIN activation in the epidermis is sufficient to induce Cytokinin signaling in the inner root cortex (Vernié *et al.*, 2015). However, CRE1-dependent signaling can also induce NIN and NIN in turn binds to the promoter of CRE1 (Vernié *et al.*, 2015). Therefore, NIN is not only involved in a negative regulation of IT formation, but also in a positive feedback loop in the cortex to initiate and maintain nodule organogenesis (Yoro *et al.*, 2014; Vernié *et al.*, 2015). But if NIN or a product of its action is involved in the coordination of the infection and organogenesis program still needs to be shown. So far, NIN was thought to be RNS-specific. However, this might be reconsidered due to the findings of Guillotin and co-workers (Guillotin *et al.*, 2016). They showed for the first time that *nin1-1* mutant plants are less colonized and having less infection points by the AMF *Rhizophagus irregularis* than the wild type (Guillotin *et al.*, 2016). However, further research needs to be done to elucidate the regulatory mechanism NIN might be involved.

Although already several further TFs have been described to be involved in root nodule formation (Combier *et al.*, 2006; De Zélicourt *et al.*, 2012; Ariel *et al.*, 2012; Laporte *et al.*, 2014). Their precise positioning within a signaling pathway and downstream targets still need to be elucidated.

1.3.3. AM-Specific Signaling Components

On the side of the AM-specific signaling components downstream of the CSP major progress has been made by elucidating the importance of several GRAS domain TFs in the regulation of AM. In 2012, RAM1 from *Medicago* was described the first time and is a direct downstream target of the CSP (Gobbato *et al.*, 2012; Pimprikar *et al.*, 2016). RAM1 is essential to support arbuscule hyphae branching and the formation of hyphopodia at the root surface (Gobbato *et al.*, 2012; Park *et al.*, 2015; Xue *et al.*, 2015; Pimprikar *et al.*, 2016). A direct target of RAM1 is RAM2, a glycerol-3-phosphate acyl transferase, which is necessary for hyphopodia and arbuscule

formation by producing cutin monomers as plant signaling molecules (Wang *et al.*, 2012b; reviewed in: Murray *et al.*, 2013).

The importance of DELLAs for the establishment of a beneficial interaction between the plants and its symbiont was already mentioned above. Besides NSP1 and NSP2 two further AM-specific GRAS-type transcription factors have been identified to be interaction partners of DELLAs: (1) DELLA INTERACTING PROTEIN 1, which is important for AMF colonization and (2) MYCORRHIZA INDUCED GRAS 1, which regulates the cortical radial cell expansion during arbuscule development (Yu *et al.*, 2014; Heck *et al.*, 2016). Moreover, REQUIRED FOR ARBUSCULE DEVELOPMENT, an AM-specific GRAS-type TF as well, interacts with RAM1 and regulates arbuscule number (Xue *et al.*, 2015). All these results point to the existence of a GRAS-type dependent regulatory complex, including DELLAs, which is important for the regulation of AM-associated gene expression.

After identifying the described DELLA-involved induction complex downstream of the CSP, the next challenging step will be to elucidate the direct targets of this complex and how the AM-specific signaling pathway is further maintained.

1.4. The Evolution of AM and RNS

450 million years ago land was colonized by terrestrial plants. Fossil findings support a concomitant evolution of beneficial interaction between a photosynthetic organism and a fungus (Taylor *et al.*, 1995; Redecker *et al.*, 2000). This symbiosis probably facilitated plant terrestrialization and true root development by assisting plants to absorb water and nutrients from soil (Humphreys *et al.*, 2010; Selosse *et al.*, 2015). The work of Humphreys *et al.* (2010) supported the theory of root development by showing the mutualistic interaction between thalloid liverworts (belonging to most basal plant groups) and AM fungus.

By applying phylogenetic comparison approaches and cross-species complementation between rice and legumes with CSP components the co-appearance of land colonization and AM was supported (Wang *et al.*, 2010). The presence of LysM-receptor-like kinases, DMI1 and IPD3 in advanced charophytes indicates the evolution of this CSP signaling module already prior to land colonization by plants (Delaux *et al.*, 2015a). Studies on the evolution of CCaMK/DMI3 propose that this gene originated through gene duplication from *CALCIUM-DEPENDENT PORTEIN*

KINASE during green algae evolution and gained its function by neo-functionalization (Wang *et al.*, 2010; Delaux *et al.*, 2015a). This was most likely the general evolution motif for the full signaling pathway necessary to establish AM in first land plants (Delaux *et al.*, 2014, 2015a). These results further supported the theory that genes, necessary for symbiotic plant-fungus interaction, have been present in the common ancestor of land plants and green algae.

The symbiosis between nitrogen-fixing bacteria and plants evolved several times with the first appearance approx. 65 million years ago (Herendeen *et al.*, 1999; Soltis *et al.*, 2000; Adams, 2002). Besides the symbiosis between plants from the FaFaCuRo clade and the bacteria of the genus *Rhizobia* or *Frankia*, symbioses between plants and cyanobacteria have developed across several plant clades (reviewed in Sprent, 2008; Delaux *et al.*, 2015b). Furthermore, the finding that several components of the AM signaling pathway are important for the successful establishment of this second symbiosis led to the hypotheses that (a) the last common ancestor of AM- and RNS-capable plants gained a predisposition to form nodules and that (b) parts of the evolutionary older AM signaling pathway have been recruited to the RNS pathway thereby establishing the CSP (Soltis *et al.*, 1995; Kistner & Parniske, 2002; Markmann & Parniske, 2009). Werner *et al.* could show that the innovation of a single precursor of all nitrogen-fixing symbioses is the best explanation for the current distribution within the plant kingdom (Werner *et al.*, 2014).

The hypothesis of AM signaling components being recruited to develop the evolutionary younger RNS pathway was supported by the studies using *Parasponia andersonii*. This non-legume specie, which can establish RNS belongs to the genus *Parasponia* and is phylogenetically positioned next to Fabaceae, but gained the RNS ability more recently than legumes (Akkermans *et al.*, 1978; Soltis *et al.*, 2000). By comparing the genomes of *Parasponia* and legumes, parallel genetic developments can be identified that have led to the evolution of RNS. *P. andersonii* plants posse a single NFP-like receptor gene (*PaNFP*), which is necessary for AM and RNS and an ortholog to NFR5/NFP (Op den Camp *et al.*, 2011b).

The comparison of non-AM-, AM-only-, AM and RNS- and RNS-only-host (e.g. *Lupinus*) genomes, as it is currently undergoing, will give further hints on how evolution took place and which components of the signaling pathways both symbioses

have in common and which are specific (Delaux *et al.*, 2014; Favre *et al.*, 2014; De Mita *et al.*, 2014; Bravo *et al.*, 2016).

2. Remorins – A Plant Specific Multi-Gene Family

Remorin proteins belong to a plant-specific protein family that can be found in angiosperms, gymnosperms, ferns and mosses, but is absent in algae. The proteins consist of a very conserved C-terminal domain that harbors the canonical Remorin-C domain. In contrast, the N-terminal domain is highly diverse. The remorin protein family can be further subdivided into six separate groups, with group 2 remorins only existing in legumes and poplar (Raffaele *et al.*, 2007). Protein modeling showed that the C-terminal part folds into a coiled-coil domain and that the N-terminal domain shows all features of an intrinsically disordered region, like low mean hydrophobicity and relatively high net charge (Marín & Ott, 2012; Marín *et al.*, 2012). Protein interaction studies revealed that the C-terminal domain is important for stable protein-protein interaction and can undergo homo- and heterooligomerization (Bariola *et al.*, 2004; Marín *et al.*, 2012; Tóth *et al.*, 2012). Remorins can be phosphorylated in a stimulus-dependent manner and are mainly phosphorylated in the N-terminal domain (Farmer *et al.*, 1989; Marín & Ott, 2012; Marín *et al.*, 2012; Tóth *et al.*, 2012; Gui *et al.*, 2016).

In recent years more and more studies have revealed that remorins play an important role in abiotic stress processes, but also pathogenic and symbiotic interactions (Benschop *et al.*, 2007; Raffaele *et al.*, 2009; Lefebvre *et al.*, 2010; Checker & Khurana, 2013; Yue *et al.*, 2014; Gui *et al.*, 2016). For example, the remorin REM1.3 from *Solanum tuberosum* (potato) was shown to be involved in the restriction of the cell-to-cell movement of Potato Virus X by modulating the plasmodesmal size exclusion limit (Raffaele *et al.*, 2009; Perraki *et al.*, 2014). The remorins REM1.2 and REM1.3 from *Arabidopsis thaliana* have been identified to be phosphorylated in a flg22-dependent manner (Benschop *et al.*, 2007). Interestingly, it could be now shown that these remorins positively correlate with the plant immune receptor FLAGELLIN-SENSITIVE 2 (FLS2) regarding their MD localization (Bücherl *et al.*, 2017). But if these remorins are directly phosphorylated by FLS2 still needs clarification.

2.1. Symbiotic Remorins

Besides remorins being involved in pathogen interaction as mentioned previously, the legume-specific remorin REM2.2 was found to be highly induced during RNS (Colebatch *et al.*, 2004; El Yahyaoui, 2004). This remorin was later named SYMBIOTIC REMORIN1 (SYMREM1) (Lefebvre *et al.*, 2010). SYMREM1 localizes to the PM in distinct membrane domains along the IT and symbiosome membrane in nodules of *Medicago truncatula*. SYMREM1 homooligomerizes and interacts with NFP, LYK3 and DMI2 (Lefebvre *et al.*, 2010). These interactions could be verified for the *Lotus* SYMREM1, as well (Tóth *et al.*, 2012). Interestingly, the interaction of SYMREM1 and NFR1 could be visualized in defined hotspots in the PM, resembling MDs (Jarsch *et al.*, 2014). SYMREM1 can be phosphorylated *in vitro* by NFR1 and SYMRK kinase domains in the N-terminal domain (Tóth *et al.*, 2012). Phenotypical studies in *Medicago* revealed the involvement of SYMREM1 in the successful and controlled nodule infection by rhizobia (Lefebvre *et al.*, 2010) while overexpression of SYMREM1 in *Lotus* led to the increased formation of nodules (Tóth *et al.*, 2012).

Interestingly, the second member (REM2.1) of the legume-specific subgroup two was identified in a screen for AM-specific marker genes and was called REMORIN-LIKE 1 (later MYCORRHIZA-INDUCED REMORIN (MYCREM)) (Kistner *et al.*, 2005; Raffaele *et al.*, 2007). RML was strongly induced 12 days after AMF inoculation (Kistner *et al.*, 2005). However, apart from this unexpected strong AM-specific induction, the function of RML1 is elusive.

2.2. Remorins as Membrane Domain Marker

2.2.1. *The Compartmentalized Plasma Membrane*

When Singer and Nicolson postulated their 'fluid-mosaic' model in 1972 they envisioned the plasma membrane as a fluid bilayer of phospholipids with embedded and freely moving integral proteins (Singer & Nicolson, 1972). Since then our view on the structure of the plasma membrane got more diverse and led to several new models. However, all of these models share the view on the PM as a subdivided and

compartmentalized continuum with regard to lipids and proteins with additional restricting influences by the actin cytoskeleton (and the cell wall in plants) (Lingwood & Simons, 2010; Kusumi *et al.*, 2012; Malinsky *et al.*, 2013; Nicolson, 2014).

2.2.1.1. Membrane Compartmentalization

In plants the main components of the lipid bilayer are glycerolipids (mainly phospholipids), sphingolipids and sterols (Mongrand *et al.*, 2004; Kierszniowska *et al.*, 2009; Li-Beisson *et al.*, 2013). Due to their different intrinsic properties like hydrophobicity, and self-association of sterols and sphingolipids via hydrogen bonds, these lipids do not mix homogeneously within the bilayer, but separate into different clusters containing either mainly phospholipids or sphingolipids and sterols (Simons & Ikonen, 1997; Simons & Gerl, 2010). The patches containing mainly sphingolipids and sterols are called “raft domains” or “lipid rafts” (Kusumi *et al.*, 2005; Lingwood & Simons, 2010). These raft domains are small (2-20 nm in diameter), heterogeneous and highly dynamic. However, these raft domains can assemble to larger domains that can be visualized by fluorescent light microscopy (Pike, 2006; Raffaele *et al.*, 2009; Demir *et al.*, 2013; Jarsch *et al.*, 2014), which are then also called meso-scale MDs (Konrad & Ott, 2015). This assembly process can be stabilized by lipid-lipid, lipid-protein and protein-protein interactions (Pike, 2006, 2009).

A prominent example for sterol-dependent domain localization of a protein is PINFORMED1 (PIN1) and PIN2, both auxin efflux carriers. In a wild type plant these proteins show a polar plasma membrane localization to establish an auxin gradient within the root (Wiśniewska *et al.*, 2006; Boer *et al.*, 2013). Within this polar localization the efflux carriers form distinct domains, which were dependent on the sterol content in the PM (Men *et al.*, 2008; Pan *et al.*, 2009; Kleine-Vehn *et al.*, 2011). An interesting study on the different RNS-related MDs of LYK3 and FLOT4 in *Medicago* showed MD co-localization as a physiological response. While the LYK3-labelled domains were mobile in buffered-treated samples, the FLOT4-labelled domains showed a stable behavior. However, after inoculation with rhizobia the LYK3 domains got static and co-localized with the FLOT4-domains (Haney *et al.*, 2011).

Besides the MDs, the membrane is also subdivided into larger areas (40 – 300 nm in diameter) by the membrane associated actin cytoskeleton, which is also named

“membrane skeleton” (Lenne *et al.*, 2006; Kusumi *et al.*, 2012; Szymanski *et al.*, 2015). This membrane skeleton can be imagined like a “fence” that compartmentalizes the PM and also restricts the diffusion of proteins (Kusumi *et al.*, 2005). It was shown that these “fences” are distributed all over the inner PM leaflet. Furthermore transmembrane proteins are anchored to and associated with this actin network and function like “pickets” to slow down the free diffusion of phospholipids and proteins (Saxton, 1990; Edidin *et al.*, 1991; Bussell *et al.*, 1995; Suzuki *et al.*, 2005; Morone *et al.*, 2006; Li *et al.*, 2011; Martinière *et al.*, 2012; Szymanski *et al.*, 2015; Koldsø *et al.*, 2016). Although this view of the PM was first gained by experiments on mammalian PM systems, the “picket - fence” model can be also used for plant the PM. For instance, disturbing the membrane skeleton by different drug treatments led to an alteration of the size of Rem1.2-MDs (Szymanski *et al.*, 2015). While raft domains and membrane skeleton influence the localization and the dynamics of PM proteins, the cell wall has also a great impact on protein’s mobility (Martinière *et al.*, 2012). The PM therefore has to be viewed as a compartmentalized membrane skeleton MD cell wall continuum.

2.2.2. Membrane Domain Marker

Remorins localize to the PM and have been identified in several proteomic studies on PM and in Detergent-Insoluble-Membrane (DIM) fractions (Watson *et al.*, 2003; Mongrand *et al.*, 2004; Bhat & Panstruga, 2005; Valot *et al.*, 2006; Lefebvre *et al.*, 2007). DIMs have been thought to be the biochemical counterpart of MDs and are obtained from PM fractions that are treated with ice-cold nonionic detergent like Triton-X-100. However, since sterols tend to cluster due to their intrinsic properties, this extraction method is prone to artifacts (Brown & Rose, 1992; Tanner *et al.*, 2011). Despite this disadvantage of this technique, the appearance of a protein in a DIM fraction can be seen as a first hint for putative MD localization but has to be verified by microscopy techniques (Kierszniowska *et al.*, 2009; Tanner *et al.*, 2011; Tapken & Murphy, 2015). Due to their constant appearance in DIM proteomic approaches and their punctate localization in the PM, remorin proteins are used as MD markers (Mongrand *et al.*, 2004; Lefebvre *et al.*, 2007, 2010; Kierszniowska *et al.*, 2009; Raffaele *et al.*, 2009; Demir *et al.*, 2013).

In a large (co-) localization approach of all 16 *Arabidopsis thaliana* remorins and four further MD localized proteins (three FLOTs and POTASSIUM CHANNEL IN ARABIDOSIS THALIANA 1) the coexistence of highly distinct MDs was demonstrated (Jarsch *et al.*, 2014). The remorin-labeled MDs have been characterized by different parameters like domain size, width, intensity, circularity and domain density. Furthermore, by tracking the fluorophore-tagged proteins over a time period of 20 min a high lateral stability of the MDs could be shown. The co-expression of 45 different remorin-pairs identified the existence of 14 co-localizing pairs and 12 pairs strictly excluding each other, but also random localization has been observed. Interestingly, besides the coexistence of several distinct MDs on the PM plane, it could be demonstrated that the MD formation of REM1.2 and REM1.3 may be dynamically under different developmental stages or environmental cues (Jarsch *et al.*, 2014).

With this set of MD marker proteins, an *in vivo* tool is now available to verify MD localization of other proteins of interest apart from the artificial DIM extraction method.

2.3. Membrane Anchoring Mechanism of Remorins

PM proteins can be categorized according to their PM binding mechanism into either integral or peripheral membrane proteins. Integral membrane proteins are embedded into the PM via secondary proteins structures. These can be one or several α -helices, called transmembrane domain(s) (TMD), β -strands building a barrel-like structure or amphipathic α -helices, that inserts only into one leaflet of the PM bi-layer (Macasev *et al.*, 2004; McMahon & Gallop, 2005; Chen *et al.*, 2006; Wang *et al.*, 2006). The PM attachment of peripheral proteins can be achieved via protein interaction with integral membrane proteins, via electrostatic interactions or by protein lipidation (Boyes *et al.*, 1998; Hemsley *et al.*, 2005; van den Bogaart *et al.*, 2011). Protein lipidation describes a post-translational protein modification that increases the affinity to PM by adding a hydrophobic moiety (reviewed in: Hemsley, 2014). The known lipid modification types in plants are (1) prenylation, (2) N-myristoylation, (3) S-acylation and (4) glycosylphosphatidylinositol (GPI) modification.

Prenylation and N-myristoylation are irreversible additions of either farnesyl or geranylgeranyl chains or of a 14 carbon myristoyl chain by specific transferases

(Cutler *et al.*, 1996; Running *et al.*, 2004; Traverso *et al.*, 2013). The S-acylation, formerly also known as palmitoylation, is a reversible modification. It describes the addition of a palmitate or stearate moiety to a cysteine residue through a thioester bond. This reaction is catalyzed by a large protein family, the protein-S-acyl transferases (PATs), which are integral membrane proteins (Hemsley *et al.*, 2005; Batistič *et al.*, 2012). In a proteomic screen several TMD containing proteins, like FLS2, could be shown to be S-acylated as an additional PM anchoring mechanism (Hemsley *et al.*, 2013).

So far, the GPI anchor modification is the only modification of proteins associated to the outer leaflet and proteins with this modification predominantly localize to MDs (Sherrier *et al.*, 1999; Mongrand *et al.*, 2004; Lefebvre *et al.*, 2007; Kierszniowska *et al.*, 2009). This large and complex glycolipid modification is added to the protein in the endoplasmic reticulum (reviewed in: Maeda & Kinoshita, 2011).

It was hypothesized that S-acylation contributes to MD localization of membrane proteins due to the high similarity to the lipids associated with MDs (Levental *et al.*, 2010b; Blaskovic *et al.*, 2013). But if this lipidation is sufficient as signal for MD localization in the inner leaflet or if this mediated by protein intrinsic signal motifs still an open question.

2.3.1. Current Anchoring Model Hypotheses

Although remorins are predicted to be highly hydrophilic and without any TMD or any other anchoring domain they localize to the PM in distinct MDs. Furthermore, it could be shown that remorins attach to the cytosolic leaflet and are as strongly anchored to the PM as integral membrane proteins (Raffaele *et al.*, 2009; Perraki *et al.*, 2012). A study in 2012 on the remorin StREM1.3 identified the last C-terminal 26 aa as a dynamic anchoring region (RemCA for Remorin C-terminal Anchor) (Perraki *et al.*, 2012). For this RemCA an intrinsic property to bind to lipids was postulated. Due to this finding the authors proposed a two-step anchoring mechanism with (1) attaching of the unfolded RemCA to the PM with its positively charged residues. By this (2) the folding of the RemCA into a tight hairpin of α -helices is induced. A hydrophobic pocket gets formed that mediates the tight PM anchoring (Perraki *et al.*, 2012). In addition a predominant co-purification of the RemCA domain with DIM-

fractions was shown, from which they concluded that the RemCA domain also harbors an intrinsic signal for MD localization.

However, remorins were also identified in a large proteomic study to be S-acylated (Hemsley *et al.*, 2013). Therefore, it still remains unclear how a general anchoring mechanism of remorins could function. Specially, if the RemCA domain really contains a MD localization signal or if the S-acylation localizes remorins to MDs needs further investigation.

3. Aims Of This Study

3.1. SYMREM1

Based on the amino acid sequence of remorins no PM anchoring domain or modification was predictable. Therefore, the mechanism how remorins are anchored to the inner leaflet of the PM, and especially to MD, was not known at the beginning of this thesis. During the initial phase of my PhD the findings of two studies postulated two different mechanisms for remorins to anchor to the PM. One hypothesized a mechanism, which includes the folding of a tight α -helical hairpin of a C-terminal RemCA domain and the other showed remorins of the group 1 to be present in a proteomic study of S-acylated proteins.

To fully unravel the anchoring mode of remorins the PM localization behavior of different SYMREM1 protein variants (truncations and point mutations) have been studied in a homologous and heterologous expression system. To be able to make a general statement on the anchoring mechanism of remorins, *Arabidopsis thaliana* remorin family proteins have been included in this study as well (Konrad *et al.*, 2014). In the frame of this work also the question was addressed whether S-acylation or an intrinsic protein motif mediated MD localization of remorins.

In a smaller second part on SYMREM1 the available mutant lines have been further phenotypically characterized. Additionally, the lack of a functional SYMREM1 in these mutant lines could be verified as the reason for the observed phenotype via complementation experiments (Stratil *et al.* manuscript 2)

3.2. MYCREM (formerly REMORIN-LIKE 1)

To gain a better understanding of the physiological relevance of an AM-induced legume-specific remorin, a large phenotypical approach was initiated. A *mycrem* mutant line was studied under three different symbiotic interaction conditions (AM, RNS and AM/RNS simultaneous). Additionally, an evolutionary approach was undertaken to understand the discrepancy between being highly induced under AM conditions but being absent in other AM-host plants than legumes. Studies on unraveling the genetic position of MYCREM within the AM and RNS related pathways have been initiated (Popp *et al.* manuscript 1).

Moreover, by studying MYCREM I addressed the first time the question how the tripartite symbiotic interaction of legumes, AMF and rhizobia, as it occurs in nature, can be spatially controlled downstream of the CSP.

B) Publications and Manuscripts

1. Overview Publications and Manuscripts

Publication 1:

Konrad, S.S.A.*, Popp, C.*, Stratil, T.F., Jarsch, I.K., Thallmair, V., Folgmann, J., Marin, M., and Ott, T.

S-acylation anchors remorin proteins to the plasma membrane but does not primarily determine their localization in membrane microdomains.

The New Phytologist **203**, 758-769

Publication 2:

Tóth, K., Stratil, T.F., Madsen, E.B., Ye, J., Popp, C. Antolín-Llovera, M., Grossmann, C., Jensen, O.N., Schüßler, A., Parniske, M. and Ott, T.

Functional Domain Analysis of the Remorin Protein LjSYMREM1 in *Lotus japonicas*. PLoS ONE, **7**, e30817

Manuscript 1:

Popp, C., Bittencourt-Silvestre J., Thallmair, V., Mysore, K.S., Wen, J., Delaux, PM., and Ott, T.

A remorin protein controls symbiotic dualism in the legume *Medicago truncatula*, *Proceedings of the National Academy of Sciences*, USA

Manuscript 2:

Stratil, T.F., Popp, C., Konrad, S.S.A., Marín, M., Folgmann, J., and Ott, T.

The formation of an infection-related membrane domain is controlled by the sequential recruitment of scaffold and receptor proteins. *Proceedings of the National Academy of Sciences*, USA

1.1. Publication 1

S-acylation anchors remorin proteins to the plasma membrane but does not primarily determine their localization in membrane microdomains.

Konrad, S.S.A.*, Popp, C.*, Stratil, T.F., Jarsch, I.K., Thallmair, V.,
Folgmann, J., Marin, M., and Ott, T.

The New Phytologist **203**, 758-769

Status: published | Year: 2014 | DOI: 10.1111/nph.12867

* These authors contributed equally to this study.

S-acylation anchors remorin proteins to the plasma membrane but does not primarily determine their localization in membrane microdomains

Sebastian S. A. Konrad*, Claudia Popp*, Thomas F. Stratil, Iris K. Jarsch, Veronika Thallmair, Jessica Folgmann, Macarena Marín and Thomas Ott

Ludwig-Maximilians-University (LMU) Munich, Institute of Genetics, 82152 Martinsried, Germany

Summary

Author for correspondence:

Thomas Ott

Tel: +49 (0)89 2180 74704

Email: Thomas.Ott@biologie.uni-muenchen.de

uni-muenchen.de

Received: 7 March 2014

Accepted: 22 April 2014

New Phytologist (2014)

doi: 10.1111/nph.12867

Key words: membrane domain, palmitoylation, protein–protein interaction, remorin, S-acylation.

- Remorins are well-established marker proteins for plasma membrane microdomains. They specifically localize to the inner membrane leaflet despite an overall hydrophilic amino acid composition. Here, we determined amino acids and post-translational lipidations that are required for membrane association of remorin proteins.
- We used a combination of cell biological and biochemical approaches to localize remorin proteins and truncated variants of those in living cells and determined S-acylation on defined residues in these proteins.
- S-acylation of cysteine residues in a C-terminal hydrophobic core contributes to membrane association of most remorin proteins. While S-acylation patterns differ between members of this multi-gene family, initial membrane association is mediated by protein–protein or protein–lipid interactions. However, S-acylation is not a key determinant for the localization of remorins in membrane microdomains.
- Although remorins bind via a conserved mechanism to the plasma membrane, other membrane-resident proteins may be involved in the recruitment of remorins into membrane domains. S-acylation probably occurs after an initial targeting of the proteins to the plasma membrane and locks remorins in this compartment. As S-acylation is a reversible post-translational modification, stimulus-dependent intracellular trafficking of these proteins can be envisioned.

Introduction

It has now been widely accepted that plasma membranes (PM) are functionally compartmentalized. These structures, called membrane micro-domains, are defined by a dynamic crosstalk between different lipids, membrane-resident proteins and probably the cortical cytoskeleton that results in the assembly of membrane subcompartments in the micrometer range (reviewed in Lingwood & Simons, 2010; Li *et al.*, 2013; Malinsky *et al.*, 2013). While life cell imaging of lipids revealed a heterogeneous distribution in cells and tissues (Vermeer *et al.*, 2009; Horn *et al.*, 2012), most work done in plants so far has focused on the roles of sterols. Such sterol-enriched sites can harbour a large number of signalling proteins and are important during plant-microbe interactions (reviewed in Zappel & Panstruga, 2008; Jarsch & Ott, 2011; Urbanus & Ott, 2012). Focal accumulation of membrane domain proteins during host cell infection indicates the existence of active cellular processes that specifically direct

signalling complexes to infection sites (Bhat *et al.*, 2005; Haney & Long, 2010; Lefebvre *et al.*, 2010; Underwood & Somerville, 2013). Increasing evidence suggests that a large number of PM-resident proteins do not freely diffuse inside the PM bilayer as single molecules but are preassembled into distinct subdomains (Kusumi *et al.*, 2012). However, not much is known about the mechanisms that target individual proteins to membrane domains in plant cells. Transmembrane proteins might not only assemble specific lipids in their vicinity and thereby directly contribute to the assembly of specific lipid shells, but also interact with other membrane-resident proteins and the actin cytoskeleton. Such interactions, among others, support the formation of larger domain clusters (Lingwood & Simons, 2010; van den Bogaart *et al.*, 2011). For extracellular proteins, the addition of glycosylphosphatidylinositol (GPI) moieties has been shown to contribute to their specific association with the apoplastic face of sterol-enriched membrane domains (Varma & Mayor, 1998). Accordingly, proteins carrying GPI-anchors are overrepresented in sterol-enriched detergent-resistant membranes (DRMs), indicating that addition of this lipid moiety directs

*These authors contributed equally to the work.

extracellular proteins into these fractions (Kierszniowska *et al.*, 2009). In plants, only few proteins have been identified that associate with membrane domains at the cytosolic face of the PM, among them flotillins and remorins (Raffaele *et al.*, 2009; Haney & Long, 2010; Li *et al.*, 2012; Jarsch *et al.*, 2014). Flotillins evolved in multicellular eukaryotes and form a small gene family with three members in *Arabidopsis thaliana*. They bind the inner leaflet via lipid modifications, called myristoylation and S-acylation (Neumann-Giesen *et al.*, 2004). Myristoylation is an irreversible modification of an N-terminal glycine residue while S-acylation (formerly called palmitoylation) of cysteine residues can occur throughout the entire protein (Blaskovic *et al.*, 2013). Importantly, S-acylation contributes not only to membrane association of proteins but also to the regulation of protein–protein interactions (Blaskovic *et al.*, 2013). The acylation reaction itself is either catalysed by membrane-resident protein acyl-transferases (PATs) or, rarely, occurs spontaneously (Bharadwaj & Bizzozero, 1995). In contrast to other lipid modifications that mediate PM association, S-acylation is reversible. This feature allows dynamic regulation of protein complexes. As such regulatory modes are required during signal transduction, it appears a natural consequence that a number of plant signalling proteins, such as small GTPases (Sorek *et al.*, 2007), calcium-dependent kinases (Martin & Busconi, 2000) and heteromeric G-proteins (Adjobo-Hermans *et al.*, 2006; Hemsley *et al.*, 2008), have been shown to be S-acylated. More globally, a recent proteomic study in *A. thaliana* reported the presence of 581 S-acylated proteins, among them two plant-specific remorins (Hemsley *et al.*, 2013). Remorins form a multigene family with 16 members in *A. thaliana* (Raffaele *et al.*, 2007). Plants that undergo root nodule symbiosis have evolved an additional subgroup that also comprises the SYMBIOTIC REMORIN 1 (SYMREM1) (Lefebvre *et al.*, 2010; Tóth *et al.*, 2012). The SYMREM1 protein interacts with symbiosis related receptor-like kinases and localizes in membrane microdomains along nodular infection threads (Lefebvre *et al.*, 2010; Tóth *et al.*, 2012). Knockout mutants in *Medicago truncatula* revealed that the protein controls rhizobial infections as these mutants developed more prematurely aborted nodules compared with wildtype plants (Lefebvre *et al.*, 2010; Tóth *et al.*, 2012). Remorins consist of a conserved C-terminal region that contains a canonical remorin signature. By contrast, their phosphorylated and intrinsically disordered N-terminal regions are highly variable in sequence composition and length and may serve regulatory functions during protein–protein interactions (Marín & Ott, 2012; Marin *et al.*, 2012; Tóth *et al.*, 2012). Remorins localize to distinct membrane domains at the cytosolic leaflet of the PM (Raffaele *et al.*, 2009; Lefebvre *et al.*, 2010; Perraki *et al.*, 2012; Demir *et al.*, 2013; Jarsch *et al.*, 2014) and serve as established marker proteins for PMs and membrane microdomains. Structurally these proteins lack a transmembrane domain and exhibit an overall hydrophilic amino acid profile (Reymond *et al.*, 1996; Raffaele *et al.*, 2009). Although they have been numerous found at the PM, their mode of association has not been fully understood. A recent study proposed that the potato remorin StREM1.3 physically inserts into the PM through a tight hairpin structure comprising amphipathic α -helices and that a

corresponding ‘remorin C-terminal anchor’ (RemCA) is required and sufficient for membrane binding of this remorin (Perraki *et al.*, 2012). Considering the fact that the homologous protein from *A. thaliana* is S-acylated (Hemsley *et al.*, 2013), the mode of membrane binding and localization to membrane microdomains remains to be fully elucidated.

In this study, we have finally unravelled the molecular mechanism that targets these membrane domain marker proteins to the PM and analysed the structural requirements for their specific localization.

Materials and Methods

Molecular cloning and sequence analyses

Remorin constructs were cloned from cDNA templates by Golden Gate cloning or standard Gateway (GW) technology using self-assembled level I and II plasmids or the pDONR207 entry vector, respectively (Binder *et al.*, 2014). In *Nicotiana benthamiana* Domin, all remorins were expressed using the pAM-PAT-YFP-GW vector. For expression in *Medicago truncatula* Gaertn. roots, the modified destination vector pUBi-YFP-GW-HYG was used, where the standard recombination site was replaced with an YFP-GW cassette via the sites KpnI and XbaI. Point mutations were introduced into the respective entry clones via inverted PCR.

Plant transformation and fluorescence microscopy

For analysis of SYMREM1, *M. truncatula* (ecotype A17) roots were transiently transformed as described previously (Boisson-Dernier *et al.*, 2001) with slight modifications. Plants were then grown on Fahraeus medium for 3 wk before imaging of the samples. For methyl- β -cyclodextrin (mbCD) treatments, roots expressing a genomic SYMREM1 construct with N-terminally fused yellow fluorescent protein (YFP) were incubated in 30 mM mbCD on the microscope slide and images were taken consecutively directly during immersion in the drug. Control experiments were performed in water. Images were taken 3 wk after transformation.

For heterologous expression, constructs were transformed into *Agrobacterium tumefaciens* strains GV3101 and AGL1. Transformation of *N. benthamiana* leaves was performed as previously described (Tóth *et al.*, 2012). All transformations were repeated at least three times independently. It should be noted that, in the case of *N. benthamiana* transformations, all cells represent independent transformation events.

Confocal laser scanning microscopy was performed using a Leica TCS SP5 confocal microscope equipped with $\times 63$ and $\times 20$ HCX PL APO water immersion lenses (Leica Microsystems, Mannheim, Germany). The YFP fluorophores were excited with the 514 nm argon laser line and emission was detected at 525–600 nm. FM4-64 fluorescence was excited using the argon laser line at 476 nm and emission was detected between 690 and 750 nm. In all cases, maximum projections of z-stacks are shown.

In silico analysis of SYMREM1

Ab initio modelling of SYMREM1 was performed using the I-TASSER server (Zhang, 2008; Roy *et al.*, 2010). Models for the N- and C-terminal regions were constructed independently and subsequently fused. Predictions of putative regions involved in protein interactions were performed using the PPI-Pred server (http://bioinformatics.leeds.ac.uk/ppi_pred/index.html) (Bradford & Westhead, 2005). Molecular graphics were produced using the UCSF Chimera package (<http://www.cgl.ucsf.edu/chimera>) (Pettersen *et al.*, 2004).

The hydrophobicity plot was generated on the basis of the SYMREM1 amino acid sequence (GenBank accession AEX20500) using the ExPasy Webserver (<http://web.expasy.org/cgi-bin/prot-scale/protscale.pl>).

Microsomal fractionation

Microsomal fractions were prepared by the addition of extraction buffer (230 mM sorbitol, 50 mM Tris/HCl (pH 7.5), 10 mM KCl, 3 mM ethylene glycol tetraacetic acid and protease inhibitors) to ground tissue of the microscopically examined material. Samples were spun at 20 000 *g* for 40 min before the extract was passed through two layers of Miracloth. The obtained supernatant was then spun down at 100 000 *g* for 1 h. The resulting pellets containing the microsomal fractions were resuspended in Tris-buffered saline (TBS) and used for western blot analysis. The supernatant contained all cytosolic proteins.

Biotin switch assays

Two *N. benthamiana* plants were independently infiltrated per construct, with *A. tumefaciens* carrying the respective plasmids. Before protein extraction, expression of the constructs was microscopically confirmed, using a Leica DMI 6000 epifluorescence microscope. Three fluorescent leaves per plant were harvested and samples were pooled for further processing. The biotin switch assay itself was conducted as described previously (Hemslay *et al.*, 2008). In brief, all free sulphhydryls were blocked by incubation in N-ethylmaleimide. Hydroxylamine-induced cleavage of the acylthioester bond resulted in removal of the fatty acid moiety and the generation of free sulphhydryls that were labelled using a sulphhydryl-reactive biotin, forming a biotinylated cysteine. S-acylated proteins were then purified using neutravidin-coupled agarose beads. Methanol/chloroform precipitations were carried out as described earlier (Wessel & Flugge, 1984). This experiment was repeated two to three times independently and always yielded the same result.

Quantification of bands on the Western blot was performed using ImageJ. Mean intensity values were obtained after subtraction of the background.

Western blot analysis

After sodium dodecyl sulfate–polyacrylamide gel electrophoresis (SDS-PAGE), proteins were transferred overnight at 4°C to

polyvinylidene fluoride membranes. Membranes were blocked in TBS containing 0.1% Tween 20 (TBS-T) and 5% milk for 10 h at 4°C. All constructs were detected using a polyclonal α -GFP antibody (Rockland Immunochemicals, Gilbertsville, PA, USA) at a 1 : 5000 dilution in TBS-T 5% milk overnight at 4°C. The membrane was washed three times with TBS-T before incubation with a horseradish peroxidase-conjugated α -rabbit antibody (GE Healthcare, Munich, Germany) at a 1 : 20 000 dilution in TBS-T 5% milk for 1 h at room temperature. Detection of chemiluminescence was carried out according to the ECL reagent manufacturer's instructions (Pierce; Thermo Fischer, Bonn, Germany).

Expression of SYMREM1 constructs in yeast

SYMREM1, SYMREM1^{C197A}, RemCA and truncated variants were cloned into the yeast expression vector pAG424GAL-EYFP-ccdB (Addgene, Cambridge, MA, USA) via Gateway technology. Yeast transformation in the NMY32 strain was performed as described earlier (Tóth *et al.*, 2012). Transformants were selected on synthetic dropout (SD) medium supplemented with 2% galactose to induce transgene expression. For microscopy, yeast cells were immobilized on glass slides with a 5% low melt agarose film.

For protein extractions, pellets from 12 ml cultures were washed with 1 mM ethylenediaminetetraacetic acid before disruption by glass beads in 50 mM Tris-HCl supplemented with protease inhibitors. Microsomal and cytosolic fractions were obtained by differential centrifugation as described earlier and subjected to western blot analysis.

Results

Sterol-dependent localization of SYMREM1 in membrane microdomains

In a first experiment, we assessed PM localization of SYMREM1 in detail. When ectopically expressing a SYMREM1 fusion protein in transgenic *M. truncatula* roots, we observed the expected labelling of PM microdomains (Fig. 1a). Interestingly, most observed membrane domains were immobile over the 30 min observation period (Fig. 1b, arrowheads). This is in agreement with previous localization studies of native SYMREM1 in root nodules (Lefebvre *et al.*, 2010) and other remorins (Raffaele *et al.*, 2009; Demir *et al.*, 2013; Jarsch *et al.*, 2014). Because formation of membrane domains has often been associated with the enrichment of sterols, we tested sterol-dependency of SYMREM1-labelled microdomains in living cells. For this, transgenic roots were incubated in the presence of 30 mM mbCD, a cyclic oligosaccharide that interacts with hydrophobic molecules, including sterols, and depletes them from membranes (Roche *et al.*, 2008). Indeed, most microdomains dissolved within the first 10 min upon mbCD application, indicating sterol-dependency of these membrane domains (Fig. 1c). Cell viability during mbCD treatment was confirmed by the persistent presence of cytoplasmic streaming in living root hair cells incubated in water (Fig. 1d) and 30 min after mbCD application (Fig. 1e).

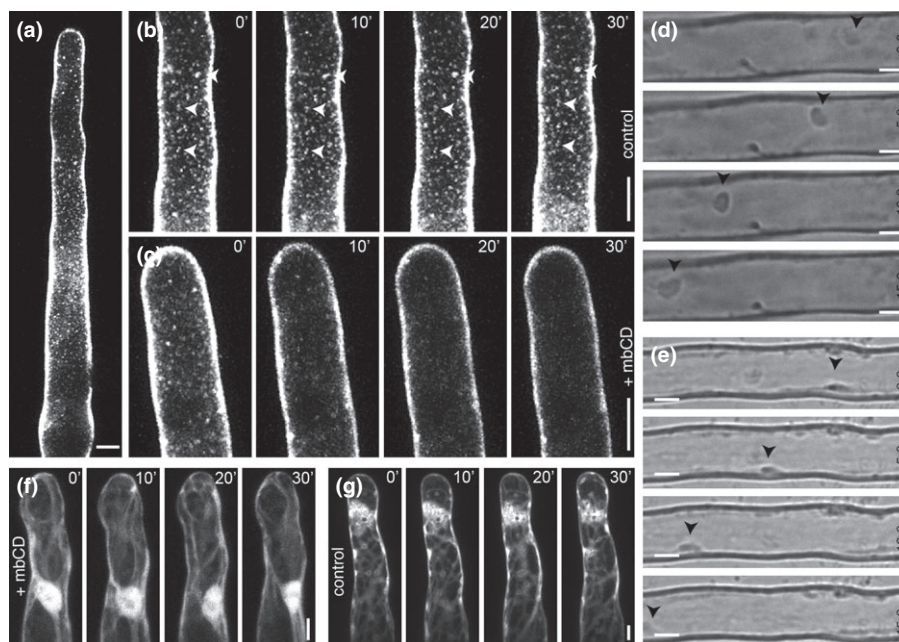


Fig. 1 SYMREM1 labels sterol-dependent membrane domains *in vivo*. (a) Image of a mature transgenic root hair from *Medicago truncatula* ectopically expressing a YFP-SYMREM1 fusion protein. (b) Membrane domain patterns did not change during imaging. Images were taken in 10 min intervals. Arrowheads mark laterally immobile membrane domains. (c) Application of 30 mM methyl- β -cyclodextrin (mbCD)-depleted membrane domains. Images were taken at 10 min intervals. (d, e) Cytoplasmic streaming was observed in 5 s intervals before (d) and after (e) incubation of roots in 30 mM mbCD for 30 min. Arrowheads point towards mobile cytosolic particles that allowed detection of cytoplasmic streaming. (f, g) Transgenic root hairs expressing free yellow fluorescent protein (YFP). No changes in fluorescence were observed when roots were treated with 30 mM mbCD for 30 min (f) or water as a control (g), indicating that the treatment did not affect the fluorophore alone. All images are z-projections. Bars: (a–c, f, g) 10 μ m; (d, e) 5 μ m.

Furthermore, we could exclude the possibility that the mbCD treatment affected the fluorophore itself, as application of the drug did not result in any difference from water-treated controls when we expressed free YFP protein in transgenic roots (Fig. 1f, g). These experiments demonstrate that SYMREM1 localizes to membrane domains in a sterol-dependent manner *in vivo*.

Identification of the membrane-binding site

As other remorins, the SYMREM1 protein shows an overall hydrophilic pattern (Fig. 2a). However, the C-terminal 35 residues may form a hydrophobic core out of which 19 residues are predicted to be intrinsically disordered and thus do not contain any secondary structure in solution. Using the PPI-Pred server, we found that 25 of these terminal residues are predicted to be involved in protein–protein interactions (indicated in red; Supporting Information, Fig. S1a). As hydrophobic sites are required for both direct membrane binding and protein–protein interactions, we generated a series of truncation variants of SYMREM1 N-terminally fused to a YFP fluorophore (YFP-SYMREM1), to investigate the role of its different protein regions in membrane binding. These constructs were expressed in transgenic *M. truncatula* roots, and secant (median) planes of root epidermal cells were analysed by confocal laser scanning microscopy. The results are shown in Fig. 2 as maximum intensity projections of z-stack images. As expected, the full-length protein entirely resided in the PM (Fig. 2b). The N-terminal region of SYMREM1 (residues 1–73; Fig. 2c) showed the same cytoplasmic localization pattern as the sole YFP fluorophore (Fig. S1b). By

contrast, the C-terminal region (residues 74–205) remained fully associated with the PM (Fig. 2d). Expression of C-terminally truncated proteins, where deletions were introduced in front of the predicted helical structure at position Cys171 (residues 1–170) or between the predicted intrinsically disordered C-terminal residues (residues 1–190), resulted in a predominantly cytosolic SYMREM1 protein (Fig. 2e, f). These results indicate that residues within the C-terminal region mediate PM localization. This was confirmed in a reciprocal experiment where a YFP fluorophore was found to be entirely associated with the PM when being fused to these 35 residues (SYMREM1^{171–205}) (Fig. 2g). In all cases, localization and integrity of the fusion proteins were biochemically confirmed by Western blot analyses after microsomal fractionation (Fig. 2, panels below images). Faint signals were still observed in the microsomal fractions of the truncated variants SYMREM1^{1–170} and SYMREM1^{1–190} (Fig. 2e, f), indicating that a proportion of the protein resided in the PM independently of the C-terminal 35 amino acid residues. In general, these data are in agreement with a recently published report, where the corresponding region in the remorin StREM1.3 from potato (RemCA) was shown to be required for membrane binding of this protein (Perraki *et al.*, 2012). For consistency we therefore used the term ‘RemCA’ throughout our study.

The presence of few C-terminal residues is indispensable for membrane localization of remorin proteins

Next we asked whether the C-terminal hydrophobic core is generally required for PM association of remorin proteins. To

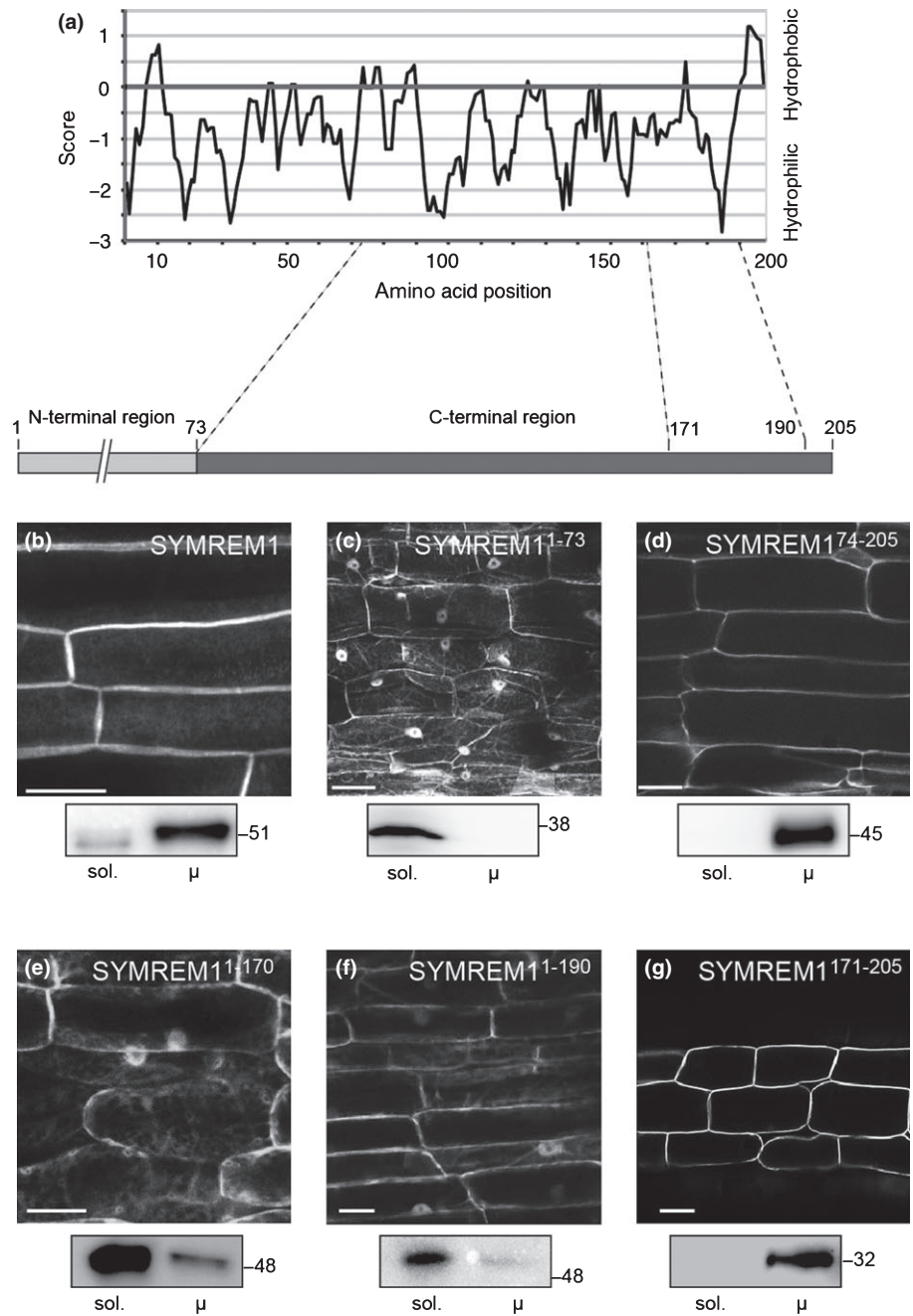


Fig. 2 The C-terminal residues mediate membrane anchoring of SYMREM1. (a) Hydrophobicity plot of SYMREM1. (b–g) Confocal images of transgenic *Medicago truncatula* roots expressing different full-length SYMREM1 (b) or truncated protein variants (c–g). The yellow fluorescent protein (YFP) fluorophore was always fused to the N-terminus of SYMREM1 protein variants. All images are z-projections of secant planes without the plasma membrane (PM) surface. Bars, 20 μ m. Western blot analysis shows the presence of intact fusion proteins (panels below images). sol., soluble protein fraction; μ , microsomal protein fraction.

investigate this, we cloned and expressed the coding regions of the closely related remorin At2g45820 (190 residues) and the three distantly related remorins, At2g41870 (274 residues), At4g36970 (427 residues) and At2g02170 (486 residues), from *A. thaliana*. As expected, all full-length proteins localized to the PM when being expressed in *N. benthamiana* leaf epidermal cells (Fig. 3a–d). Next, we truncated these proteins in front of the predicted terminal helix, as was done for SYMREM1. In analogy, expression of these truncated variants (At2g45820^{1–161}, At2g41870^{1–243}, At4g36970^{1–384}, At2g02170^{1–453}) resulted in an entire loss of PM binding of all proteins *in planta* (Fig. 3e–h). These data were verified for the shortest and the longest remorins by labelling PMs with the dye FM4-64. While full-length

At2g45820 and At2g02170 colocalized perfectly with FM4-64 (Fig. 3i,j), the truncated versions showed clear cytoplasmic localizations (Fig. 3k,l).

To reciprocally test if these regions were always sufficient to anchor YFP to the PM as shown for SYMREM1 (Fig. 2g), the C-terminal 35 amino acids (RemCAs) of all 16 *A. thaliana* remorins were fused to this fluorophore and expressed in *N. benthamiana* leaf epidermal cells. Surprisingly, only four of these RemCA peptides (At4g36970, At2g02170, At1g30320, At5g61280) were sufficient to fully anchor the YFP protein to the PM (Fig. S2a–d, Table 1). In all other cases, strong cytoplasmic localizations of the fusion proteins were observed (Fig. S2e–p). To test whether this cytoplasmic localization may (partially) derive

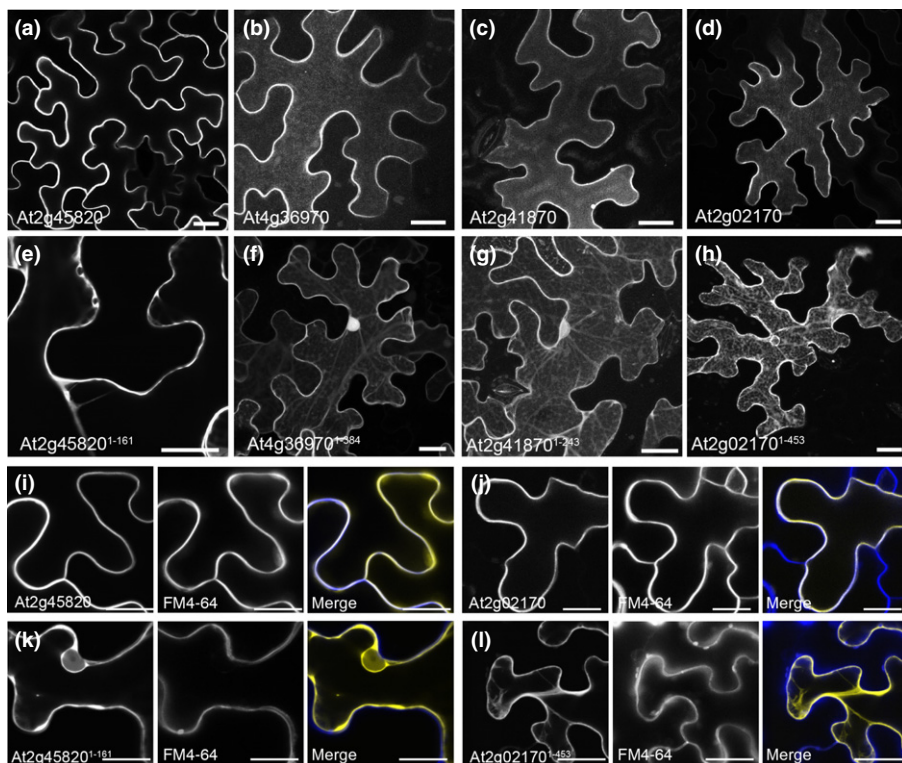


Fig. 3 The C-terminal residues determine membrane association throughout the remorin family. (a–h) All tested full-length proteins localized to the plasma membrane (PM) (a–d), while all mutant variants that were truncated by the respective remorin C-terminal anchor (RemCA) peptide were predominantly found in the cytosol when being expressed in *Nicotiana benthamiana* leaf epidermal cells (e–h). (i, j) PM counterstaining with the styryl dye FM4-64 showed colocalization with full-length At2g45820 and At2g02170. (k, l) No colocalization was observed between FM4-64 and the truncated variants At2g45820^{1–161} (k) and At2g02170^{1–453} (l). Yellow fluorescent protein (YFP) fluorescence is shown in yellow, and the FM4-64 stain is represented in blue. Bars, 20 μm .

from fluorophore cleavage, proteins were extracted and compared with free YFP by Western blot analysis (Fig. S2q). Indeed, partial cleavage was detected for At1g69325, At4g00670, At3g57540, At2g41870, At1g45207, At4g36970 and At1g13290. Those proteins were therefore further subjected to microsomal fractionations to determine the degree of cytosolic and membrane localization. In all cases, the intact fusion protein localized predominantly to the cytosolic fraction (Fig. S2r). This implies that these RemCA peptides were not sufficient for strong immobilization of the fluorophore at the PM.

As all remorins contain a hydrophobic stretch at the C-terminus (Table 1), we excluded the possibility that the chemical properties of these residues alone are the sole determinants for PM localization of the proteins.

C-terminal cysteine residues contribute to PM localization of remorins

As stated earlier, post-translational lipid modifications often confer PM binding of proteins. Following a recent global approach in *A. thaliana*, where two remorins were found to be S-acylated (Hemsley *et al.*, 2013), we used the CSS-PALM 3.0 algorithm (<http://csspalm.biocuckoo.org/>) to predict putative S-acylation sites in all *A. thaliana* remorin proteins and SYMREM1. Except for At3G48940, At3G57540 and At2G41870, all remorins were found to harbour at least one C-terminal cysteine residue that may serve as putative sites of S-acylation (Table 1).

To test whether S-acylation is a key determinant for membrane association of RemCA peptides, we chose SYMREM1 and At4g36970, which have one and two predicted S-acylated

cysteines in their RemCA sequences, respectively. High-resolution imaging (*c.* $\times 10$ higher magnification than used here) recently revealed labelling of membrane microdomains by the full-length variants of these proteins (Jarsch *et al.*, 2014). The RemCA peptides of both remorins were sufficient to fully associate a fluorophore to the PM when expressed in *N. benthamiana* (Figs 4c, S2a). At3g61260 was used as a control. This *A. thaliana* remorin is the homolog of the well-studied StREM1.3 protein (Perraki *et al.*, 2012) and was found to be S-acylated (Hemsley *et al.*, 2013). It should be noted that the RemCA peptides of neither At3g61260 nor its closely related proteins At3g48940, At2g45820 and At5g23750 were sufficient to anchor soluble YFP to the PM (Table 1; Fig. S2).

To test the impact of point mutations at the predicted cysteine residues, we expressed a number of mutant variants in *N. benthamiana*. Introduction of a cysteine to alanine mutation at the predicted S-acylation site Cys197 in SYMREM1 did not lead to a significant decrease of PM localization of the full-length protein (Fig. 4b). Western blot analysis on microsomal fractions of protein extracts from *N. benthamiana* plants expressing wildtype SYMREM1 and mutated SYMREM1^{C197A} confirmed predominant PM association of both proteins (Fig. S3a). Interestingly, a small but reproducible band shift was observed in the SYMREM1^{C197A} mutant, indicating a possible modification on this residue (Fig. S3b). In contrast to the full-length protein, introduction of the same point mutation into the isolated membrane-binding domain of SYMREM1 (RemCA, SYMREM1^{171–205}) resulted in an entire loss of PM association of the fusion protein and labelling of mobile structures in the cytoplasm (Fig. 4d), while the wildtype peptide resided at the PM (Fig. 4c). These

Table 1 Subcellular localization of remorin C-terminal anchor (RemCA) peptides of all *Arabidopsis thaliana* remorins plus SYMREM1 and predications of S-acylation sites

Name	aa	predominant subcellular localization	Predicted S-acylation sites	Score	Cutoff	C-terminal 20 aa sequence
At3g48940	175	Cytosol	n.d.	n.d.	n.d.	EMAAKYRATGTAPT KL FGFF*
At3g61260	212	Cytosol	Cys209 Cys211	1.524 2.204	0.308 0.497	ETAAKYRATGILVPKATCGCF*
At2g45820	190	Cytosol	Cys187 Cys189	1.386 2.065	0.308 0.497	EMGAKYRATGVVPKATCGCF*
At5g23750	202	Cytosol	Cys106 Cys201	0.367 1.983	0.308 1.225	ELAAKYRATGTAPK KL FGCM*
At1g69325	120	Cytosol	Cys119	2.380	1.225	KVKEKANLMRTTGRK PS TCL*
At4g00670	123	Cytosol	Cys122	2.562	1.225	AAARFQAAGKIPK SS LS CF *
At3g57540	296	Cytosol	n.d.	n.d.	n.d.	ANLMRAVGRPPAKRS F FSL*
At2g41870	274	Cytosol	n.d.	n.d.	n.d.	ANLMRALGRPPAKRS F FSF*
At1g45207	555	Cytosol	Cys549 Cys552	1.805 1.355	0.308 1.225	KRSGKKI PS LSGCF TC HVF*
At2g02170	486	Plasma membrane	Cys481 Cys485	1.690 2.954	0.308 0.497	QIRRTGKVP SLL FS CF S FC S*
At1g30320	509	Plasma membrane	Cys504 Cys505	2.262 1.455	0.308 1.225	IRETGRIPASSYKI CC GWFS*
At1g53860	442	Cytosol	Cys432 Cys434 Cys437 Cys441	0.567 0.796 0.843 1.361	0.308 0.497 0.497 0.497	GYLVTGRSS CG CL PC NNT CH *
At4g36970	427	Plasma membrane	Cys413 Cys420	0.986 2.681	0.308 0.308	TPFMT CF FAPRV DC RK SS SAL*
At1g67590	347	Cytosol	Cys344 Cys346	1.213 1.733	0.497 0.308	GHLPSSF SF SFKL PS R WC Q*
At1g13920	345	Cytosol	Cys343 Cys344	2.298 2.959	1.225 1.225	KEKAGVIR ST GKLP GN AC CF *
At5g61280	263	Plasma membrane	Cys259	1.219	0.308	VKKMSRTGKVP NN Y FC ER CY *
SYMREM1	205	Plasma membrane	Cys197	1.048	0.308	TRGYQ RR LL GC FS GL RFFS*

RemCA peptides of all 16 *A. thaliana* remorins and the *Medicago truncatula* SYMREM1 protein were expressed as yellow fluorescent protein (YFP) fusion proteins in *Nicotiana benthamiana* leaf epidermal cells and subcellular localizations were scored microscopically (Fig. S2). Putative S-acylation sites were predicted for all using the CCS-PALM server (<http://csspalm.biocuckoo.org/>). Scores and cutoff values for the predictions are provided. S-acylation was biochemically determined for those remorins marked in green. The C-terminal 20 amino acid (aa) residues are provided, and predicted S-acylated residues are indicated by the zig-zag line. Colour coding indicates Kyte–Doolittle hydrophobicity score of individual amino acids (red, hydrophobic; blue, hydrophilic). n.d., not detected; Cys, cysteine; *, stop codon.

data show that Cys197 stabilizes PM attachment of SYMREM1, whereas it is indispensable for PM binding of the membrane-binding domain alone.

A different pattern was observed for At4g36970. Here, PM association of the full-length protein was affected by single point mutations in the predicted S-acylation sites Cys413 (Fig. 4f) and Cys420 (Fig. 4g). Both mutations resulted in a strong accumulation of the proteins in immobile membrane domains. Furthermore, the mutation in Cys413 led to an additional nuclear and cytosolic localization (Fig. 4f). A C413A/C420A double mutant

was also targeted to these immobile foci and showed nuclear localization, resembling the pattern of the C413A mutant (Fig. 4h).

To test whether these putative cysteine lipidations are key determinants for membrane localization of the At4g36970-derived RemCA, the same mutations were introduced into the respective constructs. Expression of a fluorophore-tagged RemCA construct of At4g36970 (residues 384–427) revealed labelling of the PM and mobile vesicles in the cytosol (Fig. 4i). While the replacement of Cys420 with alanine did not affect PM targeting

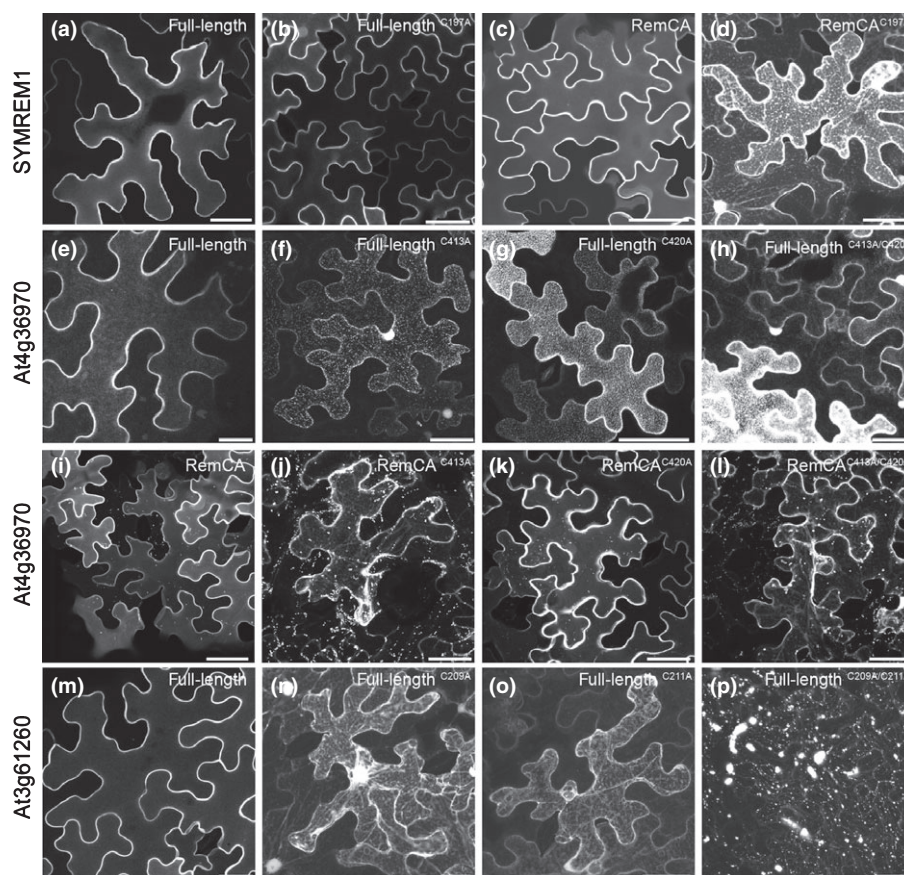


Fig. 4 Mutations in C-terminal cysteine residues alter localization patterns of remorin proteins when being expressed in *Nicotiana benthamiana* leaf epidermal cells. (a, b) Full-length SYMREM1 and the mutant variant SYMREM1^{C197A} remained plasma membrane (PM)-localized. (c, d) PM association of the remorin C-terminal anchor (RemCA) peptide of SYMREM1 is dependent on Cys197. Introduction of a C197A mutation in this residue resulted in an entire loss of membrane binding (d). (e–h) Mutations in the two predicted C-terminal S-acylation sites, Cys413 (f) and Cys420, of At4g36970 resulted in altered membrane domain patterning and partial cytosolic/nuclear localization of the C413A mutant (f). (h) The At4g36970 double cysteine mutant resembled both single mutations. (i) The yellow fluorescent protein (YFP)-RemCA peptide of At4g36970 is targeted to the PM and some mobile vesicles. PM localization is altered in the C413A (j) but not in the C420A (k) mutant of the At4g36970 RemCA peptide. (l) The At4g36970 RemCA double cysteine mutant resembled the C413A mutation. (m–p) Both C-terminal cysteines of At3g61260 are required for PM association of the protein. (p) The respective double mutant strongly aggregated in the cytoplasm. All images are z-projections. Bars, 50 μ m.

(Fig. 4k), a mutation in Cys413 led to cytosolic and nuclear localization of the YFP fusion protein. In line with this, the C413A/C420A double mutant followed the same localization pattern as observed for the C413A single mutant (Fig. 4l). All results were confirmed in colocalization experiments with the lipophilic dye FM4-64 (Fig. S4a,b). These data are consistent with our results from *in planta* localization studies of mutated SYMREM1 and show that C-terminal cysteine residues are crucial for membrane attachment of the remorin membrane-anchoring motif.

Finally, we introduced mutations into the predicted S-acylation sites of At3g61260, a protein that has been shown to be S-acylated (Hemsley *et al.*, 2013). While the full-length protein was exclusively found at the PM (Fig. 4m), mutations of the C-terminal residues Cys209 and Cys211 resulted in both cytoplasmic and, for Cys209, additional nuclear localization (Fig. 4n, o). Interestingly, the double mutant (C209A/C211A) strongly aggregated in large, mobile clusters in the cytosol (Fig. 4p). Again, these data were confirmed by colocalization experiments with FM4-64 (Fig. S4c).

In all three cases, the mutation of *in silico* predicted S-acylation sites resulted in an altered localization pattern. The entire loss of PM attachment in mutant variants of the remorin membrane-binding domain from two different remorins and the alteration of localization of the full-length At3g61260 protein highlight the importance of these residues in PM targeting.

Interestingly, three *A. thaliana* remorins (At3g48940, At3g57540 and At2g41870) are entirely devoid of cysteine residues. Thus no putative S-acylation sites could be detected in these proteins when using the CSS PALM algorithm (Table 1). However, as shown for At2g41870, these proteins also require the C-terminal 35 residues to associate with the PM (Fig. 3c,g), indicating a possible alternative mode of membrane binding.

Remorins are S-acylated proteins

Next, we asked, whether the identified and mutated cysteine residues are indeed post-translationally modified. To verify the presence of S-acyl moieties, we performed a biotin switch assay, a

method that was successfully used to determine S-acylation of plant proteins (Hemsley *et al.*, 2008). We confirmed functionality of the assay on full-length At3g61260, where the presence of a band in the elution fraction of hydroxylamine-treated samples indicates S-acylation of the protein (Fig. S5a,b). Strong S-acylation signals were also observed for SYMREM1, and its RemCA peptide (Fig. 5a). By contrast, no S-acylation was detected in the C197A mutant of the full-length SYMREM1 protein and the isolated membrane-binding domain. This demonstrates that Cys197 is the only S-acylated residue in the SYMREM1 protein (Fig. 5a).

Accordingly, the At4g36970 RemCA peptide was also found to be S-acylated (Fig. 5b). A mutation in Cys413 of the At4g36970 RemCA was sufficient to abolish S-acylation of the peptide (Fig. 5b), demonstrating that this residue is an essential S-acylation site in the membrane-binding domain. These data are supported by the fact that no change in S-acylation was observed for the C420A mutation. Thus, this residue is not S-acylated (Fig. 5b). It should be noted that we were unfortunately unable to perform these experiments reliably on full-length At4g36970, because of the insolubility of the protein.

S-acylation is dispensable for SYMREM1 targeting to membrane microdomains

S-acylation has been suggested to contribute to microdomain localization of membrane-resident proteins (Blaskovic *et al.*, 2013). Therefore, we asked whether S-acylation is required for membrane domain localization of the SYMREM1 protein in

transgenic *M. truncatula* roots. Expression of full-length SYMREM1 or the C-terminal region (SYMREM1^{74–205}) resulted in clear labelling of membrane microdomains in root epidermal cells (Fig. 6a,b). Interestingly, this pattern was also observed when expressing the S-acylation mutant variant SYMREM1^{C197A}, albeit to weaker extent (Fig. 6c). By contrast, the YFP protein fused to the SYMREM1 membrane-binding domain (RemCA, SYMREM1^{171–205}) did not label such distinct sites in the majority of cells (Fig. 6d). These data imply that S-acylation and the presence of the hydrophobic core alone are not sufficient to target SYMREM1 into membrane domains. As remorins are able to form oligomers (Bariola *et al.*, 2004; Marin *et al.*, 2012; Tóth *et al.*, 2012), membrane localization of SYMREM1 could be mediated by interactions with other members of the remorin family. Therefore we expressed wildtype SYMREM1, SYMREM1^{74–205}, SYMREM1^{C197A} and SYMREM1^{170–205} in *Saccharomyces cerevisiae* (yeast), a biological system devoid of remorin proteins. Indeed, all fusion proteins that contained the full-length C-terminal region localized to the PM and clearly labelled distinct membrane domains in the PM independently of S-acylation at Cys197 (Fig. 6e–g). Reciprocally, expression of the PM binding domain alone was not sufficient to label membrane domains in yeast cells (Fig. 6h), although western blot analysis revealed the predominant presence of the fusion protein in the microsomal fraction (Fig. S6). These data clearly indicate that interaction with other remorins is not the basis for PM association of SYMREM1 and that other factors than S-acylation alone contribute to membrane domain targeting.

Discussion

Association of soluble proteins with the cytoplasmic leaflet of the PM can be mediated by interactions with other membrane-resident (e.g. transmembrane) proteins or post-translational lipidations. These lipid modifications, for example, S-acylation, can serve as key determinants for polar signalling, which enables cells to rapidly respond to extracellular stimuli and to efficiently organize proteins in a polar manner (Grunewald & Friml, 2010; Kleine-Vehn *et al.*, 2011). Prominent examples are small GTPases of the Rho of plants (ROP) family that laterally segregate in plant cells. ROP6, a type-I ROP that is involved in ABA signalling, is S-acylated upon activation and subsequently copurifies with DRM fractions (Sorek *et al.*, 2007). Furthermore, expression of deacylated ROP variants in transgenic plants resulted in nonpolar accumulation of reactive oxygen species (ROS), indicating that polar segregation of ROPs depends on S-acylation (Sorek *et al.*, 2010).

Plant-specific remorin proteins, for which putative roles during hormone responses, plant–microbe and plant–virus interactions have been suggested (Alliotte *et al.*, 1989; Raffaele *et al.*, 2009; Lefebvre *et al.*, 2010; Tóth *et al.*, 2012; Demir *et al.*, 2013), are canonical marker proteins for sterol-rich DRM fractions. More importantly, these proteins label membrane microdomains *in vivo* (Fig. 1) (Raffaele *et al.*, 2009; Lefebvre *et al.*, 2010; Peraki *et al.*, 2012; Demir *et al.*, 2013; Jarsch *et al.*, 2014). The mechanism that is used by remorin proteins to specifically target

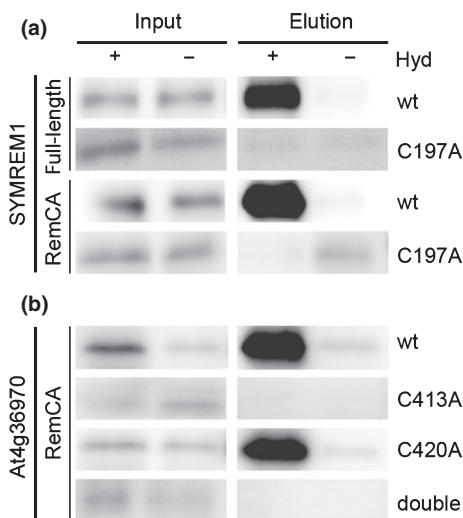


Fig. 5 Remorins are S-acylated proteins. S-acylated cysteine residues of remorin proteins purified from *Nicotiana benthamiana* were labelled by a biotin switch assay. (a) S-acylation of SYMREM1 and its corresponding membrane binding domain is indicated by the presence of a band in the elution fraction of the hydroxylamine (Hyd)-treated samples (+). Absence of this band in the C197A mutant variant revealed that Cys197 is the only S-acylated residue in this protein. wt, wildtype. (b) The remorin C-terminal anchor (RemCA) peptide of the remorin protein At4g36970 is S-acylated. Absence of a signal in the C413A mutant indicates S-acylation of this residue, while Cys420 is not S-acylated.

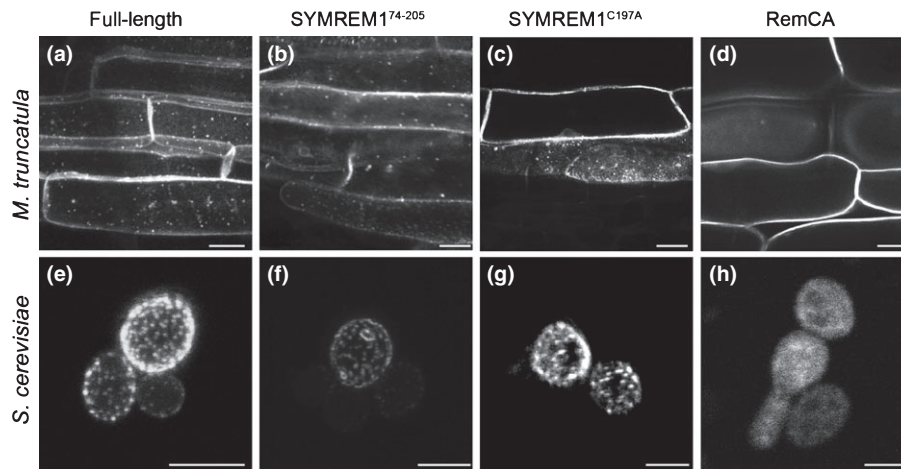


Fig. 6 Localization of remorins in membrane domains is not primarily determined by S-acylation. (a–d) Expression of different SYMREM1 constructs in transgenic *Medicago truncatula* roots revealed strong labelling of microdomains at the plasma membrane (PM) by the wildtype full-length construct (a) and the C-terminal region of SYMREM1 (b). Weaker labelling of membrane domains was also observed when expressing the deacylated mutant variant SYMREM1^{C197A} (c), while the membrane binding domain (remorin C-terminal anchor, RemCA) mostly showed uniform distribution on the PM (d). (e–h) Expression of different SYMREM1 constructs in yeast (*Saccharomyces cerevisiae*). Membrane domains were labelled by the wildtype full-length construct (e), the C-terminal region (f) and the deacylated mutant variant SYMREM1^{C197A} (g), while the membrane binding domain showed uniform distribution on the PM (h). All images are z-projections. Bars: (a–d) 10 μ m; (e–h) 5 μ m.

the inner leaflet of membrane domains remained controversial, especially as two different modes were proposed recently (Perraki *et al.*, 2012; Hemsley *et al.*, 2013). In this study, we have finally unravelled the binding mechanism of plant-specific remorin proteins on a molecular level. Our data clearly demonstrate that membrane binding of most remorins is mediated by S-acylation of cysteine residues in a C-terminal hydrophobic core, and is thus a combination of both models (Figs S1a, S7).

S-acylation is catalysed by transmembrane PATs (Roth *et al.*, 2002; Hemsley *et al.*, 2005). Therefore, remorins need to be initially directed to the PM to serve as S-acylation substrates. We propose that the C-terminal region with its terminal hydrophobic core mediates this initial affinity to the PM. This can occur via two routes: by direct protein–lipid interactions or by protein–protein interactions (Fig. S7). Indeed, recombinant StREM1.3 bound artificial, protein-free liposomes directly and showed a preferred interaction with phosphatidylinositol 3,4-bisphosphate (PI(3,4)P₂) *in vitro* (Perraki *et al.*, 2012). However, it remains to be tested whether the recombinant protein was post-translationally modified in bacteria before purification and whether this modification mediated membrane binding of StREM1.3. Our data support such a concern, as single point mutations in two C-terminal cysteine residues of the homologous remorin (At3g61260) from *A. thaliana* abolished membrane binding of the protein (Fig. 4n–p). Furthermore, none of the deacylated RemCA peptides remained associated with the PM (Figs 4, 5).

We demonstrated that despite only a few of the 35 C-terminal residues (RemCA) of different remorins are sufficient to confer membrane association of soluble fluorophores (Table 1), they are always indispensable for membrane binding of the full-length proteins (Fig. 3). It should be noted that *ab initio* modelling of SYMREM1 indicated that its RemCA peptide probably contributes to protein–protein

interactions (Fig. S1a). This prediction is experimentally supported as the C-terminal region of remorins was shown to be essential for oligomerization (Marin *et al.*, 2012; Tóth *et al.*, 2012) and interaction with other proteins (Marin *et al.*, 2012; Tóth *et al.*, 2012). In the case of SYMREM1, such interaction and membrane binding of its RemCA peptide are independent of other members of the remorin family, as PM association was also observed in yeast (Fig. 6e–h). As S-acylation may also control protein–protein interactions (Blaskovic *et al.*, 2013), the extent to which this feature also contributes to membrane association of remorin proteins remains to be studied.

Membrane domain localization of proteins in living cells can also be achieved by combinatorial lipidation, mainly myristoylation and S-acylation. In plants, double lipidation of *b*-type thiorodoxins (TRX) was shown to target these proteins to membrane microdomains *in planta* (Traverso *et al.*, 2013). By contrast, domain markers from *A. thaliana* and *M. truncatula* like flotillin and remorin proteins lack N-terminal glycine residues and are therefore not myristoylated. Thus, the possibility that membrane association of remorins *in vivo* is supported by protein–protein interactions independently of S-acylation could be especially essential for those remorins that are devoid of cysteine residues (At3g48940, At3g57540 and At2g41870) and that are therefore unlikely to be acylated. This hypothesis is further substantiated by the finding that an unacylated SYMREM1 protein remains in the PM (Fig. 4b).

We showed that S-acylation is not required for localization of remorins in immobile membrane domains *per se*, as the mutated SYMREM1^{C197A} protein still labelled these membrane compartments in plants and in yeast (Fig. 6), albeit to a lower extent. Interestingly, deacylation of At4g36970 even resulted in increased association of the protein with immobile membrane domains (Fig. 4f–h), indicating that S-acylation may eventually

restrict certain domain labelling patterns of some remorins. Therefore it is likely that another, as yet unknown factor contributes to their highly specific targeting of membrane domains.

Acknowledgements

This work was supported by the German Research Foundation (Deutsche Forschungsgemeinschaft, DFG) through an Emmy-Noether grant to T.O. (OT 423/2-1) and by two PhD fellowships from the Universität Bayern e.V. (S.S.A.K. and I.K.J.).

References

- Adjobo-Hermans MJ, Goedhart J, Gadella TW Jr. 2006. Plant G protein heterotrimers require dual lipidation motifs of Galpha and Ggamma and do not dissociate upon activation. *Journal of Cell Science* 119: 5087–5097.
- Alliotte S, Tircé C, Engler G, Peleman J, Caplan A, Van Montagu M, Inzé D. 1989. An auxin-regulated gene of *Arabidopsis thaliana* encodes a DNA-binding protein. *Plant Physiology* 89: 743–752.
- Bariola PA, Retelska D, Stasiak A, Kammerer RA, Fleming A, Hijri M, Frank S, Farmer EE. 2004. Remorins form a novel family of coiled coil-forming oligomeric and filamentous proteins associated with apical, vascular and embryonic tissues in plants. *Plant Molecular Biology* 55: 579–594.
- Bharadwaj M, Bizzozero OA. 1995. Myelin P0 glycoprotein and a synthetic peptide containing the palmitoylation site are both autoacylated. *Journal of Neurochemistry* 65: 1805–1815.
- Bhat RA, Miklis M, Schmelzer E, Schulze-Lefert P, Panstruga R. 2005. Recruitment and interaction dynamics of plant penetration resistance components in a plasma membrane microdomain. *Proceedings of the National Academy of Sciences, USA* 102: 3135–3140.
- Binder A, Lambert J, Morbitzer R, Popp C, Ott T, Lahaye T, Parniske M. 2014. A modular plasmid assembly kit for multigene expression, gene silencing and silencing rescue in plants. *PLoS ONE* 9: e88218.
- Blaskovic S, Blanc M, van der Goot FG. 2013. What does S-palmitoylation do to membrane proteins? *FEBS Journal* 280: 2766–2774.
- van den Bogaart G, Meyenberg K, Risselada HJ, Amin H, Willig KI, Hubrich BE, Dier M, Hell SW, Grubmüller H, Diederichsen U *et al.* 2011. Membrane protein sequestering by ionic protein–lipid interactions. *Nature* 479: 552–555.
- Boisson-Dernier A, Chabaud M, García F, Becard G, Rosenberg C, Barker DG. 2001. *Agrobacterium rhizogenes*-transformed roots of *Medicago truncatula* for the study of nitrogen-fixing and endomycorrhizal symbiotic associations. *Molecular Plant-Microbe Interactions* 14: 695–700.
- Bradford JR, Westhead DR. 2005. Improved prediction of protein–protein binding sites using a support vector machines approach. *Bioinformatics* 21: 1487–1494.
- Demir F, Horntrich C, Blachutzik JO, Scherzer S, Reinders Y, Kierszniowska S, Schulze WX, Harms GS, Hedrich R, Geiger D *et al.* 2013. Arabidopsis nanodomain-delimited ABA signaling pathway regulates the anion channel SLAH3. *Proceedings of the National Academy of Sciences, USA* 110: 8296–8301.
- Grunewald W, Friml J. 2010. The march of the PINs: developmental plasticity by dynamic polar targeting in plant cells. *EMBO Journal* 29: 2700–2714.
- Haney CH, Long SR. 2010. Plant flotillins are required for infection by nitrogen-fixing bacteria. *Proceedings of the National Academy of Sciences, USA* 107: 478–483.
- Hemsley PA, Kemp AC, Grierson CS. 2005. The TIP GROWTH DEFECTIVE1 S-acyl transferase regulates plant cell growth in Arabidopsis. *Plant Cell* 17: 2554–2563.
- Hemsley PA, Taylor L, Grierson CS. 2008. Assaying protein palmitoylation in plants. *Plant Methods* 4: 2.
- Hemsley PA, Weimar T, Lilley KS, Dupree P, Grierson CS. 2013. A proteomic approach identifies many novel palmitoylated proteins in Arabidopsis. *New Phytologist* 197: 805–814.
- Horn PJ, Korte AR, Neogi PB, Love E, Fuchs J, Strupat K, Borisjuk L, Shulaev V, Lee YJ, Chapman KD. 2012. Spatial mapping of lipids at cellular resolution in embryos of cotton. *Plant Cell* 24: 622–636.
- Jarsch IK, Konrad SSA, Stratil TF, Urbanus SL, Szymanski W, Braun P, Braun KH, Ott T. 2014. Plasma membranes are subcompartmentalized into a plethora of coexisting and diverse microdomains in *Arabidopsis* and *Nicotiana benthamiana*. *Plant Cell* 26: 1698–1711.
- Jarsch IK, Ott T. 2011. Perspectives on remorin proteins, membrane rafts, and their role during plant-microbe interactions. *Molecular Plant-Microbe Interactions* 24: 7–12.
- Kierszniowska S, Seiwert B, Schulze WX. 2009. Definition of Arabidopsis sterol-rich membrane microdomains by differential treatment with methyl-beta-cyclodextrin and quantitative proteomics. *Molecular and Cellular Proteomics* 8: 612–623.
- Kleine-Vehn J, Wabnik K, Martiniere A, Langowski L, Willig K, Naramoto S, Leitner J, Tanaka H, Jakobs S, Robert S *et al.* 2011. Recycling, clustering, and endocytosis jointly maintain PIN auxin carrier polarity at the plasma membrane. *Molecular Systems Biology* 7: 540.
- Kusumi A, Fujiwara TK, Chadda R, Xie M, Tsunoyama TA, Kalay Z, Kasai RS, Suzuki KG. 2012. Dynamic organizing principles of the plasma membrane that regulate signal transduction: commemorating the fortieth anniversary of Singer and Nicolson's fluid-mosaic model. *Annual Review of Cell and Developmental Biology* 28: 215–250.
- Lefebvre B, Timmers T, Mbengue M, Moreau S, Herve C, Toth K, Bittencourt-Silvestre J, Klaus D, Deslandes L, Godiard L *et al.* 2010. A remorin protein interacts with symbiotic receptors and regulates bacterial infection. *Proceedings of the National Academy of Sciences, USA* 107: 2343–2348.
- Li R, Liu P, Wan Y, Chen T, Wang Q, Mettzbach U, Baluska F, Samaj J, Fang X, Lucas WJ *et al.* 2012. A membrane microdomain-associated protein, Arabidopsis Flot1, is involved in a clathrin-independent endocytic pathway and is required for seedling development. *Plant Cell* 24: 2105–2122.
- Li X, Luu DT, Maurel C, Lin J. 2013. Probing plasma membrane dynamics at the single-molecule level. *Trends in Plant Science* 18: 617–624.
- Lingwood D, Simons K. 2010. Lipid rafts as a membrane-organizing principle. *Science* 327: 46–50.
- Malinsky J, Opekarova M, Grossmann G, Tanner W. 2013. Membrane microdomains, rafts, and detergent-resistant membranes in plants and fungi. *Annual Review of Plant Biology* 64: 501–529.
- Marin M, Ott T. 2012. Phosphorylation of intrinsically disordered regions in remorin proteins. *Frontiers in Plant Science* 3: 86.
- Marin M, Thallmair V, Ott T. 2012. The intrinsically disordered N-terminal region of ATREM1.3 remorin protein mediates protein–protein interactions. *Journal of Biological Chemistry* 287: 39982–39991.
- Martin ML, Busconi L. 2000. Membrane localization of a rice calcium-dependent protein kinase (CDPK) is mediated by myristoylation and palmitoylation. *Plant Journal* 24: 429–435.
- Neumann-Giesen C, Falkenbach B, Beicht P, Claasen S, Luers G, Stuermer CA, Herzog V, Tikkanen R. 2004. Membrane and raft association of reggie-1/flotillin-2: role of myristoylation, palmitoylation and oligomerization and induction of filopodia by overexpression. *Biochemical Journal* 378: 509–518.
- Perraki A, Cacas JL, Crowet JM, Lins L, Castroviejo M, German-Retana S, Mongrand S, Raffaele S. 2012. Plasma membrane localization of *Solanum tuberosum* remorin from group 1, homolog 3 is mediated by conformational changes in a novel C-terminal anchor and required for the restriction of *Potato virus X* movement. *Plant Physiology* 160: 624–637.
- Petterson EF, Goddard TD, Huang CC, Couch GS, Greenblatt DM, Meng EC, Ferrin TE. 2004. UCSF Chimera – a visualization system for exploratory research and analysis. *Journal of Computational Chemistry* 25: 1605–1612.
- Raffaele S, Bayer E, Lafarge D, Cluzet S, German Retana S, Boubekeur T, Leborgne-Castel N, Carde JP, Lherminier J, Noirot E *et al.* 2009. Remorin, a *Solanaceae* protein resident in membrane rafts and plasmodesmata, impairs *Potato virus X* movement. *Plant Cell* 21: 1541–1555.

- Raffaele S, Mongrand S, Gamas P, Niebel A, Ott T. 2007. Genome-wide annotation of remorins, a plant-specific protein family: evolutionary and functional perspectives. *Plant Physiology* 145: 593–600.
- Reymond P, Kunz B, Paul-Pletzer K, Grimm R, Eckerskorn C, Farmer EE. 1996. Cloning of a cDNA encoding a plasma membrane-associated, uronide binding phosphoprotein with physical properties similar to viral movement proteins. *Plant Cell* 8: 2265–2276.
- Roche Y, Gerbeau-Pissot P, Buhot B, Thomas D, Bonneau L, Gresti J, Mongrand S, Perrier-Cornet JM, Simon-Plas F. 2008. Depletion of phytosterols from the plant plasma membrane provides evidence for disruption of lipid rafts. *FASEB Journal* 22: 3980–3991.
- Roth AF, Feng Y, Chen L, Davis NG. 2002. The yeast DHHC cysteine-rich domain protein Akr1p is a palmitoyl transferase. *Journal of Cell Biology* 159: 23–28.
- Roy A, Kucukural A, Zhang Y. 2010. I-TASSER: a unified platform for automated protein structure and function prediction. *Nature Protocols* 5: 725–738.
- Sorek N, Poraty L, Sternberg H, Bar E, Lewinsohn E, Yalovsky S. 2007. Activation status-coupled transient S acylation determines membrane partitioning of a plant Rho-related GTPase. *Molecular and Cellular Biology* 27: 2144–2154.
- Sorek N, Segev O, Gutman O, Bar E, Richter S, Poraty L, Hirsch JA, Henis YI, Lewinsohn E, Jurgens G *et al.* 2010. An S-acylation switch of conserved G domain cysteines is required for polarity signaling by ROP GTPases. *Current Biology* 20: 914–920.
- Tóth K, Stratil TF, Madsen EB, Ye J, Popp C, Antolin-Llovera M, Grossmann C, Jensen ON, Schussler A, Parniske M *et al.* 2012. Functional domain analysis of the remorin protein LjSYMREM1 in *Lotus japonicus*. *PLoS ONE* 7: e30817.
- Traverso JA, Micalella C, Martinez A, Brown SC, Satiat-Jeunemaitre B, Meinel T, Giglione C. 2013. Roles of N-terminal fatty acid acylations in membrane compartment partitioning: Arabidopsis h-type thioredoxins as a case study. *Plant Cell* 25: 1056–1077.
- Underwood W, Somerville SC. 2013. Perception of conserved pathogen elicitors at the plasma membrane leads to relocalization of the Arabidopsis PEN3 transporter. *Proceedings of the National Academy of Sciences, USA* 110: 12492–12497.
- Urbanus SL, Ott T. 2012. Plasticity of plasma membrane compartmentalization during plant immune responses. *Frontiers in Plant Science* 3: 181.
- Varma R, Mayor S. 1998. GPI-anchored proteins are organized in submicron domains at the cell surface. *Nature* 394: 798–801.
- Vermeer JE, Thole JM, Goedhart J, Nielsen E, Munnik T, Gadella TW Jr. 2009. Imaging phosphatidylinositol 4-phosphate dynamics in living plant cells. *Plant Journal* 57: 356–372.
- Wessel D, Flugge UI. 1984. A method for the quantitative recovery of protein in dilute solution in the presence of detergents and lipids. *Analytical Biochemistry* 138: 141–143.
- Zappel NF, Panstruga R. 2008. Heterogeneity and lateral compartmentalization of plant plasma membranes. *Current Opinion in Plant Biology* 11: 632–640.
- Zhang Y. 2008. I-TASSER server for protein 3D structure prediction. *BMC Bioinformatics* 9: 40.

Supporting Information

Additional supporting information may be found in the online version of this article.

Fig. S1 Protein interaction scores within the SYMREM1 protein and free YFP in root epidermal cells.

Fig. S2 Analysis of RemCA-mediated PM binding throughout the remorin protein family.

Fig. S3 Western blots of microsomal fractionations of wildtype and mutated SYMREM1 fusion proteins.

Fig. S4 Colocalization studies for different mutant variants.

Fig. S5 Biotin switch assay and quantification.

Fig. S6 Western blot analysis of SYMREM1 constructs expressed in yeast.

Fig. S7 Proposed model for membrane-binding of remorin proteins.

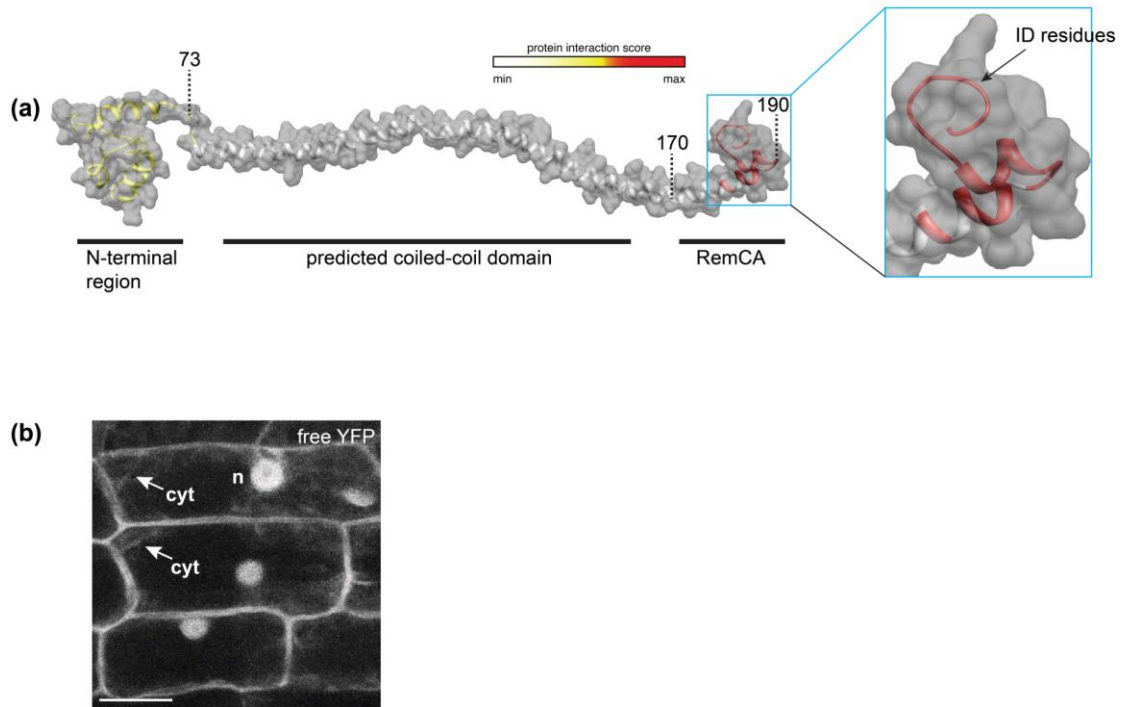
Please note: Wiley Blackwell are not responsible for the content or functionality of any supporting information supplied by the authors. Any queries (other than missing material) should be directed to the *New Phytologist* Central Office.

***New Phytologist* Supporting Information Figs S1–S7**

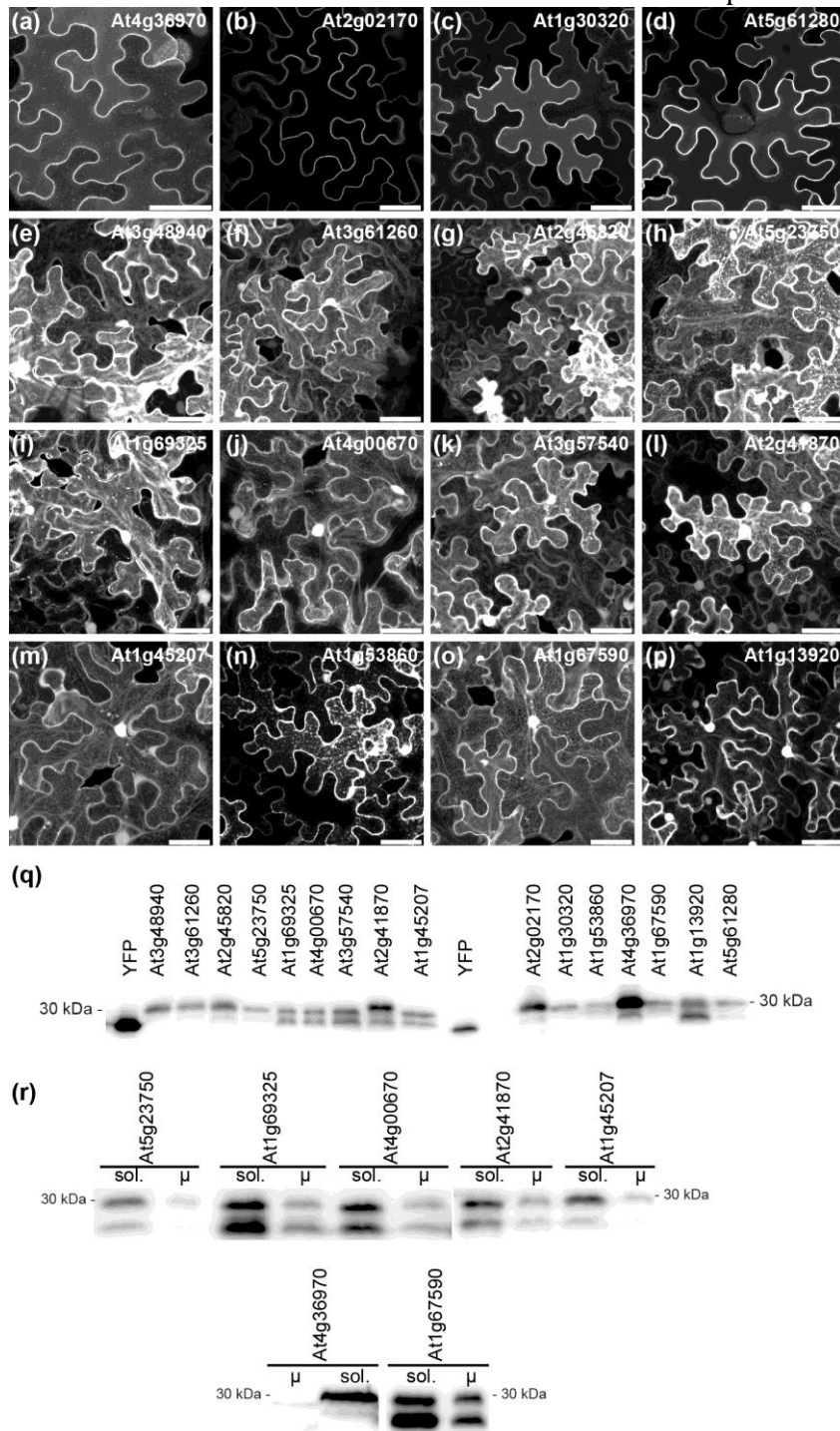
S-acylation anchors Remorin proteins to the plasma membrane but does not primarily determine their localization in membrane micro-domains

Sebastian S. A. Konrad, Claudia Popp, Thomas F. Stratil, Iris K. Jarsch, Veronika Thallmair, Jessica Folgmann, Macarena Marín and Thomas Ott

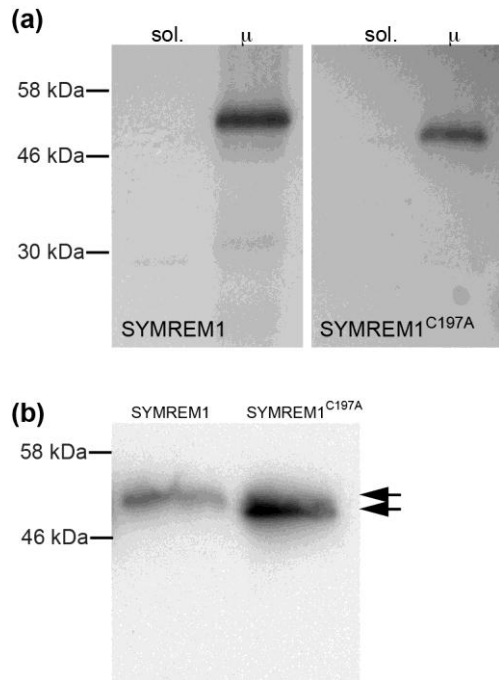
The following Supporting Information is available for this article:



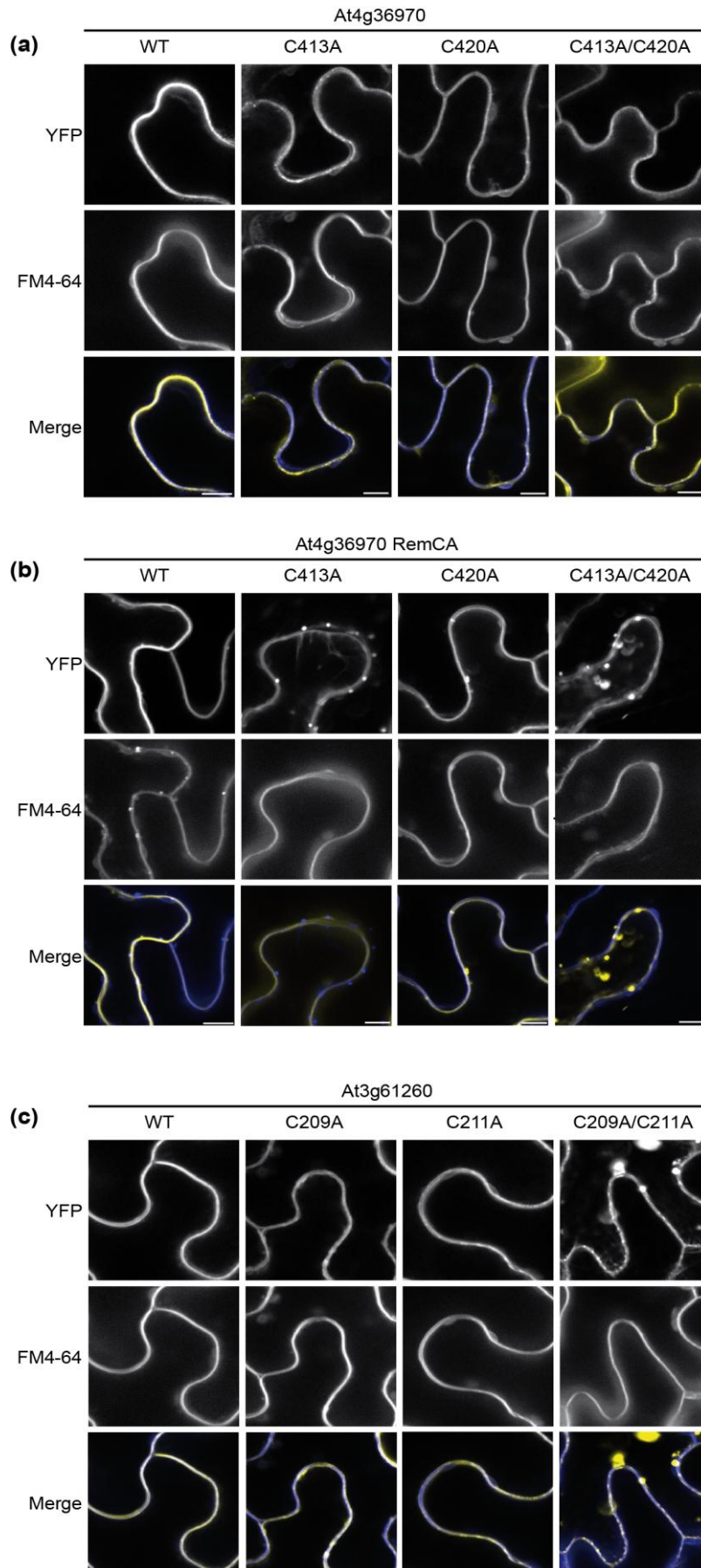
Supporting Information Fig. S1 Protein interaction scores within the SYMREM1 protein and free YFP in root epidermal cells. (a) *Ab initio* modelling of the SYMREM1 protein and colour-coded representation of putative regions that may contribute to protein interactions. Models for the N- and C-terminal regions were constructed independently and fused subsequently. Details can be found in the Materials and Methods section. ID, intrinsically disordered (b) *M. truncatula* root epidermal cell expressing a free YFP protein. The image shows a maximum intensity projection of a z-stack. n, nucleus; cyt, cytoplasmic strands. Bar, 5 μ m.



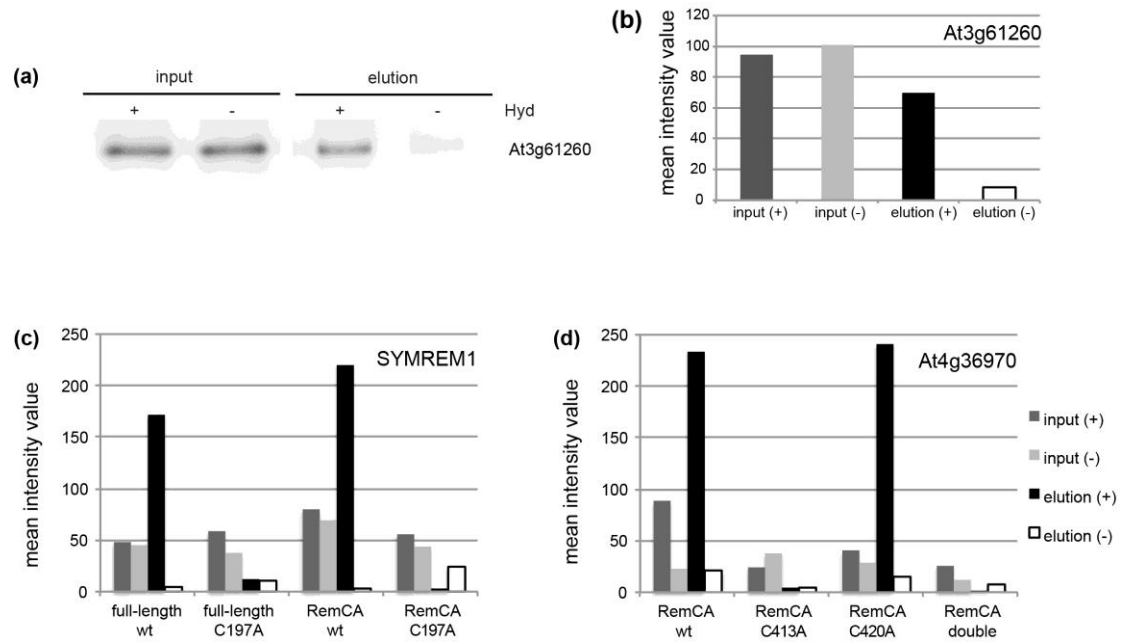
Supporting Information Fig. S2 Analysis of RemCA-mediated PM-binding throughout the Remorin protein family. (a–d) Four out of 16 RemCA peptides were sufficient to target the fluorophore almost exclusively to the plasma membrane of *N. benthamiana* root epidermal cells. (e–p) Representative images of the remaining twelve RemCA peptides show at least partial cytoplasmic and nuclear labelling. Bars, 20 μm. (q) Western Blot on total protein extracts from *N. benthamiana* leaves expressing different RemCA peptides. Double bands indicate partial cleavage of the fusion protein. Samples were compared to free YFP. (r) Microsomal fractionations of total protein extracts were performed to assess partial cleavage of the respective constructs. sol., soluble protein fraction; μ, microsomal fraction.



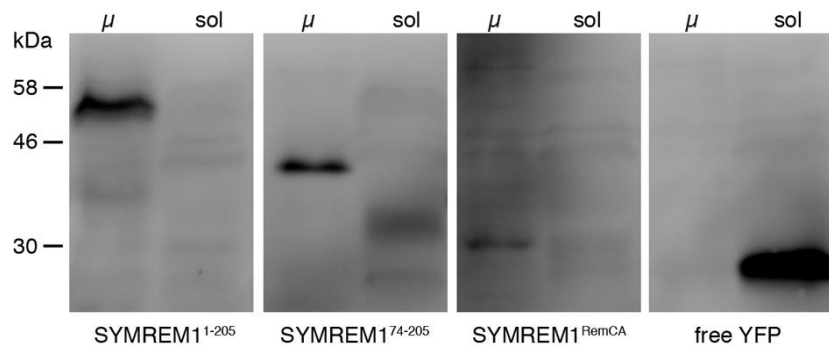
Supporting Information Fig. S3 Western Blots and microsome fractionations of wild-type and mutated SYMREM1 fusion proteins. (a) Microsomal fractions were obtained from *N. benthamiana* leaves expressing YFP-SYMREM1 and YFP-SYMREM1^{C197A} fusion proteins. Both wild-type and the mutant variant were found in the microsomal fraction, indicating that they remained at the plasma membrane. (b) Microsomal fractions of wild-type and mutated SYMREM1 showed a band shift pattern. Western blots were probed with α -GFP antibodies.



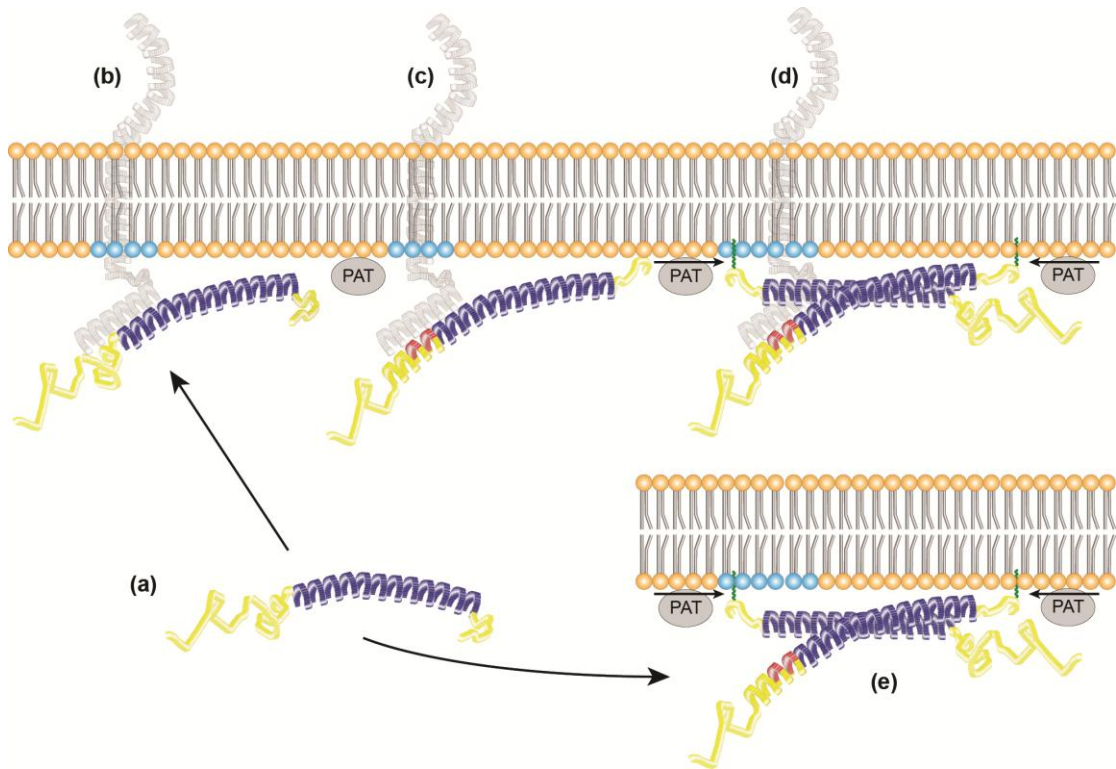
Supporting Information Fig. S4
 Co-localization studies for different mutant variants. YFP-tagged proteins were expressed in *N. benthamiana* leaf epidermal cells and counterstained with FM4-64. All images show maximum projections of z-stacks taken of secant planes. Bars, 5 μ m.



Supporting Information Fig. S5 Biotin switch assay and quantification. (a) Control experiment to prove functionality of the assay. Full-length At3g61260 is S-acylated as previously demonstrated in Hemsely *et al.* (2013). S-acylation of proteins is indicated by the presence of a band in the elution fraction of the hydroxylamine treated samples (+). (b) Quantification of the Western Blot in (a) using ImageJ. (c, d) Quantification of Western Blots shown in Fig. 5. Values were normalized to background levels. double, double mutant.



Supporting Information Fig. S6 Western blot analysis of YFP-SYMREM1 constructs expressed in yeast. Free YFP was expressed as a control for the fractionation procedure. Microsomal fractions were obtained and the corresponding SYMREM1 proteins were detected using a α -GFP antibody. μ , microsomal fraction; sol., soluble proteins.



Supporting Information Fig. S7 Proposed model for membrane-binding of Remorin proteins. Remorins are soluble proteins (a) that are initially immobilized at the PM via interactions with a membrane resident protein (b) or by direct protein-lipid interactions via their C-terminal hydrophobic core (e). (c) Interaction with a protein partner leads to partial disorder-to-order transition of the intrinsically disordered N-terminal region. This may involve protein phosphorylation (red). (d, e) A membrane-localized protein acyl transferase (PAT) S-acylates (green line) C-terminal cysteine residues of Remorins and possibly others throughout the protein. This lipidation tightly binds the protein to the PM and may confer some degree of specificity to sterol-rich sites (blue) in the PM. Oligomerization of Remorins contributes to the formation of larger domain platforms (hypothetical).

1.2. Publication 2

Functional Domain Analysis of the Remorin Protein LjSYMREM1 in *Lotus japonicas*.

Tóth, K., Stratil, T.F., Madsen, E.B., Ye, J., Popp, C. Antolín-Llovera, M.,
Grossmann, C., Jensen, O.N., Schüßler, A., Parniske, M. and Ott, T.

PLoS ONE, 7, e30817

Status: published | Year: 2012 | DOI: 10.1371/journal.pone.003081

Functional Domain Analysis of the Remorin Protein LjSYMREM1 in *Lotus japonicus*

Katalin Tóth^{1,2,9}, Thomas F. Stratil^{1,9}, Esben B. Madsen^{1,3}, Juanying Ye⁴, Claudia Popp¹, Meritxell Antolín-Llovera¹, Christina Grossmann³, Ole N. Jensen⁴, Arthur Schübler¹, Martin Parniske¹, Thomas Ott^{1*}

1 Department of Genetics, University of Munich, Martinsried, Germany, **2** Department of Genetics, Eötvös Loránd University, Budapest, Hungary, **3** Centre for Carbohydrate Recognition and Signalling, Department of Molecular Biology, Aarhus University, Aarhus C, Denmark, **4** Department of Biochemistry and Molecular Biology, University of Southern Denmark, Odense, Denmark

Abstract

In legumes rhizobial infection during root nodule symbiosis (RNS) is controlled by a conserved set of receptor proteins and downstream components. MtSYMREM1, a protein of the Remorin family in *Medicago truncatula*, was shown to interact with at least three receptor-like kinases (RLKs) that are essential for RNS. Remorins are comprised of a conserved C-terminal domain and a variable N-terminal region that defines the six different Remorin groups. While both N- and C-terminal regions of Remorins belonging to the same phylogenetic group are similar to each other throughout the plant kingdom, the N-terminal domains of legume-specific group 2 Remorins show exceptional high degrees of sequence divergence suggesting evolutionary specialization of this protein within this clade. We therefore identified and characterized the MtSYMREM1 ortholog from *Lotus japonicus* (LjSYMREM1), a model legume that forms determinate root nodules. Here, we resolved its spatio-temporal regulation and showed that over-expression of *LjSYMREM1* increases nodulation on transgenic roots. Using a structure-function approach we show that protein interactions including Remorin oligomerization are mainly mediated and stabilized by the Remorin C-terminal region with its coiled-coil domain while the RLK kinase domains transiently interact *in vivo* and phosphorylate a residue in the N-terminal region of the LjSYMREM1 protein *in vitro*. These data provide novel insights into the mechanism of this putative molecular scaffold protein and underline its importance during rhizobial infection.

Citation: Tóth K, Stratil TF, Madsen EB, Ye J, Popp C, et al. (2012) Functional Domain Analysis of the Remorin Protein LjSYMREM1 in *Lotus japonicus*. PLoS ONE 7(1): e30817. doi:10.1371/journal.pone.0030817

Editor: Richard James Morris, John Innes Centre, United Kingdom

Received: August 25, 2011; **Accepted:** December 21, 2011; **Published:** January 23, 2012

Copyright: © 2012 Tóth et al. This is an open-access article distributed under the terms of the Creative Commons Attribution License, which permits unrestricted use, distribution, and reproduction in any medium, provided the original author and source are credited.

Funding: This work is supported by the Deutsche Forschungsgemeinschaft (DFG) (www.dfg.de) in frame of an Emmy-Noether grant (TO, project OT423/2-1) and of the Priority Program SPP1212 PlantMicro (Pa493/5-1; MA-L and MP) of the DFG. Two consecutive research fellowships to KT provided by the Bayerisches Hochschulzentrum für Mittel-, Ost- und Südosteuropa and the German Academic Exchange Service. JY and OJ were supported by a grant from the Danish Research Council "Plant Phosphoproteomics" and CG was funded by the Danish National Research Foundation. The funders had no role in study design, data collection and analysis, decision to publish, or preparation of the manuscript.

Competing Interests: The authors have declared that no competing interests exist.

* E-mail: Thomas.Ott@biologie.uni-muenchen.de

⁹ These authors contributed equally to this work.

Introduction

Root nodule symbiosis (RNS) in legumes requires a complex molecular dialogue between the plant host and bacteria belonging to the *Rhizobiaceae* family. Upon perception of different flavonoid compounds released by the plant under nitrogen starvation, rhizobia secrete strain-specific lipochitooligosaccharide signaling molecules, called nod factors (NF), which are recognized by at least two receptor-like kinases (RLKs). In *L. japonicus* two LysM-type Nod Factor receptors NFR1 and NFR5 confer NF recognition specificity [1,2,3]. They trigger downstream physiological and morphological processes such as calcium-spiking, root-hair curling and activation of gene expression [4,5]. In *Medicago truncatula* NFP and LYK3 have been described to serve these functions [6,7,8]. However, the fact that initial responses to NFs can be observed in an *hcl1/bk3* mutant indicates the presence of another LysM RLK to be involved in NF perception. A closely related LYK4 protein has been proposed to be a likely candidate for a NF receptor component [8]. Phenotypical analysis of *M. truncatula* plants, where

the NF receptors have been post-transcriptionally silenced by RNA interference (RNAi), and spatial analysis of receptor gene expression support the hypothesis, that these proteins are not only required for initial recognition of NFs prior to bacterial invasion but for the entire intracellular infection process. This was also suggested for the leucine-rich repeat RLK DMI2 from *M. truncatula* [9,10]. While DMI2 and its homolog in *L. japonicus* SYMRK [11] have been originally isolated based on their infection phenotypes, recent genetic data suggest that SYMRK is rather required for nodule organogenesis and activation of a calcium-calmodulin dependent protein kinase (CCaMK) [12], a protein that decodes NF induced calcium-spiking.

Upon perception of NFs the root hair curls around rhizobia and entraps them in a micro-colony. Infection occurs via formation of infection threads (ITs), invaginations of the plant plasma membrane (PM) that surround rhizobia throughout the entire symbiotic interaction [13,14]. While the IT progresses intracellularly towards the root cortex, cell divisions occur directly below the IT in outer cortical cells. They branch within the developing

nodule primordium and finally release rhizobia into symbiosomes. These are spatially defined by the PM encapsulating the bacteria (the symbiosome membrane) and contain differentiated bacteroids, the nitrogen-fixing state of rhizobia.

We have recently shown that a Remorin protein from *M. truncatula* (MtSYMREM1) is able to interact with the putative NF receptors NFP and LYK3 as well as with DMI2. MtSYMREM1 localizes to infection threads within the nodular infection zone and symbiosomes membranes and is required for bacterial infection [15]. Remorins are plant-specific proteins that comprise a gene family with 16 members in *Arabidopsis thaliana* while only 10 genes have so far been identified in *M. truncatula* [16]. Members of all Remorin groups can be found in all higher plants, except group 2 Remorins, which are only present in legumes and poplar. This subgroup is comprised of two members. While MtSYMREM1 has so far only been described to be activated in response to rhizobia [15], the second gene is transcriptionally induced during arbuscular mycorrhiza symbiosis [17]. Furthermore recent data indicate that remorins belonging to the group 1 are function during plant-viral [18] and plant-microbe interactions [19]. While the exact mechanisms remain to be understood, the structural composition of Remorins with their highly conserved C-terminal region that harbors a coiled-coil domain and a set of conserved positively charged and aliphatic amino acid residues suggest

similar core functions. In contrast, the N-terminal region is highly variable or absent in between the different Remorin groups [16] indicating functional specification.

Results

Evolutional divergence of *L. japonicus* LjSYMREM1

Legumes develop two main types of nodules. *Medicago truncatula* develops indeterminate nodules that have persistent meristem activity and are continuously infected. Other legumes such as *Lotus japonicus* develop determinate nodules that lose the ability to get infected and thus have a defined lifespan. Based on expression profiles [20,21] we identified a *REMORIN* gene in *L. japonicus* that was significantly induced during nodulation, a feature that was also described for *MtSYMREM1* in *M. truncatula* [15]. The *LjSYMREM1* gene (chr4.CM0004.60.r2.d; <http://www.kazusa.or.jp/lotus/>) is comprised of 5 exons and 4 introns. Sequencing the genomic fragment of the putative *Medicago* ortholog *MtSYMREM1*, revealed a gene structure similar to *LjSYMREM1* (Figure 1A). Errors in the publicly available annotation of *MtSYMREM1* (Medtr8g098650.1; <http://www.medicago.hapmap.org/>) led to a previously reported incomplete annotation [15]. Thus the *MtSYMREM1* genomic sequence has been submitted to GenBank (Accession number JQ061257). Phylogenetic analysis

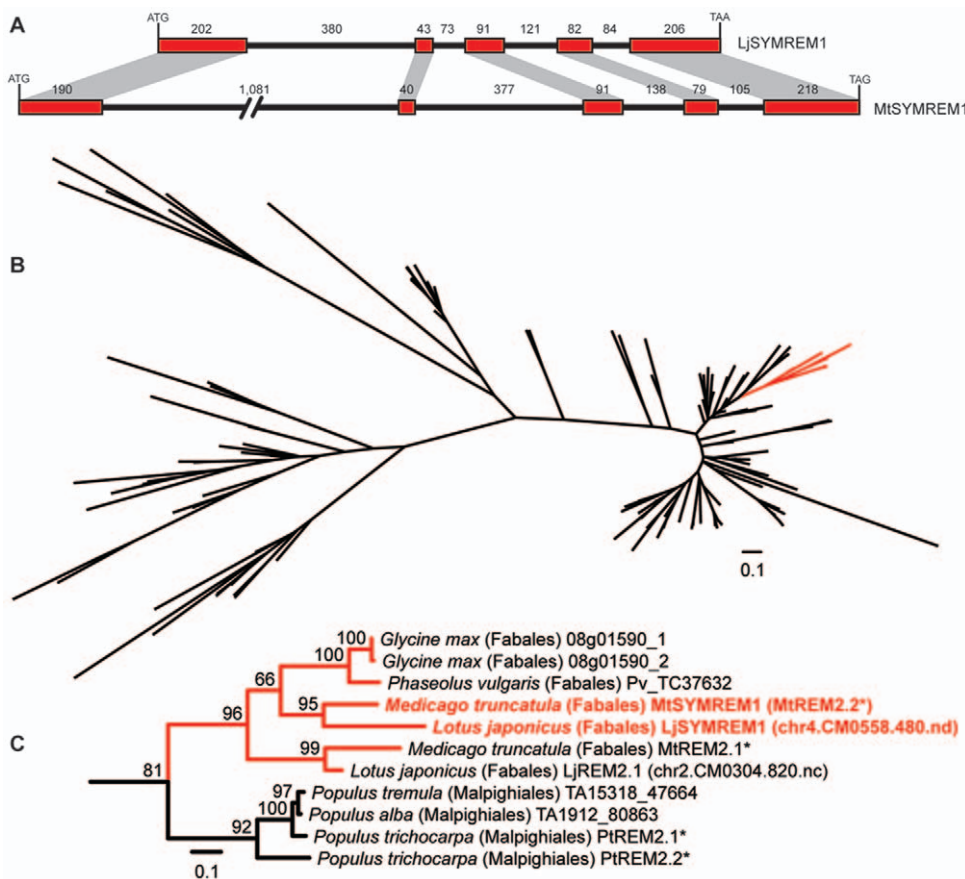


Figure 1. Identification and analysis of orthologous SYMREM1 genes and proteins. The *LjSYMREM1* sequence is similar to the previously published one of *MtSYMREM1*. Both genes show the same exon-intron structure even though the *MtSYMREM1* gene is comprised of longer introns (A). Phylogenetic analysis based on 147 amino acid Remorin sequences using 101 unambiguously aligned residues in the conserved C-terminal region identifies the group 2 (B). Amino acid sequences of 11 group 2 Remorins from legumes and poplar were aligned and analyzed in 172 positions (C). *MtSYMREM1* and *LjSYMREM1* clearly cluster indicating that these proteins are orthologous to each other. Names marked with an asterisk were introduced in [16].

doi:10.1371/journal.pone.0030817.g001

revealed that *LjSYMREM1* and *MtSYMREM1* are closely related and directly evolved from a common ancestral gene, by speciation (Figure 1B–1C). They thus are orthologous genes.

Surprisingly, both proteins only share an overall similarity 67.1% (Table S1A) resulting from only 38.3% similarity in the N-terminal region while the C-terminal part of the protein is rather similar to *MtSYMREM1* (85.3% similarity). Such low conservation was also found when comparing the N-terminal region of *MtSYMREM1* with those of the closest homologs in soybean, poplar, common bean and grape wine (38.7% similarity) (Table S1A). This sequence divergence between the N-terminal regions of the SYMREM1 proteins of *Medicago* and *Lotus* is in sharp contrast to scores found for the symbiotic receptor-like kinases NFP/NFR5 and DMI2/SYMRK, the so-called ‘common symbiosis’ proteins DMI1/POLLUX, DMI3/CCAMK, IPD3/CYCLOPS, the putative transcription factors NSP2 and NIN and the late nodulin leghemoglobin 1 where the average sequence similarity is 81.9% with NIN only showing 67.5% similarity between the two legumes (Table S1B). This high sequence divergence of *Medicago* and *Lotus* SYMREM1 proteins that suggests high evolutionary pressure on the N-terminal region prompted us to functionally characterize the *Lotus* LjSYMREM1 protein, to analyze the contributions of the individual domains to SYMREM1 localization, function and to the interaction with the symbiotic RLKs NFR1, NFR5 and SYMRK.

Overexpression of *LjSYMREM1* increases nodulation

To show the importance of LjSYMREM1 genetically, we intensively screened the *L. japonicus* mutant population at RevGen, Norwich, UK (<http://www.lotusjaponicus.org/tillingpages/homepage.htm>) by a Targeted Induced Local Lesion in Genomes (TILLING) approach. Unfortunately, no potential homozygous knock-out mutant could be obtained while 15 non-allelic mutations that were identified with six being located in non-coding regions, four missense mutations, three silent mutations and one being located at the splice site did not show any phenotypical differences (data not shown). Thus we generated a LjSYMREM1:mOrange fusion construct that was driven by the *Lotus* poly-ubiquitin promoter (pUbi) [23] to assess the nodulation phenotype upon overexpression of *LjSYMREM1*. Transgenic roots expressing this construct were generated and inoculated for 28 days with *Mesorhizobium loti* (MAFF DsRed). Roots over-expressing *LjSYMREM1* developed significantly more mature nodules (24.6%; $p < 0.01$) without any macroscopical alterations (Figure 2A) compared to the empty vector control while both genotypes exhibited similar numbers of immature nodules (bumps). However, transgenic roots overexpressing LjSYMREM1:mOrange did not show more infection threads at 28 dpi (neither mature nor aborted infection threads; data not shown).

To confirm overexpression of the construct we isolated proteins from transgenic roots expressing the *pUbi:LjSYMREM1:mOrange* construct and showed presence of the fusion protein at different time points (Figure 2B, left panel). In contrast LjSYMREM1:YFP protein expressed in stable transgenic lines under control of the native promoter (described below) could only be detected in roots 15 days after inoculation with *M. loti* (Figure 2B, right panel). Expression of the transgene was also verified by microscopy prior to phenotypical analysis where patterns as described later in the text were observed. However, natively expressed LjSYMREM1 protein was never detected microscopically in root cells (see below).

Spatial expression of the *LjSYMREM1* gene

Next we assessed spatio-temporal expression of *LjSYMREM1* since such data have not been provided for any SYMREM1 gene.

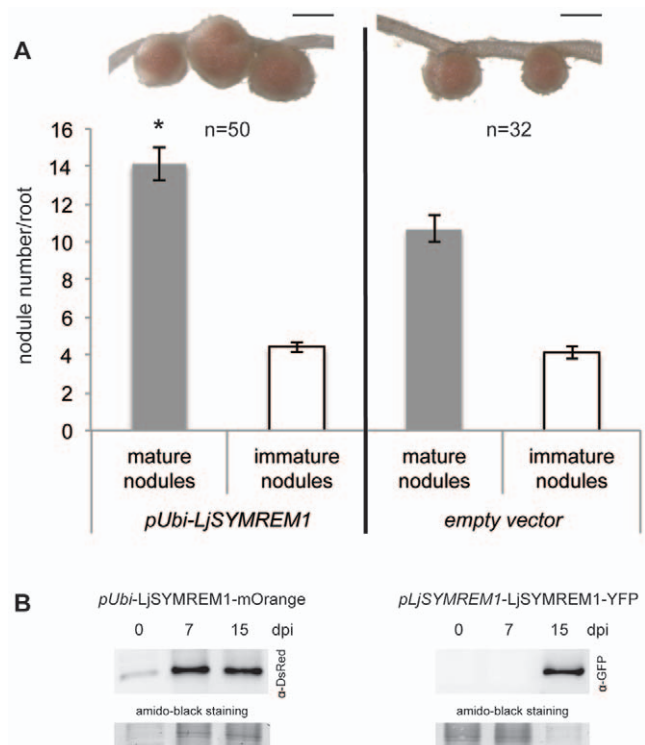


Figure 2. Overexpression of *LjSYMREM1* leads to increased nodule numbers. LjSYMREM1 was overexpressed as a mOrange fusion protein in transgenic *L. japonicus* roots (A). Nodule number and morphology was assessed 28 dpi with *M. loti* (MAFF303099-DsRed). Nodules were grouped into mature/pink and immature/white nodules and counted. Nodule morphology was not altered as indicated by the representative inlets above. Scale bars indicate 500 μ m. Error bars represent standard errors and significance levels that were determined by student's t-test are indicated by an asterisk ($p < 0.01$). Western Blot analysis to determine expression levels of *LjSYMREM1* in transgenic roots (B). Proteins from transgenic roots of chimeric plants expressing a *pUbi:LjSYMREM1:mOrange* construct (left) and stable transgenic plants expressing a *pLjSYMREM1:LjSYMREM1:YFP* construct (right) were transferred to a PVDF membrane and probed with the respective antibodies. Amounts of proteins loaded transferred the membrane is indicated by Amido black staining.
doi:10.1371/journal.pone.0030817.g002

Thus we cloned a 975 bp fragment of the putative *LjSYMREM1* promoter (*pLjSYMREM1*) and generated transcriptional fusions to the β -glucuronidase (*GUS*) gene. The *pLjSYMREM1:GUS* reporter construct was transformed into *L. japonicus* roots using *Agrobacterium rhizogenes* mediated gene transfer. No *GUS* staining was observed in uninoculated transgenic roots after five hours of staining (Figure 3A). However, some weak staining of vascular tissue and root tips was occasionally observed after extended staining time, but this was also observed in roots transformed with the empty *GUS*-vector and was thus regarded as background staining (data not shown). To test promoter activation upon application of isolated NFs we applied 10^{-8} M isolated *Mesorhizobium loti* NFs as a droplet in the root hair elongation zone above the root tip to these transformed roots. This zone was previously described to be most susceptible to rhizobial infections [22]. *GUS*-activity was observed 24 hours post inoculation (hpi) in epidermal and cortical cells in the area where NFs were applied confirming inducibility of the *LjSYMREM1* gene by these bacterial signaling molecules (Figure 3B; S1A). Next we tested promoter activation during symbiotic interaction in transgenic roots carrying the *pLjSYMREM1:GUS* construct. Plants were inoculated with *M. loti* (expressing a

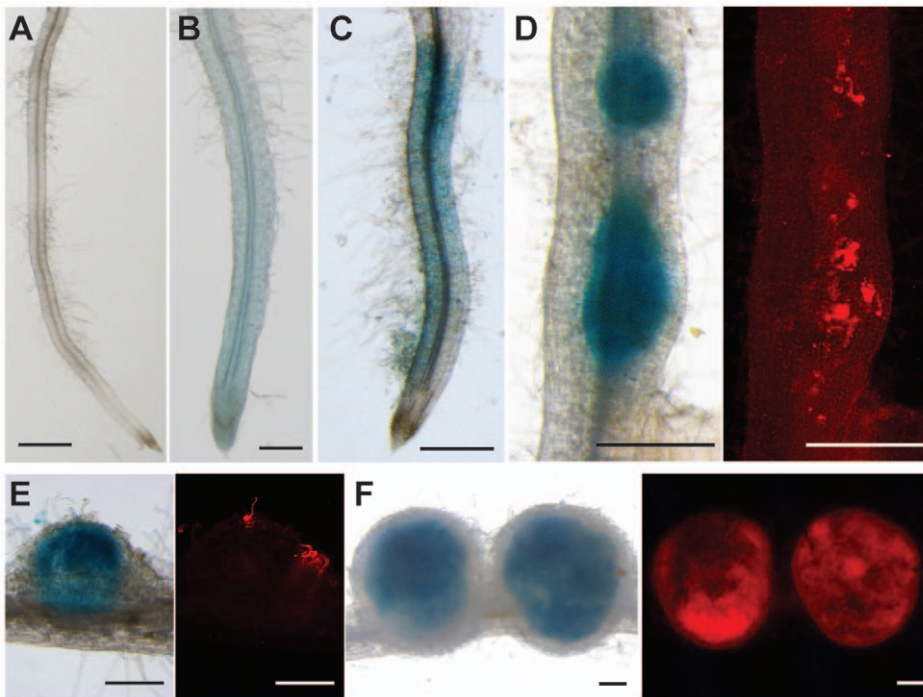


Figure 3. Analysis of *LjSYMREM1* promoter activity during rhizobial infection. Uninoculated transgenic roots transformed with the promoter:GUS construct (A). Application of 10^{-8} M purified Nod Factors for 24 hours induced promoter activity in the root infection zone (1–5 cm above the root tip) (B). Root 48 hours after inoculation with DsRed expressing *M. loti* MAFF303099 (no infections) (C). Root segment with nodule primordia at 4dpi (D). Red fluorescence deriving from the bacteria shows their presence at the root surface. Young nodule at 6dpi with bacteria infecting the cortex (E). Mature nodules at 21dpi that are entirely infected by rhizobia (F). Bars indicate 500 μ m. doi:10.1371/journal.pone.0030817.g003

fluorescent DsRed marker) by application of rhizobia to the whole root system and stained for GUS-activity 2, 4, 6 and 21 days post inoculation (dpi). As shown after NF application *LjSYMREM1* promoter activity was observed in a distinct zone above the root tip at 2 dpi (Figure 3C). Roots that had been inoculated for four days showed strong β -glucuronidase-activity that localized specifically around nodule primordia with progressing bacterial infection, while the epidermal staining, that was observed at pre-infection stages, was entirely diminished in these roots (Figure 3D). From 4 dpi onwards GUS-staining coincided with the presence of bacteria. In developing and mature nodules GUS-activity was detected in infected cells in the central zone of the nodule hosting nitrogen-fixing bacteroids but not in outer cortical cells (Figure 3E–3F). This was confirmed by sectioning these nodules prior to GUS staining. There, *LjSYMREM1* promoter activity was clearly found in inner nodule parenchyma cells that were not infected, as well as in infected cells (Figure S1B).

Localization of *LjSYMREM1* in legume nodules

To study localization of the native *LjSYMREM1* protein, we generated a construct where the promoter together with the intron-containing version of *LjSYMREM1* that was amplified from genomic DNA was cloned and fused to the yellow fluorescent protein (YFP; g*LjSYMREM1*:YFP). Using *A. tumefaciens* mediated gene transfer we created stable transgenic lines in the *L. japonicus* ecotype MG-20 background. In T2 plants, we could not detect distinguishable YFP fluorescence in NF-treated roots due to high levels of intrinsic auto-fluorescence. However, a clear and specific YFP signal was detected in infected cells of mature nodules at 21 dpi (Figure 4A–4H). In comparison no YFP signal was detected in untransformed control nodules of MG-20 wild-type plants (21dpi) (Figure 4I–4L). In

transgenic nodules the g*LjSYMREM1*:YFP fluorescence co-localized with the DsRed signal derived from *M. loti* expressing this fluorophore (Figure 4D,4G,4H and Figure S2A) suggesting localization of the protein on symbiosome membranes surrounding bacteroids in infected cells. A more detailed view on nodular infection threads also showed presence of *LjSYMREM1* on these infection structures (Figure S2B). These data are in agreement with localizations reported for MtSYMREM1 that was detected by immuno-localization experiments on nodular ITs in the infection zone and on symbiosome membranes of indeterminate *Medicago* nodules [15].

The C-terminal domain of *LjSYMREM1* is mediating PM localization

The *LjSYMREM1* protein is comprised of two main parts, the conserved C-terminal region with a strong prediction for a coiled-coil domain (COILS probability >90%) and the variable N-terminal region. While the C-terminal region (amino acids 79–207; *LjSYMREM1*_C) has a predicted globular structure (GlobDoms by Russell/Linding definition), almost only random coils and unfolded structures are predicted for the N-terminal part (amino acids 1–78; *LjSYMREM1*_N). Next we identified the domain responsible for PM localization. *LjSYMREM1*_N and *LjSYMREM1*_C regions were individually fused to the mOrange fluorophore and expressed under control of the *Lotus* polyubiquitin promoter in *L. japonicus* hairy roots (Figure 5A–5C). As expected the full-length *LjSYMREM1* protein localized to the periphery of root epidermal cells (Figure 5A) indicating membrane association of the protein. This localization was also detected when expressing *LjSYMREM1*_C (Figure 5B) while *LjSYMREM1*_N localized to the cytosol and the nucleus (Figure 5C) indicating that the PM binding motif is located in the C-terminal region of the protein. However,

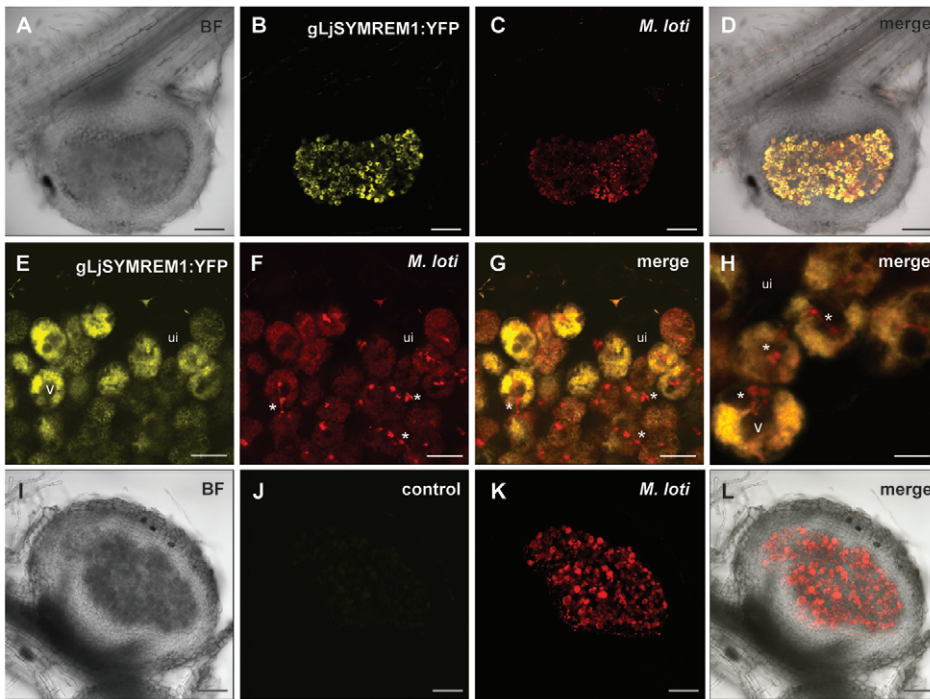


Figure 4. Stable transgenic *Lotus japonicus* plant expressing gLjSYMREM1:YFP. A genomic construct consisting of the *LjSYMREM1* native promoter ($p_{LjSYMREM1}$) and the *LjSYMREM1* gene was fused to YFP (gLjSYMREM1:YFP). Roots were inoculated with *M. loti* MAFF303099-DsRed and three week old nodules of stable transgenic T2 plants were analyzed as 150 μ m thick sections. Nodule of a transgenic *Lotus* plant shows strong YFP-fluorescence in infected cells that co-localizes with *M. loti* (A–D). Close-ups of infected (yellow) and uninfected (ui; no fluorescence) cells at the periphery of the nodule cortex (E–H). Vacuoles (V) are visible in the center of infected cells. Remnant trans-cellular infection threads lacking gLjSYMREM1:YFP protein are marked with an asterisk. Cross-section of an untransformed control nodule shows no fluorescence (I–L). Bars indicate 100 μ m (A–D, I–L), 20 μ m (E–G) and 10 μ m (H). BF = bright-field.
doi:10.1371/journal.pone.0030817.g004

nuclear localization of the LjSYMREM1_N:mOrange construct was not expected, but due to the small size and the unordered structure of the N-terminal region, the fusion may not interfere with the nuclear import of free fluorophores.

LjSYMREM1 oligomerizes and interacts with symbiotic RLKs

To understand the roles of the domains we tested interactions between individual LjSYMREM1 domains and other proteins. Since the *in planta* approaches currently require expression of the proteins in a heterologous system such as *N. benthamiana* leaves we first tested whether localizations of these constructs follows those observed in *Lotus* roots. Indeed the full-length protein as well as LjSYMREM1_C localized to the PM (Figure 5D–E) as it was also shown for NFR1 (Figure 5F). In contrast, LjSYMREM1_N was detected in the cytosol (Figure 5G). Co-localization of LjSYMREM1_N with free Cerulean fluorophore protein in *N. benthamiana* leaves confirmed cytosolic localization (Figure 5H–5I).

As a proof of concept we then tested for possible interactions between the LjSYMREM1 protein and the symbiotic RLKs NFR5, NFR1 and SYMRK from *L. japonicus* using Bimolecular Fluorescence Complementation (BiFC) (Figure 6A–6I) and the yeast split-ubiquitin system (SUS) (Figure 6J) to assess if LjSYMREM1 exhibits the same interaction patterns as its homolog MtSYMREM1.

For BiFC (also termed split-YFP), we individually fused the proteins to the N- (Y_N) and C-terminal (Y_C) halves of YFP and expressed different combinations in leaves of *N. benthamiana* for two days. Interaction between proteins should result in re-assembly of the functional YFP protein and thus in fluorescence at the sites of

interaction. Co-expression of LjSYMREM1:Y_C and LjSYMREM1:Y_N resulted in strong fluorescence in epidermal cells indicating interaction of the proteins (Figure 6A). This is in agreement with the previously reported homo-oligomerization when expressing Y_C:MtSYMREM1 and Y_N:MtSYMREM1 together in *N. benthamiana* leaves [15]. When both proteins were C-terminally fused to the individual halves of YFP hetero-oligomerization was also observed between LjSYMREM1 and MtSYMREM1 (Figure 6B). In contrast co-expression of LjSYMREM1:Y_C and Y_N:MtSYMREM1 did not show fluorescence (Figure 6C) presumably since both halves of the YFP protein were physically separated by changing the fusion direction. Thus they served as negative controls. Due to cleavage of the fluorescent tag of a YFP:LjSYMREM1 construct *in planta* (data not shown), reciprocal experiments could not be performed. Next, we fused the *Lotus* RLKs NFR5, NFR1 and SYMRK to the N-terminal half of the YFP protein and co-expressed them together with LjSYMREM1:Y_C. Interaction between LjSYMREM1 and the RLK proteins was detected in all three cases (Figure 6D–6F). Fluorescence localized to the periphery of the cells indicating PM resident interactions of the proteins. However, expression frequently led to formation of PM associated foci (inlet Figure 6E). Interestingly, no fluorescent signal was detected when these RLKs were co-expressed with the Y_C:MtSYMREM1 construct (Figure 6G–6I).

To verify the RLK interaction data we used the yeast split-ubiquitin system. Similar to the principle of BiFC the ubiquitin protein was split in two halves. Upon protein interaction re-assembly of the full ubiquitin molecule occurs. The assembled ubiquitin serves as a recognition site for proteolytic cleavage that results in the release of the LexA transcriptional activator that is fused to a VP16 DNA binding domain that are coupled to the C-

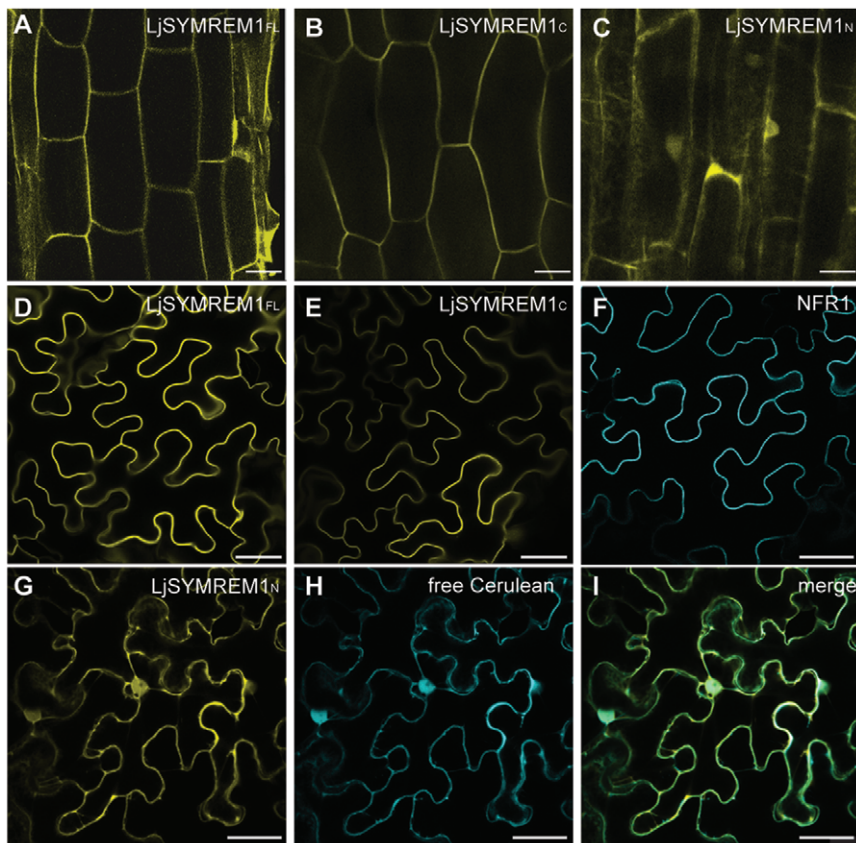


Figure 5. Expression of LjSYMREM1 variants in *L. japonicus* roots and *N. benthamiana* leaves. Clones derived from cDNA of LjSYMREM1 were C-terminally tagged with the mOrange fluorophore and expressed under control of the *Lotus* polyubiquitin promoter in transgenic *L. japonicus* roots (A–C) and as a CaMV-35S promoter-driven construct in leaf epidermal cells of *N. benthamiana* (D,E,G). The full-length (FL) protein and the C-terminal region of LjSYMREM1 (LjSYMREM1_C) are associated to the PM while the N-terminal region (LjSYMREM1_N) is cytosolic indicated by visible cytoplasmic strands. In addition NFR1: Cerulean (F) and free Cerulean (H) were expressed in *N. benthamiana* leaves resulting in PM and cytosolic localization, respectively. Bars indicate 200 μm (A–C) and 50 μm (D–I). doi:10.1371/journal.pone.0030817.g005

terminal half (Cub). Diffusion of this construct into the nucleus leads to activation of a HIS3-reporter enabling the yeast to complement its histidine auxotrophy and thus growth on medium lacking histidine. For these assays we generated Cub:LjSYMREM1 fusions while the C-termini of the RLKs were fused to the mutated N-terminal part of ubiquitin (NubG) that is unable to auto-interact with Cub. As negative control we co-expressed the yeast resident ER protein Alg5 as a Cub construct together with the RLKs while Alg5:NubG was used as control to test auto-activation of the reporter system by Cub:LjSYMREM1. Yeast was grown on medium depleted in leucine and tryptophan (–LW) to select for the presence of both plasmids. To select for positive protein interactions these colonies were stamped onto –LWH medium that was additionally depleted in histidine and supplemented by 15 mM 3-amino-1,2,4-triazole (3-AT) to suppress residual levels of endogenous histidine biosynthesis. Yeast growth was sustained when Cub:LjSYMREM1 was co-expressed with the *Lotus* RLKs indicating an interaction between these proteins while no growth was observed when these proteins were co-expressed with the negative controls Alg5:NubG and Alg5:Cub (Figure 6J).

The C-terminal LjSYMREM1 domain is required for oligomerization and receptor interactions

To assess the individual contributions of both protein regions for Remorin oligomerization LjSYMREM1 (full-length), LjSYM-

REM1_C and LjSYMREM1_N were tested on a one-to-one basis. Cytoplasmic localization of LjSYMREM1_N (Figure 5C, 5G) only allowed the use of the NubG fusion because the split-ubiquitin assay requires the bait construct (Cub) to be anchored to the plasma membrane, in order to avoid auto-activation of the reporter gene. Co-expression of the LjSYMREM1_C construct with full-length LjSYMREM1 resulted in yeast growth under selective conditions indicating that oligomerization of the LjSYMREM1 protein occurs along the C-terminal region of the protein (Figure 7A). Co-transformation of LjSYMREM1_N with either LjSYMREM1_C or full-length LjSYMREM1 resulted in slight yeast growth on selective conditions to the same extent as observed in the negative controls (Figure 7B). Thus the N-terminal region has no major contribution on LjSYMREM1 oligomerization.

To test domain-specific interactions with the RLKs we co-expressed the different LjSYMREM1 constructs together with the *Lotus* RLKs NFR1, NFR5 and SYMRK. Co-transformation of the LjSYMREM1_C construct with the individual RLKs resulted in yeast growth under triple selective conditions indicating a strong interaction (Figure 7A). Since co-expression of the negative control Alg5:NubG resulted in almost no yeast growth it can be concluded that the observed interactions specifically result from the RLK-LjSYMREM1 interaction. In contrast, no interaction was found when these RLKs were co-transformed with LjSYMREM1_N (Figure 7B). However, yeast grew on –LWH plates after co-

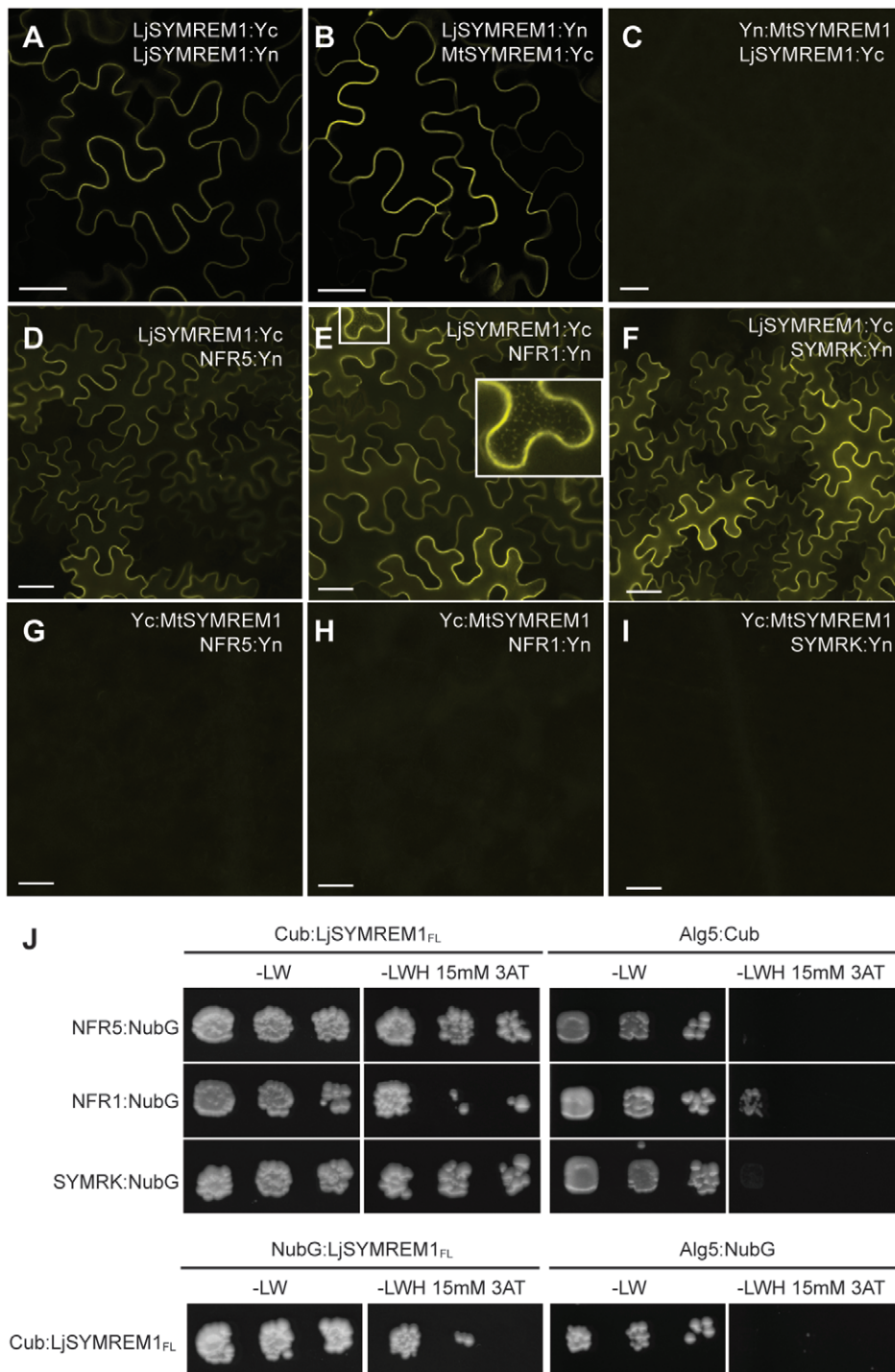


Figure 6. Interactions between LjSYMREM1 and symbiotic RLKs. Bimolecular complementation (BiFC) experiments show that LjSYMREM1 is able to interact with itself and MtSYMREM1 as indicated by the presence of YFP fluorescence (A,B). However, no signal was observed when the MtSYMREM1 protein was N-terminally fused to one half of the YFP protein (C). This demonstrates that overexpression alone is not sufficient to re-assemble the YFP protein. LjSYMREM1 is also able to interact with the three RLKs NFR5, NFR1 and SYMRK (D–F). Bars indicate 40 μ m. Occasionally fluorescent foci were observed (E, inset). The yeast split-ubiquitin assay was used to test interactions between full-length LjSYMREM1 itself and the RLKs NFR1, NFR5 and SYMRK (J). The coding regions were fused to the C-terminal half (Cub) and the N-terminal half (NubG) of ubiquitin and interaction was tested on an individual basis. Yeast growth on medium lacking leucine and tryptophan (–LW) shows the presence of both constructs. Interaction was tested on medium additionally lacking histidine (–LWH) that was supplemented with 15 mM 3-amino-1,2,4-triazole (3-AT) to suppress residual levels of endogenous histidine biosynthesis. The yeast resident ER protein Alg5 was used as negative control (Alg5:NubG and Alg5:Cub) (J).

doi:10.1371/journal.pone.0030817.g006

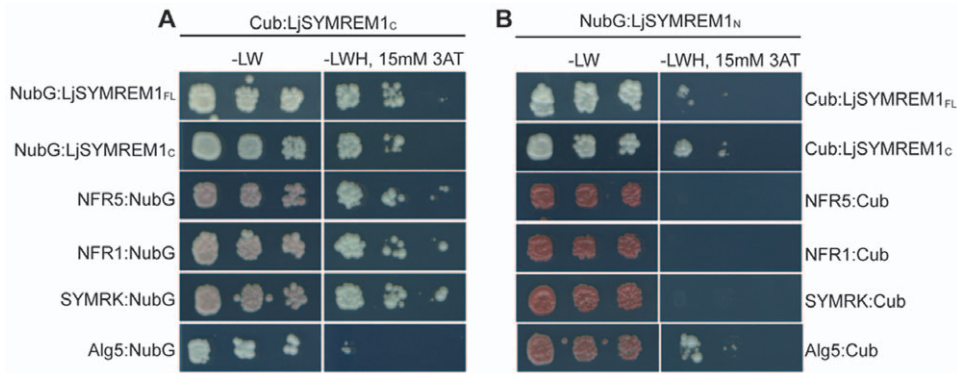


Figure 7. The C-terminal domain of the LjSYMREM1 protein mainly contributed to protein interactions. The yeast split-ubiquitin assay was used to test interactions between the LjSYMREM1 variants and the RLKs NFR1, NFR5 and SYMRK. The coding regions were fused to the C-terminal half (Cub) and the N-terminal half (NubG) of ubiquitin and interaction was tested on an individual basis. Yeast growth on medium lacking leucine and tryptophan (–LW) indicates presence of both constructs. Interaction was tested on medium additionally lacking histidine (–LWH) that was supplemented with 15 mM 3-amino-1,2,4-triazole (3-AT) to suppress residual levels of endogenous histidine biosynthesis. The yeast resident ER protein Alg5 was used as negative control (Alg5:NubG and Alg5:Cub). Yeast growth was sustained on –LWH medium indicating strong interaction of the RLKs and Remorins variants with LjSYMREM1_C (A). Weak interaction of LjSYMREM1_N with the RLKs and Remorins variants indicates minor or transient contribution of the N-terminal region to protein interactions (B). Pigmentation of yeast indicates severe adenine deficiency as a consequence of lacking interaction. A series of three dilutions (non-diluted, 10⁻¹ and 10⁻²) are shown in each panel from left to right). doi:10.1371/journal.pone.0030817.g007

transformation of the RLKs with the positive control Alg5:NubG proving expression of the fusion proteins (Figure S3).

Since both yeast split-ubiquitin and BiFC assays are mostly suitable to qualitatively detect stable protein-interactions we performed fluorescence lifetime imaging microscopy (FLIM) to characterize and quantify interaction by Foerster resonance energy transfer (FRET). We used a Cerulean-mOrange FRET pair, where one protein is fused to the donor fluorophore (Cerulean) while the second protein is fused to mOrange which functions as energy acceptor [24]. FRET occurs when both fluorophores are brought into physical proximity (<10 nm) by interaction of the target proteins. In brief, when measuring FRET by FLIM (FLIM-FRET), the average time electrons of the donor molecule (after photon absorption) stay in the excited state is determined by measuring the exponential ‘decay’ rate by time-resolved measurement of the emitted photons. This is then transformed into ‘fluorescence lifetime’ values. Upon occurrence of FRET, the Cerulean fluorescence lifetime becomes shorter (the ‘decay’ is faster) because the excited donor-electrons drop to the ground state faster, due to the direct energy transfer to the acceptor (mOrange).

For this approach we used the mOrange fusions with LjSYMREM1, LjSYMREM1_C and LjSYMREM1_N while NFR1, which was taken as a representative RLK, was fused to the Cerulean protein. *N. benthamiana* leaves were co-infiltrated three times independently with *A. tumefaciens* carrying the respective fusion constructs. FLIM-FRET data recording was performed two days post infiltration. For every tested combination (see Table S2), 6–13 lifetime images were collected per tobacco leaf (n = 3–5). To determine the Cerulean lifetime under non-interacting conditions we expressed NFR1:Cerulean alone. To assess a possible effect of acceptor fluorophore over-accumulation on the donor lifetime, NFR1:Cerulean was expressed together with free mOrange. No significant differences between lifetimes of solely expressed NFR1:Cerulean (2.18 ± 0.013 ns) and NFR1:Cerulean/free mOrange (2.16 ± 0.014 ns) were detected (Table S2) indicating that acceptor-accumulation did not have any impact on the donor lifetime. When co-expressing NFR1:Cerulean and LjSYMREM1:mOrange the Cerulean lifetimes were significantly reduced to 1.99 ± 0.022 ns, corresponding to a FRET efficiency of

8.8%. Similar values were obtained when NFR1:Cerulean and LjSYMREM1_C:mOrange were co-expressed. The observed lifetime decreased to 1.97 ± 0.021 ns with a FRET efficiency of 9.6% clearly indicating physical interaction of NFR1 and the C-terminal region of the LjSYMREM1 protein (Table S2). Moderately but also significantly reduced lifetimes were measured when co-expressing NFR1:Cerulean and LjSYMREM1_N:mOrange (2.09 ± 0.019 ns; FRET efficiency of 4.1%) (Table S2). These data indicate that primarily the C-terminal region of LjSYMREM1, containing the coiled-coil domain, contributes to NFR1-LjSYMREM1 interaction while the N-terminal region only weakly or transiently interacts with NFR1.

Phosphorylation of LjSYMREM1 by kinase domains of NFR1 and SYMRK

As shown above the C-terminal region of the LjSYMREM1 forms a stable interaction with the RLKs while the N-terminal domain may undergo weak or transient interaction. Since Remorins were reported to be phosphorylated *in vivo* [25,26,27,28] we decided to test if the putative transient interactions between the RLKs and the LjSYMREM1_N domain is a result of rapidly occurring protein phosphorylation. Contact between proteins should occur along the intracellular region (juxtamembrane region, kinase domain and C-terminal region) of the RLKs since Remorins are anchored to the cytosolic face of the PM [18]. Therefore, we tested if the cytoplasmic domains (CDs) of these symbiotic RLKs are able to phosphorylate LjSYMREM1 *in vitro*. It should be noticed that NFR5 is a pseudokinase that lacks several kinase subdomains including the activation loop and has recently been shown to lack kinase activity *in vitro* [1,29]. Purified LjSYMREM1 was tested with the recombinant CDs of NFR1, NFR5 and SYMRK. As illustrated in Figure 8A SYMRK was able to phosphorylate LjSYMREM1. A clear, but weaker, phosphorylation of LjSYMREM1 was found when the protein was incubated with NFR1 alone or in the presence of both NFR1 and NFR5. No phosphorylation was observed when purified MBP protein was used as substrate of NFR1, demonstrating that the phosphorylation of LjSYMREM1 did not derive from phosphorylation of the MBP tag (Figure S4).

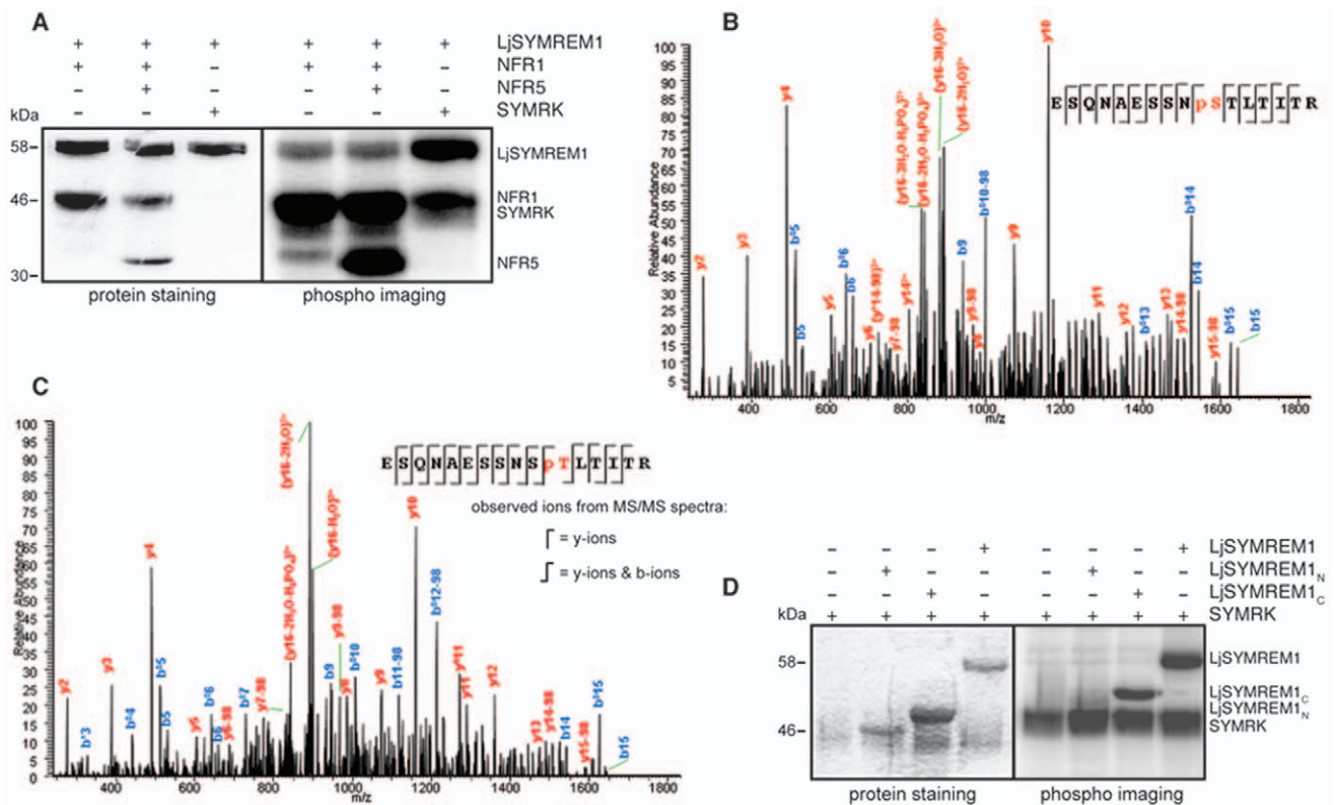


Figure 8. NFR1 and SYMRK kinase domains are able to phosphorylate LjSYMREM1 *in vitro*. Recombinant proteins purified from *E. coli* were tested for phosphorylation *in vitro*. LjSYMREM1 was N-terminally fused to the maltose binding protein (MBP). While NFR1 and NFR5 kinase domains (CD; cytosolic domains of the RLKs were used) were used as untagged proteins, SYMRK-CD contained a His-tag at its C-terminal end. Phosphorylation was visualized by detection of integrated radioactively labeled γ - ^{32}P -ATP. Both CDs were able to phosphorylate LjSYMREM1 even though NFR1 to a lower extent than SYMRK (A). Autophosphorylation of NFR1 and SYMRK kinase domains as well as trans-phosphorylation of NFR5-CD (inactive) by NFR1 were observed. Presence of NFR5 did not change the level of LjSYMREM1 phosphorylation. Protein staining of the SDS-PAGE shows presence of used proteins. Due to high kinase activity of SYMRK-CD protein amounts used for the assay were decreased to 0.25 μg and thus not visible on the gel (A). Representative MS/MS spectra of phosphorylated peptide ESQNAESSNSPTLTITR (NFR1-LjSYMREM1) (B) and ESQNAESSNSPTLTITR (SYMRK-LjSYMREM1) (C) were obtained when mapping the phosphorylation sites S48 and T49 on the LjSYMREM1 protein, respectively. While SYMRK was able to phosphorylate the C-terminal part of the protein, the LjSYMREM1 N-terminal region alone could not be phosphorylated *in vitro* (D).
doi:10.1371/journal.pone.0030817.g008

To map the phosphorylation sites on the LjSYMREM1 protein, phosphorylation reactions were repeated under non-radioactive conditions, LjSYMREM1 bands were excised from the SDS-polyacrylamide gel and tandem mass spectrometric analysis (MS/MS) was performed. Phosphorylated residues were neither detected on the LjSYMREM1 nor on the MBP proteins in the absence of NFR1 and SYMRK, indicating the absence of LjSYMREM1 and MBP phosphorylation by bacterial kinases. MS/MS analysis of LjSYMREM1 phosphorylated by NFR1 and SYMRK revealed that serine S48 and threonine T49 located within the N-terminal region of the SYMREM1 protein, were phosphorylated by these kinase domains, respectively (Figure 8B–8C). The obtained Mascot score were 54 for the T49 and 57 for phosphorylation of the S48 while the MS/MS spectra did not permit us to rule out that only one of the residues was phosphorylated. However, bioinformatic predictions (NetPhos2.0) indicate high P-site probabilities for S48 (0.994) while T49 is unlikely to represent an active P-site (score 0.180). These results are also supported by the fact that S48 is conserved in both MtSYMREM1 and LjSYMREM1 while T49 can only be found in the *Lotus* protein. Despite a high LjSYMREM1 sequence coverage (92%) the possibility cannot be excluded that S91, S130 and/or T131 may also be phosphorylated, as the 89-VESQK-93 and 127-

KASTQAK-134 peptide fragments could not be detected during the experiments.

To test this we purified recombinantly expressed LjSYMREM1_C and LjSYMREM1_N proteins and used them independently in a kinase assay with SYMRK that was shown to be the strongest phosphorylating kinase (Figure 8A). Indeed SYMRK could phosphorylate LjSYMREM1_C indicating the presence of an additional phosphorylation site in the C-terminal region. Interestingly, when LjSYMREM1_N was co-incubated with SYMRK, no phosphorylation of this domain was detected (Figure 8D) suggesting that the C-terminal region form a stable kinase-LjSYMREM1 interaction that subsequently allows phosphorylation of the Remorin N-terminal domain.

Discussion

Despite the fact that most signaling proteins involved in RNS are highly conserved between *M. truncatula* and *L. japonicus*, SYMREM1 proteins from legumes show a remarkable variability in their N-terminal regions (Figure 1; Table S1) indicating either high evolutionary pressure on group 2 N-terminal regions or dispensability of the domain. Given the emerging roles of Remorins to act as novel modulators in plant signaling cascades

we therefore characterized the LjSYMREM1 protein from *Lotus japonicus* in more detail with the aim to determine its spatio-temporal regulation and domains within the protein that contribute to the RLK-Remorin complex formation. The finding that purified NFs were sufficient to induce the promoter in root epidermal and cortical cells and that *LjSYMREM1* expression followed nodule primordium formation supports putative role of the protein during initial stages of rhizobial infection. Epidermal activation of the promoter was entirely abolished during nodule organogenesis and infection while GUS staining was continuously observed in infected cells of mature determinate nodules of *Lotus* (Figure 3) where the native LjSYMREM1 protein strongly accumulates (Figure 4). Whether the spatial expression of the *Lotus* RLKs NFR1, NFR5 and SYMRK matches the profile of *LjSYMREM1* during later stages of the nodulation process remains to be studied. However, continuous expression of the orthologous RLKs from *M. truncatula* in nodule primordia has been shown while in nodules transcripts have only been detected in the infection zone [6,9,30]. These data suggest roles of these RLKs also during later stages of infection. Whether the receptors are also present on symbiosome membranes has not been reported, yet. LjSYMREM1 is also present on trans-cellular infection threads that connect infected cells in mature nodules (Figure S2B). These data complement the findings that MtSYMREM1 localizes to nodular infection threads within the infection zone (zone II) [15], however no MtSYMREM1 protein was detected on remnant trans-cellular infection threads in the fixation zone (zone III) of *Medicago* nodules (Ton Timmers, LIPM Toulouse, *personal communication*).

In order to better understand the biology of Remorins and the structural requirements for RLK-Remorin interactions we separated the N- and C-terminal regions according to the presence of the coiled-coil domain in the C-terminal part and the lack of sequence conservation compared to other Remorins in the N-terminal region. As expected, due to the fact that PM association has been suggested for the entire Remorin family, the solely expressed C-terminal region localized to the plasma membrane (Figure 5) while the N-terminal region does not contribute to the subcellular localization of LjSYMREM1. Furthermore data presented here show that both, Remorin oligomerization and interaction with RLKs are mainly mediated also by the C-terminal part as shown in yeast (Figure 6), by FLIM analysis (Table S2) and by *in vitro* kinase assays (Figure 8B). The lack of fluorescence in the BiFC assay when co-expressing Yc:MtSYMREM1 and LjSYMREM1:Yn (Figure 6) indicates that Remorins may assemble in a parallel fashion leading to a physical distance of the split YFP halves and thus the lack of fluorescent signal. Whether phosphorylation of C-terminal residues is required for oligomerization remains to be studied. However, the fact that Yc:MtSYMREM1 does not interact with any of the *Lotus* RLKs (Figure 6) may also suggest that the N-terminal region of the both homologs has a steric impact on these interactions. Thus the function of the N-terminal region remains to be studied in detail and will likely provide further functional insights into SYMREM1 function.

Coiled-coil motifs are well known domains required for protein-protein interactions and several CCD containing proteins involved in cellular signaling processes have been described [31,32]. This domain has been previously hypothesized to be involved in Remorin oligomerization [33]. Since PM association of LjSYMREM1 is mediated by residues in the C-terminal region (Figure 5) we assume that LjSYMREM1_C tightly associates with the kinase- and/or juxtamembrane domains of the receptors in close proximity to the PM. However, our FLIM data indicate that the N-terminal region weakly or transiently interacts with the RLK

cytoplasmic domains (Table S2). In line with this we mapped the NFR1 and SYMRK phosphorylation site (S48/T49) to the N-terminal region of LjSYMREM1 (Figure 8). This phosphorylation possibly requires formation of a stable receptor-Remorin complex *in vivo*. It remains to be investigated whether phosphorylation of S48 induces a conformational change in the N-terminal region of the protein that allows interaction with other proteins and how specificity for recognition of interaction partners is achieved.

Molecular scaffold proteins are able to recruit proteins in membrane subdomains such as membrane rafts and facilitate assembly of multi-component signaling complexes. We hypothesize that LjSYMREM1 also serves such function. However, the fact that NFR1 and NFR5 are able to interact with each other in the absence of LjSYMREM1 at least when heterologously overexpressed in *N. benthamiana* [29] implies that the protein might be required for recruitment of RLKs into membrane rafts and to facilitate complex assembly in these subdomains. The fact that a large-scale proteomic study of *M. truncatula* membrane raft localized proteins did not identify LYK3, NFP or DMI2 in membrane rafts [34] may rather reflect low abundance of the RLK proteins. However it was recently nicely shown that LYK3 localizes to mobile membrane micro-domains in *Medicago* root hairs. Application of Nod Factors immobilized these foci and led to co-localization with the flotillin protein FLOT4 [35] that has been previously shown to be required during rhizobial infections [36]. It remains an intriguing question for the future if direct interactions between symbiotic RLKs and flotillins together with remorin proteins occur.

Materials and Methods

Phylogenetic and sequence analyses

Alignments and phylogenetic trees were computed using the CIPRES web-portal. Alignments were computed with MAFFT 6.822 (JTT matrix, E-INS-i setting) and RAxML 7.2.7 for fast maximum likelihood analyses [37]. For RAxML, the JTT PAM matrix for amino acid substitutions was chosen and the GTRGAMMA model was used for both, the bootstrapping phase and the final tree inference model, with 1000 bootstraps.

The 147 Remorin protein sequences available from public databases were analyzed to study their relationship, using 101 unambiguously aligned amino acid positions of the conserved C-terminal region. A second dataset contained 96 aligned sequences of group 2 Remorins only, allowing the analysis of 172 positions.

For sequence comparisons (Table S1 A-C) sequences were pairwise aligned using the EMBOSS Stretcher Algorithm (http://www.ebi.ac.uk/Tools/psa/emboss_stretcher/).

Plant Growth, Hairy Root Transformation and Stable Transformation

Transgenic roots were generated using *Agrobacterium rhizogenes* AR1193 [38] carrying the relevant construct. Roots of all plants were removed and seedlings were dipped into *Agrobacterium* suspension. Transformed plants were plated onto Gamborg's B5 medium [39], incubated in dark for 2 days before being grown at 24°C (8 h dark/16 h light, 60% humidity). Removal of *Agrobacterium* was achieved by transferring plants on Gamborg's B5 medium containing Cefotaxim 5 days after transformation.

Four weeks after transformation, plants were infected with *Mesorhizobium loti* MAFF 303099 (expressing DsRed fluorophore) and grown in glass jars on sand-vermiculite (1:1) mixture for the time indicated in the individual experiments.

Stable transformation of *Lotus japonicus* MG20 wild-type plants was performed as described earlier [40] with slight modifications.

The offspring of primary transformed plants (T2) was selected by hygromycin resistance and grown in glass jars on sand-vermiculite and were infected with *M. loti* MAFF 303099.

Promoter Analysis - Histochemical GUS-Staining/ β -Glucuronidase Assay

For analysis of promoter activity a 975 bp fragment upstream of the translational start codon was cloned into pBI101 binary vector and fused to the *uidA* (GUS) reporter gene. Transgenic roots of composite plants carrying the 975 bp construct as well as the empty vector - as negative control - were harvested periodically one week after inoculation with *M. loti* MAFF 303099 and incubated in GUS-staining solution (0.1 M NaPO₄; 1 mM EDTA; 1 mM K₃Fe(CN)₆; 1 mM K₄Fe(CN)₆; 1% Triton- \times 100; 1 mM X-Gluc) at 37°C in dark for 5 hours.

For imaging nodules were embedded in 5% Low-melt Agarose and sectioned via a Leica VT1000s Vibratome into 100 μ m thick sections. For GUS-staining (Figure S1) nodules were sectioned prior to GUS staining and staining was performed over-night.

Cloning and Constructs

All cloning steps (if not specifically indicated) were performed using Gateway technology. Created entry clones were verified by sequencing. All LjSYMREM1 and RLK constructs are based on cDNA templates until stated differently. SYMRK constructs that were used for *in planta* expression derived from genomic based clones.

For BiFC vectors were used as described earlier [15]. For FLIM analysis p35S-GW-Cerulean-nos and p35S-GW-mOrange-nos [41] vectors were used.

To analyze the localizations of LjSYMREM1 in the homologous *L. japonicus* background, we generated C-terminal fusions of the different LjSYMREM1 constructs to mOrange fluorophore in a vector that was described earlier [23] where the mOrange fluorophore was inserted after the recombination cassette.

To generate a stable *L. japonicus* line for protein localization expressed under its native promoter, we fused a 975 bp native promoter sequence and the full-length genomic sequence of LjSYMREM1 C-terminally to the eYFP fluorophore using the pH7YWG2.0 vector (modified after [42]) after removal of the CaMV-35S-promoter.

Protein Extraction and Western-blot Analysis

Total protein extraction was performed from transgenic *Lotus* roots expressing LjSYMREM1-mOrange under control of the *Lotus* polyubiquitin promoter and from roots of the stable transgenic plants expressing LjSYMREM1-YFP under its endogenous promoter. Roots were ground in liquid nitrogen and homogenized in denaturing buffer (10 mM EDTA, 50 mM Hepes, 150 mM NaCl, 10% Sucrose, 5 M Urea, 2 M Thiourea, 1% Triton-X 100, 1% SDS, 2 mM DTT, plant protease inhibitor cocktail from Sigma) and incubated for 1 hour at 37°C. Proteins were separated on a 12% SDS gel and transferred overnight at 4°C onto PVDF membranes. Membranes were blocked in 5% milk in TBS (with 0.1% Tween 20) and incubated overnight at 4°C with primary antibody. For detection of mOrange and the YFP fluorophore primary α -DsRed (rabbit, polyclonal; 1:5000) and primary α -GFP (mouse, monoclonal; 1:5000) antibodies were used, respectively.

Yeast two-hybrid interaction assay

We used the yeast split-ubiquitin system (SUS) for testing protein-protein interactions using the NMY32 yeast strain. The

Remorin constructs were cloned into the bait vector pBT3-N (Cub – C-terminal half of the Ubiquitin molecule – N-terminal fusion to the protein) and into the prey vector pDSL-Nx (NubG – mutated N-terminal Ubiquitin domain - N-terminal fusion to the protein) using SfiI restriction sites. RLK bait constructs were cloned into pTMBV4 (NFR1, SYMRK) and in pBT3-C (NFR5). For using the RLKs as prey constructs genes were cloned into pDL2xN. Co-transformations to investigate and confirm interactions and crude protein extraction were performed as described by the manufacturer (DUALsystem). Transformants were tested for interactions on SD (0.67% yeast nitrogen base, 2% glucose, 2% Bacto-agar and amino acid mix) without the appropriate auxotrophic markers and in the presence of 15 mM 3-amino-1,2,4-triazole (3-AT) in different dilution series: ND (non-diluted), 10⁻¹, 10⁻² up to 10⁻⁵.

BiFC studies and FLIM-FRET analysis

BiFC experiments were performed as described earlier [29]. Imaging was performed with a spectral TCS SP5 MP confocal laser-scanning microscope (Leica Microsystems, Mannheim, Germany) using an argon laser at an excitation wavelength of 514 nm. The water immersion objective lens HCX PL APO 20.0 \times 0.70 IMM UV was used for imaging tobacco epidermal cells for confocal imaging and FLIM analysis.

For FLIM-FRET analysis *Agrobacterium*-infiltration of tobacco leaves was performed as described above using *A. tumefaciens* GV3101 C58 carrying the respective constructs. For confocal laser scanning microscopy (CLSM) Cerulean fusion proteins were excited with a 405 nm diode laser, whereas mOrange fusion proteins were excited with a 514 nm argon laser line [41]. Cerulean fluorescence emission was detected between 485 and 535 nm, whereas mOrange fluorescence emission was detected between 545 and 600 nm. For spectroscopic analysis, the emission spectra of Cerulean and mOrange were recorded by λ -scanning between 450–590 nm and 540–720 nm, respectively.

For FLIM-FRET measurements, multiphoton (MP) excitation was used. Cerulean was excited with 810-nm light using a Spectra Physics Ti:Sapphire Mai Tai laser running at 80MHz with 1.2 ps pulse lengths. A FLIM PMT detector build in the spectral scanhead of the above mentioned microscope (Becker & Hickl [B&H] FLIM setup, implemented by Leica Microsystems, Mannheim, Germany) was used for time resolved photon detection for 5 min in 64 scanning cycles (\approx 5 s/cycle) at a spatial resolution of 256 \times 256 pixel, using the B&H photon counting software TCSPC 2.80. The MP excitation laser-power used was at setting that resulted in less than 10% photobleaching over the 5 min measuring time.

Selected magnified areas of the cells were then subjected to analyses performed with the B&H SPCImage software. Significance levels were calculated by student's t-test (with $p < 0.01$ being significantly different).

In Vitro Phosphorylation Assay

For this study the different LjSYMREM1 constructs were fused to the C-terminus of *E. coli* maltose-binding protein MalE (MBP) in pKM596 using the pENTR/TEV/D-TOPO entry clones. Proteins were expressed in *E. coli* Rosetta cells upon induction with 0.5 mM IPTG, cells were harvested after incubation at 21°C for 6 hours. Proteins were purified by amylose resin affinity chromatography (binding buffer: 20 mM Tris-HCl pH 7.4, 200 mM NaCl, 10 mM β -mercaptoethanol, 1 mM EDTA and 1 protease inhibitor tablet per 200 ml) and eluted samples (elution buffer: 20 mM Tris-HCl pH 7.4, 200 mM NaCl, 10 mM β -mercaptoethanol, 1 mM EDTA, 10 mM maltose and 1 protease inhibitor tablet per 200 ml) were tested on 10% SDS gel.

Purified MBP-LjSYMREM1, MBP-LjSYMREM1c and MBP-LjSYMREM1_N were incubated with the respective kinases (NFR1-CD (residues 254–622), NFR5-CD (residues 276–596), SYMRK-CD (residues 541–923)) for 45 min in kinase buffer (10 mM HEPES pH 7.4; 2 mM MgCl₂; 2 mM MnCl₂; 0.2 mM DTT; 2 μM ATP). For radioactive labeling proteins were incubated as described above in the presence 10 μCi [γ -³²P]ATP.

In Gel Digestion

Protein bands were excised from the SDS gels and bands were cut into 11 mm³ pieces and destained with 30% acetonitrile. The samples were reduced with 10 mM dithiothreitol in 25 mM ammonium bicarbonate for 30 min at 56°C and subsequently alkylated with 55 mM iodoacetamide in 25 mM ammonium bicarbonate for 45 min at room temperature in the dark. Then, the gel pieces were washed with water and ACN and dried under vacuum. Finally, proteins were digested with trypsin (1:20, w/w) in 25 mM ammonium bicarbonate (pH 8.0) overnight at 37°C.

Phosphopeptide enrichment with TiO₂ micro-column

Peptides were extracted from the gel by 5% FA 30% ACN. Phosphopeptides were enriched using micro-column as described earlier [43,44]. A small C8 plug (3 M C8 disk) was made using a HPLC syringe and placed at the constricted end of the Geloader tip. The TiO₂ material in 100% ACN was packed on top of the C8 plug. The dried peptides were resuspended with 50 μl of TiO₂ loading buffer and directly loaded onto the TiO₂ micro-column. After washing one time with 20 μl loading buffer and twice with 20 μl washing buffer (80% ACN, 1% TFA), the bound peptides were eluted with 20 μl 1 M NH₃·H₂O and 5 μl of 0.5 M NH₃·H₂O in 30% ACN. The elution was acidified with 1 μl 100% formic acid and dried prior to LC-MS analysis.

LC MS/MS Analysis and Data Interpretation

LC-MS/MS analysis was performed using a nanoliter flow EasyLC system (Thermo Fisher Scientific, Odense, Denmark) interfaced to an LTQ-Orbitrap XL mass spectrometer (Thermo Fisher Scientific, Bremen, Germany) as described earlier [29,45].

Supporting Information

Figure S1 Sections of nodules expressing an pLjSYMREM1:GUS construct. The construct was expressed in *L. japonicus* roots and GUS staining was performed 24 hours after Nod Factor application (A) and 21 dpi with *M. loti* (B). GUS staining was found in outer and inner root cortical cells (A), infected cells of nodules containing nitrogen-fixing bacteroids as well as in outer parenchyma cells that are not infected by the bacteria (B). Root material and nodules were sectioned after or prior to GUS staining that was performed over-night, respectively. Scale bars indicate 25 μm (A) and 500 μm (B). (TIF)

Figure S2 LjSYMREM1:YFP localizes to the symbiosome membrane and to nodular infection threads. A genomic construct consisting of the *LjSYMREM1* native promoter and the *LjSYMREM1* gene was fused to YFP. Roots were inoculated with *M. loti* MAFF303099 and three week old nodules of stable transgenic T2 plants were analyzed. Infected cells were disrupted by mechanical force to separate symbiosomes. Individual symbiosomes showed clear YFP fluorescence indicating presence of LjSYMREM1 on the symbiosome membrane (A). YFP fluorescence was also detected on nodular infection thread

remnants that are found in between infected cells (B). Bars indicate 5 μm (A) and 10 μm (B). (TIF)

Figure S3 All membrane-anchored clones were expressed in the yeast split-ubiquitin system. The Nubl tag is able to reconstitute together with Cub to the full-length ubiquitin and thus activates expression of the *HIS3*-reporter. Yeast growth on medium lacking leucine and tryptophan (–LW) shows the presence of both constructs. Interaction was tested on medium additionally lacking histidine (–LWH) that was supplemented with 15 mM 3-amino-1,2,4-triazole (3-AT) to suppress residual levels of endogenous histidine biosynthesis. (TIF)

Figure S4 NFR1 and SYMRK kinase domains are unable to phosphorylate maltose binding protein (MBP). MBP was recombinantly expressed and purified. Since no phosphorylation of MBP was detected in kinase assays it can be concluded that phosphorylation that was observed with MBP-LjSYMREM1 does not derive from MBP phosphorylation. (TIF)

Table S1 Group 2 remorins exhibit unusual sequence diversity in their N-terminal region. Sequence comparison of full-length (overall), N- and C-terminal protein sequences of legume remorins that were found to be most closely related to each other (Figure 1) revealed that sequence conservation of the C-terminal region is in accordance with similarities of other legumes signaling proteins (Table S1B) while the N-terminal region is unusually diverse (Table S1A). (DOCX)

Table S2 Testing interaction between LjSYMREM1 domains and NFR1 by FLIM analysis. LjSYMREM1:mOrange and NFR1:Cerulean were co-expressed in *N. benthamiana* leaves under control of the CaMV 35S-promoter. Shorter Cerulean lifetimes indicate interaction between the proteins. Strong interaction was observed between NFR1 and LjSYMREM1_{FL}/LjSYMREM1_C while mild but significant reduction in lifetime was also observed between NFR1 and LjSYMREM1_N. Numeric values are provided in the table inset. Significance levels were calculated by student's t-test (with $p < 0.01$ being significantly different). Free mOrange was co-expressed with NFR1:Cerulean to demonstrate that simple protein accumulation by over-expression of the acceptor fluorophore is not sufficient to reduce donor lifetimes. (PDF)

Acknowledgments

We would like to thank Jessica Folgmann and Karl-Heinz Braun for their excellent technical assistance. Entry clones were kindly provided by Jens Stougaard (University of Aarhus, Denmark). We would also like to acknowledge Riyaz A. Bhat (CEA/CNRS/Mediterranean University Aix-Marseille, Cadarache, France) for providing the vectors p35S-GW-Cerulean-nos and p35S-GW-mOrange-nos. Furthermore we would also like to thank Zsuzsanna Buzás (University of Budapest, Hungary) for providing the empty yeast split-ubiquitin vectors and for her scientific support of the project. We also thank the LMU Exzellenz-Initiative that kindly funded the FLIM-FRET equipment (grant ZUK 22/1).

Author Contributions

Conceived and designed the experiments: KT TS TO. Performed the experiments: KT TS EM JY AS TO. Analyzed the data: KT TS EM JY AS TO. Contributed reagents/materials/analysis tools: CP MA-L CG MP OJ. Wrote the paper: KT TS TO.

References

- Madsen EB, Madsen LH, Radutoiu S, Olbryt M, Rakwalska M, et al. (2003) A receptor kinase gene of the LysM type is involved in legume perception of rhizobial signals. *Nature* 425: 637–640.
- Radutoiu S, Madsen LH, Madsen EB, Felle HH, Umehara Y, et al. (2003) Plant recognition of symbiotic bacteria requires two LysM receptor-like kinases. *Nature* 425: 585–592.
- Radutoiu S, Madsen LH, Madsen EB, Jurkiewicz A, Fukai E, et al. (2007) LysM domains mediate lipochitin-oligosaccharide recognition and *Nfr* genes extend the symbiotic host range. *EMBO J* 26: 3923–3935.
- Oldroyd GE, Downie JA (2008) Coordinating nodule morphogenesis with rhizobial infection in legumes. *Annu Rev Plant Biol* 59: 519–546.
- Popp C, Ott T (2011) Regulation of signal transduction and bacterial infection during root nodule symbiosis. *Curr Opin Plant Biol* 14: 458–467.
- Arrighi JF, Barre A, Ben Amor B, Bersoult A, Soriano LC, et al. (2006) The *Medicago truncatula* lysin motif-receptor-like kinase gene family includes NFP and new nodule-expressed genes. *Plant Physiol* 142: 265–279.
- Smit P, Limpens E, Geurts R, Fedorova E, Dolgikh E, et al. (2007) *Medicago* LYK3, an entry receptor in rhizobial nodulation factor signaling. *Plant Physiol* 145: 183–191.
- Limpens E, Franken C, Smit P, Willemsse J, Bisseling T, et al. (2003) LysM domain receptor kinases regulating rhizobial Nod factor-induced infection. *Science* 302: 630–633.
- Bersoult A, Camut S, Perhald A, Kereszt A, Kiss GB, et al. (2005) Expression of the *Medicago truncatula* DMI2 gene suggests roles of the symbiotic nodulation receptor kinase in nodules and during early nodule development. *Mol Plant Microbe Interact* 18: 869–876.
- Limpens E, Mirabella R, Fedorova E, Franken C, Franssen H, et al. (2005) Formation of organelle-like N₂-fixing symbiosomes in legume root nodules is controlled by DMI2. *Proc Natl Acad Sci U S A* 102: 10375–10380.
- Stracke S, Kistner C, Yoshida S, Mulder L, Sato S, et al. (2002) A plant receptor-like kinase required for both bacterial and fungal symbiosis. *Nature* 417: 959–962.
- Madsen LH, Tirichine L, Jurkiewicz A, Sullivan JT, Heckmann AB, et al. (2010) The molecular network governing nodule organogenesis and infection in the model legume *Lotus japonicus*. *Nat Commun* 1: 1–12.
- Gage DJ (2002) Analysis of infection thread development using Gfp- and DsRed-expressing *Sinorhizobium meliloti*. *J Bacteriol* 184: 7042–7046.
- Gage DJ (2004) Infection and invasion of roots by symbiotic, nitrogen-fixing rhizobia during nodulation of temperate legumes. *Microbiology and Molecular Biology Reviews* 68: 280–300.
- Lefebvre B, Timmers T, Mbengue M, Moreau S, Herve C, et al. (2010) A remorin protein interacts with symbiotic receptors and regulates bacterial infection. *Proc Natl Acad Sci U S A* 107: 2343–2348.
- Raffaële S, Mongrand S, Gamas P, Niebel A, Ott T (2007) Genome-wide annotation of remorins, a plant-specific protein family: evolutionary and functional perspectives. *Plant Physiol* 145: 593–600.
- Kistner C, Winzer T, Pitzschke A, Mulder L, Sato S, et al. (2005) Seven *Lotus japonicus* genes required for transcriptional reprogramming of the root during fungal and bacterial symbiosis. *Plant Cell* 17: 2217–2229.
- Raffaële S, Bayer E, Lafarge D, Cluzet S, German Retana S, et al. (2009) Remorin, a *Solanaceae* protein resident in membrane rafts and plasmodesmata, impairs potato virus X movement. *Plant Cell* 21: 1541–1555.
- Jarsch IK, Ott T (2011) Perspectives on remorin proteins, membrane rafts, and their role during plant-microbe interactions. *Mol Plant Microbe Interact* 24: 7–12.
- Colebatch G, Desbrosses G, Ott T, Krusell L, Montanari O, et al. (2004) Global changes in transcription orchestrate metabolic differentiation during symbiotic nitrogen fixation in *Lotus japonicus*. *Plant Journal* 39: 487–512.
- Hogslund N, Radutoiu S, Krusell L, Voroshilova V, Hannah MA, et al. (2009) Dissection of symbiosis and organ development by integrated transcriptome analysis of *Lotus japonicus* mutant and wild-type plants. *PLoS One* 4: e6556.
- Heidstra R, Geurts R, Franssen H, Spaik HP, Van Kammen A, et al. (1994) Root Hair Deformation Activity of Nodulation Factors and Their Fate on *Vicia sativa*. *Plant Physiol* 105: 787–797.
- Mackawa T, Kusakabe M, Shimoda Y, Sato S, Tabata S, et al. (2008) Polyubiquitin promoter-based binary vectors for overexpression and gene silencing in *Lotus japonicus*. *Mol Plant Microbe Interact* 21: 375–382.
- Koushik SV, Vogel SS (2008) Energy migration alters the fluorescence lifetime of Cerulean: implications for fluorescence lifetime imaging Forster resonance energy transfer measurements. *J Biomed Opt* 13: 031204.
- Benschop JJ, Mohammed S, O'Flaherty M, Heck AJ, Slijper M, et al. (2007) Quantitative phosphoproteomics of early elicitor signaling in Arabidopsis. *Mol Cell Proteomics* 6: 1198–1214.
- Farmer EE, Moloshok TD, Saxton MJ, Ryan CA (1991) Oligosaccharide signaling in plants. Specificity of oligouronide-enhanced plasma membrane protein phosphorylation. *J Biol Chem* 266: 3140–3145.
- Reymond P, Kunz B, Paul-Petzer K, Grimm R, Eckerskorn C, et al. (1996) Cloning of a cDNA encoding a plasma membrane-associated, uronide binding phosphoprotein with physical properties similar to viral movement proteins. *Plant Cell* 8: 2265–2276.
- Widjaja I, Naumann K, Roth U, Wolf N, Mackey D, et al. (2009) Combining subproteome enrichment and Rubisco depletion enables identification of low abundance proteins differentially regulated during plant defense. *Proteomics* 9: 138–147.
- Madsen EB, Antolin-Llovera M, Grossmann C, Ye J, Vieweg S, et al. (2011) Autophosphorylation is essential for the in vivo function of the *Lotus japonicus* Nod factor receptor 1 and receptor-mediated signalling in cooperation with Nod factor receptor 5. *Plant J* 65: 404–417.
- Mbengue M, Camut S, de Carvalho-Niebel F, Deslandes L, Froidure S, et al. (2010) The *Medicago truncatula* E3 ubiquitin ligase PUB1 interacts with the LYK3 symbiotic receptor and negatively regulates infection and nodulation. *Plant Cell* 22: 3474–3488.
- Rairdan GJ, Collier SM, Sacco MA, Baldwin TT, Boettrich T, et al. (2008) The coiled-coil and nucleotide binding domains of the Potato Rx disease resistance protein function in pathogen recognition and signaling. *Plant Cell* 20: 739–751.
- Skirpan AL, McCubbin AG, Ishimizu T, Wang X, Hu Y, et al. (2001) Isolation and characterization of kinase interacting protein 1, a pollen protein that interacts with the kinase domain of PRK1, a receptor-like kinase of petunia. *Plant Physiol* 126: 1480–1492.
- Bariola PA, Retelska D, Stasiak A, Kammerer RA, Fleming A, et al. (2004) Remorins form a novel family of coiled coil-forming oligomeric and filamentous proteins associated with apical, vascular and embryonic tissues in plants. *Plant Mol Biol* 55: 579–594.
- Lefebvre B, Furt F, Hartmann MA, Michaelson LV, Carde JP, et al. (2007) Characterization of lipid rafts from *Medicago truncatula* root plasma membranes: a proteomic study reveals the presence of a raft-associated redox system. *Plant Physiol* 144: 402–418.
- Haney CH, Riely BK, Tricoli DM, Cook DR, Ehrhardt DW, et al. (2011) Symbiotic Rhizobia Bacteria Trigger a Change in Localization and Dynamics of the *Medicago truncatula* Receptor Kinase LYK3. *Plant Cell*.
- Haney CH, Long SR (2010) Plant flotillins are required for infection by nitrogen-fixing bacteria. *Proc Natl Acad Sci U S A* 107: 478–483.
- Stamatakis A, Hoover P, Rougemont J (2008) A rapid bootstrap algorithm for the RAxML Web servers. *Syst Biol* 57: 758–771.
- Stougaard J, Petersen TE, Marcker KA (1987) Expression of a Complete Soybean Leghemoglobin Gene in Root-Nodules of Transgenic *Lotus-Corniculatus*. *Proceedings of the National Academy of Sciences of the United States of America* 84: 5754–5757.
- Gamborg OL, Miller RA, Ojima K (1968) Nutrient requirements of suspension cultures of soybean root cells. *Exp Cell Res* 50: 151–158.
- Lombardi P, Ercolano E, El Alaoui H, Chiurazzi M (2005) *Agrobacterium*-mediated in vitro transformation. In: Márquez AJ, Stougaard J, Udvardi M, Parniske M, Spaik H, et al. (2005) *Lotus japonicus* handbook Springer. 384 p.
- Bayle V, Nussaume L, Bhat RA (2008) Combination of novel green fluorescent protein mutant TSapphire and DsRed variant mOrange to set up a versatile in planta FRET-FLIM assay. *Plant Physiol* 148: 51–60.
- Karimi M, De Meyer B, Hilson P (2005) Modular cloning in plant cells. *Trends Plant Sci* 10: 103–105.
- Larsen MR, Thingholm TE, Jensen ON, Roepstorff P, Jorgensen TJ (2005) Highly selective enrichment of phosphorylated peptides from peptide mixtures using titanium dioxide microcolumns. *Mol Cell Proteomics* 4: 873–886.
- Thingholm TE, Jorgensen TJ, Jensen ON, Larsen MR (2006) Highly selective enrichment of phosphorylated peptides using titanium dioxide. *Nat Protoc* 1: 1929–1935.
- Ye J, Zhang X, Young C, Zhao X, Hao Q, et al. (2010) Optimized IMAC-IMAC protocol for phosphopeptide recovery from complex biological samples. *J Proteome Res* 9: 3561–3573.

Supporting Information

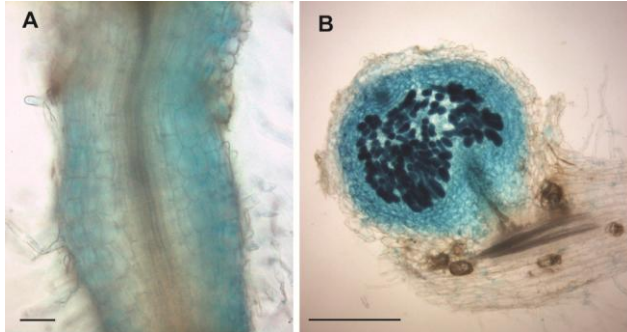


Figure S1

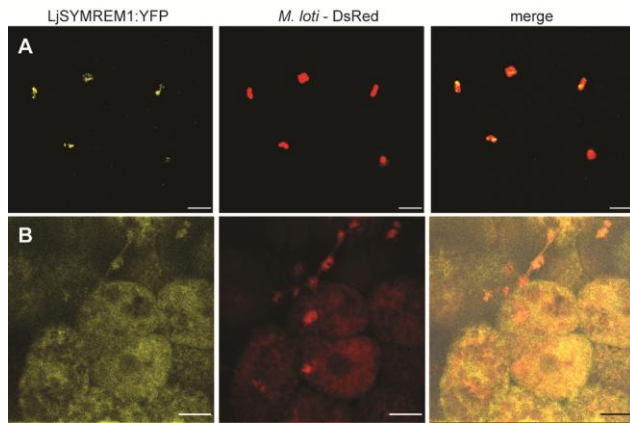


Figure S2

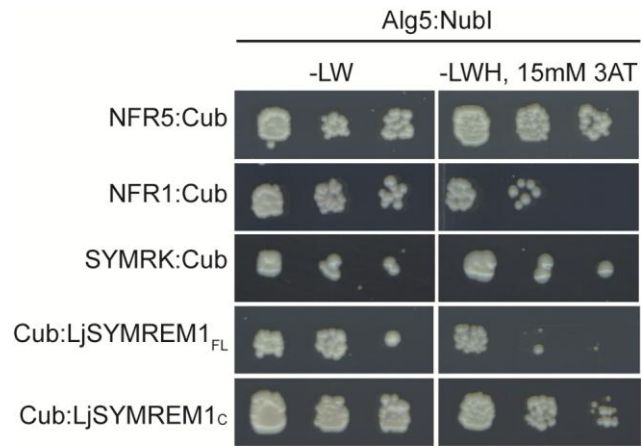


Figure S3

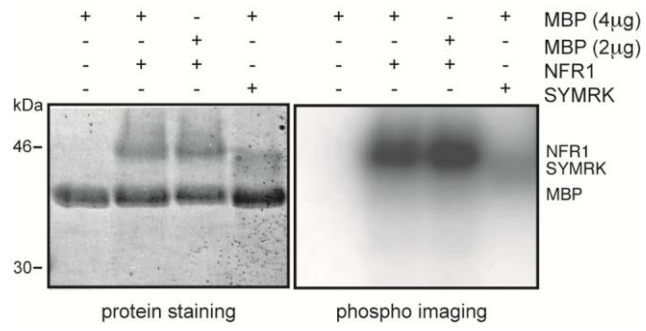


Figure S4

Sequence comparison between different group 2 Remorins that derived from the best BLAST hit against the genome sequences (Table S1A) and sequence analysis for symbiotic signaling proteins and nodulins (Table S1B).

Table S1A

Identity/Similarity values in % for putative SYMREM1 homologs (based on MtSYMREM1)						
domain	<i>Medicago</i>	<i>Lotus</i>	soybean	poplar	Common bean	<i>Vitis</i>
Full-length	100	55.5/67.1	53.1/65.1	49.8/62.9	52.4/65.0	42.9/59.0
C-term	100	72.9/85.3	67.4/79.1	63.6/76.0	67.4/79.1	58.9/76.0
N-term	100	27.2/38.3	30.0/42.5	26.3/40.8	27.3/41.6	15.8/30.3

Medicago truncatula= MtSYMREM1*; *Lotus japonicus*= chr4.CM0004.60.r2.d; soybean=Glyma08g01590.1; poplar= PtREM2.2*; common bean= Pv_TC37632; *Vitis vinifera*= Vv_XP_002267609; nomenclature introduced and sequences provided in Raffaele et al., (2007) (*) and Lefebvre et al. (2010) (#).

Table S1B

<i>Medicago</i>	<i>Lotus</i>	identity	similarity
NFP	NFR5	72.0%	82.8%
DMI2	SYMRK	81.6%	87.6%
DMI1	POLLUX	80.8%	85.3%
DMI3	CCAMK	85.7%	92.2%
IPD3	CYCLOPS	78.2%	87.1%
NIN	NIN	57.4%	67.5%
NSP2	NSP2	73.9%	83.4%
Leghemoglobin 1	Leghemoglobin 1b	70.3%	80.4%

Accession numbers for sequences used in this analysis: NFP (ABF50224), NFR5 (CAZ66917), DMI2 (CAD10811), SYMRK (AAM67418), DMI1 (AAS49490), POLLUX (BAD89022), DMI3 (Q6RET7), CCAMK (CAJ76700), IPD3 (ABN45743), CYCLOPS (ABU63668), MtNIN (ACN58567), LjNIN (CAB61243), MtNSP2 (CAH55768), LjNSP2 (BAE72690), Lb1 (P72992), Lb1b (BAB18108).

NFR1: Cerulean	+	+	+	+	+
free mOrange	-	+	-	-	-
SYMREM1:mOrange	-	-	LjSYMREM1 _{FL}	LjSYMREM1 _C	LjSYMREM1 _N
lifetime [ns]	2.18	2.16	1.99	1.97	2.09
std. error	0.013	0.014	0.022	0.021	0.019
n	35	19	40	38	36
p-value	0.2221		1.32×e ⁻¹⁰	1.47×e ⁻¹⁰	0.0001

Table S2

1.3. Manuscript 1

A remorin protein controls symbiotic dualism in the legume *Medicago truncatula*,

Popp, C., Bittencourt-Silvestre J., Thallmair, V., Mysore, K.S., Wen, J., Delaux, PM.,
and Ott, T.

Proceedings of the National Academy of Sciences, USA

Status: Invited for resubmission | Year: NN | DOI: NN

A remorin protein controls symbiotic dualism in the legume *Medicago truncatula*

Claudia Popp¹, Joana Bittencourt-Silvestre¹, Veronika Thallmair^{1,§}, Kirankumar S. Mysore², Jiangqi Wen², Pierre-Marc Delaux³ and Thomas Ott^{1,4*}

¹ Ludwig-Maximilians Universität München, Institute of Genetics, Großhaderner Str. 2-4, 82152 Martinsried, Germany

² Plant Biology Division, The Samuel Roberts Noble Foundation, 2510 Sam Noble Parkway, Ardmore, OK 73401, USA

³ Laboratoire de Recherche en Sciences Végétales, Université de Toulouse, CNRS, UPS, 24 chemin de Borde Rouge, Auzeville, BP42617, 31326, Castanet Tolosan, France.

⁴ Albert-Ludwigs-Universität Freiburg, Institute Biology II - Cell Biology, Schänzlestr. 1, 79104 Freiburg, Germany

[§] present address: Philipps Universität Marburg, Department of Neurophysiology, Deutschhausstr. 2, 35037 Marburg, Germany

* corresponding author: Thomas.Ott@biologie.uni-freiburg.de

ABSTRACT:

About 65 million years ago legumes evolved the almost unique ability to concurrently host two symbioses, the arbuscular mycorrhiza (AM) and the root nodule symbiosis (RNS). Being therefore able to grow in phosphate- and nitrogen-deprived environments, this feature provided a significant competitive advantage in natural ecosystems. Consequently it has become a major aim to understand the molecular networks governing both bipartite interactions. One of the key events was the implementation of an already existing signalling cascade operating during AM into RNS, commonly referred to as the ‘common symbiosis pathway’ (CSP). However, the fact that only RNS but not AM triggers the onset of an entire organogenesis programme downstream of the CSP raises the ultimate need for additional regulatory circuits. In this study we provide first evidence for the existence of a legume-specific pathway that controls CSP-dependent nodule organogenesis during the tripartite interaction between the host, the AM fungus and rhizobia. As a first member of such novel control layer, we characterized the legume-specific remorin protein MYCREM that strictly co-evolved with symbiotic dualism in all tested legumes. Genetically, MYCREM negatively regulates nodulation in the presence of both symbionts but not during sole bipartite host-rhizobium interactions in *Medicago truncatula*. The protein functions as a nodule organogenesis suppressor and interferes with the expression of a rhizobia-induced host infection marker. We propose that MYCREM represents a first component of a novel pathway that fine-tunes cellular events required to maintain effective symbiotic dualism in legumes in natural environments.

SIGNIFICANCE STATEMENT

INTRODUCTION

Arbuscular mycorrhiza (AM) symbiosis is one of the oldest and most frequently found symbiotic associations on earth as the respective fungi belonging to the monophyletic *Glomeromycota* phylum colonize about 80% of all terrestrial land plants (1-3). The recognition of fungal lipochitooligosaccharides (LCOs) by LysM-type receptor-like kinases (4) (RLKs) results in host cell reprogramming including initial cellular, physiological and transcriptional responses such as cell polarization, calcium spiking and the expression of specific marker genes, respectively (5-8). The primary intracellular passage of AM fungi (AMF) such as *Rhizophagus irregularis* across the host epidermis and outer cortical cells is guided by the formation of a cytoplasmic bridge, the pre-penetration apparatus (PPA), which precedes the direct cellular colonization by the symbiont (9, 10). In the model legume *Medicago truncatula* this stage is followed by an intercellular expansion of the intraradical hyphae along the root axis prior to the penetration of inner cortical cells. Within these cells fungal hyphae undergo extensive branching to form the symbiotic organ, the arbuscule (7). Interestingly, colonization of inner root cortical cells by AMF does not trigger any significant cell proliferation or tissue re-organization in this susceptible zone.

In contrast to almost any other plant family, legumes evolved the ability to undergo a second mutualistic interaction, the root nodule symbiosis (RNS) mostly with gram-negative alpha-proteobacteria of the *Rhizobaeaceae* family. Phylogenetic analyses revealed that RNS evolved several times independently about 65 million years ago (14) with one of these events occurring early in the evolution of the Papilionoideae subfamily, the largest legume subfamily with more than 13,000 species (15). With the perception of LCOs - the so-called Nod Factors - by host LysM-type RLKs (16-19), regular calcium spiking (20-22), the formation of the pre-infection thread (PIT) (23, 24) - a structure similar to the PPA - and the intracellular colonization of the host root (25, 26), both symbioses share remarkable similarities. The most striking one, however, is the use of an identical molecular signalling cascade, the 'common symbiosis pathway' (CSP), downstream of LCO perception (14). Loss of function mutations in any of the CSP genes results in the inability to form AM and RNS or to severe perturbations during colonization. Most of the CSP components known to date localize to the nuclear envelope (27-33) or the nucleoplasm (34-37). Among them are

the *M. truncatula* calcium-calmodulin-dependent kinase DOES NOT MAKE INFECTIONS 3 (DMI3) (34, 38) and the transcriptional activator INTERACTING PROTEIN OF DMI3 (IPD3) (39) as well as their respective orthologs in *L. japonicus* CCaMK and CYCLOPS (36, 37). The DMI3/IPD3 (CCaMK/CYCLOPS) complex probably decodes calcium-spiking signatures during AM and RNS (40). Interestingly, the presence of the phospho-mimetic and auto-active versions CCaMK-T265D or CYCLOPS-S50D-S154D (CYCLOPS-DD) result in the formation of spontaneous nodules (SPN) even in the absence of rhizobia (36, 41). Considering that the CSP is absolutely indispensable for establishing or maintaining both symbioses raises a so far unsolved paradox with respect to a key difference between AM and RNS: In contrast to AM, the colonization of the root by rhizobia results in the formation of an entirely new organ, the root nodule, that hosts differentiated, membrane-encapsulated and nitrogen-fixing bacteroids (42). In *M. truncatula* the respective organogenetic programme is initiated by cell divisions in the pericycle and inner root cortical cells that result in the formation of a nodule primordium, which subsequently further differentiates into a mature nodule (43). As the formation of lateral roots, which are induced during RNS and AM (44, 45), is also initiated in the pericycle and the endodermis and followed by cell divisions within the most inner cortical cell layer (46) both organogenetic programmes might be genetically overlapping in *M. truncatula*.

In this study we asked the question: What enables legumes to spatially control two morphologically different symbioses after using a genetically identical signalling pathway? While this feature is not required when inoculating legumes with only one symbiont at a time, as currently done under laboratory conditions in most molecular and cell biological studies, they are exposed to both symbionts simultaneously in natural environments. This study aimed to gather evidence for the existence of a novel regulatory pathway that coordinates simultaneous existence of this globally important symbiotic dualism on the same root segment.

RESULTS

To illustrate the simultaneous and physical presence of both symbioses under natural conditions we harvested field-grown Medicago and stained the roots for AM structures. As expected all roots were populated with nodules as well as densely

colonized by AMF that were found in close proximity to each other (Fig. 1A-E). To be able to investigate this symbiotic dualism under laboratory conditions we established a novel co-inoculation assay where plants were grown in sterilized substrate and inoculated with both symbionts, *Sinorhizobium meliloti* and *R. irregularis*. As observed for field-grown plants both symbioses were located adjacent to each other when grown under these co-inoculation conditions in a controlled laboratory environment (Fig. 1F).

MYCREM evolved with symbiotic dualism in legumes

As the molecular composition of protein complexes that mediate the hypothesized regulatory system are unknown, we assumed that scaffold proteins such as members of the remorin protein family could serve as promising candidates to test for the existence of such pathway. Therefore, we took advantage of the fact that these proteins function as molecular hubs by interacting with a number of different and most likely pathway-specific components. Previous analysis identified a legume-specific subclade (clade II) within the remorin family that is represented by two members in the *M. truncatula* genome (*MtREM2.1* and *MtREM2.2* (*SYMREM1*)) (47). *SYMREM1* is exclusively induced during RNS and controls rhizobial infection (48, 49). In contrast, *REMORIN-LIKE 1* (*RML1*), the *L. japonicus* homolog of *MtREM2.1* is induced during later stages of AM (50) although it also belongs to the same clade as *SYMREM1* (47, 49). Therefore, we called this gene *MYCORRHIZA-INDUCED REMORIN* (*MYCREM*).

This raised the intriguing question about the possible function of AM-induced but legume-specific genes such as *MYCREM* as it is unlikely that they are essential for AM due to their phylogenetic restriction. To unravel the evolutionary pattern of clade II remorins we took a phylogenetic approach and identified homologous sequences in the main legume lineages and closely related species (see Supplementary Table S1). To identify actual orthologs among them, a phylogenetic tree was constructed and rooted with the potential orthologs from the closely related Rosales species and the Fabales *Quillaja saponaria* (Fig. 2). Three clades were recovered by both Neighbor-joining and Maximum-likelihood analyses (Fig. 2). The basal one is composed of the Caesalpinioideae *Bauhinia tomentosa* and *Copaifera officinalis* and the Mimosoideae *Acacia argyrophylla*. Although the branching order within this clade (polyphyletic in

the ML tree) is not resolved strongly it suggests that a single ortholog, MYCREM-like, is present in these lineages (Fig. 2). The two other clades are composed of homologs from the Papilionoideae subfamily with species represented in both clades. One of them contains the *Medicago* and *Lotus* SYMREM1 whereas the other one encompasses *Medicago* and *Lotus* MYCREM. In addition, each clade contains sequences from other Papilionoideae. Orthologs of MYCREM were identified in most Papilionoideae species with only transcriptome data available, irrespectively of the sampled tissues. By contrast, SYMREM1 orthologs were only found in few transcriptomes generated from root samples (Supplementary Table S1). Focusing on species with sequenced genomes, both MYCREM and SYMREM1 were recovered in all of them, including the Dalbergieae *Arachis ipoensis*. The only exception was *Lupinus angustifolius* where only SYMREM1 was found. In support of the absence of MYCREM in *Lupinus*, orthologs were also not detected in the three *Lupinus* transcriptomes included in the analysis (Supplementary Table S1).

Taken together, these results indicate that *SYMREM1* and *MYCREM* originate from a duplication event at the base of the Papilionoideae clade, after the divergence of the Mimosoideae, and strongly suggest that *MYCREM* was lost in the *Lupinus* genus while *SYMREM1* has been retained. Although *Lupinus* is able to form the root nodule symbiosis, species belonging to this genus are not able to form the AM symbiosis. It has been previously demonstrated that the loss of AM in the *Lupinus* genus is associated with the loss of genes specifically required to form this symbiotic association, while the ones specific of RNS, such as *SYMREM1*, are conserved (6, 51). From this we concluded that *MYCREM* evolved with the ability of legumes to maintain both AM and RNS at the same time.

***MYCREM* transcripts accumulate during AM**

The *M. truncatula* *MYCREM* gene (Medtr5g010590) is transcribed at basal levels in control roots (mock) (Fig. 3A) and isolated young nodules (Fig. 3B). Elevated mRNA levels were found in nodulated as well as mycorrhized roots (Fig. 3A). To gain cell-type specific resolution we generated transgenic roots expressing a reporter construct (ProMYCREM::GUS). In non-inoculated roots (mock) the *MYCREM* promoter was weakly activated along the vasculature, inner cortical cells (Fig. 3C,D) and in lateral root primordia (Fig. 3D). Upon rhizobial inoculation, GUS staining was also observed

in nodule primordia (Fig. 3F,G) as well as in the nodule meristem and the distal zone II of mature nodules (Fig. 3E). In root segments without nodules the promoter remained activated in inner cortical cells, the vasculature and lateral root primordia (Fig. 3H). These basal cortical expression levels were also observed on roots carrying extraradical *R. irregularis* hyphae (Fig. 3I) while the reporter was reproducibly induced in inner root cortical cells that hosted intraradical hyphae (Fig. 3J) or arbuscules (Fig. 3K).

MYCREM is dispensable for the sole formation of AM and RNS

To genetically assess MYCREM function, we screened (52, 53) the *M. truncatula* *Tnt1*-retrotransposon insertion population and identified a single *mycrem* mutant line (NF8847; *mycrem-1*). Re-sequencing of the *MYCREM* locus in this line revealed that the retrotransposon inserted at the end of the fourth intron at nucleotide position 1484 (Supplementary Fig. S1A). Quantitative RT-PCR analysis on cDNAs obtained from five independent homozygous individuals showed a strong reduction of the full-length *MYCREM* transcript under AM condition at 6wpi (Supplementary Fig. S1B). However, this mutant did not display any phenotypical differences to wild-type plants with respect to nodule primordia number (Supplementary Fig. S1C) or intraradically hosted fungal structures such as hyphae, arbuscules and vesicles when grown under high infection (chive nurse system; Supplementary Fig. S1D) or moderate infection pressure conditions (spore inoculum; Supplementary Fig. S1E) with each symbiont being inoculated independently from the other.

Taken together these data indicate that MYCREM does not represent a core gene required for the establishment of the individual symbioses where only one type of symbiont, either AMF or rhizobia, is present at the time.

MYCREM controls nodule organogenesis under co-inoculation conditions

Following the hypothesis that genes like *MYCREM* should possess their main function in the presence of both symbionts, plants were grown under co-inoculation conditions. To ensure full colonization of the roots by AMF and to avoid systemic auto-regulation of nodulation (AON) plants were exposed for four weeks to *R. irregularis* prior to the inoculation with *S. meliloti*. Symbiotic performance was scored taking nodule

primordia as a read-out. Strikingly, *mycrem* mutant plants developed significantly more nodule primordia compared to wild-type plants under co-inoculation conditions using high (Fig. 4A) and moderate infection pressure inoculums (Fig. 4B) indicating an impaired cross-regulation of both symbioses in the *mycrem* mutant. The phenotype was genetically complemented in transgenic roots expressing a *ProMYCREM:HA-MYCREM* construct (Fig. 4C). In addition to the symbiotic phenotype, the *mycrem* mutant developed significantly more lateral roots when grown for 7 days in the absence of any symbiont (Fig. 4D).

These experiments imply that MYCREM is specifically involved in a novel regulatory mechanism that controls lateral root formation and nodulation under more complex inoculation conditions. These phenotypes raised the question whether MYCREM functions as an autonomous organogenesis suppressor in non-infected primordia.

MYCREM negatively interferes with nodule organogenesis

To genetically assess the putative organogenetic suppressor function of MYCREM in more detail we made use of the auto-active *L. japonicus* CCaMK-T265D and CYCLOPS-DD mutant variants. Indeed, individual expression of both CCaMK-T265D and CYCLOPS-DD in the R108 wild-type background resulted in the formation of SPN with significantly fewer organogenesis events observed for CYCLOPS-DD (Fig. 5A). Furthermore, SPNs induced by CCaMK-T265D developed into elongated structures (Fig. 5B,D) while those induced by the expression of CYCLOPS-DD were arrested in the young primordium stage (Fig. 5C,E) and therefore were significantly smaller (Supplementary Fig. S2). Genotype-based comparison revealed that significantly more SPNs were formed on *mycrem* compared to wild-type roots that expressed CCaMK-T265D, an effect that was less pronounced using CYCLOPS-DD (Fig. 5A). Furthermore, expression of both auto-active versions resulted in the formation of cluster-like roots (as illustrated for CYCLOPS-DD; Fig. 5F) with the effect being more prominent upon expression of CYCLOPS-DD (Fig. 5H). This phenomenon was not observed or greatly reduced when expressing CCaMK-T265D and CYCLOPS-DD in the *mycrem* mutant, respectively (Fig. 5G,H). These results clearly demonstrate that MYCREM acts as a negative regulator of organogenesis.

As the CCaMK/CYCLOPS complex defines the genetic branch point at the end of the CSP where AM and RNS related signalling diverges again (54), we tested the ability of these auto-active variants to transcriptionally induce endogenous remorin genes. While ectopic expression CCaMK-T265D only resulted in mildly elevated *MYCREM* transcript levels the presence of CYCLOPS-DD lead to a significant induction of the gene in the wild-type but not in the *mycrem* mutant (Supplementary Fig. S3A). Interestingly, the infection marker and closely related *SYMREMI* gene, which is strongly activated in young nodules (Supplementary Fig. S3C,D) was exclusively induced by CCaMK-T265D in the wild-type but completely blocked in the *mycrem* mutant (Supplementary Fig. S3B). Given our finding that CYCLOPS-DD selectively induces the onset of lateral roots and nodule organogenesis we concluded that CCaMK-T265D is able to trigger additional cell-specific infection- and organogenesis-related processes as represented by the induction of *SYMREMI* that are inhibited in the *mycrem* mutant (Supplementary Fig. S3B). This suggests that, mechanistically, MYCREM might be able to locally suppress expression of genes linked to rhizobial infection such as *SYMREMI* in the presence of both symbionts.

DISCUSSION

About 65 million years ago (14, 55) legumes evolved the capability to simultaneously host RNS and AM in close proximity to each other (Fig. 1). This symbiotic dualism creates at least two obstacles: First, as legumes integrate the initial perception of specific microbe-derived signalling molecules via the same genetic pathway, the CSP, they require mechanisms to maintain this specificity downstream of the CSP in order to ensure the observed differential responses. Second, since RNS is energetically extremely costly for the host plant (56), legumes need regulatory circuits that allow local fine-tuning of rhizobial infection in AM colonized roots. This includes spatial separation of both symbioses and the molecular integration of environmental constrains where host plants favour one over the other symbiosis (e.g. under drought conditions that positively regulate AM (57)). Our phylogenetic approach revealed that *MYCREM* strictly co-evolved with symbiotic dualism (Fig. 2), a feature that this is most likely not restricted to this gene. In addition *MYCREM* is not found within the canonical genes required for AM (5, 6, 51) although the gene is induced in AMF

colonized roots and arbuscule containing cells. This strongly imposes a potential function of *MYCREM* in coordinating both symbioses and being a component of a cell-type specific pathway that spatially controls cross talk between the two symbioses in the inner root cortex. Indeed *MYCREM* is transcriptionally activated in these cells and uninfected nodule primordia (Fig. 3C-K) that are potentially susceptible to intracellular colonization by symbiotic microbes and to cell division (43). In these cells *MYCREM* appears to be regulated by at least two routes: First, its reduced transcript stability in nodules (Fig. 3B) implies the locally confined regulation on a post-transcriptional level during a sole bipartite rhizobium-host interaction as shown for a number of RNS-related genes (59-61). Second, the CSP-dependent activation of *MYCREM* and *SYMREMI* relies on a specific phosphorylation pattern within the CCaMK/CYCLOPS complex (Supplementary Fig. S3). The CCaMK-T265D-mediated induction of *SYMREMI*, which is blocked in the *mycrem* mutant (Supplementary Fig. S3B), supports a possible model where *MYCREM* might be able to desensitize AMF colonized inner cortical cells for subsequent rhizobial infection by inhibiting CSP-dependent activation of infection related genes such as *SYMREMI*.

Besides a CSP-dependent regulation of *MYCREM* expression, global transcriptome data indicate that the gene is induced during nitrate-mediated nodule senescence but not upon treatment of uninoculated roots with high nitrate (62). Additionally, prolonged drought that coincides with elevated abscisic acid (ABA) concentrations, a phytohormone that promotes AM but inhibit RNS (63, 64), lead to a constant accumulation of *MYCREM* mRNAs, which were immediately reduced upon re-watering (65). These data indicate an additional hormonal and metabolic control of *MYCREM* and a possible involvement of local AON, which is able to inhibit the initiation of nodule primordium formation in legumes such as *M. truncatula* that develop indeterminate nodules (66, 67), in spatially controlling this symbiotic dualism.

In summary, our data indicate the existence of a so far overlooked regulatory and multi-factorial pathway that co-evolved with the ability to maintain symbiotic dualism in legumes coordinates the concurrent colonization of roots by symbiotic bacteria and fungi. *MYCREM*, a first representative of such system acts as a negative regulator of organogenesis in a CSP-dependent manner under co-inoculation conditions. As a

molecular scaffold protein, the proposed function of remorins, MYCREM might decrease susceptibility of AM-colonized cells for subsequent rhizobial infection.

MATERIALS AND METHODS

Plant material, Growth conditions, genotyping and Agrobacteria mediated-root transformation

Promoter activation studies were performed in the *M. truncatula* Jemalong A17 background. For phenotypic analysis the *M. truncatula* mutant line *mycrem* (NF 8847) and its corresponding wild type background R108 were used throughout the whole study.

The *mycrem* mutant line was obtained upon reverse screening of the mutant population at The Samuel Roberts Noble Foundation. Seeds from the R1 generation of the *M. truncatula* R108 *Tnt1* retrotransposon insertion line were propagated and screened for homozygous mutant plants via PCR (primers see Table S3).

Agrobacterium rhizogenes (ARqua1) carrying different vector constructs was used for transient hairy root transformation as described previously . In brief, seeds were surface sterilized for 1 min using 1.2% sodium hypochlorite and 0.1% SDS, after a sulfuric acid treatment for 5-15 min and 4 washing steps with sterile H₂O. The seeds were vernalized for at least 3 days at 4°C in darkness. Agrobacteria used for the transformation were grown two days on plate at 28°C. Prior transformation seeds were germinated for 18 h at 24°C in darkness. For transformation roots were removed, the remaining seedlings were inoculated with Agrobacteria and grown for three days on Fahraeus medium in darkness at 22°C for four days at 22°C in 16 h light /8 h dark cycle in a growth chamber. Then seedlings were transferred to fresh Fahraeus medium plates and grown for another 14 days at 24°C in 16h light /8h dark cycles. Positive transformants were selected by fluorescence.

Plants were grown in sand (quartz sand, BayWa, Germany)/vermiculite (size 2-3 mm, Deutsche vermiculite Dämmstoff GmbH, Germany) (1:1) mixture in open pots for all experiments. They were fertilized once per week with Fahraeus medium and watered regularly.

Lateral root density was determined seven days after growth on Fahraeus medium plates.

Rhizobia, Fungi and Co-inoculation conditions

Rhizobia inoculation

For promoter induction studies plants were inoculated with *Sinorhizobium meliloti*-mCherry with an OD₆₀₀ of 0.001. For RNS phenotype analysis the *S. meliloti*-CFP strain (Sm 2011-CFP) was used (69) with the same OD₆₀₀ for inoculation. Each plant was inoculated with 5 mL of bacteria suspension.

Fungi inoculation (spore inoculation and chive nurse system) and quantification

To determine the AM phenotype of *mycrem* mutant plants and for MYCREM promoter induction under AM wild type and mutant plants were either inoculated with 500 spores/plant (in about 200ml sand/vermiculite) of *Rhizophagus irregularis* (SYMPLANTA, Munich Germany) or were grown in chive (*Allium schoenoprasum*) nurse pot system containing *Rhizophagus irregularis* (in-house root culture inoculum), as well. Plants were watered every second or third day and fertilized once per week either with B&D or ¼ Hoagland medium, respectively. Ink/ vinegar staining was used to visualize fungal structures within the root (70). Root length colonization was analyzed four weeks after inoculation by using a modified gridline intersect method (71) and 10x magnification at a light microscope.

Co-Inoculation

For co-inoculation studies plants were pre-inoculated with *R. irregularis* as described above for 4 to 5 weeks. After verifying fungal colonization via ink/vinegar staining plants were inoculated with *S. meliloti* CFP as already described.

All phenotyping experiments have been repeated at least 3 to 5 times independently. The complementation experiment and the SPN experiment were repeated two times with the same results.

Expression analysis

Total RNA extraction was performed according to the Spectrum Plant Total RNA Kit (Sigma-Aldrich, Germany) manual. Root material was grinded in liquid nitrogen and

100 mg per root sample was used for extraction. Extracted RNA was treated with DNase I, Amp Grade (Invitrogen, Germany). The absence of genomic DNA was verified via PCR. Synthesis of cDNA was performed with 700 ng of RNA in a total reaction volume of 20 μ l using the Superscript III kit from Invitrogen (Invitrogen, Germany). For qRT-PCR analysis a Fast SYBR Green Master Mix (Applied Biosystems, Germany) was used in a 10 μ l reaction volume. A CFX96™ Real-Time system (Bio-Rad, Germany) was used for PCR reactions and detection. Expression was normalized either to *EFL-alpha* or *Ubiquitin*. At least three biological replicates were analyzed in technical duplicates per treatment. Primers used within this study are listed in Table S3.

Histochemical Promoter analysis (GUS-staining), WGA staining and Microscopy

MYCREM promoter induction was analyzed via β -Glucuronidase (GUS) activity. Transgenic roots were stained in GUS-staining solution (0.1 M NaPO₄; 1 mM EDTA; 1 mM K₃Fe (CN)₆; 1 mM K₄Fe (CN)₆; 1% Triton-X 100; 1 mM X-Gluc) at 37°C for 4 h in the dark. For fluorescent visualization of fungal structure colonized roots were fixed in 50% ethanol for at least 12h and afterwards cleared for 2 days at root temperature in 10% KOH. After a washing step with distilled water roots have been incubated in 0.1 M HCl for 1 h at RT. Prior the final staining roots have been washed with distilled water and rinsed once with PBS (phosphate buffered saline; pH7.4). Roots were placed in a PBS-WGA–AlexaFluor594 staining solution (0.2 μ g/mL WGA-AlexaFluor594 from Thermo Fisher Scientific, Germany) for at least 6 h at 4°C in dark. For documentation a stereomicroscope and an inverted fluorescence microscope were used.

Phylogenetic analysis

Sequence collection

Sequences were collected by tBLASTn using the protein sequences of *Lotus japonicus* SYMREM1 and MYCREM as queries on a homemade database of genomes and transcriptomes. This database includes genomes of the legumes *Phaseolus vulgaris* (72), *Medicago truncatula* (73), *Lotus japonicus* (74), *Cicer arietinum* (75), *Glycine max* (76), *Arachis ipoensis* (77), *Trifolium pratense* (78), *Lupinus angustifolius* (79, 80) and the closely related Rosales *Canabis sativa* (81),

several transcriptomes from the 1KP initiative (82) including those of early diverging Fabaceae (83) and three transcriptome assemblies of *Lupinus* species (Table S1). For each species the top five hits (based on E-values) were collected for further analyses. In addition, for *Lupinus albus* transcriptome, the top ten hits based on % identity were also collected to avoid excluding sequences based on contigs length. In addition, SYMREM sequences were amplified by PCR from *Vigna* sp., *Pisum sativum*, *Vicia* and *Trigonella* using primers shown in Table S3.

Alignment and phylogeny

The collected DNA sequences were translated and aligned using MAFFT (84). This initial alignment also included two additional sequences from *Medicago truncatula* previously identified as outgroups (Medtr1g100647.1 and Medtr8g031370.1) (47). A first phylogeny was then conducted using Fastree in Geneious v8.1.7. From this initial analysis a clade rooted with clades encompassing the two *Medicago* outgroups and including the *Lotus japonicus* SYMREM1 and MYCREM sequences was extracted. These 35 sequences (Table S2) were then re-aligned as previously described. The best substitution model and rate were determined (JTT+G) and phylogenetic trees reconstructed using Maximum-likelihood (ML) and Neighbor-joining (NJ) algorithms implemented in MEGA6 (85). Both phylogenies were tested using 500 bootstrap replicates. Trees were rooted with the Rosales sequences and the basal Fabales *Quillaja saponaria*. Both analyses were also ran after discarding all positions with gaps or only on the highly conserved C-terminal domain. These analyses yielded the same result as the analysis with full length sequences.

Cloning and Constructs

For promoter induction studies 1 kb upstream of the ATG of the *MYCREM* gene was amplified via PCR from genomic DNA (A17) and cloned into the pENTR/D-TOPO vector. The ProMYCREM (1kb):eGFP-GUS was created by LR-reaction of pKGWFS7-vector and pENTR/D-TOPO: ProMYCREM (1 kb). The expression vector pProUbi:CCaMK-T265D_Pro35S:GFP was also created by LR-reaction of pProUbi:GW_Pro35S:GFP and pENTR:CCaMK-T265D (37). The expression vectors for the complementation experiment were cloned according to the Golden Gate protocol from (86) (see also Table S4).

Statistical analysis

For data display and statistical analysis the program 'R studio' version 0.99.486 (©2009-2015 R Studio. Inc.) and the packages 'XLConnect Jars' (Mirai Solutions GmbH), 'XLConnect' (Mirai Solutions GmbH), 'multcomp' (87) and 'multcompView' were used. If more than two samples have been compared statistical significance was calculated by a one-way ANOVA followed by a TukeyHSD (all-vs-all) or by a Dunnett's (all-vs-one) test. If only two samples have been compared a Student's t-test was performed.

ACKNOWLEDGEMENTS

We would like to thank Karl Heinz Braun and Richard Valentini for their valuable contributions, Sylvia Singh for providing the pUbi-CCaMK-T265D vector and Macarena Marín for critical reading of the manuscript. This work was funded by the Priority Programme (Schwerpunktprogramm) SPP1212 of the Deutsche Forschungsgemeinschaft (grants OT423/1-1 and OT423/1-2) and an Emmy Noether Fellowship awarded to T.O. (grant OT423/2-1).

REFERENCES

1. Bonfante P & Genre A (2008) Plants and arbuscular mycorrhizal fungi: an evolutionary-developmental perspective. *Trends Plant Sci* 13 (9):492-498.
2. Redecker D, Kodner R, & Graham LE (2000) Glomalean fungi from the Ordovician. *Science* 289 (5486):1920-1921.
3. Remy W, Taylor TN, Hass H, & Kerp H (1994) Four hundred-million-year-old vesicular arbuscular mycorrhizae. *Proc Natl Acad Sci U S A* 91 (25):11841-11843.
4. Op den Camp R, *et al.* (2011) LysM-type mycorrhizal receptor recruited for rhizobium symbiosis in nonlegume *Parasponia*. *Science* 331 (6019):909-912.
5. Delaux PM, *et al.* (2015) Algal ancestor of land plants was preadapted for symbiosis. *Proc Natl Acad Sci U S A* 112 (43):13390-13395.
6. Delaux PM, *et al.* (2014) Comparative phylogenomics uncovers the impact of symbiotic associations on host genome evolution. *PLoS Genet* 10 (7):e1004487.
7. Gutjahr C & Parniske M (2013) Cell and developmental biology of arbuscular mycorrhiza symbiosis. *Annu Rev Cell Dev Biol* 29:593-617.
8. Parniske M (2008) Arbuscular mycorrhiza: the mother of plant root endosymbioses. *Nature Reviews Microbiology* 6 (10):763-775.
9. Genre A, Chabaud M, Faccio A, Barker DG, & Bonfante P (2008) Prepenetration Apparatus Assembly Precedes and Predicts the Colonization Patterns of Arbuscular Mycorrhizal Fungi within the Root Cortex of Both *Medicago truncatula* and *Daucus carota*. *Plant Cell* 20:1407-1420.
10. Genre A, Chabaud M, Timmers T, Bonfante P, & Barker DG (2005) Arbuscular mycorrhizal fungi elicit a novel intracellular apparatus in *Medicago truncatula* root epidermal cells before infection. *Plant Cell* 17 (12):3489-3499.
11. Harrison MJ (2012) Cellular programs for arbuscular mycorrhizal symbiosis. *Curr Opin Plant Biol* 15 (6):691-698.
12. Javot H, Penmetsa RV, Terzaghi N, Cook DR, & Harrison MJ (2007) A *Medicago truncatula* phosphate transporter indispensable for the arbuscular mycorrhizal symbiosis. *Proc Natl Acad Sci U S A* 104 (5):1720-1725.
13. Pumplun N, Zhang X, Noar RD, & Harrison MJ (2012) Polar localization of a symbiosis-specific phosphate transporter is mediated by a transient reorientation of secretion. *Proc Natl Acad Sci U S A* 109 (11):E665-672.
14. Kistner C & Parniske M (2002) Evolution of signal transduction in intracellular symbiosis. *Trends in Plant Science* 7 (11):511-518.
15. Werner GD, Cornwell WK, Sprent JI, Kattge J, & Kiers ET (2014) A single evolutionary innovation drives the deep evolution of symbiotic N₂-fixation in angiosperms. *Nat Commun* 5:4087.
16. Amor BB, *et al.* (2003) The NFP locus of *Medicago truncatula* controls an early step of Nod factor signal transduction upstream of a rapid calcium flux and root hair deformation. *Plant J* 34 (4):495-506.
17. Limpens E, *et al.* (2003) LysM domain receptor kinases regulating rhizobial Nod factor-induced infection. *Science* 302 (5645):630-633.

18. Madsen EB, *et al.* (2003) A receptor kinase gene of the LysM type is involved in legume perception of rhizobial signals. *Nature* 425 (6958):637-640.
19. Radutoiu S, *et al.* (2003) Plant recognition of symbiotic bacteria requires two LysM receptor-like kinases. *Nature* 425 (6958):585-592.
20. Ehrhardt DW, Wais R, & Long SR (1996) Calcium spiking in plant root hairs responding to Rhizobium nodulation signals. *Cell* 85 (5):673-681.
21. Oldroyd GE & Downie JA (2004) Calcium, kinases and nodulation signalling in legumes. *Nat Rev Mol Cell Biol* 5 (7):566-576.
22. Oldroyd GE & Downie JA (2006) Nuclear calcium changes at the core of symbiosis signalling. *Curr Opin Plant Biol* 9 (4):351-357.
23. Timmers AC, Auriac MC, & Truchet G (1999) Refined analysis of early symbiotic steps of the Rhizobium-Medicago interaction in relationship with microtubular cytoskeleton rearrangements. *Development* 126 (16):3617-3628.
24. van Brussel AA, *et al.* (1992) Induction of pre-infection thread structures in the leguminous host plant by mitogenic lipo-oligosaccharides of Rhizobium. *Science* 257 (5066):70-72.
25. Gage DJ (2004) Infection and invasion of roots by symbiotic, nitrogen-fixing rhizobia during nodulation of temperate legumes. *Microbiology and Molecular Biology Reviews* 68 (2):280-300.
26. Parniske M (2000) Intracellular accommodation of microbes by plants: a common developmental program for symbiosis and disease? *Curr Opin Plant Biol* 3 (4):320-328.
27. Ane JM, *et al.* (2004) Medicago truncatula DMI1 required for bacterial and fungal symbioses in legumes. *Science* 303 (5662):1364-1367.
28. Charpentier M, *et al.* (2008) Lotus japonicus CASTOR and POLLUX are ion channels essential for perinuclear calcium spiking in legume root endosymbiosis. *Plant Cell* 20 (12):3467-3479.
29. Charpentier M, *et al.* (2016) Nuclear-localized cyclic nucleotide-gated channels mediate symbiotic calcium oscillations. *Science* 352 (6289):1102-1105.
30. Groth M, *et al.* (2010) NENA, a Lotus japonicus homolog of Sec13, is required for rhizodermal infection by arbuscular mycorrhiza fungi and rhizobia but dispensable for cortical endosymbiotic development. *Plant Cell* 22 (7):2509-2526.
31. Imaizumi-Anraku H, *et al.* (2005) Plastid proteins crucial for symbiotic fungal and bacterial entry into plant roots. *Nature* 433 (7025):527-531.
32. Kanamori N, *et al.* (2006) A nucleoporin is required for induction of Ca²⁺ spiking in legume nodule development and essential for rhizobial and fungal symbiosis. *Proc Natl Acad Sci U S A* 103 (2):359-364.
33. Saito K, *et al.* (2007) NUCLEOPORIN85 is required for calcium spiking, fungal and bacterial symbioses, and seed production in Lotus japonicus. *Plant Cell* 19 (2):610-624.
34. Levy J, *et al.* (2004) A putative Ca²⁺ and calmodulin-dependent protein kinase required for bacterial and fungal symbioses. *Science* 303 (5662):1361-1364.

35. Messinese E, *et al.* (2007) A novel nuclear protein interacts with the symbiotic DMI3 calcium- and calmodulin-dependent protein kinase of *Medicago truncatula*. *Mol Plant Microbe Interact* 20 (8):912-921.
36. Tirichine L, *et al.* (2006) Deregulation of a Ca²⁺/calmodulin-dependent kinase leads to spontaneous nodule development. *Nature* 441 (7097):1153-1156.
37. Yano K, *et al.* (2008) CYCLOPS, a mediator of symbiotic intracellular accommodation. *Proc Natl Acad Sci U S A* 105 (51):20540-20545.
38. Mitra RM, *et al.* (2004) A Ca²⁺/calmodulin-dependent protein kinase required for symbiotic nodule development: Gene identification by transcript-based cloning. *Proc Natl Acad Sci U S A* 101 (13):4701-4705.
39. Horvath B, *et al.* (2011) *Medicago truncatula* IPD3 is a member of the common symbiotic signaling pathway required for rhizobial and mycorrhizal symbioses. *Mol Plant Microbe Interact* 24 (11):1345-1358.
40. Miller JB, *et al.* (2013) Calcium/Calmodulin-dependent protein kinase is negatively and positively regulated by calcium, providing a mechanism for decoding calcium responses during symbiosis signaling. *Plant Cell* 25 (12):5053-5066.
41. Singh S, Katzer K, Lambert J, Cerri M, & Parniske M (2014) CYCLOPS, a DNA-binding transcriptional activator, orchestrates symbiotic root nodule development. *Cell Host Microbe* 15 (2):139-152.
42. Popp C & Ott T (2011) Regulation of signal transduction and bacterial infection during root nodule symbiosis. *Curr Opin Plant Biol* 14:458-467.
43. Xiao TT, *et al.* (2014) Fate map of *Medicago truncatula* root nodules. *Development* 141 (18):3517-3528.
44. Gutjahr C & Paszkowski U (2013) Multiple control levels of root system remodeling in arbuscular mycorrhizal symbiosis. *Frontiers in plant science* 4:204.
45. Olah B, Briere C, Becard G, Denarie J, & Gough C (2005) Nod factors and a diffusible factor from arbuscular mycorrhizal fungi stimulate lateral root formation in *Medicago truncatula* via the DMI1/DMI2 signalling pathway. *Plant J* 44 (2):195-207.
46. Herrbach V, Rembliere C, Gough C, & Bensmihen S (2014) Lateral root formation and patterning in *Medicago truncatula*. *J Plant Physiol* 171 (3-4):301-310.
47. Raffaele S, Mongrand S, Gamas P, Niebel A, & Ott T (2007) Genome-wide annotation of remorins, a plant-specific protein family: evolutionary and functional perspectives. *Plant Physiol* 145 (3):593-600.
48. Lefebvre B, *et al.* (2010) A remorin protein interacts with symbiotic receptors and regulates bacterial infection. *Proc Natl Acad Sci U S A* 107 (5):2343-2348.
49. Tóth K, *et al.* (2012) Functional Domain Analysis of the Remorin Protein LjSYMREM1 in *Lotus japonicus*. *PLOS ONE* 7 (1):e30817.
50. Kistner C, *et al.* (2005) Seven *Lotus japonicus* genes required for transcriptional reprogramming of the root during fungal and bacterial symbiosis. *Plant Cell* 17 (8):2217-2229.
51. Bravo A, York T, Pumplin N, Mueller LA, & Harrison MJ (2016) Genes conserved for arbuscular mycorrhizal symbiosis identified through phylogenomics. *Nat Plants* 2:15208.

52. Cheng X, *et al.* (2014) An efficient reverse genetics platform in the model legume *Medicago truncatula*. *New Phytol* 201 (3):1065-1076.
53. Cheng X, Wen J, Tadege M, Ratet P, & Mysore KS (2011) Reverse genetics in *Medicago truncatula* using Tnt1 insertion mutants. *Methods Mol Biol* 678:179-190.
54. Madsen LH, *et al.* (2010) The molecular network governing nodule organogenesis and infection in the model legume *Lotus japonicus*. *Nat Commun* 1 (1):1-12.
55. Sprent JI (2007) Evolving ideas of legume evolution and diversity: a taxonomic perspective on the occurrence of nodulation. *New Phytol* 174 (1):11-25.
56. Pate JS & Layzell DB (1990) Energetics and biological costs of nitrogen assimilation. *The biochemistry of plants, Intermediary Nitrogen Metabolism*, eds Stumpf PK & Conn EE (Academic Press, San Diego), Vol 16, pp 1-43.
57. Ruiz-Lozano JM, Collados C, Barea JM, & Azcon R (2001) Arbuscular mycorrhizal symbiosis can alleviate drought-induced nodule senescence in soybean plants. *New Phytologist* 151 (2):493-502.
58. Gaude N, Bortfeld S, Duensing N, Lohse M, & Krajinski F (2012) Arbuscule-containing and non-colonized cortical cells of mycorrhizal roots undergo extensive and specific reprogramming during arbuscular mycorrhizal development. *Plant J* 69 (3):510-528.
59. Boualem A, *et al.* (2008) MicroRNA166 controls root and nodule development in *Medicago truncatula*. *Plant J* 54 (5):876-887.
60. Combier JP, *et al.* (2006) MthAP2-1 is a key transcriptional regulator of symbiotic nodule development regulated by microRNA169 in *Medicago truncatula*. *Genes Dev* 20 (22):3084-3088.
61. De Luis A, *et al.* (2012) Two microRNAs linked to nodule infection and nitrogen-fixing ability in the legume *Lotus japonicus*. *Plant Physiol* 160 (4):2137-2154.
62. Benedito VA, *et al.* (2008) A gene expression atlas of the model legume *Medicago truncatula*. *Plant J* 55 (3):504-513.
63. Charpentier M, Sun J, Wen J, Mysore KS, & Oldroyd GE (2014) Abscisic acid promotion of arbuscular mycorrhizal colonization requires a component of the PROTEIN PHOSPHATASE 2A complex. *Plant Physiol* 166 (4):2077-2090.
64. Ding Y, *et al.* (2008) Abscisic acid coordinates nod factor and cytokinin signaling during the regulation of nodulation in *Medicago truncatula*. *Plant Cell* 20 (10):2681-2695.
65. Zhang JY, *et al.* (2014) Global reprogramming of transcription and metabolism in *Medicago truncatula* during progressive drought and after rewatering. *Plant Cell Environ* 37 (11):2553-2576.
66. Den Herder G & Parniske M (2009) The unbearable naivety of legumes in symbiosis. *Curr Opin Plant Biol* 12 (4):491-499.
67. Wasson AP, Pellerone FI, & Mathesius U (2006) Silencing the flavonoid pathway in *Medicago truncatula* inhibits root nodule formation and prevents auxin transport regulation by rhizobia. *Plant Cell* 18 (7):1617-1629.

68. Boisson-Dernier A, *et al.* (2001) Agrobacterium rhizogenes-transformed roots of Medicago truncatula for the study of nitrogen-fixing and endomycorrhizal symbiotic associations. *Mol Plant Microbe Interact* 14 (6):695-700.
69. Fournier J, *et al.* (2015) Remodeling of the infection chamber before infection thread formation reveals a two-step mechanism for rhizobial entry into the host legume root hair. *Plant Physiol* 167 (4):1233-1242.
70. Vierheilig H, Coughlan AP, Wyss U, & Piche Y (1998) Ink and vinegar, a simple staining technique for arbuscular-mycorrhizal fungi. *Appl Environ Microbiol* 64 (12):5004-5007.
71. McGonigle TP, Miller MH, Evans DG, Fairchild GL, & Swan JA (1990) A new method which gives an objective measure of colonization of roots by vesicular-arbuscular mycorrhizal fungi. *New Phytol* 115 (3):495-501.
72. Schmutz J, *et al.* (2014) A reference genome for common bean and genome-wide analysis of dual domestications. *Nat Genet* 46 (7):707-713.
73. Young ND, *et al.* (2011) The Medicago genome provides insight into the evolution of rhizobial symbioses. *Nature* 480 (7378):520-524.
74. Sato S, *et al.* (2008) Genome structure of the legume, Lotus japonicus. *DNA Res* 15 (4):227-239.
75. Varshney RK, *et al.* (2013) Draft genome sequence of chickpea (Cicer arietinum) provides a resource for trait improvement. *Nat Biotechnol* 31 (3):240-246.
76. Schmutz J, *et al.* (2010) Genome sequence of the palaeopolyploid soybean. *Nature* 463 (7278):178-183.
77. Bertoli DJ, *et al.* (2016) The genome sequences of Arachis duranensis and Arachis ipaensis, the diploid ancestors of cultivated peanut. *Nat Genet* 48 (4):438-446.
78. De Vega JJ, *et al.* (2015) Red clover (Trifolium pratense L.) draft genome provides a platform for trait improvement. *Sci Rep* 5:17394.
79. Yang H, *et al.* (2015) Application of whole genome re-sequencing data in the development of diagnostic DNA markers tightly linked to a disease-resistance locus for marker-assisted selection in lupin (Lupinus angustifolius). *BMC Genomics* 16:660.
80. Yang H, *et al.* (2013) Draft genome sequence, and a sequence-defined genetic linkage map of the legume crop species Lupinus angustifolius L. *PLOS ONE* 8 (5):e64799.
81. van Bakel H, *et al.* (2011) The draft genome and transcriptome of Cannabis sativa. *Genome Biol* 12 (10):R102.
82. Matasci N, *et al.* (2014) Data access for the 1,000 Plants (1KP) project. *Gigascience* 3:17.
83. Cannon SB, *et al.* (2015) Multiple polyploidy events in the early radiation of nodulating and nonnodulating legumes. *Mol Biol Evol* 32 (1):193-210.
84. Katoh K & Standley DM (2013) MAFFT multiple sequence alignment software version 7: improvements in performance and usability. *Mol Biol Evol* 30 (4):772-780.
85. Tamura K, Stecher G, Peterson D, Filipowski A, & Kumar S (2013) MEGA6: Molecular Evolutionary Genetics Analysis version 6.0. *Mol Biol Evol* 30 (12):2725-2729.

86. Binder A, *et al.* (2014) A modular plasmid assembly kit for multigene expression, gene silencing and silencing rescue in plants. *PLOS ONE* 9 (2):e88218.
87. Hothorn T, Bretz F, & Westfall P (2008) Simultaneous inference in general parametric models. *Biom J* 50 (3):346-363.

FIGURES

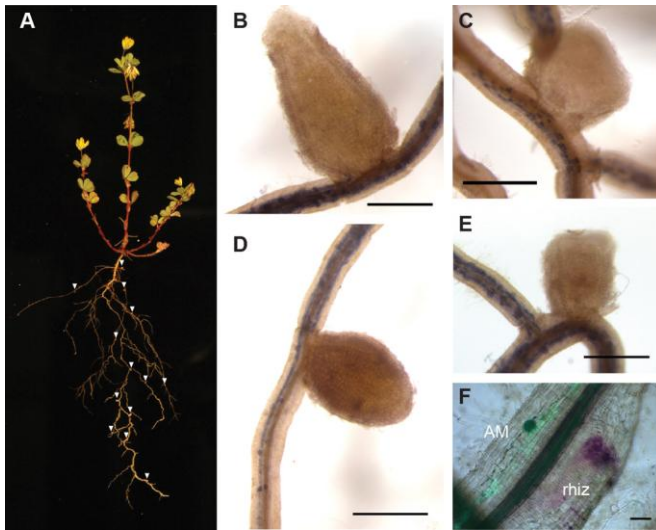


Figure 1: Field-grown Medicago plants showed simultaneous colonization with rhizobia and AM fungus. (A) Example of a field-grown Medicago plant with a nodulated root system. Arrowheads point to nodules. **(B-E)** Close-ups of ink/vinegar stained root segments showing root nodules and AM structures in direct proximity to each other. **(F)** *Medicago truncatula* wild-type root segment co-inoculated with and colonized by *R. irregularis* and *S. meliloti* 2011 LacZ under laboratory conditions. The AM fungus was stained with WGA-Alexa488. *S. meliloti* (rhiz) colonization was indirectly shown via LacZ-staining. [Scale bars=500 μ m (B, C, D and E); 100 μ m (F)].

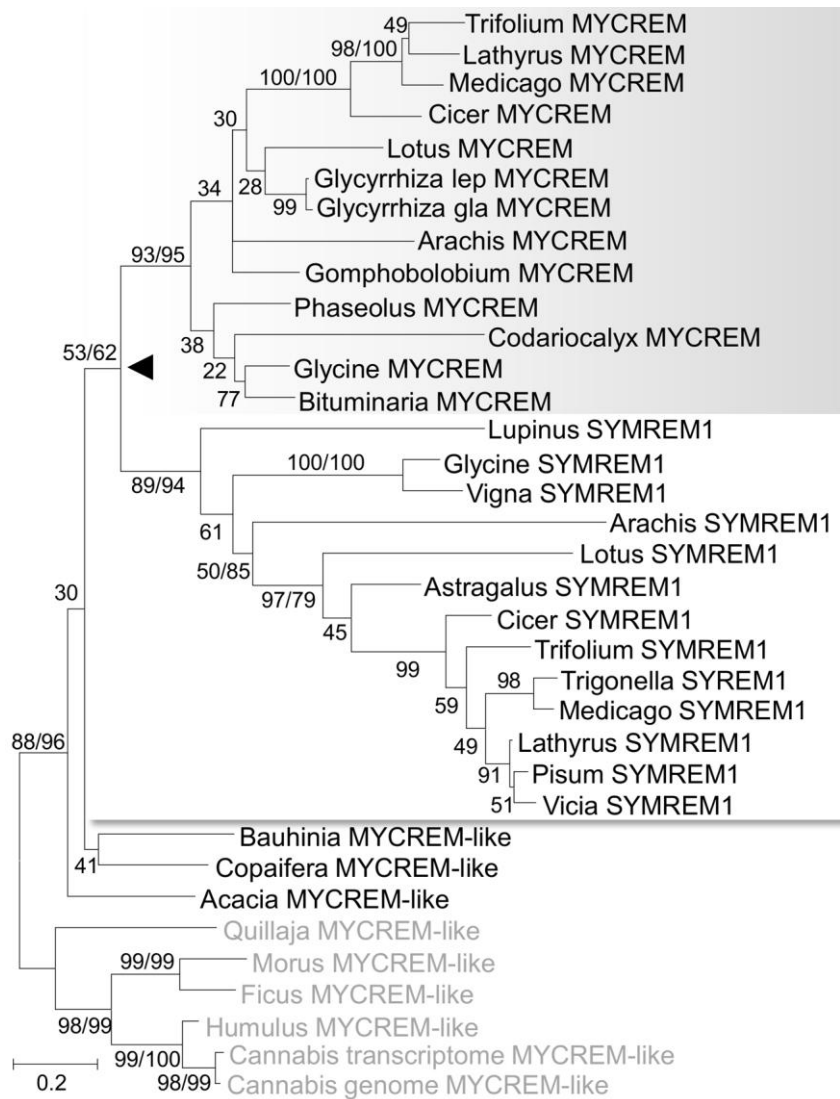


Figure 2: MYCREM evolved with symbiotic dualism. Maximum-likelihood (ML) tree of SYMREM1 and MYCREM. Bootstraps for the ML/NJ trees are indicated. Branches with a single value are only supported in the ML analysis. The black arrowhead indicates the duplication that led to the MYCREM (grey background) and SYMREM1 (white background) clades.

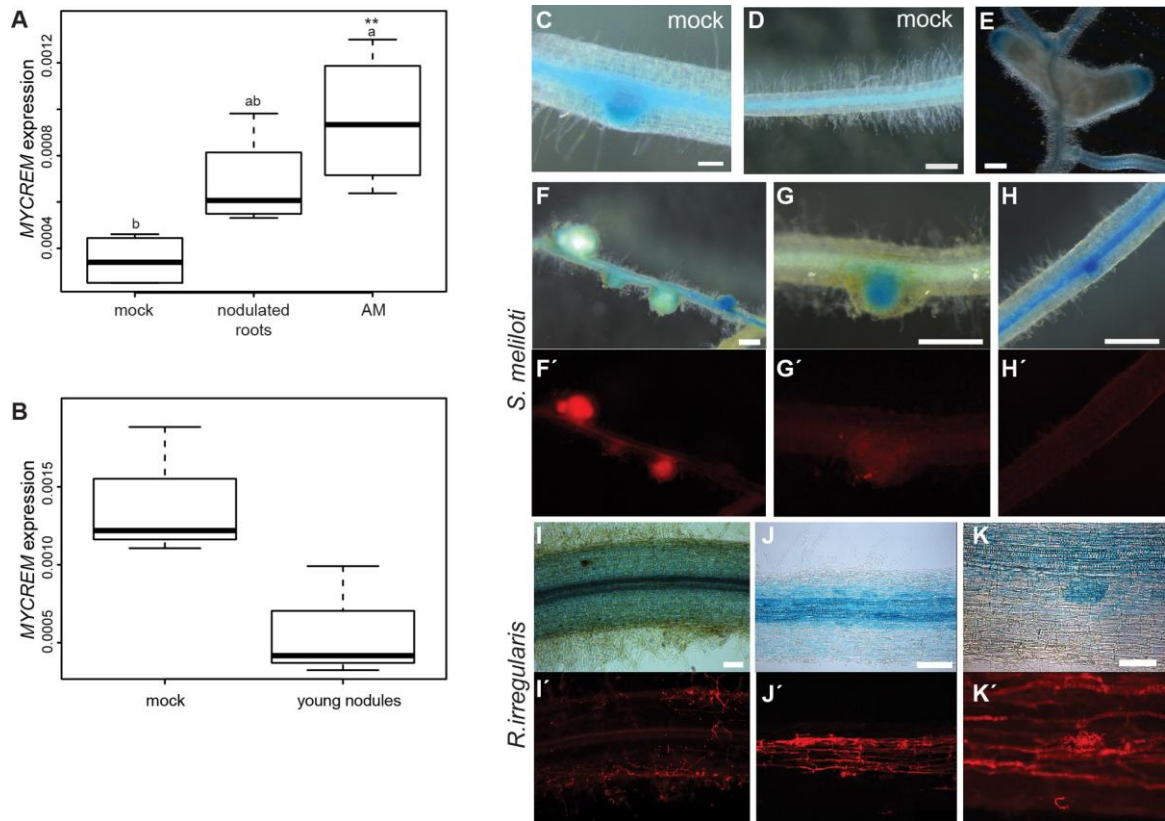


Figure 3: Global and spatial transcriptional regulation of *MYCREM*. (A-B) *MYCREM* transcripts were determined in whole root material (wild-type R108) after 5 weeks mock treatment (mock) or 4 weeks mock + 7 dpi with *S. meliloti* CFP (RNS) or 5 weeks inoculated with *R. irregularis* (AM) (n=4) (A). Expression levels were determined in 7 days old infected primordia and 7 days old uninoculated root material (n=3 x 3 pooled samples) (B). For statistical analysis a one-way ANOVA was performed followed by a TukeyHSD (significant differences indicated with small letters) and Dunnett test (significant differences indicated with an asterisk; p-value<0.05). (C-K) Analysis of *MYCREM* promoter activation using a Pro*MYCREM*::GUS reporter in transformed roots of the R108 wild-type background. (C-D) Detection of GUS staining in the vascular tissue and weakly in cortical cells (C) as well as in lateral root primordia under mock conditions (D). (E) Promoter activation in 28 days old mature nodules in the meristematic and distal zone II. (F-H) GUS activity was restricted to uninfected nodule primordia (F-G and F'-G') and LR primordia (H), but neither found in infected root nodules (F and F') nor in root cortex and epidermis cells (G and H) in roots 7-10 dpi with *S. meliloti* carrying a mCherry marker (I-K) *MYCREM* promoter activation in root 4-5 wpi with *Rhizophagus*

irrgularis. Fungal structures were stained with WGA-Alexa594 (I'-K'). Cortical root cells showed GUS staining when fungal hyphae have been present at the epidermal surface, but not the epidermal cells (I and I'). Fully colonized roots showed GUS activity in cortical cells and increased staining in arbuscule containing cells (j and k, J' and K'). [Scale bars=500µm (d-h); 100µm (C,I,J and K)].

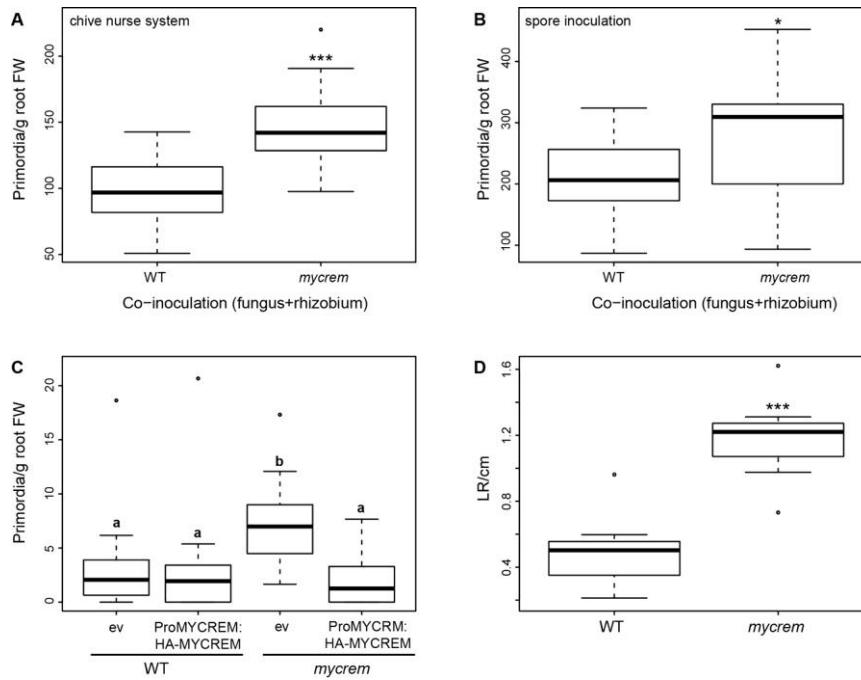


Figure 4: The *mycrem* mutant develops more nodule primordia under co-inoculation conditions. (A-B) Wild type and *mycrem* plants were inoculated with *R. irregularis* for 4 weeks in a chive nurse system (A) or with 500 spores/plant (B). Subsequently they were inoculated with *S. meliloti* CFP for 7 days. Primordia number was normalized to root fresh weight, n=20/18 in (A), n=19/20 in (B). Statistical significance was calculated via Student's t test, p<0.001 in (A), p<0.01 in (B). **(C)** For complementation analysis wild type and *mycrem* plants were transformed with either the empty vector control or with a ProMYCREM:HA-MYCREM construct. Plants positive for the transformation marker were transferred to pots containing the chive nurse system. After four weeks plants were inoculated with *S. meliloti* CFP. A one-way ANOVA with TukeyHSD post hoc test was used for statistical analysis, p<0.001, n=26/26/16/30. **(D)** The *mycrem* plants showed a higher lateral root density 7 days after growth on plates in absence of any symbiont, n=10, Student's t test, p<0.001.

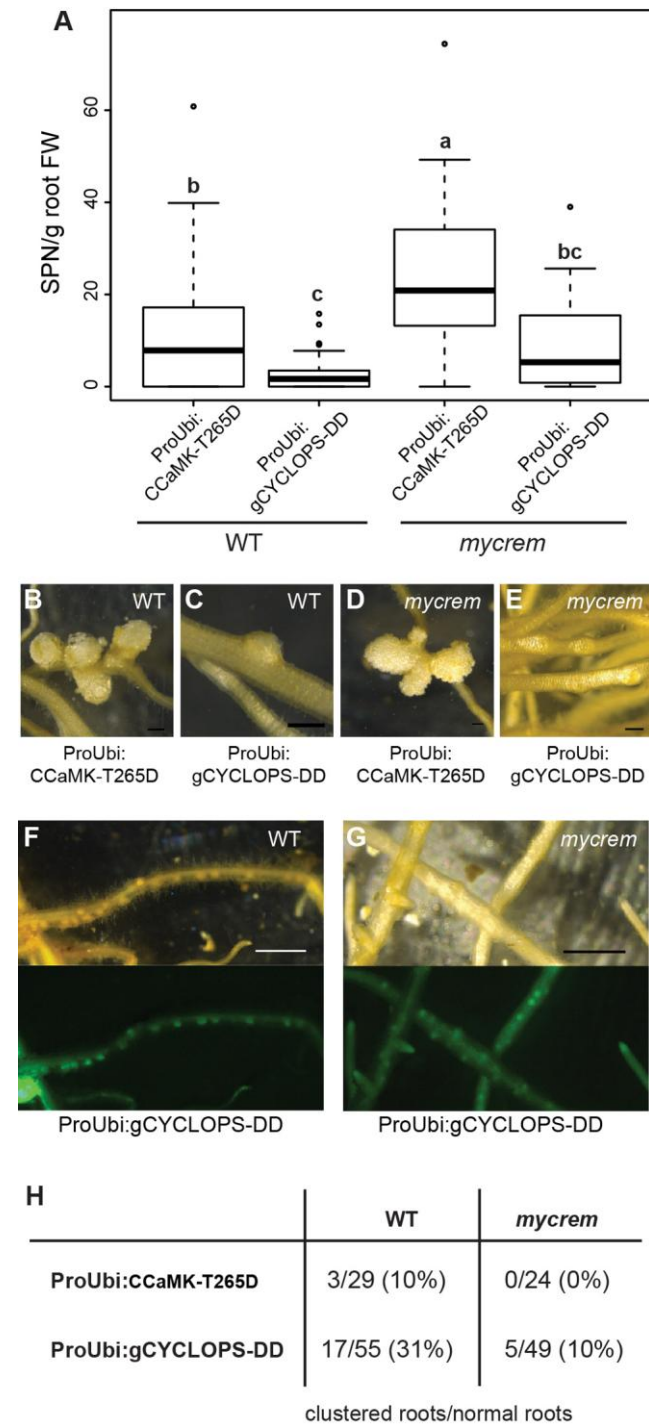
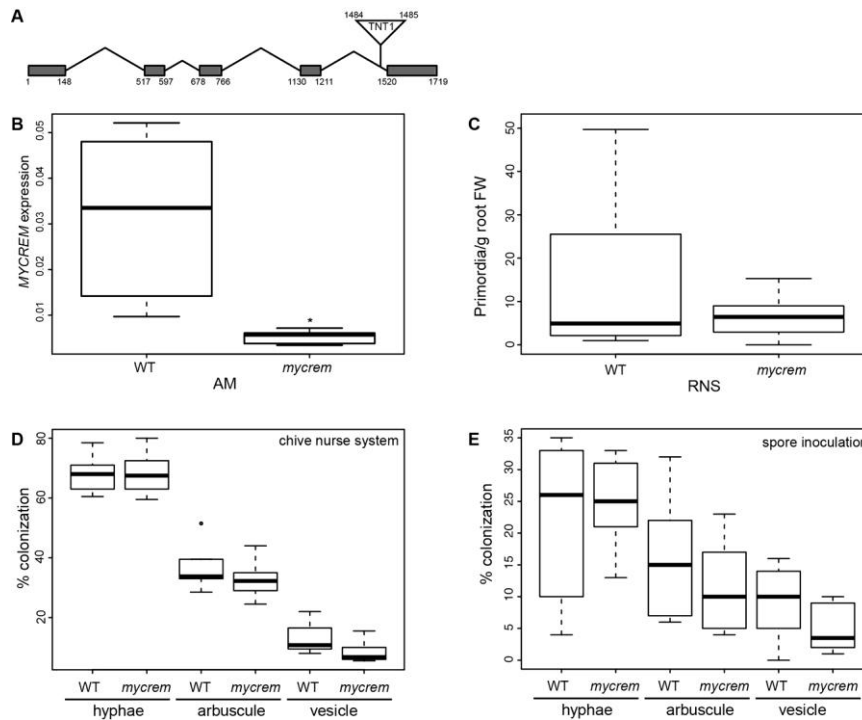
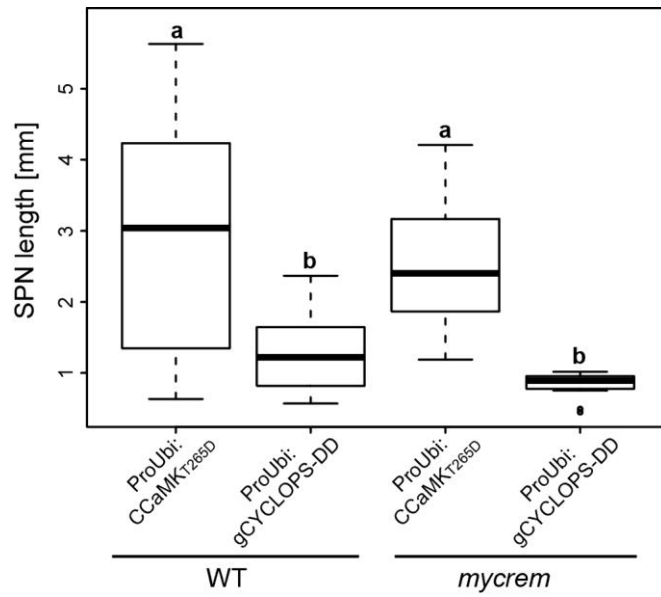


Figure 5: Overexpression of either CCaMK-T265D or gCYCLOPS-DD induced more SPN on the *mycrem* mutant. (A) Wild type and *mycrem* plants were transformed with either ProUbi:CCaMKT265D or ProUbi:gCYCLOPS-DD constructs. Seven weeks after transformation SPN were counted and normalized to the root fresh weight. Statistical significance was calculated via a one-way ANOVA with a TukeyHSD post hoc test, $p < 0.001$, $n = 33/31/24/23$. (B-C) Examples of SPN structures that were formed when overexpressing either CCaMKT265D (B) or

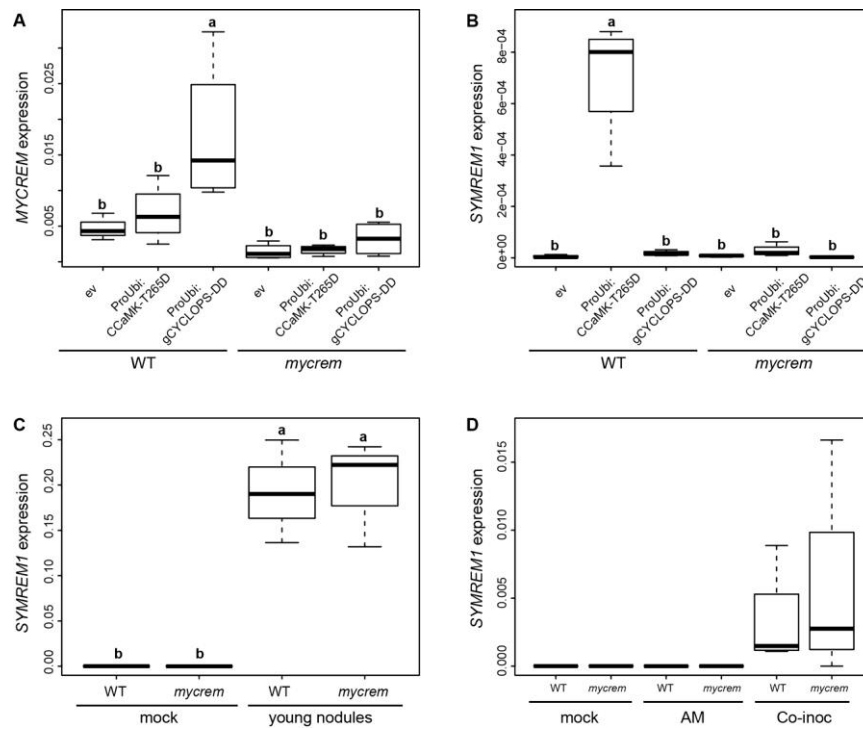
gCYCLOPS-DD (C) in the wild type background. **(D-E)** Examples of SPN structures that were formed overexpressing either CCaMKT265D (D) or gCYCLOPS-DD (E) in the *mycrem* mutant background. [Scale bars=100 μ m (B-E)]. **(F-G)** Examples of clustered roots in wild type (F) or *mycrem* (G) when overexpressing gCYCLOPS-DD. Green fluorescence indicates expression of the GFP transformation marker. [Scale bar=500 μ m]. **(H)** Number of clustered roots out of normal roots in wild type or *mycrem* when overexpressing CCaMKT265D or gCYCLOPS-DD. The relative percentage is indicated in brackets.



Supplementary Fig. 1: The *mycrem* mutant does not display a common AM and RNS phenotype. (A) Exon/intron structure of the *MYCREM* gene. In the *mycrem* mutant line the Tnt1 retrotransposon insertion was detected at the position 1484/1485. (B) *MYCREM* transcript expression normalized to *Ubiquitin* in wild type and *mycrem* mutant plants. For RNA extraction AMF colonized whole root systems of individual wild type and mutant plants were used. Roots were harvested 6wpi. Statistical significance was calculated via Student's t test, $p < 0.05$, $n = 5$ per genotype. (C) Wild type and *mycrem* plants were pre-grown for 4 weeks under non-symbiotic conditions and subsequently inoculated with *S. meliloti*-CFP in open pots for 7 days. The number of primordia was standardized to the root fresh weight ($n = 20$). (D-E) Colonization rates of the fungus *R. irregularis* four weeks after inoculation using a chive nurse system (D) and a spore inoculum (E). In both experiments $n = 6$ per genotype. No significant differences were observed in (C-E).



Supplementary Fig. 2: Spontaneous nodules do not differ in size when comparing wild type and *mycrem*. Images of SPN were evaluated using ImageJ. Size of measured SPN is shown in mm. Statistical significance was calculated by a one-way ANOVA and TukeyHSD post hoc test, $p < 0.001$, $n = 26/11/32/11$.



Supplementary Fig. 3: Transcriptional regulation of *MYCREM* and *SYMREM1*.

(A-B) *MYCREM* (A) and *SYMREM1* (B) transcript show an opposite induction in wild type background when overexpressing CCaMK-T265D or gCYCLOPS-DD and no induction in the *mycrem* background. Expression was normalized to *EF1-alpha*. For quantitative RT-PCR total RNA was extracted from whole root material of transgenic roots that showed SPN structures. Statistical significance was determined by one-way ANOVA and TukeyHSD post hoc test, $p < 0.01$ in (A), $p < 0.001$ in (B), $n = 4$ in (A) and (B). **(C)** *SYMREM1* expression in young infected primordia (7dpi) compared to mock control in wild type and *mycrem*. Expression was normalized to *Ubiquitin*. For statistical analysis a one-way ANOVA was performed followed by a Tukey HSD post hoc test, $p < 0.01$, $n = 3 \times 3$ pooled samples. **(D)** *SYMREM1* transcript expression normalized to *Ubiquitin* in wild type and *mycrem* mutant plants. RNA was extracted from whole root material either after 5 weeks mock treatment (mock) or 5 weeks inoculated with *R. irregularis* (AM), or 4 weeks inoculated with *R. irregularis* + 7 days after inoculation with *S. meliloti* CFP (Co-inoc) ($n = 4$).

Supplementary Table S1: List of the datasets used to collect sequences for the phylogenetic analysis.

Supplementary Table S2: List of sequences used to generate the phylogenetic tree in Fig. 2.

Supplementary Table S3: List of primers that have been used in this study.

Supplementary Table S4: List of expression vectors that have been used in this study. Nuclear Export Signal (NES); hemagglutinin (HA); coding signal (cds).

Supplementary Table S4: List of expression vectors that have been used in this study. Nuclear Export Signal (NES); hemagglutinin (HA); coding signal (cds).

Experiment	Vector	Reference
Fig 1	ProMYCREM(1kb):eGFP-GUS (pKGWFS7)	This work
Fig 4	LIIIβfin-ProUbi:NES_mCherry	This work
	LIIIβfin-ProMYCREM:HA-MYCREMcds_ProUbi:NES-mCherry	This work
Fig 5	pProUbi:GW__Pro35S:GFP	Maekawa et al. 2008
	pProUbi:CCaMKT _{265D} __Pro35S:GFP	Entry clone (Yano et al. 2008) and this work
	pProUbi:gCYCLOPS-DD__Pro35S:GFP	Singh et al. 2014

Supplementary Table S3: List of primers that have been used in this study.

Experiment	Name	Sequence /Reference
Genotyping	MYCREM FL 3F (WT allele)	CACCATGGGAGAATCAGAAGGTTCC
	REM2 in 2R	GTGCAACTCCACGACTACGA
	TNT F2	TCTTGTTAATTACCGTATCTCGGT
Promoter cloning	MYCREM_1Kprom_1F	CACCTTAAATGAAATGGGCGATCC
	MYCREM_1Kprom_1R	GACTTGTTCTGTGGATATATACACAG
	Bpil Bsal A ProMYCREM Fw (GG)	TTGAAGACTTTACGGGTCTCAGCGGATTTATTAATGAAATGGGCGATCC
	Bpil mut ProMYCREM Rev (GG)	ATGAAGACTT GTGTTCCATATGGCATCTC
	Bpil mut ProMYCREM Fw	ATGAAGACTT ACACCAATAAATGTTTG
MYCREMcds cloning	Bpil Bsal B ProMYCREM Rev (GG)	ATGAAGACTTCAGAGGTCTCACAGAGACTTGTTCTGTGGATATATACAC
	Bsal C MYCREM Fw (GG)	TTGGTCTCACACCGGAGAATCAGAAGGTTCCAGC
	Bsal D MYCREM Rev (GG)	TTGGTCTCACCTTAGCACTAAAGCATCCAAAC
Transcript analysis	gPCR_Ubiquitin_1F	GCAGATAGACACGCTGGGA
	gPCR_Ubiquitin_1R	AACTCTTGGGCAGGCAATAA
	EF-1 alpha-L1	Javot et al. 2011
	EF-1 alpha-R1	Javot et al. 2011
	qPCR MYCREM R108 1F	CCTGTTGTGGAAAAGGAATCTG
	qPCR MYCREM R108 1R	TATTATCAGCATGATCATCTG
	SYMREM1_f	Lefebvre et al. 2010
	SYMREM1_r	Lefebvre et al. 2010
	NIN F	Plet et al. 2011
	NIN R	Plet et al. 2011
Sequenece analysis of SMYREM1	UPM Primer1	CTAATACGACTCACTATAGGGCAAGCAGTGGTATCAACGCAGAGT
	UPM Primer2	CTAATACGACTCACTATAGGGC
	NUP	AAGCAGTGGTATCAACGCAGAGT
	5`RACE-SYMREM1-R	CTTTTGTCTTCTCATTTTCTTCCCATGC
	Nested 5`RACE-SYMREM1-R	GATTCAACCCTTGCTAGTACAGCATC
	3`RACE-Vigna-F	AGTGCATGCCATAACCTCTAC
	3`RACE-Cicer-F	GAGCTTAGACATTATGGAAGAAT

3`RACE-Trigonella-F
3`RACE-Trifolium-F
3`RACE-Pisum-F
3`RACE-Vicia-F
Nested 3`RACE-Vigna-F
Nested 3`RACE-Cicer-F
Nested 3`RACE-Trigonella-F
Nested 3`RACE-Trifolium-F
Nested 3`RACE-Pisum-F
Nested 3`RACE-Vicia-F
Vigna SYMREM1-R
Cicer SYMREM1-R
Trigonella SYMREM1-R
Trifolium SYMREM1-R
Pisum SYMREM1-R
Vicia SYMREM1-R

GGAAGTTTAATAGAAATTCTGTT
TAGAGATTCAGCTTCCATAAC
GGAATATAAATTCTGCTACCTT
ACCGCAACGTTAGACATAAATAA
ATGGAAGAACTGGGATGCAAC
ATGGAAGAATCATCACAATCAG
ATGGAAGAATCAAAGAACGGG
ATGGAAGAGACATTAAGAATG
ATGGAAGAATCAAAGAAGGAA
ATGGAAGAATCAAAGAAGGAA
TTAACTGCCAAAGCATGGAAGAAA
TTAAAACAACCTTTAAACCAAACAT
TTAACTGAAAAACCTTAAACCGCT
TTAACGGAAAGCCCTTACACCG
TTAACGAAAAAACCTTAAACCGA
TTAACGAAAAAGTCTTAAACCA

Supplementary Table S2. List of sequences used to generate the phylogenetic in Figure 2

Gene name and accession number	Species	Sequence ID	Sequence
scaffold-OQHZ-2069702- Quillaja_saponaria	<i>Quillaja saponaria</i>	Quillaja MYCREM-like	MGVEVADEAEKEAKKAEARNDIAEESKSNVIVSNNKKAASPVVQKIAGPAIEKSSGGSTSQDVLQAQVEAEKRLALIKA WEESEKTKAENKAYKKSFAVGSWENRRRKASVDAELKQIEEKWERKKAIEYEEKMKKKIAEIHQVAEEKKAMVEAKRRE MGEEEPKATESTETETPDPVPATPPLQATDQDDQDRMAVEKKEEKEEKKDQEKAGKEEKKDVAEEKSLSPVP QEKAVQKIADPVVEKNQEVDRDAVLAQVETEKRLALIKAWEESEKTKSENKAYKLSAVGAWENSKAAVEAELRAIE EKLAKKRAEYTEKMKNKVAEVHKLAEERAFVEANRREELKVEETAAKFRASGFIPKKFLRCFGS MAEEEEPKAETETPDPVPATPPLAGTDQDQGHKKEDEKQKKGKLDDEEGAKKDVAAEEKSLSPVPQEKVAPAIVC KIADPVVEKTSDEKNQEVSIDRDAVLAQVETEKRLALIKAWEESEKTKAENKAYKLSAVGAWENSKRAAVEAELRAI EEKLEKKRAEYIEKMKNKVAEVHKLAEERAFVEANRREELKVEETAAKFRASGFIPKKFLRCFGS MAEEEEAKRAEPQPPENPPPVAEEEEKKEEKEEKEAENTKDVCASEEKSLSPVPSEKPLPAPAIVQKIADPPIEKNT EVAVDRDAVLAQVETEKRLALIKAWEESEKTKADNKAYKLSAVESWENSKRAAVEAELKQIEEKFEKKRAEYTEKMK NKVVELHKVAEEKRALVEANRQEEFLKVEETAAKFRASGYSPPKFFACFSA MAEEEEAKRVPEQPPENPSPVAEEQLKKEEAKKEEVEVNSKDVCASEEKSLSPVPLEKPLPAPAIVQKVVDPFVEKNS EVAVDRDAVLAQVETEKRLALIKAWEESEKTKADNKAYKLSAVESWENSKRAAVEAELKQIEEKFEKKRAEYTEKMK KNKVVELHKIAEEKRAMVEANRQEEFLKVEETAAKFRASGYSPPKFFACFSA MAEEEEAKRVPEQPPENPSPVAEEQLKKEEAKKEEVEVNSKDVCASEEKSLSPVPLEKPLPAPAIVQKVVDPFVEKNS EVAVDRDAVLAQVETEKRLALIKAWEESEKTKADNKAYKLSAVESWENSKRAAVEAELKQIEEKFEKKRAEYTEKMK KNKVVELHKIAEEKRAMVEANRQEEFLKVEETAAKFRASGYSPPKFFACFSA MGEEETKTEPKPESTSSVNPQPPEPVAVEPEKLEKRDPAQVQEQNKVTPPPVQKVDSATKQESKDFADKDS VLARVETEKRLALIKAWEESEKTKAENRAYKLSAVGLWEDSKNASIEAQLKRIEELKREKAESVERMKNKMAVH QSAEGKRAMVEAQRREQLKVEETAEKFRSSGLYPRGFLSCFTA MAEEEEAKKSESPSQPGPPPIQDKQKEDKADPPNGVAAQHTVPVQKQVADPAKKDENDSVDRDSVFAKVEAEK RLALIKAWEESEKTKAENRAYKLSAVGLWENTKKAASVEAQLKQIEEKLERKKAIEYVEKMNNKMAEIHQSAAEKRA VVEAQRKEEFLKVEDTAAKYRSSGYAPRKLACFGA MAEEEEANKPQTQPEPQPTVSEPADPSPPSVKESDSAKEDFPNGVVQAPPSAVQKQVADPPAKNDSVDRDSV LARVVTEKRLALIKAWEESEKTKVDNKSYYKHSVAVGLWEDSKKASVQAQLKQIEEKLEKKAIEYVEKKNKIAGIHQ LAEKRAMVEANRQEEFLKVEETAASKFRAS MGEEVSNKTETESHSAVVDSVPPLQEKESDKPDPNSNENVTSPSPVQKVEDHAAEKDTEDSVSKDVMLARVLTEK RLALIKAWEESEKTKAENRAYKLSAVELWEDSRKASVEAELKQIEENMERKKAIEYVEKMKNKVAEIHRLAEEKRA NVKAQKREEFLGVEETAEKFRSRGVTPRKFFACFSA MGEEVSYKTEPESELHSPVQEHNSAQEKELEKPEPPNDKVTSPSPVAQEVADHASKKDTESVDKGHSINKL KLLKQVEKRNIFHIVLPDAMLAKVLTEKRLALIKAWEESEKTKAENRAYKLSAVGLWEDSKKASVEAQLKQIEESM EKKKAIEYVEKMKNKVAEIHRLAEEKKAIEAQAQKREEFIDLEETASKFRSRGDVPRKFFACFGG MGEEVSNKTEPETEPHVDSPVAEAEHNSPVLEKESDKPEPPNDKPTSPSPLAQDVADHANKDTEESVDKDA MLARVVTEKRLALIKAWEESEKTKAENRAYKLSAVGLWEDSKKASVEAELKQIEENLEKKAQYVEKLNKAAEI HRLAEEKRAIVEAQAQKREEFIDLEETASKFRSRGDAP MGEEEDSNLNVESQTEFVDSVSEQEPQVEEKESEKPEAVTQEPHKEVPSPIVQNVADDDAKKVTGDSVDRDAA LARVVTEKRLALIKAWEESEKTKAENRAYKLSAVGLWEDSRKASIEAELKQIEENLERKKAIEYAEKMKNKIAEIHQ AAEEKRATVEANKKEEFLEVEETAAKFRSRGVAPKLLFACFSA
scaffold-XVJB-2052865- Morus_nigra	<i>Morus nigra</i>	Morus MYCREM-like	
scaffold-EDHN-2051318- Ficus_religiosa	<i>Ficus religiosa</i>	Ficus MYCREM-like	
scaffold-AQGE-2051814- Humulus_lupulus	<i>Humulus lupulus</i>	Humulus MYCREM-like	
scaffold-BJSW-2069095- BJSW-Cannabis_sativa- 4_samples_combined	<i>Cannabis sativa</i>	<i>Cannabis transcriptome</i> MYCREM-like	
CanSat genome PK08385.1	<i>Cannabis sativa</i>	<i>Cannabis genome</i> MYCREM-like	
scaffold-JETM-2090896- Bauhinia_tomentosa	<i>Bauhinia tomentosa</i>	Bauhinia MYCREM-like	
scaffold-RKLL-2063873- Copaifera_officinalis	<i>Copaifera officinalis</i>	Copaifera MYCREM-like	
scaffold-ZCDJ-2090156- Acacia_argyrophylla-Nov. Extraction	<i>Acacia argyrophylla</i>	Acacia MYCREM-like	
Phvul.002G155800.1	<i>Phaseolus vulgaris</i>	Phaseolus MYCREM	
Glyma11g02740.1	<i>Glycine max</i>	Glycine MYCREM	
scaffold-TVSH-2065612- Bituminaria_bituminosa	<i>Bituminaria bituminosa</i>	Bituminaria MYCREM	
Lotus japonicus MYCREM	<i>Lotus japonicus</i>	Lotus MYCREM	
scaffold-SUAK-2037307-	<i>Codariocalyx</i>	Codariocalyx MYCREM	MAENDSQNHETNMLSSPSPLGQNDVVDGAGKDTGDFDKDALLAKVVVEKRFALIRAWEESEKTKAENRAHK

Codariocalyx_motorius	<i>motorius</i>		KL SAVGLWEEGKKASIEAQLKKLEQDMEIKKAEYVEKMKNKVAEIHRSAAEEKRAIVKAKKMEEFVDLEDTAEKFRSL AETPRKLFSCFSL DMGELEGSDLNKTESSELEVPEEHSPVLVKESDALNTISQEPNDHQVTSIVDDDDQKVVEDHADNKETGDHDDKDDT KDSTDRDTGLAKIVAEKRLALIKAWEESEKTKAENRAYKKQSAVGLWEEERKASIEAQLKKFEENLERKKVEYVLMK KNEVAEIHQYAEKRAIVEAQKREEFLDLEDTAAKFRSRGVAPKFFACFNN NKTESQQPQPLDPVPEESSPLQENESDIVNQEPNQSSTLDDQKVADDHAENKETENHDDNKDTKGSSDKDTG LAKIVAEKRLALIKAWEDSEKTKAENRAFKKQSAVGLWEEERKASIEAQLKKFEENLERKKVEYVLMKNDIAEIHQY AEKRAIVEAQKREEFLDLEETA AKFRSRGVAPKFLGCFSS MGESEGSINKTESPQLQSLLDPVPEELSPVVEKDSSETLSTISISQEPNQQAISTLDDQKVADDHADNKETGDHDDK KDAKSTDRDAGLAKIVAEKRLALIKAWEESEKTKAENRAYKKQSSVGLWEEERKASIEAQLKKFEENLERKKVEY VSKMKNELAEIHQYAEKRAIVEAQKREECLELEETA AKFRSRGVAPKFLGCFSA MESSQLHSLDSVQVKELEKDPPTASAVSHQSLEEPKEHAITAPLVQKVEDSGGNKGTVDSVDRDAELARVVSEKR LALIKAWEESEKTKAENRAYKKLSAVGLWESKKNASVEAQLKIIENLERKKA EYAEKMKNKIADIIHRSAAEEKRAMVE AQKREEFIELEETA AKFRSSGRTPAKFFACFKA MEQEGSNSNKTESQPQPVDSVPEEHSLSLAQETESEKPDNPNTASHLTSQVVQQTADHAGIKDEGDSVDRDAG LARVVAEKRLALIKAWEESEKTKAENRAYKKLSAVGLWEDSKKASIEAQLKKIEENLERKKA EYVEKMKNKIAEIH SAEDKRTIVEAQKKEEFLELEETASKFRSRGDMPRKFFACFSG MEEEGSNVNTKTESPQLDSVPEEQEHSPVQKEESEKPDPSNAVVNQKPNQVTSPLVQKVADDAGKDDTGD SIDRDAGLARVVAEKRLALIKAWEESEKTKAENRAYKKLSAVGSWEEERKASIEAQLKKIEEDLERKKA EYVEKMRN KIAEIHQSAEERRAIVEAQKREEFLEVEDTA AKFRSRGVTPRKFFACFSG MEEEGSNVNTKTESPQLDSVPEEQEHSPVQKKEESEKLDPSNAVVNQEPNEQVTSPLVQKVADDAGKDDTGD SIDRDAGLARVVAEKRLALIKAWEESEKTKAENRAYKKLSAVGSWEEERKASIEAQLKKIEEDLERKKA EYVEKMRN KIAEIHQSAEERRAIVEAQKREEFLEVEDTA AKFRSRGVTPRKFFACFSG MGEDGNEKAKSKSES VVFVATPSSSFPTPPHQSPLEHGEDPKSPRSSNFVQQUESTLMSHLINIPILKHMGTSP MVQKVEDESPDAETDTKVLVDRGDVHARVEEEKRSLIKAWEDNEKTKVENGAYKQSSIGFWEDSKKASVEAN LKKFEEKLERKKA EYVEKMKNKIAQIHLIAEERKATIKAKREEELKVEETA AKFRSSGGYSPRKLFPFCFGG MGVSGNQRGKEVENTHTSSGVRQEYAFSPLNLSLFAKWNRFRSFLVILSKKVKKKVPTTTRTDSKDSVDRDAV LARVESEKRLALIRAWEESEKTKAENRAYKRHNNAVVLWENSKKASAEHLKRIEEKLDRNKAKCVEKMQNNVAE IHRTAEKRAMIEANRGEFLEIEEKA AKFRTRGYSPRKYLPFCFGSS MEETGMQLGKEVNEGTSNTVKERSISPLDLGLFDIWNRFRSFLVILSKKVKKKVPPITRSDTKDSIDRDAV LARVES EKRVALIKAWEESEKTKAENRAYKRHNNAVVLWENSKKASAEHLKRIEEKLDRNKAKCVEKMQNNVAE KRAMIEAYKGEFLEIEEKA AKFRTRGYSPRKLFPFCFGS MFMGETSDNNSNSSDSEDVPHYSYTENNLLKYQEAATSSARKDGTDLGGLARLEAEKRALIKAWEESEKTKI DNRAYKMQFVAVGLWEDSKKASVEAKLKNAEKLERKKA EYFEKMQNKIAEIHMAEEKRAGIEAQRGKGLLKIED TAENFRTRGYSPKKILSCFTA MGEETKHCDQCGASASASEATVLSQLRLSEVLKLESQNAESSNSTLTITRQGSTTNPSPYPLDQDLDAETDN INTSIDRDAV LARVESQKRLALIKAWEESEKTKAENRAYKRHNNAVVLWENSKKASAEHLKRIEEKLDRNKAKCVEKMQNNVAE IMQNKIAETHRLADEKKALIEAQKGEVLEKVEETA AKFRTRGYVPPKFLSCFNFSF MAESGNEKPESSSVATPPPPPPQTQELSQLLKLKEPEHAEASSSVKQEHNDPPLDQVPTVGNTKDSIDRDAV LARVES EKRVALIKAWEESEKTKAENRAYKRHNNAVVLWENSKKASAEHLKRIEEKLDRNKAKCVEKMQNNVAE QEKKALIEAQKGEFLEKVEETA AKFRTRGYVPRKLLACFGI MEESSQSESVATPITPPPPQSPQLRELSHFVKEKPEPQGTSTNIVKQEYTDQFFQPKDHATSSLDQIPDAGTDT KDSVDRD TVLARVESQKRLALIKAWEESEKTKAENRAFQKMSAVDLWEDNKKASIEAKFKGIEVRLDKKKT EYVE IMQNKIAEIHHSAAEEKKAMIEAQKGEELKVEETA AKFRTRGYVPRRLLGCFGLKLF
Trifolium pratense GAOU01009771.1	<i>Trifolium pratense</i>	Trifolium MYCREM	
scaffold-KNMB-2011028- Lathyrus_sativus	<i>Lathyrus sativus</i>	Lathyrus MYCREM	
Medtr5g010590.1	<i>Medicago truncatula</i>	Medicago MYCREM	
Araip.10030403.1	<i>Arachis ipaensis</i>	Arachis MYCREM	
scaffold-VLNB-2073520- Gompholobium_polymorphum	<i>Gompholobium polymorphum</i>	Gompholobium MYCREM	
scaffold-JTQQ-2067397- Glycyrrhiza_lepidota	<i>Glycyrrhiza lepidota</i>	Glycyrrhiza lep MYCREM	
scaffold-PEZP-2008216- Glycyrrhiza_glabra	<i>Glycyrrhiza glabra</i>	Glycyrrhiza gla MYCREM	
Lupinus angustifolius KB405353.1	<i>Lupinus angustifolius</i>	Lupinus SYMREM1	
GLYMA_08g012800	<i>Glycine max</i>	Glycine SYMREM1	
Vigna	<i>Vigna</i>	Vigna SYMREM1	
Araip.10033874.1	<i>Arachis ipaensis</i>	Arachis SYMREM1	
LjSYMREM1	<i>Lotus japonicus</i>	Lotus SYMREM1	
scaffold-HJMP-2071780- Astragalus_membranaceus	<i>Astragalus membranaceus</i>	Astragalus SYMREM1	
Cicer XP_012572140	<i>Cicer arietinum</i>	Cicer SYMREM1	

Trifolium pratense	<i>Trifolium pratense</i>	Trifolium SYMREM1	MEETLKNEQSIDTPNAPPDQPLELSYFVEEKKPKNEGTSSSIVKQERIVRDHATSPLNQIPPAAGTDTKDSVDRDA VLARVESQKRLALIKAWEEENEKTKVENRAYKMQSAVDLWEDNKKSSIEAKFKGIEVKLDKKKSEYIEVMQNKIAEIH LSAEEKKAMIEAQKGEEIVKVEETAAKFRTRGYEPRRLLGCFGFGVRAFR MEESKNGKIESLDTPLLPQSEPEPREFSYFLEEKEPENEGTSNSVVKQERITSDHATSSLDQTPGSGTDTKDSV DRVPLDAVLARVESQKRLALIKAWEEENEKTKVENRAYKMQSAVDLWEDNKKASIEAKFKGIEVKLERKKSEYVEV MQNKIGIEIHKSAAEEKKAMIEAQKGEEILKVEETAAKFRTRGYQPRKLLGCFSGLRFFS MEESKNKQLELVDLTLPLPQSESEPREFSYFLEEKEPGNEGTSSSVVKQERVVSDHATSSVDQTTAAGTDTKDS VDRDAVLARVESQKRLALIKAWEEENEKTKVENRAYKMQSAVDLWEDDKKASIEAKFKGIEVKLDRKKSEYVEVM QNKIGIEIHKSAAEEKKAMIEAQKGEEILKVEETAAKFRTRGYQPRRLLGCFSGLRFFS MEESKKEQLESDDDDTPSPPPQSQELSYFLKENEPENEGTSNSVVKQERNERDHASSLDQIPGAGIDTKDSVDRD AVLARVESQKRLALIKAWEEENEKTKVENRAYKMQSAVDLWEDNKKSSIEAKFKGIEVKLDQKKSEYVEDMQNKI AEIHKSAAEEKKAMIEAQKGEEILKVEETAAKFRTRGYEPRRLLGCFGLRFR MEESKKEQLESDDDDTPSPLPQSQELSYFLKEKEPENEGTSNSAVKQERNERDYASSSLNQIPGGGTDTKDSVD RDAVLARVESQKRLALIKAWEEENEKTKVENRAYKMQSAVDLWEDNKKSSIEAKFKGIEVKLDQKKSEYVEDMQ NKIAEIHKSAAEEKKAMIEAQKGEEILKVEETAAKFRTRGYEPRRLLGCFGLRFR MEESKKEQQPESDDDDIPSPPPQSQELSYFLKENEPENEGTSNNVVKQERNERDHALDQIAGGGTDTKDSVERD AVLARVESQKRLALIKAWEEENEKTKVENRAYKMQSAVDLWEDNKKSSIEAKFKGIEVRLDQKKSEYVESMQNKIA EIHKSAAEEKKAMIEAQKGEEILKVEETAAKFRTRGYEPRRFLGCFGLRFR MGEEDSNINKTEPESLDSVPEENFTIQENESEKPNLNTINHESNELVASSLDPKVVVDHADSKETGEHDDKDDTT RDSTGRDAGLTRIVTEKRLALIKAWEESEKTKAENRAYKQSAVVLWEESRKASIEAQLKFKFEDKLERKKVEYVE KMKNEIAEIHQYAEKRAIVEAQKGEEILELEETASKFRSRGVVPRKFFGCFSG*
Trigonella	<i>Trigonella</i>	Trigonella SYREM1	
Medtr8g097320.1	<i>Medicago truncatula</i>	Medicago SYMREM1	
scaffold-KNMB-2012141-Lathyrus_sativus	<i>Lathyrus sativus</i>	Lathyrus SYMREM1	
Pisum	<i>Pisum sativum</i>	Pisum SYMREM1	
Vicia	<i>Vicia</i>	Vicia SYMREM1	
Cicer XP_004511588.1	<i>Cicer arietinum</i>	Cicer MYCREM	

Supplementary Table S1. List of the datasets used to collect sequences for the phylogenetic analysis.

Order	Family	Sub-family (for Fabaceae)	tribe (for Fabaceae)	Data type	Tissues (for transcriptomes)	database
Fabales	Fabaceae	Mimosoideae	Acacieae	transcriptome	not described	http://www.onekp.com/blast.html
Fabales	Fabaceae	Papilionoideae	Dalbergieae	genome		http://peanutbase.org/
Fabales	Fabaceae	Papilionoideae	Galegeae	transcriptome	shoot and roots	http://www.onekp.com/blast.html
Fabales	Fabaceae	Caesalpinioideae	Cercideae	transcriptome	leaves	http://www.onekp.com/blast.html
Fabales	Fabaceae	Papilionoideae	Psoraleeae	transcriptome	leaves and buds	http://www.onekp.com/blast.html
Rosales	Cannabaceae			transcriptome	stems	http://www.onekp.com/blast.html
Rosales	Cannabaceae			genome		http://genome.ccb.utoronto.ca/cgi-bin/hgGateway
Fabales	Fabaceae	Papilionoideae	Cicereae	genome		NCBI
Fabales	Fabaceae	Papilionoideae	Desmodieae	transcriptome	leaves and stems	http://www.onekp.com/blast.html
Fabales	Fabaceae	Caesalpinioideae	Detarieae	transcriptome	leaves	http://www.onekp.com/blast.html
Rosales	Moraceae			transcriptome	leaves	http://www.onekp.com/blast.html
Fabales	Fabaceae	Papilionoideae	Phaseoleae	genome		https://phytozome.jgi.doe.gov
Fabales	Fabaceae	Papilionoideae	Galegeae	transcriptome	shoot and roots	http://www.onekp.com/blast.html
Fabales	Fabaceae	Papilionoideae	Galegeae	transcriptome	shoot and roots	http://www.onekp.com/blast.html
Fabales	Fabaceae	Papilionoideae	Mirbelieae	transcriptome	leaves and buds	http://www.onekp.com/blast.html
Rosales	Cannabaceae			transcriptome	leaves	http://www.onekp.com/blast.html
Fabales	Fabaceae	Papilionoideae	Fabeae	transcriptome	shoot and tuber	http://www.onekp.com/blast.html
Fabales	Fabaceae	Papilionoideae	Loteae	genome		http://www.kazusa.or.jp/lotus/
Fabales	Fabaceae	Papilionoideae	Genisteae	genome		NCBI
Fabales	Fabaceae	Papilionoideae	Trifolieae	genome		http://jcv.org/medicago/
Rosales	Moraceae			transcriptome	flower, stem, leaves	http://www.onekp.com/blast.html
Fabales	Fabaceae	Papilionoideae	Phaseoleae	genome		https://phytozome.jgi.doe.gov
Fabales	Quillajaceae			transcriptome	leaves	http://www.onekp.com/blast.html
Fabales	Fabaceae	Papilionoideae	Trifolieae	genome		NCBI
Fabales	Fabaceae	Caesalpinioideae	Cercideae	transcriptome	leaves and young flowers	http://www.onekp.com/blast.html

Fabales	Fabaceae	Caesalpinioideae	Cassieae	transcriptome	young leaves and shoot	http://www.onekp.com/blast.html
Fabales	Fabaceae	Mimosoideae	Mimoseae	transcriptome	young leaves and shoot	http://www.onekp.com/blast.html
Fabales	Fabaceae	Caesalpinioideae	Caesalpinieae	transcriptome	leaves and young flowers	http://www.onekp.com/blast.html
Fabales	Fabaceae	Papilionoideae	Sophoreae	transcriptome	leaves	http://www.onekp.com/blast.html
Fabales	Fabaceae	Papilionoideae	Genisteae	transcriptome	roots, phosphate starved roots	NCBI
Fabales	Fabaceae	Papilionoideae	Genisteae	transcriptome	leaves	http://www.onekp.com/blast.html
Fabales	Fabaceae	Papilionoideae	Genisteae	transcriptome	leaves and flowers	http://www.onekp.com/blast.html

1.4. Manuscript 2

The formation of an infection-related membrane domain is controlled by the sequential recruitment of scaffold and receptor proteins.

Stratil, T.F., Popp, C., Konrad, S.S.A., Marín, M., Folgmann, J., and Ott, T.

Proceedings of the National Academy of Sciences, USA

Status: Invited for resubmission | Year: NN | DOI: NN

The formation of an infection-related membrane domain is controlled by the sequential recruitment of scaffold and receptor proteins

Short title: Assembly of an infection-related microdomain

Thomas F. Stratil, Claudia Popp, Sebastian S.A. Konrad, Macarena Marín, Jessica Folgmann, Thomas Ott*

Institute of Genetics, Ludwig-Maximilians-Universität München, Großhaderner Str. 2-4,
82152 Planegg-Martinsried, Germany

* To whom correspondence should be addressed: Thomas.Ott@bio.lmu.de

Classification: BIOLOGICAL SCIENCES

Keywords: membrane microdomain, symbiosis, scaffold proteins, receptor, remorin, flotillin

ABSTRACT

Intracellular colonization of plant cells by symbiotic bacteria is a critical step for the host that requires stringent surveillance circuits at the plasma membrane to keep exclusive control over the infection process. Accumulating evidence suggests that such perception and signal transduction complexes are pre-formed in membrane compartments such as mesoscale membrane domains (MMDs). However, neither the existence of pathway-specific MMDs nor the essential steps and components for their controlled assembly have been identified. Here, we describe the sequential and spatial organization of membrane-resident signalling proteins that are indispensable for the intracellular infection of *Medicago truncatula* roots by symbiotic bacteria. Mechanistically, we show that the flotillin FLOT4 and the remorin SYMREM1 act as molecular scaffold proteins that are required and sufficient to induce compartmentalization of the entry receptor LYK3 *in vivo*. While FLOT4 provides the initial core of a symbiosis-related MMD, the stimulus-dependent recruitment of LYK3 into this site requires the presence of the second order scaffold SYMREM1. Under these conditions, as found upon the onset of rhizobial infection, all three proteins coalesce into the same and actin-dependent MMD. Reciprocally, combinatorial expression of these proteins in a heterologous cell system that is devoid of the scaffolds and LYK3 was sufficient to heterologously reconstitute this specialized membrane domain *in vivo*.

SIGNIFICANCE STATEMENT

Considering the dense packing of proteins at the plasma membrane (PM) and the plethora of environmental stimuli tissues need to perceive and to integrate simultaneously, cells evolved membrane-based substructures called ‘mesoscale membrane domains’ (MMDs). These compartments may serve as central hubs for the specific assembly of signalling complexes. Even though many individual proteins have been described to laterally segregate into MMDs at the cell surface, it has been a long-standing question whether pathway-specific components indeed localize to the same MMD. In our study we not only provide evidence for this intriguing phenomenon but also unravel essential molecular building blocks and the sequence of events that are required and sufficient to maintain an infection-related MMD *in vivo*.

INTRODUCTION

Our view on plasma membranes (PM) as being uniform bilayers has recently been entirely revised when systematic studies reported on the segregation of a large number of membrane resident proteins into distinct clusters on the PM (1, 2). One class of these inhomogeneous protein distributions appears as punctate foci on cell surfaces in so called ‘mesocale membrane domains’ (MMDs). Most likely, these structures are composed of several different proteins and their lateral mobility is restricted by cytoskeleton components such as actin (3, 4) and the cell wall (5). Conceptually, this compartmentalization of membranes allows the spatial assembly of functionally related components and possibly pre-formation of signalling complexes. This hypothesis is supported by systematic and pair-wise co-localization analyses of almost 20 different plant MMD marker proteins from the remorin and flotillin protein families, which revealed a great diversity and co-existence of different MMDs on the same cell membrane (1). Remorins are plant-specific proteins that associate with the cytosolic face of the PM by S-acylation and potentially direct lipid binding and protein-protein interactions. There, they can interact with different proteins including receptor-like kinases (6-10). Although their precise functional role has not been determined, it has been hypothesised that they might act as molecular scaffold proteins that facilitate higher order complex formation (11). Similar mechanisms have also been proposed for flotillin proteins (12, 13). As in metazoans, plant flotillins might also play roles during endocytosis (14).

Interestingly, the legume-specific remorin SYMREM1 and flotillins FLOT2 and FLOT4 from *Medicago truncatula* are required for successful root infection by *Sinorhizobium*

meliloti during root nodule symbiosis (RNS) (7, 15). This mutualistic interaction is characterized by the intracellular colonization of roots that is preceded by the formation of primary infection threads (ITs) in root hairs (16, 17). ITs are tip growing tunnel-like structures surrounded by a plasma membrane that encapsulate rhizobia during the infection process and guide them in a tightly regulated manner towards dividing root inner cortical cells, the site of intracellular release (16, 17). Infection strictly depends on the molecular recognition of strain-specific rhizobial signalling molecules, called Nod Factors (NFs)(18), which is mediated by the two plasma membrane-resident LysM-type receptor-like kinases (RLKs) NOD FACTOR PERCEPTION (NFP) (19, 20) and LYSIN MOTIF RECEPTOR KINASE 3 (LYK3) (21, 22) that can interact with SYMREM1(7). Interestingly, LYK3 was also shown to label discrete MMDs in root hairs and potentially in the L1 and L2 layers at the apex of root nodules (23, 24). While LYK3-labelled MMDs are laterally dynamic in the absence of rhizobia, the protein is immobilized upon inoculation of root hairs with *S. meliloti*. This mechanistically unresolved transition coincides with the co-localization of LYK3 and FLOT4. Therefore, RNS provides an excellent system to assess functional and multi-component compartmentalization of proteins in plants. It may also allow the identification of essential molecular MMD building blocks and to unravel the temporal sequence of events that underlay their formation *in vivo*.

Here we show that actin, FLOT4, LYK3 and SYMREM1 act as core MMD components, which are consecutively recruited into the same structure in a spatially and temporarily controlled manner. Additional phenotypical data strongly suggest that FLOT4, LYK3 and SYMREM1 act in the same signalling pathway. Combinatorial expression of these

proteins in a heterologous model system indeed allowed the molecular reconstitution of this MMD *in vivo*. Therefore, FLOT4, LYK3 and SYMREM1 act as central and specific molecular building blocks for the formation of an infection-related MMD in legumes.

RESULTS

Any functional interplay between the LYK3 receptor and the putative scaffold proteins FLOT4 and SYMREM1 requires overlapping expression profiles and phenotypical patterns. Thus we first assessed this by reinvestigating these issues for SYMREM1. For this, the promoter of *SYMREM1* was used to drive the expression of a nuclear localized tandem green fluorescent protein (GFP) (*pSYMREM1:NLS:2xGFP*) in transgenic *Medicago truncatula* hairy roots. While no induction of the reporter was detected in uninoculated control roots (Fig. 1A), the promoter was weakly but reproducibly activated upon rhizobial inoculation in root epidermal and outer cortical cells as indicated by nuclear fluorescence (Fig. 1B-E). In contrast, a *pFLOT4:NLS:2xGFP* reporter was already active in control roots (Fig. 1F) and was further induced upon rhizobial inoculation (Fig. 1G-J). This resembled patterns of the homologous *SYMREM1* gene in *L. japonicus* and those reported for *Medicago* FLOT4 and LYK3. To strengthen these data genetically, we investigated whether the *symrem1-2* mutant exhibits an early infection phenotype in addition to the effect on nodule maturation that was reported earlier (7). To test this, two independent *symrem1* mutant alleles were inoculated with the symbiont *S. meliloti* and primary infection threads in root hairs were scored 7 days post inoculation (dpi). Indeed, we found significantly less mature ITs on *symrem1* mutants in comparison to the wild-type (Fig. 1K). As these mutants still develop some wild-type like infection

threads, we reinvestigated the nodulation phenotype. While short-term exposure to rhizobia resulted in decreased nodule numbers (7), the number of mature nodules was similar to those found on wild-type plants after six weeks. However, significantly more white and aborted nodules were found on these plants (Fig. 1M) indicating that more infection attempts were required for successful infection of nodule primordia. Both phenotypes were complemented upon expression of an YFP-SYMREM1 construct (Fig. 1L-M) demonstrating the transposon insertion in the *SYMREM1* locus to be the causative mutation and functionality of the fluorophore-tagged fusion protein. Again, striking similarities with the primary infection phenotypes (aborted ITs) in FLOT4 and LYK3 knock-down experiments (15, 21) provide further strong evidence that all three proteins function in the same pathway.

In the following we addressed this question by cell biological approaches. To provide a solid basis for the interpretation of these data and conclusions, we first expressed SYMREM1 alone and carefully determined the overall MMD density at the PM. For this, all images were segmented and the resulting masks were used for quantification as described earlier (25). On average, the expression of YFP-SYMREM1 resulted in labelling of MMDs in epidermal and outer cortical cells with a density of 0.057 domains/ μm^2 (standard error (SE)=0.0051; n=47) (Fig. 2A).

Recent evidence suggests that remorins not only bind actin directly (26) but, more generally, that MMDs in plants depend on an intact cytoskeleton (1, 27). To test this, we induced drug-dependent microtubule and actin depolymerisation by applying oryzalin and cytochalasin D, respectively, to root epidermal cells expressing YFP-SYMREM1 (Fig. 2B-C). While oryzalin treatment did not significantly affect SYMREM1 domain

patterning (density= 0.062 domains/ μm^2 ; SE= 0.0058; $p= 0.54$) (Fig. 2b), the application of cytochalasin D resulted in strong and highly significant reduction of SYMREM1-labelled MMDs (density=0.018 domains/ μm^2 ; SE=0.0012; $p= 4.74\text{E}^{-10}$) (Fig. 2C). The efficiency of both treatments was independently confirmed in roots expressing the microtubule binding domain of the MICROTUBULE ASSOCIATED PROTEIN 4 (MAP4) or the actin binding peptide Lifeact (Fig. S1). In both cases application of the corresponding drug resulted in an effective distortion of the individual cytoskeleton components (Fig. S1). These data demonstrate an actin-dependency of MMDs labelled by SYMREM1 and provide the first and essential molecular building block for this domain. As previously demonstrated, the two flotillins FLOT2 and FLOT4 respond to rhizobial infection (15). Interestingly, MMDs targeted by these proteins showed wild-type like localization patterning in a range of receptor mutants while only the density of MMDs labelled by FLOT4 was significantly altered in the LYK3 mutant allele *hcl-1*. This mutant carries a glycine to glutamate mutation in the conserved GxGxxG motif of the kinase domain (22) that results in a kinase-dead variant of the LYK3 receptor (28). Thus, we tested whether SYMREM1-labelled MMDs are also altered in any of the receptor mutant alleles. The expression of the YFP-SYMREM1 fusion protein in transgenic *M. truncatula* roots (wild-type A17 background) resulted in the expected MMD-labelling pattern in root epidermal and outer cortical cells (Fig. S2A). Additionally, no differences to wild-type plants were observed upon expression of this construct in roots of the RLK mutants *nfp-2* and *dmi2-1* and the LYK3 mutant allele *hcl-4* (Fig. S2B-D). In contrast, the *hcl-1* allele showed remarkably altered SYMREM1 localization (Fig. S2E), which was restored in a complemented *hcl-1* mutant (*hcl-1* comp.; Fig. S2F) (23).

These data indicate a functional link between SYMREM1 and LYK3 and imply an association with FLOT4. To test this more specifically we co-expressed FLOT4 and SYMREM1 in wild-type *M. truncatula* roots and analysed their subcellular localization. To substantiate such experiments quantitatively and statistically we used large replicate numbers and calculated Pearson Correlation Coefficients ‘Rr’ between all pixels of the two corresponding channels in any image. In addition, we applied a Costes’ Randomization procedure where blocks of 10x10 pixels were randomized within one channel of an image (e.g. YFP-SYMREM1) and calculated the random Pearson Correlation Coefficient ‘rd Rr’ between these artificially generated and the original images of the corresponding second channel (here FLOT4-mCherry). Indeed, SYMREM1 (Fig. 3A) and FLOT4 (Fig. 3B) labelled distinct MMDs that greatly co-localized with $Rr = 0.344$ (SE= 0.027) (Fig. 3C-G). This was significantly different to values obtained by image randomization (rd Rr= 0.043; SE=0.008; $p=5.78E^{-09}$). In line with these findings, both proteins followed the observed short parallel array-like pattern when being co-expressed in the *hcl-1* mutant background (Fig. S2G-I). These data clearly demonstrate that SYMREM1 and FLOT4 are indeed targeted to the same MMD in *M. truncatula* roots. Interestingly, domain density of SYMREM1 increased by about 7-fold (density=0.395 domains/ μm^2 ; SE=0.0581) during ectopic co-expression with FLOT4 in wild-type roots compared to the individual expression of SYMREM1. This indicates that FLOT4 might be required for SYMREM1 recruitment and thus would provide a primary and essential scaffold for targeting SYMREM1 into the MMD

To test this genetically, we created a RNA interference (RNAi) construct against the 3’UTR of the endogenous *FLOT4* transcript, which was previously shown to efficiently

silence the FLOT4 and co-expressed it with YFP-SYMREM1 in the complemented *hcl-1* mutant background. While SYMREM1 labelled MMDs with a density of 0.077 MMDs/ μm^2 (SE= 0.0099) in control roots (lacking the FLOT4-RNAi construct and thus expressing the endogenous FLOT4) (Fig. 3H) significantly less domains (0.02 MMDs/ μm^2 ; SE=0.0014; $p=9.05\text{E}^{-06}$) were found in *FLOT4*-silenced roots (Fig. 3I). These data demonstrate that FLOT4 is a second essential building block of a symbiosis related MMD and is required for the lateral segregation of SYMREM1 into this structure. However, SYMREM1 strictly localized to the PM even in the absence of FLOT4 indicating that FLOT4 is not involved in membrane targeting of the SYMREM1 protein *per se*.

Assuming that we identified core components of a symbiosis related MMD we should be able to reconstitute this structure in a heterologous cell system lacking any of the three proteins. Therefore, we first expressed all three components individually in *Nicotiana benthamiana* leaf epidermal cells. The expression of SYMREM1 alone resulted in almost no labelling of distinct MMDs. Instead, SYMREM1 was mostly homogenously distributed except for its exclusion from defined tracks (Fig. 4A). For other remorin proteins these spaces have been previously described to be populated by cortical microtubules (1). This indicates a lack of essential components required for an efficient accumulation of SYMREM1 in a specialized MMD-type in these cells. In contrast, FLOT4-mCherry (Fig. 4B) and LYK3-GFP (Fig. 4C) labelled more distinct structures when being expressed individually, even though these putative MMDs did not resemble those observed in the homologous system. Strikingly, co-expression of SYMREM1 and FLOT4 in the same cell strongly induced compartmentalization of SYMREM1 (Fig. 4D)

while FLOT4 further segregated but only to moderate extent (Fig. 4E). This compartmentalized SYMREM1 localization was entirely revertible upon post-transcriptional silencing of FLOT4 (Fig. S3). Interestingly and in striking contrast to SYMREM1/FLOT4 co-localizations observed in *M. truncatula* roots (Fig. 3), these two proteins did not co-localize in *N. benthamiana* leaf epidermal cells but mutually excluded each other (Fig. 4F-G). Quantitative image analysis and segmentation confirmed a strong negative correlation indicating that both proteins remained in direct vicinity and tightly linked but failed to co-localize (Rr = -0.395, SE= 0.030; rd Rr= -0.008; rd SE= 0.005; $p=6.67E^{-13}$).

Since LYK3 is actively recruited into FLOT4-labelled domains and this process coincides with the induced expression of *SYMREM1* upon rhizobial infection (7), we tested whether the additional expression of LYK3 altered SYMREM1 localization. To avoid spectral interference of three fluorophores we expressed FLOT4-mCherry, YFP-SYMREM1 and hemagglutinin (HA)-tagged LYK3 (LYK3-HA) simultaneously. Interestingly, this combination resulted in labelling of discrete and specific MMDs by SYMREM1 (Fig. 4H) and FLOT4 (Fig. 4I). Quantitative image analysis now showed significant co-localizations within the MMDs labelled simultaneously by both proteins (Rr=0.40, SE=0.051; rd Rr=0.017; rd SE=0.017; $p=3.03E^{-06}$) (Fig. 4J-K). Additional Western Blot analysis confirmed successful expression of the HA-tagged fusion proteins (Fig. S4A). All together, these data demonstrate that LYK3 is essential for the targeting of SYMREM1 into FLOT4-labelled MMDs. Furthermore, our results show that all three components in addition to actin are required and sufficient to artificially reconstitute an essential scaffolding core of this symbiosis-related MMD in a heterologous system. The

fact that none of the endogenous and constitutively expressed flotillin or remorin proteins of *N. benthamiana* were able to induce the reconstitution further supports the specificity of the approach. To further test for specificity of this approach we cloned the second legume-specific flotillin (FLOT2) that shows a different localization and induction pattern compared to FLOT4 (15). Indeed, the co-expression of SYMREM1 and FLOT2 did not result in a co-localization (Fig. S5A-D). Although FLOT2/SYMREM1 displayed negative Pearson correlation coefficients that indicate a significant separation of the proteins ($R_r=-0.135$, $SE=0.041$; $rd\ R_r=0.041$; $rd\ SE=0.015$; $p=2.34E^{-07}$) this effect was significantly weaker compared to the exclusion observed upon co-expression of FLOT4 and SYMREM1 in leaf epidermal cells (Fig. 4D-G). Similarly, the additional expression of LYK3 did neither induce stringent segregation of SYMREM1 into distinct MMDs nor a co-localization with FLOT2 ($R_r=-0.163$, $SE=0.031$; $rd\ R_r=0.032$; $rd\ SE=0.08$; $p=8.58E^{-07}$) (Fig. S5E-H).

These data raised a mechanistically intriguing question: Is the lateral recruitment of LYK3 into FLOT4-labelled MMDs SYMREM1-dependent? To answer this we first co-expressed SYMREM1 or FLOT4 together LYK3 to test whether any of these dual combinations is sufficient for strict MMD confinement of both proteins. However, neither the SYMREM1/LYK3 (Fig. S4B-C) nor the FLOT4/LYK3 (Fig. 5A-D) pair was sufficient to induce a strong compartmentalization of any of the proteins. Therefore, FLOT4 and SYMREM1 alone are not sufficient to mediate LYK3 recruitment into this specific MMD. It should be noted here that robust image segmentation could not be applied to these images due to the comparably low degree of compartmentalization. Therefore, values are only provided for the shown dataset (Fig. 5A-D) but were

repeatedly observed throughout the replicates. However, when we expressed the HA-SYMREM1 construct in addition to FLOT4/LYK3, a significant compartmentalization and high degree of co-localization between the fluorophore-tagged FLOT4 scaffold and LYK3 receptor was observed ($R_r=0.60$, $SE=0.046$; $rd\ R_r=0.021$; $rd\ SE=0.019$; $p=4.79E^{-08}$) (Fig. 5E-H). Reciprocally, clear segregation of LYK3 also occurred in the presence of mCherry-SYMREM1 and FLOT4-HA (Fig. 5I-L) ($R_r=0.39$, $SE=0.049$; $rd\ R_r=0.046$; $rd\ SE=0.030$; $p=8.46E^{-04}$). These data provide first mechanistic insights into MMD assembly and clearly demonstrate that the recruitment of the entry receptor LYK3 into FLOT4 labelled MMDs is SYMREM1-dependent.

DISCUSSION

Although recent evidence suggests the coexistence of different MMDs in plant cells (1) it remained a mystery whether multiple proteins acting in the same biological pathway segregate into the same MMD and which molecular building blocks are required for the *de novo* assembly of such structures. First hints were provided by the stimulus-dependent co-localization of the LYK3 receptor together with the putative scaffold protein FLOT4 during rhizobial infection (23). Considering these data and those presented here, we hypothesise the sequential assembly of an infection-related MMD, which is composed of proteins that establish and determine sites for rhizobial infections during RNS. Our current model (Fig. 6) considers the root-specific but constitutive expression of the LYK3 receptor and the flotillin FLOT4. Under these conditions FLOT4, and potentially FLOT2, serve as primary scaffolds that may control a first wave of protein recruitment into this

MMD. Such a hypothesis is supported by a recent report that demonstrated MMD targeting of the brassinosteroid receptor BRI1 to be flotillin-dependent (29) and by data showing flotillins to serve as key factors for membrane compartmentalization in bacteria (12). Although the application of isolated NFs and their recognition by the NFP/LYK3 receptor complex triggers first physiological responses such as calcium spiking within minutes (30) the application was not sufficient to alter LYK3 dynamics in the observed time window despite this immobilization is strictly NF-dependent (23). However inoculation of roots with rhizobia for 24 hours induced the lateral arrest of LYK3 in root hairs (23) and this not only coincides with the initial induction of the endogenous *SYMREM1* transcript (7) but also with epidermal activation of its promoter (Fig. 1B-E). In addition, the *symrem1* phenotype clearly points to an infection related process (Fig. 1K). Data presented here indicate that downstream of the initial NF perception, SYMREM1 as well as LYK3 are mutually required for their recruitment into an infection-related MMD, which is initially formed by FLOT4 (Fig. 4; Fig. 6). This process does not require an active LYK3 kinase domain as SYMREM1 also co-localized with FLOT4 in the *hcl1* mutant background that exclusively expresses a kinase dead variant of the receptor (Fig. S2). However, *in vitro* phosphorylation data using the kinase domain of NFR1 from *Lotus japonicus*, the putative ortholog of LYK3, suggest that residues of the intrinsically disordered region (IDR) of SYMREM1 can be phosphorylated by the NFR1 kinase domain (31). Such IDRs serve as hotspots for phosphorylation and significantly contribute to protein-protein interactions in remorins (32) and other plant proteins (33). Thus, we speculate that LYK3 contributes to SYMREM1 oligomerization, which then may open further docking sites for the additional recruitment of a second set of proteins

into this specific MMD that control the infection process. These may include components of the exocytosis machinery and small ROP GTPases all of which have been described to be MMD localized and/or required for rhizobial infection (34-36).

A peculiar aspect of MMD formation in plants in comparison to metazoans is the lateral immobility of these domains that are labelled by scaffold proteins such as remorins and flotillins. An advanced model may be provided by the picket fence theory that suggests the formation of mesocale compartments in the size range of 100-200 nm that are confined by the actin network (4, 37, 38). Lateral stability may further be supported by the presence of a cell wall that has significant impact on protein diffusion inside the PM in plants (5). However, even though post-translational modifications such as the addition of lipid moieties to MMD components and biophysical properties of transmembrane domains contribute to lateral segregation (39), the molecular mechanism that precisely positions individual MMD at the PM and potentially along the actin cytoskeleton remains to be examined in the future.

ACKNOWLEDGEMENTS

We would like to thank all members of our team for their fruitful discussions throughout the project and comments on the manuscript. Christina Bielmeier and Anne-Kathrin Classen (LMU Munich) helped with different aspects during image analysis. Jana Munstermann conducted the initial experiments on FLOT4. The *hcl-1* mutant and the complemented *hcl-1* line were kindly provided by Doug Cook (UC Davis, USA). This work was funded by an Emmy-Noether grant of the Deutsche Forschungsgemeinschaft (DFG; OT423/2-1) and the Boehringer Ingelheim Foundation.

MATERIALS AND METHODS

Plant growth and phenotypical analysis

For phenotypical analysis *Medicago truncatula* wild-type R108, *symrem1-1* (NF4432) and *symrem1-2* (NF4395) seeds were scarified and sterilized before being sown on 1% agar plates for germination and kept in dark at 4°C for 3-5 days for vernalization. Germination was allowed for up to 24h at 24°C before transferring the seedlings in a closed weck-jar system filled with sand/vermiculte mixture and Fahraeus liquid media for rhizobia inoculation. After 3 days plants were inoculated with 1ml *Sinorhizobium meliloti* 2011 CFP with an OD600 of 0.001. Mature infection threads were scored 7 dpi. Complementation experiments were conducted via hairy root transformation using a pSYMREM1-YFP-SYMREM1 (nodulation) or a pUbi-YFP-SYMREM1 (IT) construct and analysed 10 days (IT) and 6 weeks (nodule) after inoculation.

Hairy Root Transformation

M. truncatula hairy root transformation was performed as previously described using the *Agrobacterium rhizogenes* strain ARqual and transferred weekly to fresh plates containing Fahraeus medium with a pH of 6.0.

Nicotiana benthamiana infiltration

N. benthamiana leaf infiltration was performed as previously described (1, 25, 31). Agrobacteria were infiltrated at a final OD 600nm of 0.4 for p35S-LYK3-GFP to 0.005 pUbi-HA-SYMREM1. Level 2 single expression vectors and Level 3 co-expression vectors obtained by Golden Gate cloning (40) were infiltrated with a final OD 600nm of

0.1 in presence of the silencing suppressor P19. The infiltration with the FLOT4-RNAi silencing construct, as well as the respective control was performed without P19. Microscopy was performed 2 and 3 days post infiltration.

Western blot analysis

N. benthamiana leaf disks were harvested 3 dpi and shock frozen with liquid nitrogen. Proteins were extracted by grinding leaf disks in lysis buffer (150 mM NaCl, 10 mM TrisHCl pH 7.5, 1% Triton-X-100, 1 mM EDTA, 2 mM DTT, Pefabloc, protease inhibitor cocktail. Samples were spun down at 14000 rpm at 4°C and pellets were discarded. The samples were diluted with 5x SDS-sample buffer and denatured at 70°C for 5 min. The protein samples were loaded onto 10% polyacrylamide SDS-polyacrylamide gels before being transferred onto a nitrocellulose membrane. For blocking and antibody incubation the SNAP i.d. 2.0 protein detection system was used. The membrane was blocked with 3% milk in 1xTBS-Tween (0.1%) and incubated with the anti-HA-antibody that was directly conjugated with horseradish peroxidase (1:3000, Roche). Detection of proteins was performed with the SuperSignal™ West Pico Chemiluminescent Substrate (Pierce).

Golden Gate and Gateway cloning/constructs

The coding sequence of *Medicago truncatula* SYMREM1 (Genbank accession JQ061257) was recombined into the Gateway (GW) compatible pUBi-YFP-GW vector(6) via LR-reaction. For complementation experiments a Gateway compatible pSYMREM1-GW vector was created by replacing the Ubiquitin promoter with the

functional SYMREM1 promoter (643bp upstream of the translational start of *SYMREM1*) using PmeI and XbaI restriction sites. All other constructs were cloned as Golden Gate compatible constructs. Bpi and BsaI restriction sites were removed from the following nucleotide templates prior to the cloning of Level 2 expression vectors: *SYMREM1* (Genbank accession: JQ061257.1), *LYK3* (Genbank accession AY372406), *MAP4* (Genbank accession: M72414), the cDNA of the genomic *FLOT4* (Genbank accession GU224281) and *FLOT2* (Genbank accession 224279), the 2kb *FLOT4* promoter (pFLOT4), as well as the *SYMREM1* promoter (pSYMREM1). A double stranded Lifeact template with flanking BsaI restriction sites was directly inserted into pUC-Bpi via blunt end StuI (NEB) cut-ligation for subsequent Golden Gate cloning. Double stranded sequences for the FLOT4-RNAi constructs with flanking BsaI sites were also cloned via blunt end StuI cut-ligation into pUC-Bpi. RNAi silencing vectors were assembled as previously described (40). The RNAi construct used that was expressed in *N. benthamiana* expanded from the 3'UTR 114 bp into 5' direction of the FLOT4 gene in order to facilitate silencing in *N. benthamiana*, since the FLOT4-mCherry constructs lack the 3'UTR.

Level 2 single expression and Level 3 co-expression vectors for microscopy were assembled in a Golden Gate compatible fashion (40).

Confocal Laser-Scanning Microscopy

Confocal laser scanning microscopy was performed on a Leica TCS SP5 confocal microscope equipped with 63x and 20x HCX PL APO water immersion lenses (Leica Microsystems, Mannheim, Germany). GFP was excited with the Argon laser (AR) line at

488 nm and the emission detected at 500-550 nm. YFP was excited with the 514 nm AR laser line and detected at 520–555nm. mCherry fluorescence was excited using the Diode Pumped Solid State (DPSS) laser at 561nm and emission was detected between 575-630 nm. Samples, co-expressing two fluorophores were imaged in sequential mode between frames. Due to low signal intensity for the pSYMREM1-NLS-2xGFP reporter, the corresponding fluorescence was detected using Leica HyD detectors. Images were taken with a Leica DFC350FX digital camera.

Quantitative Image Analysis

Image analysis was performed with the open source ImageJ/ (Fiji) software (41). For illustration, images were background subtracted according to the rolling ball algorithm, filtered with a Mean filter pixel radius of 1 and then maximum z-projected ('create stack'). Contrast was enhanced for visualization in figures but not for quantification.

Pixel based co-localizations to determine Pearson Correlation Coefficient values were performed using the Fiji Plugins 'Squassh'(42) and 'JACoP' (43). Image segmentation was performed with 'Squassh'.

Randomization was performed with the automatic Costes' Randomization method in 'JACoP' in which clusters of 10x10 pixels were randomly distributed in one channel and correlated to the original values. Additionally, randomization was also performed on maximum z-projections via horizontal flip of the mCherry channel as described previously (1, 25).

To quantify MMDs images were segmented to differentiate background from domains. For this, the background was subtracted using a rolling ball algorithm with a radius

corresponding to the largest structure of interest. I.e., the largest domain was encircled, and its dimension was used. A mean blur with radius 1 was then applied, and the slices (n=5-12 slices, with distances of 0.25 to 0.7 μm) maximum projected along the z-axis. A threshold was applied to the images and the result saved as a binary mask. The 'create selection' tool was used to mark the outlines and was overlaid onto the original image to verify proper image segmentation. Domains were counted with the 'particle analyzer' tool in Fiji.

Cytoskeleton depolymerisation

A 1mM Oryzalin stock solution in DMSO and a 10mM Cytochalasin D stock solution on EtOH were prepared. *Medicago truncatula* root samples of 1 cm length were incubated in final concentrations of 10 μM Oryzalin or 10 μM Cytochalasin D for 12 hours in water. The control samples were incubated in water with the equal amount of solvent for the same amount of time.

REFERENCES

1. Jarsch IK, *et al.* (2014) Plasma Membranes Are Subcompartmentalized into a Plethora of Coexisting and Diverse Microdomains in Arabidopsis and *Nicotiana benthamiana*. *Plant Cell* 26(4):1698-1711.
2. Spira F, *et al.* (2012) Patchwork organization of the yeast plasma membrane into numerous coexisting domains. *Nat Cell Biol* 14(6):640-648.
3. Kusumi A, *et al.* (2012) Dynamic organizing principles of the plasma membrane that regulate signal transduction: commemorating the fortieth anniversary of Singer and Nicolson's fluid-mosaic model. *Annu Rev Cell Dev Biol* 28:215-250.
4. Kusumi A, Suzuki KG, Kasai RS, Ritchie K, & Fujiwara TK (2011) Hierarchical mesoscale domain organization of the plasma membrane. *Trends Biochem Sci* 36(11):604-615.
5. Martiniere A, *et al.* (2012) Cell wall constrains lateral diffusion of plant plasma-membrane proteins. *Proc Natl Acad Sci U S A* 109(31):12805-12810.
6. Konrad SS, *et al.* (2014) S-acylation anchors remorin proteins to the plasma membrane but does not primarily determine their localization in membrane microdomains. *New Phytol* 203(3):758-769.
7. Lefebvre B, *et al.* (2010) A remorin protein interacts with symbiotic receptors and regulates bacterial infection. *Proc Natl Acad Sci U S A* 107(5):2343-2348.
8. Marin M, Thallmair V, & Ott T (2012) The intrinsically disordered N-terminal region of AtREM1.3 remorin protein mediates protein-protein interactions. *J Biol Chem* 287(47):39982-39991.

9. Perraki A, *et al.* (2012) Plasma Membrane Localization of Solanum tuberosum Remorin from Group 1, Homolog 3 Is Mediated by Conformational Changes in a Novel C-Terminal Anchor and Required for the Restriction of Potato Virus X Movement. *Plant Physiol* 160(2):624-637.
10. Raffaele S, *et al.* (2009) Remorin, a Solanaceae protein resident in membrane rafts and plasmodesmata, impairs potato virus X movement. *Plant Cell* 21(5):1541-1555.
11. Jarsch IK & Ott T (2011) Perspectives on remorin proteins, membrane rafts, and their role during plant-microbe interactions. *Mol Plant Microbe Interact* 24(1):7-12.
12. Bach JN & Bramkamp M (2013) Flotillins functionally organize the bacterial membrane. *Mol Microbiol* 88(6):1205-1217.
13. Langhorst MF, Reuter A, & Stuermer CA (2005) Scaffolding microdomains and beyond: the function of reggie/flotillin proteins. *Cell Mol Life Sci* 62(19-20):2228-2240.
14. Li R, *et al.* (2012) A membrane microdomain-associated protein, Arabidopsis Flot1, is involved in a clathrin-independent endocytic pathway and is required for seedling development. *Plant Cell* 24(5):2105-2122.
15. Haney CH & Long SR (2010) Plant flotillins are required for infection by nitrogen-fixing bacteria. *Proc Natl Acad Sci U S A* 107(1):478-483.
16. Gage DJ (2004) Infection and invasion of roots by symbiotic, nitrogen-fixing rhizobia during nodulation of temperate legumes. *Microbiol Mol Biol Rev* 68(2):280-300.

17. Oldroyd GE, Murray JD, Poole PS, & Downie JA (2011) The rules of engagement in the legume-rhizobial symbiosis. *Ann Rev Genet* 45:119-144.
18. Oldroyd GE (2013) Speak, friend, and enter: signalling systems that promote beneficial symbiotic associations in plants. *Nat Rev Microbiol* 11(4):252-263.
19. Amor BB, *et al.* (2003) The NFP locus of *Medicago truncatula* controls an early step of Nod factor signal transduction upstream of a rapid calcium flux and root hair deformation. *Plant J* 34(4):495-506.
20. Arrighi JF, *et al.* (2006) The *Medicago truncatula* lysin motif-receptor-like kinase gene family includes NFP and new nodule-expressed genes. *Plant Physiol* 142(1):265-279.
21. Limpens E, *et al.* (2003) LysM domain receptor kinases regulating rhizobial Nod factor-induced infection. *Science* 302(5645):630-633.
22. Smit P, *et al.* (2007) *Medicago* LYK3, an entry receptor in rhizobial nodulation factor signaling. *Plant Physiol* 145(1):183-191.
23. Haney CH, *et al.* (2011) Symbiotic Rhizobia Bacteria Trigger a Change in Localization and Dynamics of the *Medicago truncatula* Receptor Kinase LYK3. *Plant Cell* 23(7):2774-2787.
24. Moling S, *et al.* (2014) Nod factor receptors form heteromeric complexes and are essential for intracellular infection in *medicago* nodules. *Plant Cell* 26(10):4188-4199.
25. Jarsch IK & Ott T (2015) Quantitative Image Analysis of Membrane Microdomains Labelled by Fluorescently Tagged Proteins in *Arabidopsis thaliana* and *Nicotiana benthamiana*. *bio-protocol* 5(11):e1497.

26. Gui J, Liu C, Shen J, & Li L (2014) Grain setting defect1, encoding a remorin protein, affects the grain setting in rice through regulating plasmodesmatal conductance. *Plant Physiol* 166(3):1463-1478.
27. Szymanski WG, *et al.* (2015) Cytoskeletal Components Define Protein Location to Membrane Microdomains. *Mol Cell Proteomics* 14(9):2493-2509.
28. Klaus-Heisen D, *et al.* (2011) Structure-function similarities between a plant receptor-like kinase and the human interleukin-1 receptor-associated kinase-4. *J Biol Chem* 286(13):11202-11210.
29. Wang L, *et al.* (2015) Spatiotemporal Dynamics of the BRI1 Receptor and its Regulation by Membrane Microdomains in Living Arabidopsis Cells. *Mol Plant* 8(9):1334-1349.
30. Oldroyd GE & Downie JA (2004) Calcium, kinases and nodulation signalling in legumes. *Nat Rev Mol Cell Biol* 5(7):566-576.
31. Tóth K, *et al.* (2012) Functional Domain Analysis of the Remorin Protein LjSYMREM1 in *Lotus japonicus*. *PLOS ONE* 7(1):e30817.
32. Marín M & Ott T (2012) Phosphorylation of Intrinsically Disordered Regions in Remorin Proteins. *Front Plant Sci* 3:86.
33. Marin M & Ott T (2014) Intrinsic disorder in plant proteins and phytopathogenic bacterial effectors. *Chem Rev* 114(13):6912-6932.
34. Ivanov S, *et al.* (2012) Rhizobium-legume symbiosis shares an exocytotic pathway required for arbuscule formation. *Proc Natl Acad Sci U S A* 109(21):8316-8321.

35. Lei MJ, *et al.* (2015) The small GTPase ROP10 of *Medicago truncatula* is required for both tip growth of root hairs and nod factor-induced root hair deformation. *Plant Cell* 27(3):806-822.
36. Zhang Y, Immink R, Liu CM, Emons AM, & Ketelaar T (2013) The Arabidopsis exocyst subunit SEC3A is essential for embryo development and accumulates in transient puncta at the plasma membrane. *New Phytol* 199(1):74-88.
37. Hosy E, Martiniere A, Choquet D, Maurel C, & Luu DT (2015) Super-resolved and dynamic imaging of membrane proteins in plant cells reveal contrasting kinetic profiles and multiple confinement mechanisms. *Mol Plant* 8(2):339-342.
38. Saka SK, *et al.* (2014) Multi-protein assemblies underlie the mesoscale organization of the plasma membrane. *Nat Commun* 5:4509.
39. Konrad SS & Ott T (2015) Molecular principles of membrane microdomain targeting in plants. *Trends Plant Sci* 20(6):351-361.
40. Binder A, *et al.* (2014) A modular plasmid assembly kit for multigene expression, gene silencing and silencing rescue in plants. *PLOS ONE* 9(2):e88218.
41. Schindelin J, *et al.* (2012) Fiji: an open-source platform for biological-image analysis. *Nat Methods* 9(7):676-682.
42. Rizk A, *et al.* (2014) Segmentation and quantification of subcellular structures in fluorescence microscopy images using Squassh. *Nat Protoc* 9(3):586-596.
43. Bolte S & Cordelieres FP (2006) A guided tour into subcellular colocalization analysis in light microscopy. *J Microsc* 224(Pt 3):213-232.

FIGURES AND LEGENDS

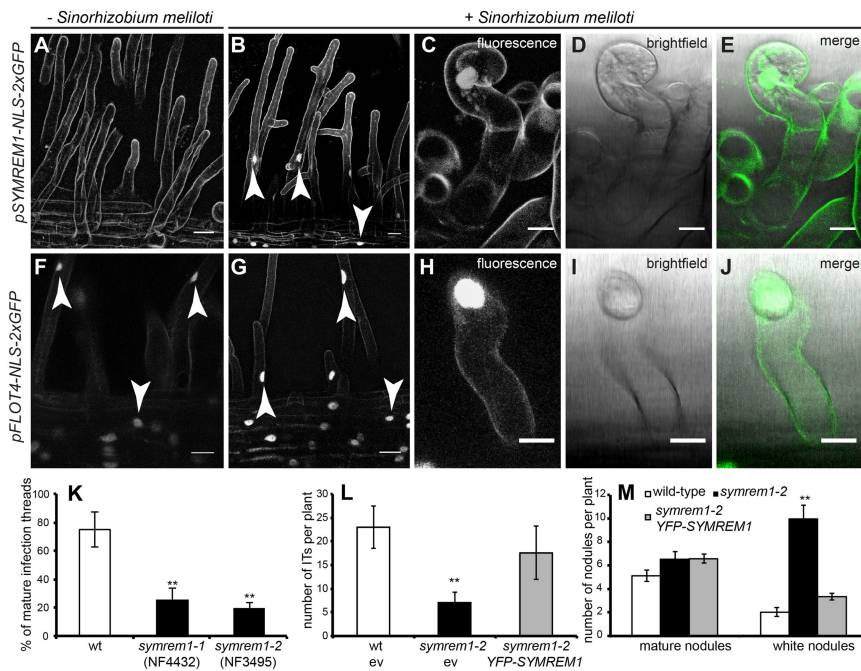


Fig. 1. Expression and phenotypal analysis of *SYMREM1* and *FLOT4*. *A-E*, Activation of the *SYMREM1* promoter as indicated by nuclear fluorescence (arrowheads) in uninoculated (*A*) and inoculated (*B-E*) conditions. (*C-E*) close-up of a curled root hair entrapping rhizobia. Autofluorescent contours of roots hairs and epidermal cells are visible due to increased sensitivity settings to detect any low intensity nuclear fluorescence. (*F-J*) Activation of the *FLOT4* promoter in uninoculated (*F*) and inoculated (*G-J*) conditions (arrowheads). (*H-J*) close-up of a curled root hair entrapping rhizobia. (*K-M*) Phenotypal analysis of *symrem1* mutants. Infection threads (ITs) were scored 7 days (*K*) and 8 days (*L*) after inoculation with *S. meliloti*. The IT (*L*) and the nodulation (*M*) phenotypes were complemented when expressing a *pUbi-YFP-SYMREM1* construct in the *symrem1-2* mutant line. Asterisks indicate results of a Student t-test with $p < 0.01$. Scale bars indicate 20 μm in *A, B, F, G* and 10 μm in *C-E* and *H-I*.

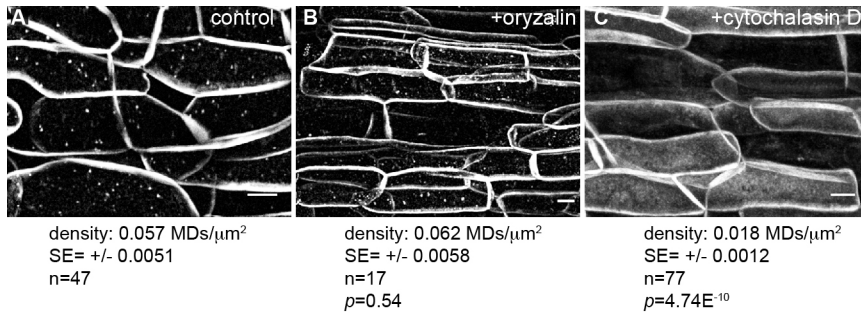


Fig. 2. SYMREM1-labelled MMDs are actin-dependent. An YFP-SYMREM1 fusion protein was ectopically expressed in transgenic *M. truncatula* roots and imaged using confocal-laser scanning microscopy. (A) YFP-SYMREM1 labelled distinct MMDs in control roots. (B) Treatment with the microtubule depolymerising drug oryzalin did not change YFP-SYMREM1 localization. (C) In contrast disruption of the actin cytoskeleton by application of cytochalasin D abolish MMD targeting of the protein. Quantitative image analysis was performed on all samples as indicated below the individual panels. SE= standard error; *p*-value= confidence interval obtained from a Student t-test. Scale bars indicate 10 μm.

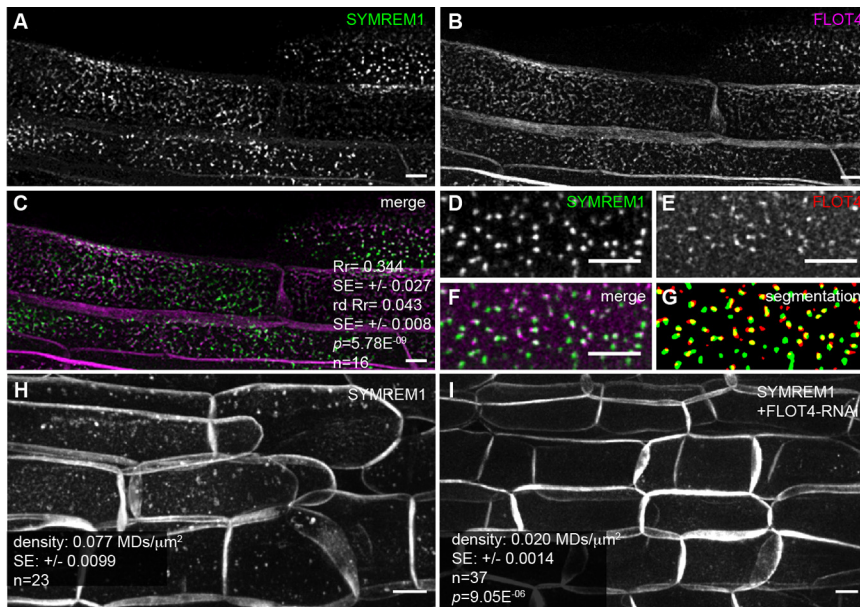


Fig. 3. FLOT4 is essential for MMD formation. (A) YFP-SYMREM1 and FLOT4-mCherry (B) co-localized (C) in epidermal cells when being expressed in transgenic *M. truncatula* roots (complemented *hcl1* mutant background). Quantitative data are provided in panel (C). Rr= Pearson correlation coefficient; rd Rr= Pearson correlation coefficient obtained after image randomization of the FLOT4-mCherry image. The respective standard errors (SE) are provided below the Pearson values. p = confidence interval obtained from a Student ttest comparing Rr and rd Rr. Close-up of YFP-SYMREM1 (D) and FLOT4-Cherry (E) microdomains at the plasma membrane surface. Overlaying both channels (F) and image segmentation (G) better illustrate co-localization between the two proteins. (H) While YFP-SYMREM1 labelled MMDs in root epidermal cells, their density was greatly reduced upon co-expression with a FLOT4-RNAi construct (I). p -value= confidence interval obtained from a Student ttest comparing roots expressing endogenous FLOT4 (as in H) and those where FLOT4 was silenced (as in I). Scale bars indicate 5 μ m (A-F) and 10 μ m (H, I).

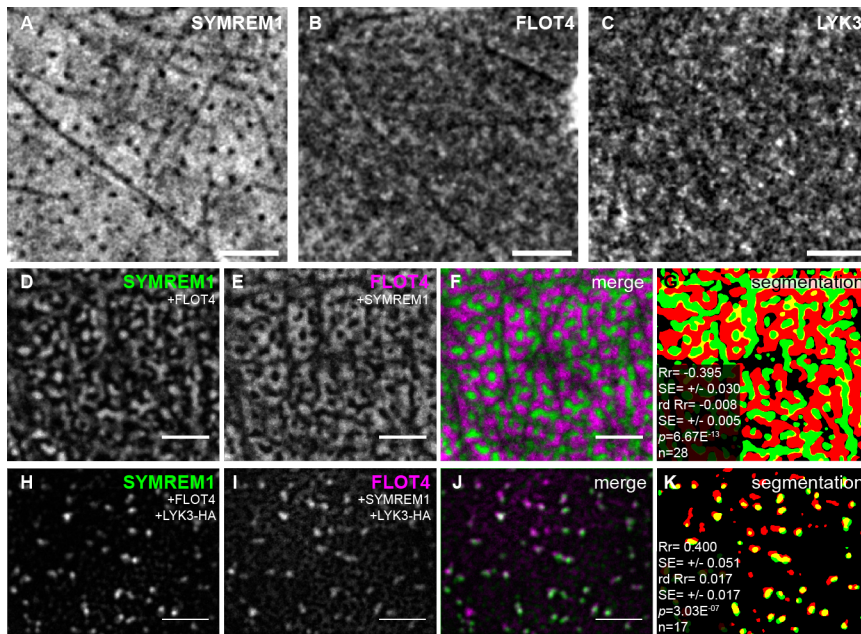


Fig. 4. *De novo* reconstitution of a symbiosis-related MMD *in vivo*. (A-C) *N. benthamiana* leaf epidermal cells individually expressing the legume-specific proteins YFP-SYMREM1, FLOT4-mCherry and LYK3-GFP revealed almost no MMDs being labelled by SYMREM1 while FLOT4 and LYK3 showed a moderate compartmentalization. (D, E) Co-expression of YFP-SYMREM1 and FLOT4-mCherry induced stronger compartmentalization of SYMREM1 and to lesser extent of FLOT4. (F, G) Overlaying the signals from both channels and image segmentation revealed a lack of co-localization and mutual exclusion of both proteins. In contrast, triple expression of fluorophore-tagged YFP-SYMREM1 and FLOT4-mCherry together with hemagglutinin (HA) tagged LYK3 resulted in specific accumulations of SYMREM1 (H) and FLOT4 (I) in MMDs that showed significant co-localization (J, K). Quantitative data are provided in panels G and K. Rr = Pearson correlation coefficient; rd Rr = Pearson correlation coefficient obtained after image randomization. The respective standard errors (SE) are provided below the Pearson values. p = confidence interval obtained from a Student t test comparing Rr and rd Rr. Scale bars indicate 5 μ m.

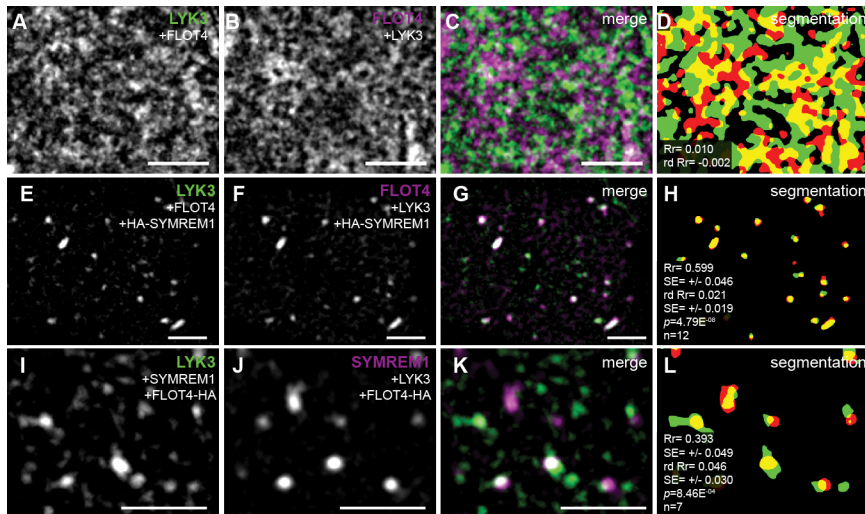


Fig. 5. SYMREM1-dependent MMD-recruitment of LYK3. Combinatorial expression of LYK3, FLOT4 and SYMREM1 in *N. benthamiana* leaf epidermal cells. Co-expression of LYK3 (A) and FLOT4 (B) in the absence of SYMREM1 resulted in moderate compartmentalization of both proteins and the lack of significant co-localization (C, D). In contrast, additional expression of HA-SYMREM1 resulted in labelling of distinct MMDs by LYK3 (E) and FLOT4 (F) that co-localized under these conditions (G, H). Similar patterns were observed for the co-expression of LYK3-GFP (I) and mCherry-SYMREM1 (J) in the presence of FLOT4-HA where the fluorophore-tagged proteins co-localized (K, L). Proteins fused to GFP are indicated in green, those fused to mCherry in red. Rr= Pearson correlation coefficient; rd Rr= Pearson correlation coefficient obtained after Costes randomization was applied to the red channel (mCherry) image. The respective standard errors (SE) are provided below the Pearson values. p = confidence interval obtained from a Student ttest comparing Rr and rd Rr. Scale bars indicate 5 μ m.

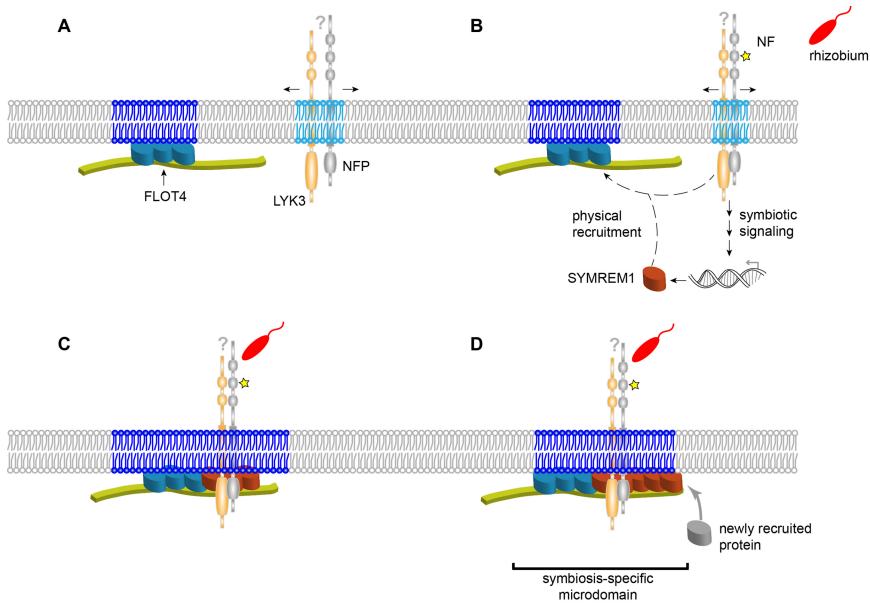


Fig. 6. Model illustrating different steps of MMD formation. (A) Constitutively expressed FLOT4 (turquoise) forms the initial MMD in an actin dependent manner that is devoid of the LYK3 receptor. (B) Nod factor (NF) perception by NFP (grey) and LYK3 (orange) occurs in a mobile microdomain and results in the activation of a symbiosis-specific signalling cascade that leads to the expression of SYMREM1 (red). (C) SYMREM1, LYK3 are actively recruited in a mutually dependent manner. (D) Phosphorylation of SYMREM1 by LYK3 leads to remorin oligomerization, which generates new docking sites for proteins required for rhizobial infection (hypothetical).

SUPPLEMENTAL INFORMATION

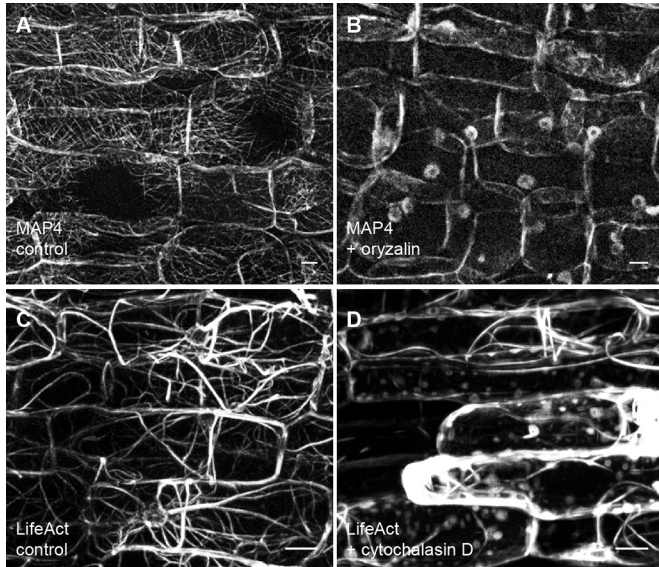


Fig. S1. Depolymerisation of microtubules and actin in *M. truncatula* roots. Expression of the microtubule (MT) associated protein MAP4-YFP clearly labelled the MT network (A) that was successfully depolymerised upon incubation with oryzalin (B). Similarly, actin strands were labelled by YFP-Lifeact (C) and their disruption monitored upon application of cytochalasin D (D). Scale bars indicate 10 µm.

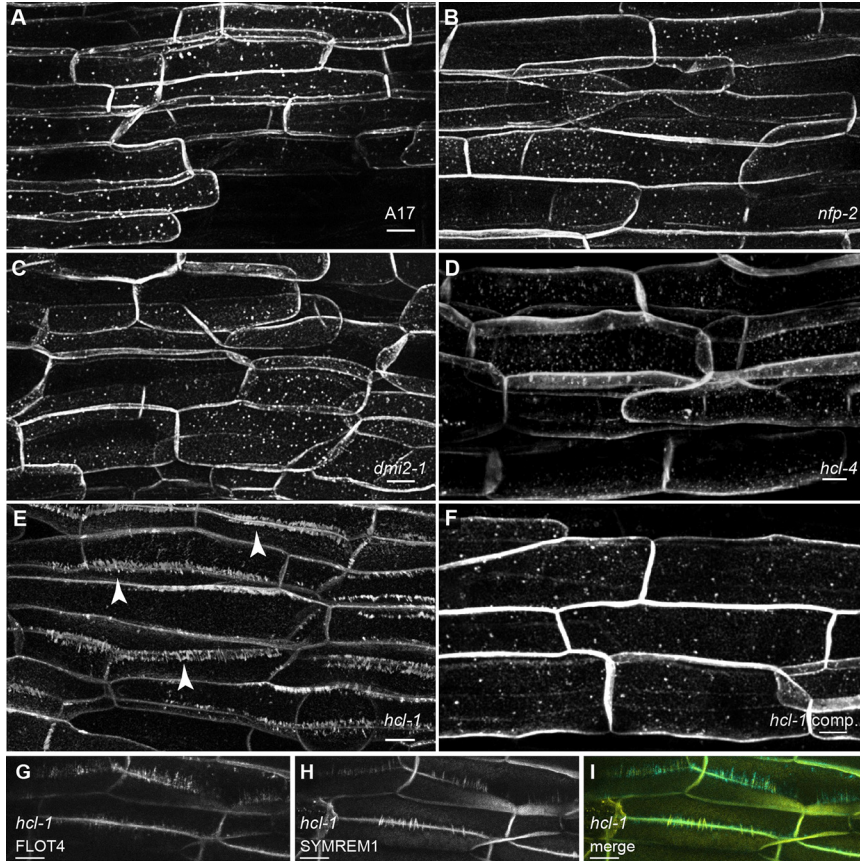


Fig. S2. SYMREM1 and FLOT4 patterns are altered in the *hcl1* mutant allele. (A) A YFP-SYMREM1 fusion protein was expressed in wild-type A17 roots. (B-D) No qualitative differences were observed upon expression of this construct in the receptor mutant backgrounds *nfp-2* (B), *dmi2-1* (C) and *hcl-4* (D). e, In contrast SYMREM1 MMD patterns were strongly altered in the *hcl-1* mutant (arrowheads). f, Wild-type like patterns were restored in a complemented *hcl-1* mutant line (23). FLOT4 followed the same parallel patterning (G) as SYMREM1 (H, I) in the *hcl-1* mutant. Scale bars indicate 10 μ m.

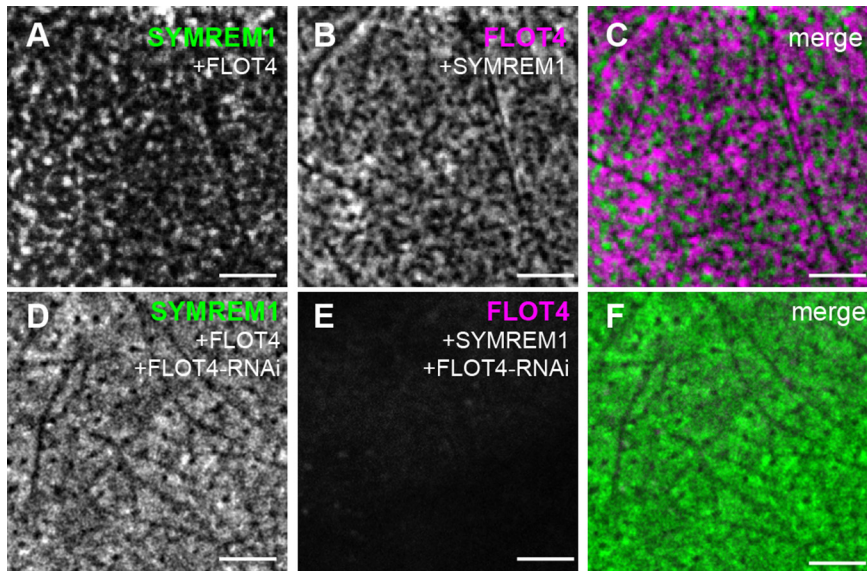


Fig. S3. Compartmentalization of SYMREM1 in leaf epidermal cells is FLOT4-dependent. Co expression of YFP-SYMREM1 (A) and FLOT4-mCherry (B) in *N. benthamiana* leaf epidermal cells resulted in compartmentalization of both proteins, although both proteins did not co-localize (C). Additional expression of a FLOT4-RNAi construct resulted in a loss of FLOT4-mCherry (E) and reverted the localization of SYMREM1 towards less compartmentalized patterns (D, F). Scale bars indicate 5 μ m.

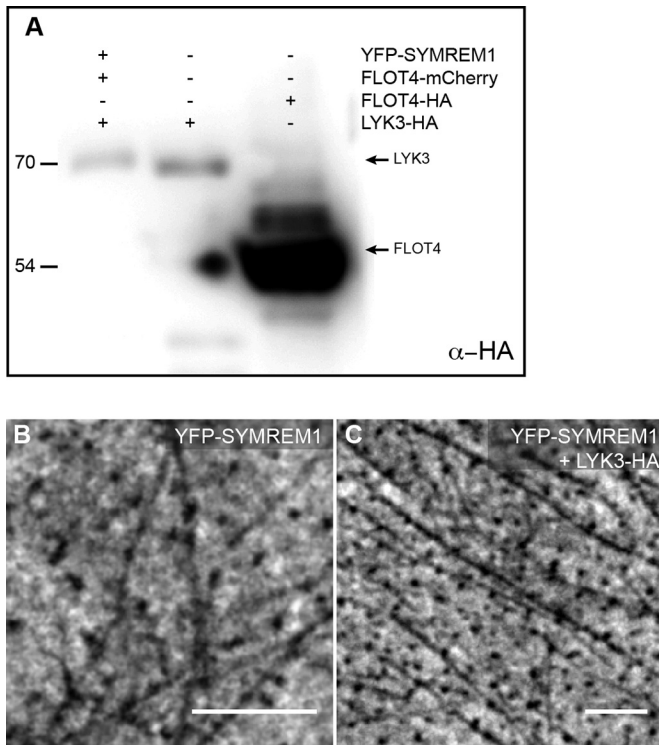


Fig. S4. Presence of LYK3 alone does not induce SYMREM1 compartmentalization. (A) Western Blot analysis confirming the presence of HA-tagged non-fluorescent LYK3 and FLOT4 as used in Fig. 4H-K and Fig. 5I-L, respectively. (B) Expression of SYMREM1 alone and (C) together with LYK3 in *N. benthamiana* leaf epidermal cells did not affect localization patterns of the proteins. Scale bars indicate 5 μ m.

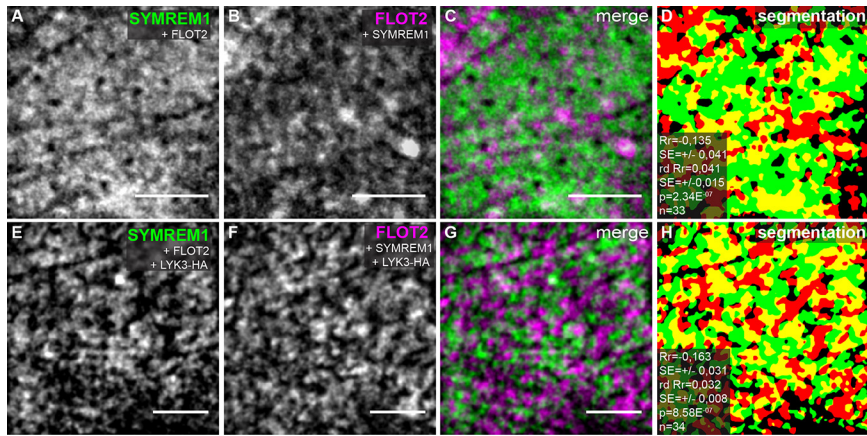


Fig. S5. FLOT2 does not induce MMD recruitment of SYMREM1. (A-D), Co-expression of SYMREM1 and FLOT2 in *N. benthamiana* leaf epidermal cells resulted in significant exclusion of the proteins even though to lesser extent than observed with FLOT4. (E-H) Additional expression of LYK3 did not result in MMD formation. Scale bars indicate 5 μm .

C) Discussion

1. SYMREM1- SYMbiotic REMorin 1

More than 25 years ago, Farmer and co-workers discovered the protein pp34 in a screen for plasma membrane (PM) proteins that were differently phosphorylated upon oligogalacturonide treatment (Farmer *et al.*, 1989). After further characterization of this protein they proposed the name 'remorin' for it. This should describe the protein's properties with regard to the hydrophilic profile of its amino acid sequence and its tight PM attachment, in analogy to remora fish that attach themselves to the surface of larger organisms (Reymond *et al.*, 1996). Since the discovery in 1989 several proteomic studies revealed the presence of further remorins in PM fractions (Mongrand *et al.*, 2004; Morel, 2006; Lefebvre *et al.*, 2007; Kierszniowska *et al.*, 2009). Due to the absence of a PM binding motif, two different anchoring mechanisms for remorins have been suggested: (a) a two-step mechanism based on findings for the remorin protein StREM1.3, which involves initial attachment to the PM due to an intrinsic lipid affinity of the StREM1.3 anchoring motif, and sequential folding of this C-terminal anchor region (RemCA) into a tight α -helical hairpin with a hydrophobic core (Perraki *et al.*, 2012). (b) In contrast, the homologous remorin REM1.2 from *Arabidopsis* was shown to harbor an S-acylation motif for PM anchoring (Hemsley *et al.*, 2013). To analyse the molecular mechanism of PM anchoring and to clarify whether this mechanism also determines the membrane domain (MD) localization of remorins, we performed biochemical and cell biological experiments with SMYREM1.

1.1. SYMREM1 anchors to the PM via S-acylation in the RemCA region

By employing immunolocalization and transmission electron microscopy, it had been shown that SYMREM1 accumulates in clusters on the PM in *Medicago truncatula* roots (Lefebvre *et al.*, 2010). Additionally, co-purification of SYMREM1 in *in vitro* experiments with Detergent Insoluble Membrane (DIM) fractions from *M. truncatula* roots can be seen as a hint for potential MD localization (Kierszniowska *et al.*, 2009; Lefebvre *et al.*, 2010). The observation of punctuate localization of transiently expressed fluorophore-tagged SYMREM1 *in vivo* in *Medicago* roots verified the

membrane domain (MD) specific localization of SYMREM1 (Konrad *et al.*, 2014; Fig. 1a and 6a).

When Perraki and co-workers investigated the anchoring mechanism of StREM1.3, they established that its last C-terminal 28 aa were crucial for PM localization (Perraki *et al.*, 2012). Further, they proposed that this RemCA region is first present in an unfolded conformation. In close proximity to a nonpolar environment like the PM, folding into two short α -helical stretches is induced. In this way, a hydrophobic pocket is formed, which anchors the protein to the PM. Similar to StREM1.3, we could show for SMYREM1 that its RemCA region is necessary for PM anchoring. In the case of SYMREM1 this region consists of the last C-terminal 35 aa, which also contains a hydrophobic stretch (Konrad *et al.*, 2014; Fig. 1g and Table 1).

In contrast to StREM1.3, the *Arabidopsis* homolog REM1.2 was demonstrated to be S-acylated and also SYMREM1 was predicted to be S-acylated on the last C-terminal Cysteine within the RemCA region (Hemsley *et al.*, 2013; Konrad *et al.*, 2014, Table 1). This post-translational modification was verified *in vitro* and mutation of the S-acylation site in the RemCA-only fusion protein led to a loss of PM localization (Konrad *et al.*, 2014; Fig. 5a and 4d). These results suggest a combination of the above-mentioned mechanisms for SYMREM1 (Konrad *et al.*, 2014; Sup Fig. S7). A combined mechanism was further supported by the analysis of *Arabidopsis* remorin proteins' RemCA regions. In line with our hypothesis, we confirmed the S-acylation of AtREM1.2 (At3g61260) and remorin At4g36970 (Konrad *et al.*, 2014; Fig. 4 and Sup Fig. S5a). Furthermore, only 4 out of 16 RemCA fluorophore-fusion proteins localized to the PM although all analysed *Arabidopsis* RemCA regions displayed a hydrophobic stretch in their RemCA domain. Based on these findings, RemCA as sole anchor motif could be excluded (Konrad *et al.*, 2014; Table 1 and Fig. S2).

S-acylation is a posttranslational modification that is added to a protein by PM located protein-S-acyl transferases (PATs) (Roth *et al.*, 2002; Huang *et al.*, 2004). Due to their localization within the cell it is hypothesized that their targets already have to be associated or anchored to the PM to become S-acylated (reviewed in Smotrys & Linder, 2004). Considering this as well, we now propose a combined membrane-binding mechanism. (1) Remorins initially associate to the PM either (a) via potential protein-protein interactions of their coiled-coil domain with already PM-integral proteins or (b) via a protein-lipid association of the hydrophobic core of the RemCA

region. (2) After this first transient PM association, PATs are able to S-acylate C-terminal cysteine residue(s) and the remorins get tightly anchored to the PM (Konrad *et al.*, 2014; Fig. S7).

In support of this hypothesis, the work of Gui *et al.* (2015) verified S-acylation in the RemCA region as the driving force for tight PM anchoring (Gui *et al.*, 2015).

As for the remorins, membrane localization mediated by S-acylation could also be shown for other proteins lacking any known PM-anchoring mechanism like TMD, e.g. calcium sensor proteins and receptor-like kinases relevant for guiding pollen tubes to the ovule (Batistic *et al.*, 2008; Batistič *et al.*, 2012; Liu *et al.*, 2013). Interestingly, these mentioned proteins have different localization sites within the cell (vacuole and plasma membrane) and are involved in different signaling pathways. Therefore, S-acylation appears to function as a general PM-anchoring motif without a specific preference with regard to localization within the cell or protein type. However, beyond its role in PM anchoring, S-acylation is also considered as a signal for specific MD association, which will be discussed below (Sorek *et al.*, 2009).

1.2. S-acylation of SYMREM1 is not required for MD localization

The glycosylphosphatidylinositol (GPI) motif is the only known post-translational modification that anchors proteins to MDs in the outer leaflet of the PM in mammalian and plant cells (Ikonen & Simons, 1998; Borner *et al.*, 2005; Sorek *et al.*, 2007; Garner *et al.*, 2007; Levental *et al.*, 2010a). For the inner PM leaflet S-acylation has been postulated as MD targeting motif in mammalian cells (Levental *et al.*, 2010b; Thaa *et al.*, 2011; Blaskovic *et al.*, 2013). However, up to now a final proof of S-acylation being a MD localization motif in plants is still missing (Blaskovic *et al.*, 2013; Hemsley, 2015). So far the only correlation between S-acylation and MD localization in plant cells that has been found was based on DIM extractions. In these studies a member of the small GTPase ROP family showed a higher affinity to DIMs compared to its deacylated protein variant (Sorek *et al.*, 2007, 2010). However, a verification of this S-acylation dependent MD recruitment via microscopy-based methods was missing. Since SYMREM1 localized to MDs and was shown to be S-acylated (Konrad *et al.*, 2014), we addressed the question whether S-acylation of the RemCA region is the determinant for MD localization of remorins.

Expression of the full-length SYMREM1 mutated in the S-acylation site did not completely abolish MD localization but led to a reduced MD localization compared to the wild type protein (Konrad *et al.*, 2014; Fig. 6a). This result suggests an alternative MD localization motif besides the S-acylation modification. The fact that the non-acylated SYMREM1 mutant variant localized to MDs when expressed in *S. cerevisiae* cells corroborated our hypothesis (Konrad *et al.*, 2014; Fig. 6h). Interestingly, when expressing only the RemCA domain from SYMREM1 either in *Medicago* roots or in yeast cells, it displayed no MD localization but was uniformly distributed (Konrad *et al.*, 2014; Fig. 6d and h). In contrast to our findings, in the work of Perraki *et al.* (2012) it was hypothesized that the RemCA has an intrinsic affinity to lipid raft lipids and this drives the remorin into MDs. As already mentioned, this theory was based on *in vitro* binding assays and DIM extractions. However, in this study an *in vivo* MD localization of a StREM1.3 RemCA-fusion protein was not shown. Therefore, a final proof for the RemCA region being the MD signal motif was missing in this work.

From our results, we concluded that the S-acylation is not the predominant MD localization signal for remorins and we could rule out that intrinsic lipid affinity of the RemCA region functions as MD determinant as had been postulated by Perraki and co-workers (Perraki *et al.*, 2012). In the light of the localization results in yeast it can also be excluded that a hetero-oligomerization is the reason for MD localization. Instead, it is very likely that a potential alternative motif responsible for MD localization may be encoded in another part of the protein.

Besides a potential MD localization motif, the interaction with another factor that is already present in the MD could also drive SYMREM1 to localize to MDs. This might be mediated by an interaction with another protein like FLOT4, which has also been shown to localize to MDs (Haney & Long, 2010; Haney *et al.*, 2011) (see also section A.2.1). When addressing the question whether SYMREM1 functions as scaffold protein, we showed that SYMREM1 and FLOT4 co-localize in the same PM domain (Stratil *et al.* manuscript (ms) 2, Fig. 3c). In the course of this work, we found that the formation of SYMREM1 MDs is FLOT4- and actin-dependent, while the co-localization of LYK3 and FLOT4 is SYMREM1-dependent (Stratil *et al.* ms 2, Fig. 5). A Nod factor-dependent co-localization of FLOT4 and LYK3 was already demonstrated, however, an evidence of direct physical interaction of FLOT4 and LYK3 was still missing (Haney *et al.*, 2011). Our findings suggest a SYMREM1-

dependent recruitment mechanism of a putative LYK3-signaling complex to the FLOT4 MDs after Nod factor induced expression of SYMREM1 (Lefebvre *et al.*, 2010b; Stratil *et al.* ms 2, Fig. 6). This recruitment causes a SYMREM1-FLOT4-LYK3 infection MD. Although, S-acylation being a MD localization motif for other proteins cannot be ruled out, these results suggested, that SYMREM1-related MD formation is driven by protein interaction rather than only by a lipid-lipid interaction (Pike, 2006, 2009; Konrad & Ott, 2015).

A physical interaction between LYK3 and SYMREM1 was already proven (Lefebvre *et al.*, 2010), but it still remains to be demonstrated whether the SYMREM1 and FLOT4 co-localization is mediated via direct protein interaction. On a more general level, the MD localization mechanism will need further investigation to fully understand how differential localization of certain remorins to distinct MDs is achieved (Jarsch *et al.*, 2014).

Although S-acylation is not the main driving force for SYMREM1 being localized to MDs, there still remains the question of whether it is important for the physiological function of SYMREM1, like it is in the case of AtCESA7. CESA7 is a component of the cellulose synthase complex and was shown to be S-acylated. Mutation of S-acylation sites of CESA7 abolished cellulose synthase complex assembly, further trafficking to the PM and thereby its physiological function (Kumar *et al.*, 2016).

Along these lines, the work of Gui *et al.* (2015) addressed to some extent the functional relevance of S-acylation for the remorin protein GRAIN SETTING DEFECTS (GSD)1. In a former work the same authors demonstrated that overexpression of GDS1 in the wild type background leads to reduced grain setting (Gui *et al.*, 2014). Based on this phenotype, the physiological function of (I) two different single point mutations of S-acylation sites, (II) a delta construct missing the whole RemCA region and (III) a variant mutated in all potential C-terminal S-acylation sites in the RemCA has been assessed by monitoring the grain setting rate. The fully mutated variant and the delta construct did not localize to the PM anymore and did not have any impact on grain setting when overexpressed. In contrast, the two single point mutation variants, which still localized to the PM, caused the already described overexpression phenotype.

Gui and co-authors concluded that these two S-acylation sites mediate PM localization and that this localization is required for a correct function (Gui *et al.*, 2015). However, based on the data presented, it remains unclear whether the point mutation variants still localize to MDs or not. All in all, their work could not clarify whether S-acylation as anchoring mechanism *per se* is necessary for the physiological protein function, or whether PM-localization of remorins by an independent mechanism is sufficient. Since the SYMREM1 S-acylation mutant variant still localizes to MDs, this protein version would be an ideal construct to test whether it can complement the *symrem1*-phenotype. This approach could clarify whether the S-acylation really has an impact on the function of SYMREM1.

Besides a role solely in PM-localization, S-acylation was postulated to function also as an activation switch, or as modification controlling specific protein-protein interactions (Blaskovic *et al.*, 2013). One possible function for the S-acylation of SYMREM1 might be modulating activation intensity of downstream signaling components after Nod factor perception. The relevance of S-acylation for signaling in response to a trigger was already shown for the plant immune receptor FLS2, which shows less efficient pathway induction when deacylated (Hemsley *et al.*, 2013). Furthermore, S-acylation can also function as an activation switch like phosphorylation (Sorek *et al.*, 2010). Given that such a mechanism is present in SYMREM1, it might have different activation stages depending on the Nod factor perceived. As long as Nod factor perception takes place, SYMREM1 might stay S-acylated and the signal could be transduced. However, to switch off further signaling, SYMREM1 might get deacylated, turn into an inactive state and/or get degraded. There is precedence for a role in regulation of protein degradation, e.g. RIN4, a member of the plant immune system, is prevented from degradation as long as it is S-acylated (Kim *et al.*, 2005). A third possible role of S-acylation could be modulation of protein-protein interaction (Yang *et al.*, 2002). An alternative function of the S-acylation of SYMREM1 therefore might be to alter the composition of the SYMREM1-FLOT4-LYK3 infection MD depending on the S-acylation status of SYMREM1. Since a S-acylation site was predicted for AtFLOT1 (Borner *et al.*, 2005), FLOT4 might also be S-acylated, which would increase the level of regulation and modulation of the signaling via the SYMREM1-FLOT4-LYK3 infection MD. However, what kind of physiological impact S-acylation might have for the function

of SYMREM1 or whether S-acylation serves only as PM anchoring needs to be shown in the future.

1.3. SYMREM1 is necessary for a successful Infection Thread formation

Depletion of SYMREM1 via an RNAi construct causes an altered infection thread (IT) phenotype (Lefebvre *et al.*, 2010). Although a reduction in nodule number was shown for a stable *Medicago* transposon-insertion line (*symrem1-1*), the IT phenotype was not monitored in this work (Lefebvre *et al.*, 2010). Therefore, in the course of this thesis the altered IT phenotype was verified for *symrem1-1* and could also be demonstrated for a second *SYMREM1* mutant allele (*symrem1-2*). For both mutant allele lines a significant reduction in the number of mature ITs was shown (Stratil *et al.* ms 2, Fig. 1K). Successful complementation with the wild type allele finally proved that the *Tnt1* transposon insertion in the *SYMREM1* gene is the reason for the observed IT and nodule phenotype in the *symrem1-2* mutant line (Stratil *et al.* ms 2, Fig. 1K and L). These findings verified the involvement of SYMREM1 in the infection process during Root Nodule Symbiosis (RNS).

A next step may be to investigate the function of SYMREM1 in the infection process in more detail. It would be necessary to visualize SYMREM1 during the infection process in the root hair and in this way the role of SYMREM1 could be studied *in vivo*. One starting point for understanding the physiological mechanism in which SYMREM1 is involved could be studying the localization of the exocytotic vesicle-associated membrane protein (VAMP721e) in the *symrem1* background. VAMP72s are involved in exocytosis by mediating the fusion of transported vesicles with a target membrane like the PM (Sanderfoot, 2007; Kwon *et al.*, 2008). Like SYMREM1, VAMP721e localizes to the symbiosome membrane and to the site of bacterial release from ITs (Lefebvre *et al.*, 2010; Ivanov *et al.*, 2012). Furthermore, it was shown that VAMP721e localizes to the newly formed infection chamber in the root hair (Fournier *et al.*, 2015). To test whether the *symrem1* phenotype is due to an alteration in an exocytotic pathway or membrane fusion, studying the localization pattern of VAMP721e in the *symrem1* mutant could be one first step.

Another question is whether there are other proteins localizing to the SYMREM1-FLOT4-LYK3 domain. LYK3 and NFP most probably act as a complex (Madsen *et al.*, 2011; Pietraszewska-Bogiel *et al.*, 2013; Moling *et al.*, 2014). Additionally, a

recent work also showed that SYMRK associates with NFR1 and NFR5 (Ried *et al.*, 2014). Since SYMREM1 interacts with all three receptors (Lefebvre *et al.*, 2010; Tóth *et al.*, 2012), the SYMREM1-domain might function as an interaction platform for this signaling complex and facilitate further signaling. SYMRK, and to some extent also LYK3 are part of the signaling cascade induced by both AM fungi and rhizobia (Stracke *et al.*, 2002; Zhang *et al.*, 2015). During RNS an unwanted AMF-dependent induction via SYMRK and LYK3 therefore needs to be prevented. By forming a specific Nod factor-dependent signaling platform with SYMREM1 as scaffold protein, SYMRK and LYK3 may be physically hindered to interact with a potential Myc factor receptor (e.g. CERK1 (Zhang *et al.*, 2015)). As a consequence, the Nod factor-dependent signaling pathway is strongly induced and an unwanted induction by the Myc factor receptor is prevented. A similar mechanism, which inhibits the induction of a signaling pathway by preventing the formation of a receptor complex, was just recently shown for the abscisic acid induced inhibition of brassinosteroid receptor complex assembly (Gui *et al.*, 2016). In this case the interaction of the co-receptor OsSERK1 (the rice BRI1-ASSOCIATED RECEPTOR KINASE 1) and the brassinosteroid receptor BRASSINOSTEROID-INSENSITIVE 1 is blocked at high abscisic acid levels due to the interaction of SERK1 and the remorin REM4.1. Similarly SYMREM1 might inhibit the interaction of LYK3 and SYMRK with CERK1 under high Nod factor concentrations.

Besides SYMRK/DMI2 another putative candidate as an additional component of the SYMREM1-dependent infection domain might be the ubiquitin ligase PUB1. PUB1 localizes to the PM and interacts with and is phosphorylated by LYK3 and DMI2. (Mbengue *et al.*, 2010; Vernié *et al.*, 2016). This phosphorylation most likely modulates the ubiquitination level of downstream signaling components through PUB1 since it could not be shown that LYK3 or DMI2 are direct targets of PUB1 (Mbengue *et al.*, 2010; Vernié *et al.*, 2016). However, whether PUB1 directly interacts with SYMREM1 and whether PUB1 is localized in MDs after all still needs to be shown.

Two other SYMRK interacting proteins might also be interesting candidates for a larger signaling infection hub, which is stabilized by the scaffold protein SYMREM1. The first one is a mitogen-activated protein (MAP) kinase kinase, a component of the MAP kinase cascade, which is known to be important for the signal transduction in

plant immune signaling. (Asai *et al.*, 2002; Chen *et al.*, 2012). The second candidate is HMGR1, a reductase that produces the second messenger mevalonate (Kevei *et al.*, 2007; Venkateshwaran *et al.*, 2015). Mevalonate was shown to be able to induce Ca^{2+} spiking and symbiotic gene expression (Venkateshwaran *et al.*, 2015). Both proteins play a role in two different modes of signal transduction (kinase cascade and second messenger production). Based on these abilities, both proteins could serve as a link between the Nod factor perception and downstream signal transduction from the SYMREM1-FLOT4-LYK3 domain to the Ca^{2+} spiking formation and transcription activation in the nucleus (Genre & Russo, 2016).

In the future unraveling potential additional components of the SYMREM1-dependent infection domain might help to get a better picture of the downstream targets of the Nod factor receptors. Furthermore, it might also shed light on the question of how specificity in downstream signaling upon Nod or Myc factor perception is achieved.

2. MYCREM - MYCorrhiza-induced REMorin

2.1. MYCREM: A putative component of a “new” regulatory pathway

Legumes have the fascinating ability to establish two different kinds of mutualistic plant-microbe interactions: The Arbuscular Mycorrhiza (AM) and the RNS. Both interactions start with a molecular dialog at the PM, where receptor kinases perceive Myc or Nod factors secreted either by the fungus or the rhizobium, respectively. Detection of this signal in both cases triggers Ca^{2+} spiking in the nucleus which is decoded by the combined action of the calcium dependent kinase DMI3/CCaMK and the transcriptional activator IPD3/CYCLOPS (for details see also section A.1.3.1). Since this signaling cascade is involved in establishing both symbioses, it is called Common Symbiosis Pathway (CSP) (Kistner & Parniske, 2002; Kistner *et al.*, 2005; Popp & Ott, 2011). Downstream of the CSP the signaling pathway is separated again and in the inner root cortex either arbuscule formation or nodule formation is initiated (Gutjahr & Parniske, 2013; Oldroyd, 2013).

2.1.1. A “New” regulatory circuit and prerequisites for a putative negative component

Under laboratory conditions AM and RNS have usually been studied as a one-to-one interaction. Consequently, it is common practice to inoculate plants with only one symbiont to investigate the signaling cascade. However, by focusing on only a single interaction, the situation as it is found in nature is completely ignored. Under open-field conditions legumes interact with both, fungus and rhizobia, in a temporal and spatial manner. More specifically, legumes do not only establish the two symbioses with both symbionts on a macroscopic level at different local positions along the root, but also form both symbiotic accommodations (arbuscule and root nodule) at the same time next to each other within the inner root cortex (Küster *et al.*, 2007; Padamsee *et al.*, 2016; Popp *et al.* ms 1, Fig. 1). However, regarding the process downstream of the CSP several questions remain unanswered, e.g.: (a) how do legumes discriminate which symbiosis should be established if both symbionts have been recognized at the epidermis? (b) How is it possible to suppress root nodule organogenesis when the fungus is growing in the inner cortex and is close to penetrating the cortical root cell to form an arbuscule? In the light of these questions, it has to be hypothesized that by gaining the ability for the RNS symbiosis, legume plants at the same time had to evolve a spatial regulatory mechanism to suppress nodule organogenesis when forming arbuscules in the inner cortical cells (Fig. 5B).

A component of such a postulated regulatory circuit has to fulfill some prerequisites: (1) it should have co-appeared with the evolution of the RNS, (2) be induced in a symbiont-dependent manner and (3) be dispensable for the establishment of both symbioses *per se*.

Phylogenetic analyses revealed that the remorin protein MYCREM co-evolved with the RNS in the legume clade but was lost again in *Lupinus angustifolius* (Popp *et al.* ms 1, Fig. 2). *Lupinus* itself lost the ability to form AM, but can still establish RNS (Oba *et al.*, 2001).

MYCREM transcript was induced under AM (Popp *et al.* ms 1, Fig. 3A) and MYCREM promoter activity was detected during AM and initial nodule organogenesis stages (Popp *et al.* ms 1, Fig. 3F-K). However, the mutant did not

display any alteration in fungal colonization or nodule number (Popp *et al.* ms 1, Fig. S1C-E). Interestingly, *MYCREM* transcript and promoter induction was down-regulated in infected nodule primordia cells (Popp *et al.* ms.1, Fig. 3B, E and G). Thus, *MYCREM* shows an AM- and RNS-dependent induction, but is dispensable for both symbioses. Although *MYCREM* is absent in *Lupinus* and strongly induced by AMF inoculation, a RNS-related relevance of *MYCREM* is supported by the fact that *MYCREM* was not detected as AM-specific gene in any proteomic or bioinformatic approach (Favre *et al.*, 2014; Bravo *et al.*, 2016). From that and in the light of all prerequisites being fulfilled, we hypothesized that a function of *MYCREM* is related to the presence of both symbioses and might play a role in the proposed negative regulatory circuit.

To our knowledge *MYCREM* is the first described gene that is induced by AMF and rhizobia, which has co-evolved with RNS, but was lost again in the RNS-only host *Lupinus*. In a phylogenetic approach addressing the presence of symbiosis-specific genes, only AM-related genes have been found to be absent in *Lupinus*, which is consistent with *Lupinus* being a non-AM host (Delaux *et al.*, 2014). In the future, comparative phylogenetic studies including AM-only, AM/RNS and RNS-only hosts should give better insight into the mechanisms of how legume plants can coordinate the tripartite interaction of plant, fungus and rhizobium.

Besides *MYCREM*, another interesting candidate at least partly fulfilling the above mentioned criteria for tripartite symbiosis regulatory component is the receptor *LYS11* from *Lotus* and *LYR1* from *Medicago*. These receptors are paralogs to *NFR5* and *NFP* (Gomez *et al.*, 2009; Lohmann *et al.*, 2010; De Mita *et al.*, 2014). *LYS11* is strongly induced in arbuscule-containing and adjacent cells. Moreover, it shows a basal promoter activity under uninoculated conditions, in lateral root primordia and a strong activation in young nodule primordia (Rasmussen *et al.*, 2016). This induction pattern is very similar to the *MYCREM* promoter (Popp *et al.* ms 1, Fig. 3). In addition, the mutant of *LYS11* shows a wild type-like phenotype under AM or RNS conditions, like it is the case for the *mycrem* mutant (Popp *et al.* ms 1, Fig. S1). Interestingly, *LYS11* co-localizes with *NFR5* in the PM and can complement the function of *NFR5* in the corresponding mutant, which implies a certain ability of *LYS11* to recognize lipooligosaccharides (Rasmussen *et al.*, 2016). Based on the expression pattern and the functional influence on RNS, it would be interesting to

monitor the phenotype under co-inoculation conditions and to analyze whether a homolog of *LYS11* is still present in *Lupinus* or not. However, whether MYCREM and LYS11/LYR1 may then be involved in the same signaling pathway remains to be investigated.

2.1.2. MYCREM - a regulatory component of root nodule organogenesis under tripartite co-inoculation conditions

If our hypothesis of MYCREM being part of a negative regulatory pathway under a tripartite interaction situation holds true, MYCREM should be relevant under conditions when both symbionts are present. Therefore, we monitored the number of developing nodules in a *Medicago truncatula mycrem* mutant, when plants were inoculated with the fungal symbiont *Rhizophagus irregularis* and *Sinorhizobium meliloti* at the same time. Indeed, our experiments demonstrated that *mycrem* plants developed significantly more root nodule primordia compared to the wild type (Popp *et al.* ms 1, Fig. 4A-C). Moreover, the complementation experiment verified the *Tnt1* insertion in the *MYCREM* being the causative mutation for the observed phenotype under co-inoculation conditions (Popp *et al.* ms 1, Fig. 4C).

Until now, only Xie and co-workers have looked at a local effect of a tripartite symbiotic interaction (Xie *et al.*, 1995, 1998). In contrast to our work, they investigated the putative impact of Nod factor application or rhizobia inoculation on AM, revealing that the co-inoculated plants show a higher AMF colonization rate. However, they did not monitor the effect of the AM colonization on the nodulation rate like we did in our study. To our knowledge, our study was the first addressing the existence of a local AM-triggered negative regulatory circuit on RNS.

Interestingly, besides an increase of primordia number under co-inoculation conditions, *mycrem* mutants develop more lateral roots, as well (Popp *et al.* ms 1, Fig. 4). The phenotype of increased nodule and higher lateral root number was also observed in mutants of genes which have been described to control nodule number under single inoculation conditions. For example, the mutant of the CSP component PUB1 shows such a phenotype (Mbengue *et al.*, 2010; Vernié *et al.*, 2016). As already mentioned above when discussing putative interaction partners of SYMREM1, it is thought that PUB1 functions via degrading downstream signaling components after Nod or Myc factor perception. One possible scenario might be that

MYCREM facilitates the interaction between PUB1 and its so far uncharacterized targets in an AM-specific manner to inhibit nodule organogenesis.

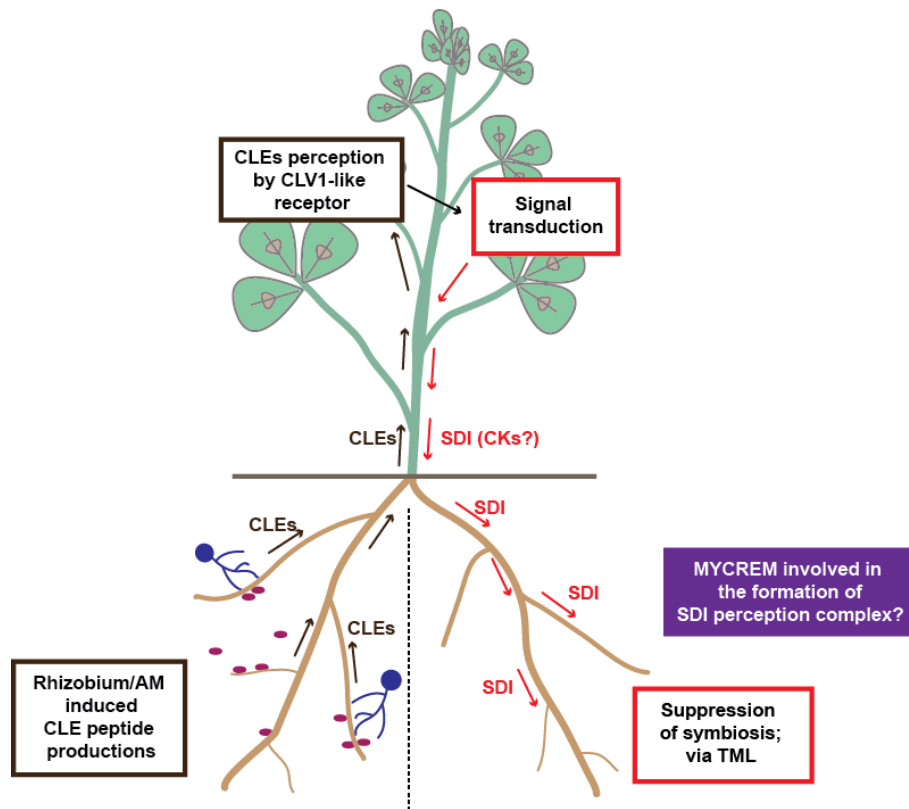


Figure 4: Systemic Autoregulation of Symbioses.

The Autoregulation of Nodulation and the Autoregulation of Mycorrhiza were shown to share signaling components and function via the same mode of function. Therefore, these two pathways are also called Autoregulation of Symbioses (Caetano-Anolles & Gresshoff, 1991; Catford *et al.*, 2003; Meixner *et al.*, 2007; Staehelin *et al.*, 2011; Mortier *et al.*, 2012; Schaarschmidt *et al.*, 2013)

The root-to-shoot-to-root signaling is activated by the perception of Nod or Myc factor, which leads to the expression of CLAVATA3/endosperm-surrounding region-related (CLE) peptides in the root (Okamoto *et al.*, 2009, 2013; Reid *et al.*, 2011; Saur *et al.*, 2011; Soyano *et al.*, 2014). These peptides are transported to the shoot (brown arrows), where they are perceived by a CLAVATA1 (CLV1)-like receptor (Krusell *et al.*, 2002; Nishimura *et al.*, 2002; Penmetsa *et al.*, 2003; Searle, 2003; Schnabel *et al.*, 2005). The perception triggers a signal transduction, which causes the formation of a shoot-derived inhibitor, most likely Cytokinins (CKs) and is again transported to the root (red arrows) (Sasaki *et al.*, 2014). In the root the putative perception of this shoot-derived inhibitor (SDI) suppresses either arbuscule or nodule formation in a so far unknown mechanism. TOO MUCH LOVE (TML), a F-box protein, acts downstream of the SDI perception, however, its precise mode of function is still unclear (Magori *et al.*, 2009; Takahara *et al.*, 2013). MYCREM might putatively be involved in the formation of a SDI perception complex (purple box).

The mutant of a CLAVATA1 (CLV1)-like receptor kinase, which is a component of a negative regulatory signaling pathway, also shows a hypernodulation phenotype and an increase in lateral root number (Day *et al.*, 1986; Szczyglowski *et al.*, 1998; Wopereis *et al.*, 2000; Krusell *et al.*, 2002; Penmetsa *et al.*, 2003; Schnabel *et al.*, 2005; Buzas & Gresshoff, 2007). This CLV1-like receptor is part of a systemic root-to-shoot-to-root regulatory mechanism to control nodule number or arbuscule number, which is called Autoregulation of Nodulation (AON) or Autoregulation of Mycorrhization (AOM), respectively (Fig. 4) (Catford *et al.*, 2003; Meixner *et al.*, 2007; Staehelin *et al.*, 2011; Schaarschmidt *et al.*, 2013). This systemic signaling is induced by Nod or Myc factor perception, which leads to the production of CLAVATA3/endosperm-surrounding region-related (CLE) peptides and their transport to the shoot (Soyano *et al.*, 2014). For the Nod factor induced AON pathway, it was shown that the CLE production is induced via the transcription factor NIN (Soyano *et al.*, 2014). In the shoot the CLV1-like receptor perceives these CLE peptides and induces a so far unknown downstream signaling cascade to produce a shoot-derived inhibitor (SDI), which is most likely a cytokinin variant (Sasaki *et al.*, 2014). However, the perception of the SDI and the downstream signaling to inhibit RNS or AM is unknown (Fig 4). In addition to this systemic AON, the CLV1-like receptor is also involved in a local regulatory circuit to inhibit nodulation in the presence of high nitrate concentrations in the soil (Fig. 5A) (Okamoto *et al.*, 2009; Reid *et al.*, 2011, 2013). Similarly, for AM a local AOM has to be postulated, which is triggered by high phosphate in the soil, leading to the formation of CLE peptides and most likely perception via the CLV1-like receptor (Morandi *et al.*, 2000; Vierheilig *et al.*, 2000; Zakaria Solaiman *et al.*, 2000; Catford *et al.*, 2003; Funayama-Noguchi *et al.*, 2011). Besides the role of the described CLE-peptide-receptor signaling module, in *Arabidopsis* such modules are known to regulate the proliferation in the shoot apical meristem (e.g. CLV3-CLV1 module) or to regulate the lateral root emergence in an N-dependent manner (e.g. CLE1/3/4/7-CLV1 module) (Clark *et al.*, 1993, 1997; Araya *et al.*, 2014). In analogy to the above-described AON CLE peptide-receptor signaling pathway, our postulated mechanism could also be triggered by a local inhibitor compound, which might be induced by the AMF in the cortex, e.g. CLE peptides. This inhibitor compound would be perceived via a receptor (e.g. CLV1-like receptor), which in turn induces downstream signaling

to achieve an inhibition of nodule organogenesis (Fig. 5B). Several remorins have been shown to interact with receptor kinases and serve as scaffold protein to form a signaling complex (Lefebvre *et al.*, 2010; Tóth *et al.*, 2012; Gui *et al.*, 2016; Bücherl *et al.*, 2017). A potential site of function of MYCREM might therefore be the formation of an AM-triggered AON signaling domain, which contains the CLV1-like receptor and potential co-receptors, like CLAVATA2 or KLAVIER (Fig. 5A and B) (Guo *et al.*, 2010; Miyazawa *et al.*, 2010; Zhu *et al.*, 2010; Krusell *et al.*, 2011; Crook *et al.*, 2016).

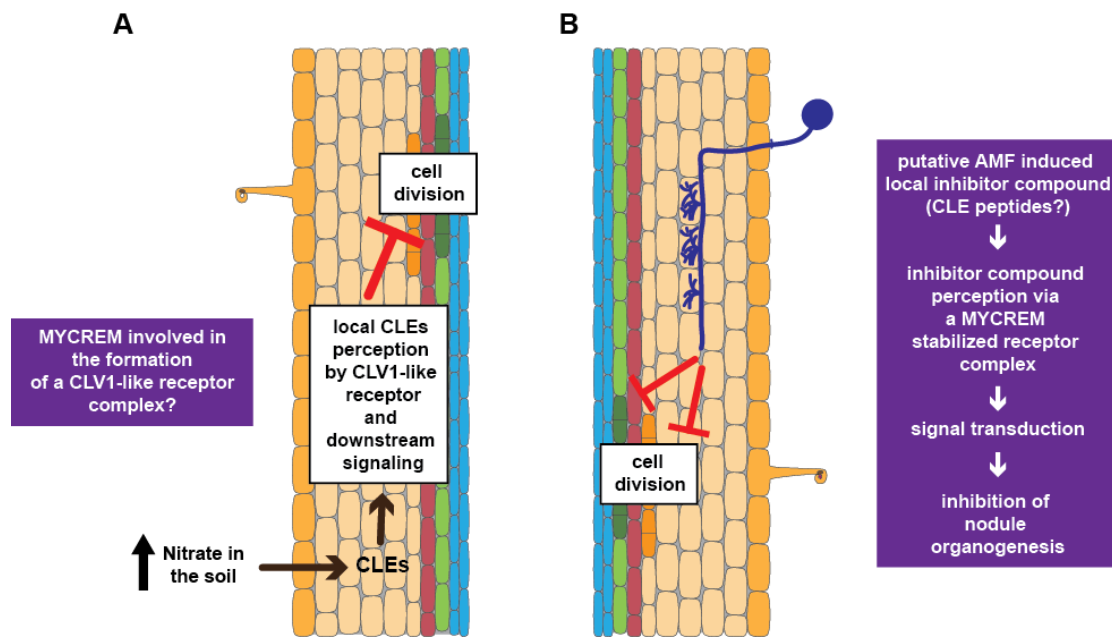


Figure 5: Local negative regulatory mechanism.

A) A high nitrate concentration in the soil induces the expression of CLE peptides, which are perceived by CLV1-like receptor, analogous to the systemic Autoregulation of Nodulation. This perception leads to the inhibition of nodule organogenesis (Okamoto *et al.*, 2009; Reid *et al.*, 2011, 2013). However, the precise downstream signaling is unknown. MYCREM might potentially be involved in the formation of a CLV1-like receptor complex (purple box).

B) Schematic description of our postulated negative regulatory circuit: The symbiotic fungus induces the formation of a local inhibitor compound (potentially CLE peptides). A MYCREM-stabilized receptor complex perceives this component and triggers downstream signaling. This inhibits nodule organogenesis at a so far unknown stage. This hypothetical pathway is depicted in a purple box.

Within the AON pathway, cytokinin signaling is involved in the negative regulation of nodule formation, as cytokinins are supposed to be the SDI signal (Sasaki *et al.*, 2014). Furthermore, it is known that cytokinins regulate lateral root development in a restrictive way (Laplaze *et al.*, 2007; Bielach *et al.*, 2012; Del Bianco *et al.*, 2013).

Moreover, cytokinin perception by the receptor CRE1/LHK1 is essential for nodule formation and is involved in lateral root formation (Tirichine *et al.*, 2007; Plet *et al.*, 2011). However, so far it is unclear which receptor is responsible for the perception of the SDI-cytokinin, either CRE1 or one of its orthologs (Gonzalez-Rizzo *et al.*, 2006; Plet *et al.*, 2011; Held *et al.*, 2014; Laffont *et al.*, 2015). These different roles of cytokinins raise the question whether specificity is achieved via dose-dependency, differently expressed Cytokinin receptors or the formation of different Cytokinin signaling complexes (Riefler *et al.*, 2006; Held *et al.*, 2014). For *Arabidopsis* it is known that specific cytokinin receptors are responsible for different pathways and that the receptors have variable affinities to different cytokinin species.

Taking these effects into account, as well as the phenotypes of *mycrem* plants (more lateral roots, increase of nodule primordia) and the overlapping promoter activity of *MYCREM* and *CRE1* (Popp *et al.* ms 1, Fig. 3C-H) (Lohar *et al.*, 2006), another possible function of *MYCREM* could be to facilitate the assembly of different cytokinin receptors with downstream interaction partners like a histidine phosphotransferase, which are known to be phosphorylated by cytokinin receptors (reviewed in Heyl *et al.*, 2012; El-Showk *et al.*, 2013) (Fig. 4 and 5 A). Being involved in the formation of a cytokinin receptor complex, *MYCREM* might nonetheless be part of a CLE-CLV1-like AON signaling pathway, however, not in the perception of the CLE peptide, but rather downstream in the signaling cascade in the perception of the SDI (cytokinins) (Fig. 4). Also within our postulated local regulatory circuit, it could well be that a potential signal by the fungus induces the expression of a cytokinin variant which is then perceived by a *MYCREM* stabilized receptor, which triggers negative effects on the root nodule organogenesis (Fig. 5B).

An initial experiment to address an involvement of *MYCREM* in a local AON pathway might be to analyze the nitrate sensitivity during RNS. Furthermore, the AM and RNS phenotypes of *mycrem* in a split-root assay could be tested to address an involvement in the systemic AON/AOM. In this kind of assay one half of the root system is inoculated, for example, with the fungus, followed by a later inoculation of the second half with rhizobia. If under these conditions *mycrem* shows an enhanced nodule number, it would indicate an involvement in a systemic mechanism. Whether *MYCREM* actually takes part in cytokinin signaling could be initially studied by

monitoring the nodule phenotype of *mycrem* in the presence of exogenously applied cytokinin.

2.1.3. Symbioses-related Remorins are inducible by the Common Symbiosis Pathway

Nodule organogenesis can be induced in the absence of rhizobia by auto-active versions of CCaMK and CYCLOPS (Miller *et al.*, 2013; Singh *et al.*, 2014; Soyano & Hayashi, 2014). To verify the negative effect of MYCREM on nodule organogenesis on a genetic basis we made use of the auto-active versions of CCaMK (CCaMK-T265D) and CYCLOPS (CYCLOPS-DD) (Yano *et al.*, 2008; Hayashi *et al.*, 2010; Singh *et al.*, 2014). The overexpression of either CCaMK-T265D or CYCLOPS-DD induced the formation of more spontaneous nodules (SPN) on *mycrem* than on wild type roots (Popp *et al.* ms 1, Fig. 5A-E). These findings support the hypothesis that *mycrem* mutants are defective in a negative regulation of nodule organogenesis. The correlation of a high MYCREM transcript level in wild type roots expressing CYCLOPS-DD compared to roots overexpressing CCaMK-T265D, and the reduced number of SPNs on roots expressing CYCLOPS-DD compared to the wild type roots expressing CCaMK-T265D strengthens our hypothesis of a negative function of MYCREM (Popp *et al.* ms 1, Fig. 5A and S3A).

The increase in MYCREM transcript by CYCLOPS-DD indicated its CSP-dependency (Popp *et al.* Fig. S3A). However, it remains to be shown whether this induction is due to a direct promoter binding of CYCLOPS or by an indirect induction via further downstream TFs, like NIN or RAM1.

Interestingly, as mentioned above, in this experiment CCaMK-T265D induced MYCREM to a lesser extent than CYCLOPS-DD (Popp *et al.* ms 1, Fig. S3A). The induction pattern by CCaMK-T265D could mean that the endogenous IPD3 cannot directly or indirectly induce MYCREM expression as strongly as the overexpressed CYCLOPS-DD due to the actual amount of active protein. Alternatively, it may be that CCaMK-T265D simultaneously induces a negative regulatory feedback, which keeps the MYCREM transcript at a certain level.

In contrast to MYCREM, the second legume-specific remorin SYMREM1 is strongly induced upon Nod factor perception and the mutant is defective in IT formation and

bacterial release. However, *SYMREM1* also co-appeared with the evolution of RNS. To test whether *MYCREM* and *SYMREM1* are induced in a similar way and whether they might be linked on the signaling level, we also analyzed the transcript induction pattern of *SYMREM1*.

For *SYMREM1* from *Medicago* it was already demonstrated, that *SYMREM1* is one of two genes showing a strongly reduced expression in uninfected *ipd3*-nodules (Bénaben *et al.*, 1995; Ovchinnikova *et al.*, 2011). Similarly, reduced induction of *Lotus* *SYMREM1* was also detected in the *cyclops* mutant background (Høgslund *et al.*, 2009; Verdier *et al.*, 2013). From these results and the fact that the *Lotus* *CYCLOPS* can complement the *Medicago ipd3* phenotype one could expect that *CYCLOPS* should be able to induce *SYMREM1* in *Medicago* (Horváth *et al.*, 2011).

However, while, overexpression of CCaMK-T265D led to a strong induction of *SYMREM1* transcription, *CYCLOPS-DD* could not induce *SYMREM1* (Popp *et al.* ms 1, Fig. S3B). Although *SYMREM1* transcription is *CYCLOPS/IPD3*-dependent in the presence of rhizobia, its transcript expression cannot be induced via *CYCLOPS-DD*. This result supports the hypothesis that the activation status of CCaMK and *CYCLOPS* may induce different downstream signaling programs, like infection, nodule organogenesis, or arbuscule formation (Hayashi *et al.*, 2010; Shimoda *et al.*, 2012; Singh & Parniske, 2012; Singh *et al.*, 2014). *CYCLOPS-DD* may be more restricted to the activation and control of nodule organogenesis (Singh *et al.*, 2014; Pimprikar *et al.*, 2016) (Popp *et al.* ms 1, Fig. S3B), whereas CCaMK-T265D in addition to the nodule organogenesis program may also induce the infection process, which can be inferred from the transcript induction of infection marker *SYMREM1* (Hayashi *et al.*, 2010; Shimoda *et al.*, 2012).

Interestingly, the CCaMK-T265D-dependent induction of *SYMREM1* is abolished in *mycrem* (Popp *et al.* ms 1, Fig. S3B). This result would suggest that *MYCREM* regulates the *SYMREM1* gene expression. Hence, the *mycrem* mutant should display a similar RNS phenotype like *symrem1* plants, which form fewer nodules. However, this is not the case since *mycrem* mutants do not show an altered RNS phenotype under single inoculation conditions (Popp *et al.* ms 1, Fig. S1C). An alternative explanation might be that abolished *SYMREM1* induction in the *mycrem* background is due to a putative regulatory mechanism that is linked to a later nodule development stage. Taking into account the mutually exclusive promoter induction pattern of

MYCREM and *SYMREM1* in elongated *Medicago* nodules, it seems as if the induction of one is excluding the other. The promoter induction study of *MYCREM* showed an induction in the meristem zone of an elongated nodule (Popp *et al.* ms 1, Fig. 3E). In contrast, *SYMREM1* is also known to be induced in the interzone II/III and nitrogen fixation zone of elongated nodules, and the protein localizes not only to the IF, but also to the symbiosome membrane after bacterial release (Lefebvre *et al.*, 2010; Popp & Ott, 2011). Since the data set for the transcriptional analyses was obtained from material that already formed elongated nodules (Popp *et al.* ms 1, Fig. D-E), it might well be that the observed lack of *SYMREM1* induction results from a putative additional function of *MYCREM* at a later stage of the nodule development, which includes a regulatory mechanism on *SYMREM1*.

To unravel the mechanism of the opposite induction pattern of *MYCREM* and *SYMREM1*, different auto-active variants of CCaMK/DIM3 and IPD3/CYCLOPS could be used. Also including the auto-active variants of the cytokinin receptor LHK1/CRE1 would help to further dissect the induction mechanism. It was shown that CCaMK-T265D can induce SPN in *cyclops* mutants (Yano *et al.*, 2008; Singh *et al.*, 2014). In contrast, DMI3¹⁻³¹¹ (the kinase domain only) cannot induce SPNs in an *ipd3* mutant, while the auto-active version CRE1-L267F does (Ovchinnikova *et al.*, 2011). Expression of both auto-active variants of DMI3 and CRE1 in an *ipd3* background could clarify whether *MYCREM* is activated downstream of DMI3, but in this case in an IPD3-independent manner, or downstream of the CRE1-mediated nodule organogenesis pathway.

Certainly, the induction patterns of *MYCREM* and *SYMREM1* need further investigation to decode the precise activation mechanism of both. In future experimental set-ups particularly the different developmental stages of a root nodule and the spatial control of RNS and AM have to be taken into consideration much more than in previous studies. This might help to discriminate between a potential early (regulation of nodule organogenesis) and a later function (a potential regulatory function of nodule meristem) of *MYCREM*.

In the course of the overexpression experiments of the auto-active CSP proteins, one puzzling result of our study was the difference in the phenotype of clustered roots when overexpressing CYCLOPS-DD in the wild type compared to overexpression in

mycrem (Popp *et al.* ms 1, Fig. 5F, G and H). This intriguing phenotype is characterized by many primordia-like foci along a transgenic root. In the light of a hypothetical AON mechanism, in which MYCREM may be involved, one explanation for the observed effect of CYCLOPS-DD on WT roots might be that CYCLOPS-DD induces lateral organ organogenesis at several spots. However, at the same time CYCLOPS-DD might activate via e.g. NIN the production of CLE peptides, which in turn are perceived by a MYCREM-stabilized CLV1-like receptor module, which induces a signaling cascade to hinder further outgrowth or development of the primordia. In contrast, in the *mycrem* mutant this inhibitory mechanism might be less effective and the primordia may further develop. For *Arabidopsis* it was already shown that CLE peptides-CLV1-like signaling modules are involved in lateral root formation (reviewed in Araya *et al.*, 2016). Besides the regulatory role in maintenance of the shoot apical meristem, CLV1 also regulates lateral root emergence in an N-dependent manner (Clark *et al.*, 1993, 1997; Araya *et al.*, 2014). However, due to CLV1 expression in companion cells of phloem, the regulation of lateral root emergence most likely depends on an additional long-distance signal (Araya *et al.*, 2014). For the CVL1-like receptor, which is involved in the local and systemic AON in legumes, a similar root phenotype and expression pattern was described as for CLV1, which might point to a similar role of the CLV1-like receptor in lateral root development (Nishimura *et al.*, 2002; Schnabel *et al.*, 2005, 2012). Another example of a CLE-peptide-receptor module that regulates lateral root outgrowth, is the CLE40-ARABIDOPSIS CRINKLY4 signaling module (Hobe *et al.*, 2003; De Smet *et al.*, 2008; Stahl *et al.*, 2009, 2013). Mutants of ARABIDOPSIS CRINKLY4 form lateral root primordia at a higher frequency and show an enhanced cell division in the pericycle (De Smet *et al.*, 2008). However, the precise mechanism of how ARABIDOPSIS CRINKLY4 restricts cell division in adjacent cells of lateral root primordia in the pericycle is still unclear. Recently, a new type of CLE peptides (CLE-like peptides) have been described to be relevant for root development (Matsuzaki *et al.*, 2010; Meng *et al.*, 2012; Fernandez *et al.*, 2013). Overexpression of two of these CLE-like peptides results in a higher, but irregular cell division rate in the pericycle, which causes an arrest of the lateral root primordia development (Meng *et al.*, 2012). For another CLE peptide-receptor signaling module it was shown that the additional knock-out of the corresponding receptor complex in

the null mutation background of the CLE peptide suppresses the CLE peptide mutant phenotype (DeYoung & Clark, 2008). Following this line of argumentation, the reduction of the clustered root phenotype in the *mycrem* mutant background could be caused by a disturbance of the CLE-receptor(s) signaling module. The proper assembly of the receptor complex would be reduced due to the loss of MYCREM, the accurate signaling might be less efficient and therefore the blockage of the lateral root organ outgrowth would be abolished.

Future research may shed light on the question whether a MYCREM-dependent formation of a CLE (-like) peptide-CLV1-like receptor signaling module is involved in the development of the observed clustered roots in wild type plants expressing CYCLSOP-DD in their roots.

2.1.4. *MYCREM* - potentially adapted from a lateral root organogenesis program?

The *MYCREM* promoter induction pattern during lateral root primordia and root nodule formation (Popp *et al.* ms 1, Fig. 3C-H) resembles the promoter activity of *CRE1*, as well as of *LONELY GUY*, which is involved in the activation of cytokinins and of *KNOX3*, a TF, which is involved in the regulation of nodule development via regulating cytokinin response genes (Lohar *et al.*, 2006; Mortier *et al.*, 2014; Di Giacomo *et al.*, 2016). These proteins also have an additional lateral root phenotype like *mycrem* (*CRE1*, *LONELY GUY*) or are known to belong to a gene family that regulates meristem activity in *Arabidopsis* (*KNOX3*) (Gonzalez-Rizzo *et al.*, 2006; Tirichine *et al.*, 2007; Plet *et al.*, 2011; Mortier *et al.*, 2014; Azarakhsh *et al.*, 2015; Laffont *et al.*, 2015) (Popp *et al.* ms 1, Fig. 4D). These similarities and the negative regulatory effect on lateral root formation lead to the question whether MYCREM might have evolved from a general lateral root organogenesis signaling pathway.

Based on proteomic approaches and mutant phenotypes, it was also postulated that parts of the lateral root organogenesis pathway were adapted to the root nodule organogenesis pathway (Desbrosses & Stougaard, 2011; Couzigou *et al.*, 2012; Limpens *et al.*, 2013; Roux *et al.*, 2014; Franssen *et al.*, 2015; Di Giacomo *et al.*, 2016). Our phylogenetic analyses showed that *MYCREM* and *SYMREMI* result from a gene duplication event at the base of the Papilionoideae clade, which occurred at the same time when RNS first appeared (Sprent, 2007; Young *et al.*, 2011). One may

speculate that the common ancestor of *MYCREM* and *SYMREM1* was originally involved in the lateral root developmental program. Later during RNS evolution, after a gene duplication of the common ancestor had taken place during the whole genome duplication event in the papilionoid legumes (Sprent, 2007; Young *et al.*, 2011), *MYCREM* might have gained its new function. In parallel, *SMYREM1* might have developed its RNS-specific function as it was shown for other paralogous RNS-related gene pairs (e.g. Type-A RRs, NFP/LYR1, ERN1/ERN2) (Lynch & Conery, 2000; Op den Camp *et al.*, 2011a; Young *et al.*, 2011; Ivanov *et al.*, 2012). However, it remains to be proven whether *MYCREM* and *SYMREM1* might have evolved their functions either by sub-neo-functionalization or by neo-functionalization after the gene duplication. In the first scenario both genes would still be redundant in some functions, but would have gained specific new functions in addition (He & Zhang, 2005). In the second scenario one gene would have kept the original function of the common ancestor (*MYCREM*) while the other would have evolved a new function (*SYMREM1*) as it was shown for the LYK3-NFR1a gene clade (Lynch & Conery, 2000; De Mita *et al.*, 2014).

2.1.5. Outlook

In summary, the data presented in this work led to the hypothesis that *MYCREM* is a component of an additional regulatory pathway to control organogenesis induced in inner cortical root cells when fungus and rhizobium concomitantly establish a symbiotic relationship with the plant.

Future experiments have to elucidate the time point at which this negative regulation of the root nodule organogenesis takes place. Additionally, comparing the root nodule phenotypes of the *CLVI-like*-receptor or the cytokinin receptors with the *mycrem* root nodule phenotype on a cellular level might provide further insights, in which signaling pathway *MYCREM* is involved (Laplaze *et al.*, 2007; De Smet *et al.*, 2008). For this detailed comparison, the cell division pattern in the inner root cortex may have to be characterized when fungus and rhizobia are forming their symbiotic structures –arbuscule or root nodule- next to each other within the root. To visualize the cell division events in the cortex the marker protein T-PLATE labeling the expanding cell plate might be a useful tool (Van Damme *et al.*, 2006, 2011).

Another approach might be to perform initial interaction studies between MYCREM and potential interaction partners like the receptors CRE1 or the CLV1-like receptor. As part of such an analysis it would be also interesting to include the above-mentioned LYR1 receptor.

All in all, we demonstrated that MYCREM plays a negative role on root nodule organogenesis under co-inoculation conditions and restricts lateral root formation. However, based on our data at the moment it is not possible to definitively place MYCREM into a precise signaling pathway. Future research has to show whether the hypothesis of MYCREM being part of an AM-triggered local AON, or of a cytokinin-dependent regulatory pathway controlling lateral root organ organogenesis holds true. In either way, taking a new view on RNS and AM by considering the interaction of symbiotic fungi, rhizobia and legume plants as a whole will not only initiate further fundamental research projects but will also help to gain a better understanding of industrial important crop plants.

D) References

- Adams DG. 2002.** Symbiotic Interactions. In: Whitton BA,, In: Potts M, eds. The Ecology of Cyanobacteria: Their Diversity in Time and Space. Dordrecht: Springer Netherlands, 523–561.
- Akiyama K, Matsuzaki K, Hayashi H. 2005.** Plant sesquiterpenes induce hyphal branching in arbuscular mycorrhizal fungi. *Nature* **435**: 824–827.
- Akkermans A, Abdulkadar S, Trinick M. 1978.** Nitrogen-fixing root nodules in Ulmaceae. *Nature (UK)*.
- Amor B Ben, Shaw SL, Oldroyd GED, Maillet F, Penmetsa RV, Cook D, Long SR, Dénarié J, Gough C. 2003.** The NFP locus of *Medicago truncatula* controls an early step of Nod factor signal transduction upstream of a rapid calcium flux and root hair deformation. *Plant Journal* **34**: 495–506.
- Andriankaja A, Boisson-Dernier A, Frances L, Sauviac L, Jauneau A, Barker DG, de Carvalho-Niebel F. 2007.** AP2-ERF Transcription Factors Mediate Nod Factor Dependent Mt ENOD11 Activation in Root Hairs via a Novel cis-Regulatory Motif. *THE PLANT CELL ONLINE* **19**: 2866–2885.
- Ané J-M, Kiss GB, Riely BK, Penmetsa RV, Oldroyd GED, Ayax C, Lévy J, Debelle F, Baek J-M, Kalo P, et al. 2004.** *Medicago truncatula* DMI1 required for bacterial and fungal symbioses in legumes. *Science (New York, N.Y.)* **303**: 1364–1367.
- Antolín-Llovera M, Ried MK, Parniske M. 2014.** Cleavage of the symbiosis receptor-like kinase ectodomain promotes complex formation with nod factor receptor 5. *Current Biology* **24**: 422–427.
- Araya T, Miyamoto M, Wibowo J, Suzuki A, Kojima S, Tsuchiya YN, Sawa S, Fukuda H, von Wirén N, Takahashi H. 2014.** CLE-CLAVATA1 peptide-receptor signaling module regulates the expansion of plant root systems in a nitrogen-dependent manner. *Proceedings of the National Academy of Sciences of the United States of America* **111**: 2029–34.
- Araya T, von Wirén N, Takahashi H. 2016.** CLE peptide signaling and nitrogen interactions in plant root development. *Plant Molecular Biology*.
- Ariel F, Brault-Hernandez M, Laffont C, Huault E, Brault M, Plet J, Moison M, Blanchet S, Ichante JL, Chabaud M, et al. 2012.** Two Direct Targets of Cytokinin Signaling Regulate Symbiotic Nodulation in *Medicago truncatula*. *The Plant Cell* **24**: 3838–3852.
- Arrighi J-F, Barre A, Amor B Ben, Bersoult A, Soriano LC, Mirabella R, de Carvalho-Niebel F, Journet E-P, Ghérardi M, Huguet T, et al. 2006.** The *Medicago truncatula* Lysine Motif-Receptor-like Kinase Gene Family Includes NFP and New Nodule-Expressed Genes [Corrected Title: The *Medicago truncatula* Lysin Motif-Receptor-like Kinase Gene Family Includes NFP and New Nodule-Expressed Genes]. *Plant Physiology* **142**: 265.
- Asai T, Tena G, Plotnikova J, Willmann MR, Chiu W-L, Gomez-Gomez L, Boller T, Ausubel FM, Sheen J. 2002.** MAP kinase signalling cascade in *Arabidopsis* innate immunity. *Nature* **415**: 977–983.
- Azarakhsh M, Kirienko a. N, Zhukov V a., Lebedeva M a., Dolgikh E a., Lutova L a. 2015.** KNOTTED1-LIKE HOMEODOMAIN 3: a new regulator of symbiotic nodule development. *Journal of Experimental Botany*: erv414.
- Bariola PA, Retelska D, Stasiak A, Kammerer RA, Fleming A, Hijri M, Frank S, Farmer EE. 2004.** Remorins form a novel family of coiled coil-forming oligomeric

- and filamentous proteins associated with apical, vascular and embryonic tissues in plants. *Plant Molecular Biology* **55**: 579–594.
- Barker DG, Bianchi S, Blondon F, Dattée Y, Duc G, Essad S, Flament P, Gallusci P, Génier G, Guy P, et al. 1990.** Medicago truncatula, a model plant for studying the molecular genetics of the Rhizobium-legume symbiosis. *Plant Molecular Biology Reporter* **8**: 40–49.
- Batistič O, Rehers M, Akerman A, Schlücking K. 2012.** S-acylation-dependent association of the calcium sensor CBL2 with the vacuolar membrane is essential for proper abscisic acid responses. *Cell research*.
- Batistic O, Sorek N, Schültke S, Yalovsky S, Kudla J. 2008.** Dual fatty acyl modification determines the localization and plasma membrane targeting of CBL/CIPK Ca²⁺ signaling complexes in Arabidopsis. *The Plant cell* **20**: 1346–62.
- Bénaben V, Duc G, Lefebvre V, Huguet T. 1995.** TE7, an inefficient symbiotic mutant of Medicago truncatula Gaertn. cv Jemalong. *Plant Physiology*.
- Benschop JJ, Mohammed S, O’Flaherty M, Heck AJR, Slijper M, Menke FLH. 2007.** Quantitative phosphoproteomics of early elicitor signaling in Arabidopsis. *Molecular & cellular proteomics : MCP* **6**: 1198–214.
- Besserer A, Puech-Pagès V, Kiefer P, Gomez-Roldan V, Jauneau A, Roy S, Portais JC, Roux C, Bécard G, Séjalon-Delmas N. 2006.** Strigolactones stimulate arbuscular mycorrhizal fungi by activating mitochondria. *PLoS Biology* **4**: 1239–1247.
- Bhat R a., Panstruga R. 2005.** Lipid rafts in plants. *Planta* **223**: 5–19.
- Del Bianco M, Giustini L, Sabatini S. 2013.** Spatiotemporal changes in the role of cytokinin during root development. *New Phytologist* **199**: 324–338.
- Bielach A, Podlesáková K, Marhavy P, Duclercq J, Cuesta C, Müller B, Grunewald W, Tarkowski P, Benková E. 2012.** Spatiotemporal regulation of lateral root organogenesis in Arabidopsis by cytokinin. *The Plant cell* **24**: 3967–3981.
- Blaskovic S, Blanc M, van der Goot FG. 2013.** What does S-palmitoylation do to membrane proteins? *FEBS Journal* **280**: 2766–2774.
- Boer RJ De, Scheres B, Tusscher K, van Berkel K, de Boer RJ, Scheres B, ten Tusscher K. 2013.** Polar auxin transport: models and mechanisms. *Development (Cambridge, England)* **140**: 1–20.
- van den Bogaart G, Meyenberg K, Risselada HJ, Amin H, Willig KI, Hubrich BE, Dier M, Hell SW, Grubmüller H, Diederichsen U, et al. 2011.** Membrane protein sequestering by ionic protein–lipid interactions. *Nature* **479**: 552–555.
- Bonfante-Fasolo P. 1984.** Anatomy and morphology of VA mycorrhizae.
- Bonfante P, Genre a, Faccio a, Martini I, Schauser L, Stougaard J, Webb J, Parniske M. 2000.** The Lotus japonicus LjSym4 gene is required for the successful symbiotic infection of root epidermal cells. *Molecular plant-microbe interactions : MPMI* **13**: 1109–1120.
- Bonfante P, Requena N. 2011.** Dating in the dark: How roots respond to fungal signals to establish arbuscular mycorrhizal symbiosis. *Current Opinion in Plant Biology* **14**: 451–457.
- Borner GHH, Sherrier DJ, Weimar T, Michaelson L V, Hawkins ND, Macaskill A, Napier JA, Beale MH, Lilley KS, Dupree P. 2005.** Plant Physiol.-2005-Borner-104-16.pdf. **137**: 104–116.
- Boyes DC, Nam J, Dangl JL. 1998.** The Arabidopsis thaliana RPM1 disease resistance gene product is a peripheral plasma membrane protein that is degraded coincident with the hypersensitive response. *Proceedings of the National Academy of Sciences of the United States of America* **95**: 15849–54.

- Bravo A, York T, Pumplin N, Mueller LA, Harrison MJ. 2016.** Genes conserved for arbuscular mycorrhizal symbiosis identified through phylogenomics. *Nature Plants* **2**: 1–6.
- Brewin NJ. 1991.** Development of the Legume Root Nodule. *Annual Review of Cell Biology* **7**: 191–226.
- Brewin NJ. 2004.** Plant cell wall remodelling in the Rhizobium-legume symbiosis. *Critical Reviews in Plant Sciences* **23**: 293–316.
- Broghammer A, Krusell L, Blaise M, Sauer J, Sullivan JT, Maolanon N, Vinther M, Lorentzen A, Madsen EB, Jensen KJ, et al. 2012.** Legume receptors perceive the rhizobial lipochitin oligosaccharide signal molecules by direct binding. *Proceedings of the National Academy of Sciences* **109**: 13859–13864.
- Brown D, Rose J. 1992.** Sorting of GPI-anchored proteins to glycolipid-enriched membrane subdomains during transport to the apical cell surface. *Cell*.
- van Brussel a N, Bakhuizen R, van Spronsen PC, Spaink HP, Tak T, Lugtenberg BJJ, Kijne JW. 1992.** Induction of preinfection thread structures in the leguminous host plant by mitogenic lipooligosaccharides of Rhizobium. *Science* **257**: 70–72.
- Bücherl CA, Jarsch IK, Schudoma C, Robatzek S, Maclean D, Ott T, Zipfel C, Genome P, National S, Biology C. 2017.** Plant immune and growth receptors share common signalling components but localise to distinct plasma membrane nanodomains. *eLife*.
- Bussell SJ, Koch DL, Hammer DA. 1995.** Effect of hydrodynamic interactions on the diffusion of integral membrane proteins: diffusion in plasma membranes. *Biophysical journal* **68**: 1836–49.
- Buzas DM, Gresshoff PM. 2007.** Short- and long-distance control of root development by LjHAR1 during the juvenile stage of *Lotus japonicus*. *Journal of Plant Physiology* **164**: 452–459.
- Caetano-Anolles G, Gresshoff PM. 1991.** Plant Genetic Control of Nodulation. *Annual Review of Microbiology* **45**: 345–382.
- Callaham DA, Torrey JG. 1981.** The structural basis for infection of root hairs of *Trifolium repens* by *Rhizobium*. *Canadian Journal of Botany* **59**: 1647–1664.
- Capoen W, Sun J, Wysham D, Otegui MS, Venkateshwaran M, Hirsch S, Miwa H, Downie JA, Morris RJ, Ané J-M, et al. 2011.** Nuclear membranes control symbiotic calcium signaling of legumes. *Proceedings of the National Academy of Sciences of the United States of America* **108**: 14348–14353.
- Catford JG, Staehelin C, Lerat S, Piché Y, Vierheilig H. 2003.** Suppression of arbuscular mycorrhizal colonization and nodulation in split-root systems of alfalfa after pre-inoculation and treatment with Nod factors. *Journal of Experimental Botany* **54**: 1481–1487.
- Cerri MR, Frances L, Kelner A, Fournier J, Middleton PH, Auriac M-C, Mysore KS, Wen J, Erard M, Barker DG, et al. 2016.** The Symbiosis-Related ERN Transcription Factors Act in Concert to Coordinate Rhizobial Host Root Infection. *Plant Physiology* **171**: pp.00230.2016.
- Cerri MR, Frances L, Laloum T, Auriac M-C, Niebel A, Oldroyd GED, Barker DG, Fournier J, de Carvalho-Niebel F. 2012.** Medicago truncatula ERN transcription factors: regulatory interplay with NSP1/NSP2 GRAS factors and expression dynamics throughout rhizobial infection. *Plant Physiology* **33**: 2155–2172.
- Chao LH, Stratton MM, Lee I-H, Rosenberg OS, Levitz J, Mandell DJ, Kortemme T, Groves JT, Schulman H, Kuriyan J. 2011.** A Mechanism for Tunable Autoinhibition in the Structure of a Human Ca²⁺/Calmodulin- Dependent

- Kinase II Holoenzyme. *Cell* **146**: 732–745.
- Charpentier M, Bredemeier R, Wanner G, Takeda N, Schleiff E, Parniske M. 2008.** Lotus japonicus CASTOR and POLLUX are ion channels essential for perinuclear calcium spiking in legume root endosymbiosis. *The Plant cell* **20**: 3467–3479.
- Charpentier M, Sun J, Martins TV, Radhakrishnan G V, Findlay K, Soumpourou E, Thouin J, Very A-AA, Sanders D, Morris RJ, et al. 2016.** Nuclear-localized cyclic nucleotide-gated channels mediate symbiotic calcium oscillations. *Science* **352**: 1102–1105.
- Checker VG, Khurana P. 2013.** Molecular and functional characterization of mulberry EST encoding remorin (MiREM) involved in abiotic stress. *Plant Cell Reports* **32**: 1729–1741.
- Chen Z, Hartmann HA, Wu M-J, Friedman EJ, Chen J-G, Pulley M, Schulze-Lefert P, Panstruga R, Jones AM. 2006.** Expression analysis of the AtMLO Gene Family Encoding Plant-Specific Seven-Transmembrane Domain Proteins. *Plant Molecular Biology* **60**: 583–597.
- Chen T, Zhu H, Ke D, Cai K, Wang C, Gou H, Hong Z, Zhang Z. 2012.** A MAP kinase kinase interacts with SymRK and regulates nodule organogenesis in Lotus japonicus. *The Plant cell* **24**: 823–38.
- Clark SE, Running MP, Meyerowitz EM. 1993.** CLAVATA1, a regulator of meristem and flower development in Arabidopsis. *Development* **119**: 397–418.
- Clark SE, Williams RW, Meyerowitz EM. 1997.** The CLAVATA1 gene encodes a putative receptor kinase that controls shoot and floral meristem size in Arabidopsis. *Cell* **89**: 575–585.
- Colebatch G, Desbrosses G, Ott T, Krusell L, Montanari O, Kloska S, Kopka J, Udvardi MK. 2004.** Global changes in transcription orchestrate metabolic differentiation during symbiotic nitrogen fixation in Lotus japonicus. *Plant Journal* **39**: 487–512.
- Combiér JP, Frugier F, De Billy F, Boualem A, El-Yahyaoui F, Moreau S, Vernié T, Ott T, Gamas P, Crespi M, et al. 2006.** MtHAP2-1 is a key transcriptional regulator of symbiotic nodule development regulated by microRNA169 in Medicago truncatula. *Genes and Development* **20**: 3084–3088.
- Coronado C, Zuanazzi JAS, Sallaud C, Quirion J-C, Esnault R, Husson H-P, Kondorosi A, Ratet P. 1995.** Alfalfa root flavonoid production is nitrogen regulated. *Plant Physiology* **108**: 533–542.
- Couzigou J-M, Zhukov V, Mondy S, Abu el Heba G, Cosson V, Ellis THN, Ambrose M, Wen J, Tadege M, Tikhonovich I, et al. 2012.** NODULE ROOT and COCHLEATA maintain nodule development and are legume orthologs of Arabidopsis BLADE-ON-PETIOLE genes. *The Plant cell* **24**: 4498–510.
- Crook AD, Schnabel EL, Frugoli JA. 2016.** The systemic nodule number regulation kinase SUNN in Medicago truncatula interacts with MtCLV2 and MtCRN. *Plant Journal* **1**: 108–119.
- Cutler S, Ghassemian M, Bonetta D, Cooney S. 1996.** A protein farnesyl transferase involved in abscisic acid signal transduction in Arabidopsis. *Science*.
- D’Haeze W, Holsters M. 2002.** Nod factor structures, responses, and perception during initiation of nodule development. *Glycobiology* **12**: 79R–105R.
- Van Damme D, Coutuer S, De Rycke R, Bouget F-Y, Inzé D, Geelen D. 2006.** Somatic cytokinesis and pollen maturation in Arabidopsis depend on TPLATE, which has domains similar to coat proteins. *The Plant cell* **18**: 3502–3518.
- Van Damme D, Gadeyne A, Vanstraelen M, Inzé D, Van Montagu MCE, De**

- Jaeger G, Russinova E, Geelen D. 2011.** Adaptin-like protein TPLATE and clathrin recruitment during plant somatic cytokinesis occurs via two distinct pathways. *Proceedings of the National Academy of Sciences of the United States of America* **108**: 615–620.
- Day DA, Lambers H, Bateman J, Carroll BJ, Gresshoff PM. 1986.** Growth Comparisons of a Supernodulating Soybean (Glycine-Max) Mutant and Its Wild-Type Parent. *Physiol Plantarum* **68**: 375–382.
- Delaux PM, Bécard G, Combier JP. 2013.** NSP1 is a component of the Myc signaling pathway. *New Phytologist* **199**: 59–65.
- Delaux P-M, Radhakrishnan G V., Jayaraman D, Cheema J, Malbreil M, Volkening JD, Sekimoto H, Nishiyama T, Melkonian M, Pokorny L, et al. 2015a.** Algal ancestor of land plants was preadapted for symbiosis. *Proceedings of the National Academy of Sciences* **112**: 201515426.
- Delaux P-MM, Radhakrishnan G, Oldroyd G. 2015b.** Tracing the evolutionary path to nitrogen-fixing crops. *Current Opinion in Plant Biology* **26**: 95–99.
- Delaux PM, Varala K, Edger PP, Coruzzi GM, Pires JC, Ané JM. 2014.** Comparative Phylogenomics Uncovers the Impact of Symbiotic Associations on Host Genome Evolution. *PLoS Genetics* **10**.
- Demchenko K, Winzer T, Stougaard J, Parniske M, Pawlowski K. 2004.** Distinct roles of *Lotus japonicus* SYMRK and SYM15 in root colonization and arbuscule formation. *New Phytologist* **163**: 381–392.
- Demir F, Hortrich C, Blachutzik JO, Scherzer S, Reinders Y, Kierszniowska S, Schulze WX, Harms GS, Hedrich R, Geiger D, et al. 2013.** Arabidopsis nanodomain-delimited ABA signaling pathway regulates the anion channel SLAH3. *Proceedings of the National Academy of Sciences* **110**: 8296–8301.
- Dénarié J, Cullimore J. 1993.** Lipo-oligosaccharide nodulation factors: a new class of signalling molecules mediating recognition and morphogenesis. *Cell* **74**: 951–954.
- Dénarié J, Debelle F, Promé J-C. 1996.** Rhizobium Lipo-Chitoooligosaccharide Nodulation Factors: Signaling Molecules Mediating Recognition and Morphogenesis. *Annual Review of Biochemistry* **65**: 503–535.
- Desbrosses GJ, Stougaard J. 2011.** Root nodulation: A paradigm for how plant-microbe symbiosis influences host developmental pathways. *Cell Host and Microbe* **10**: 348–358.
- DeYoung BJ, Clark SE. 2008.** BAM receptors regulate stem cell specification and organ development through complex interactions with CLAVATA signaling. *Genetics* **180**: 895–904.
- Dolan L, Janmaat K, Willemsen V, Linstead P, Poethig S, Roberts K, Scheres B. 1993.** Cellular organisation of the *Arabidopsis thaliana* root. *Development* **119**: 71–84.
- Edidin M, Kuo S, Sheetz M. 1991.** Lateral movements of membrane glycoproteins restricted by dynamic cytoplasmic barriers. *Science* **254**.
- Ehrhardt DW, Wais R, Long SR. 1996.** Calcium spiking in plant root hairs responding to *Rhizobium* nodulation signals. *Cell* **85**: 673–81.
- El-Showk S, Ruonala R, Helariutta Y. 2013.** Crossing paths: cytokinin signalling and crosstalk. *Development (Cambridge, England)* **140**: 1373–83.
- Endre G, Kereszt A, Kevei Z, Mihacea S, Kaló P, Kiss GB. 2002.** A receptor kinase gene regulating symbiotic nodule development. *Nature* **417**: 962–966.
- Esseling JJ, Lhuissier FGP, Emons AMC. 2003.** Nod factor-induced root hair curling: continuous polar growth towards the point of nod factor application. *Plant physiology* **132**: 1982–8.

- Farmer EE, Pearce G, Ryan C a. 1989.** In vitro phosphorylation of plant plasma membrane proteins in response to the proteinase inhibitor inducing factor. *Proceedings of the National Academy of Sciences of the United States of America* **86**: 1539–1542.
- Favre P, Bapaume L, Bossolini E, Delorenzi M, Falquet L, Reinhardt D. 2014.** A novel bioinformatics pipeline to discover genes related to arbuscular mycorrhizal symbiosis based on their evolutionary conservation pattern among higher plants. *BMC Plant Biology* **14**: 333.
- Fernandez A, Drozdzecki A, Hoogewijs K, Nguyen A, Beeckman T, Madder A, Hilson P. 2013.** Transcriptional and functional classification of the GOLVEN/ROOT GROWTH FACTOR/CLE-like signaling peptides reveals their role in lateral root and hair formation. *Plant physiology* **161**: 954–970.
- Fournier J, Teillet A, Chabaud M, Ivanov S, Genre A, Limpens E, DeCarvalho-Niebel F, Barker DG, de Carvalho-Niebel F, Barker DG. 2015.** Remodeling of the infection chamber prior to infection thread formation reveals a two-step mechanism for rhizobial entry into the host legume root hair. *Plant Physiology* **167**: pp.114.253302.
- Fournier J, Timmers ACJ, Sieberer BJ, Jauneau A, Chabaud M, Barker DG. 2008.** Mechanism of infection thread elongation in root hairs of *Medicago truncatula* and dynamic interplay with associated rhizobial colonization. *Plant physiology* **148**: 1985–1995.
- Franssen HJ, Xiao TT, Kulikova O, Wan X, Bisseling T, Scheres B, Heidstra R. 2015.** Root developmental programs shape the *Medicago truncatula* nodule meristem. *Development* **142**: 2941–2950.
- Frick M, Bright NA, Riento K, Bray A, Merrified C, Nichols BJ. 2007.** Coassembly of Flotillins Induces Formation of Membrane Microdomains, Membrane Curvature, and Vesicle Budding. *Current Biology* **17**: 1151–1156.
- Funayama-Noguchi S, Noguchi K, Yoshida C, Kawaguchi M. 2011.** Two CLE genes are induced by phosphate in roots of *Lotus japonicus*. *Journal of Plant Research* **124**: 155–163.
- Gage DJ. 2004.** Infection and invasion of roots by symbiotic, nitrogen-fixing rhizobia during nodulation of temperate legumes. *Microbiology and molecular biology reviews : MMBR* **68**: 280–300.
- Garner AE, Alastair Smith D, Hooper NM. 2007.** Sphingomyelin chain length influences the distribution of GPI-anchored proteins in rafts in supported lipid bilayers. *Molecular Membrane Biology* **24**: 233–242.
- Genre A, Chabaud M, Balzergue C, Puech-Pagès V, Novero M, Rey T, Fournier J, Rochange S, Bécard G, Bonfante P, et al. 2013.** Short-chain chitin oligomers from arbuscular mycorrhizal fungi trigger nuclear Ca²⁺ spiking in *Medicago truncatula* roots and their production is enhanced by strigolactone. *New Phytologist* **198**: 190–202.
- Genre A, Chabaud M, Faccio A, Barker DG, Bonfante P. 2008.** Prepenetration apparatus assembly precedes and predicts the colonization patterns of arbuscular mycorrhizal fungi within the root cortex of both *Medicago truncatula* and *Daucus carota*. *The Plant cell* **20**: 1407–1420.
- Genre A, Chabaud M, Timmers T. 2005.** Arbuscular mycorrhizal fungi elicit a novel intracellular apparatus in *Medicago truncatula* root epidermal cells before infection. *The Plant Cell* **17**: 3489–3499.
- Genre a., Ivanov S, Fendrych M, Faccio a., Žárský V, Bisseling T, Bonfante P. 2012.** Multiple exocytotic markers accumulate at the sites of perifungal membrane

- biogenesis in arbuscular mycorrhizas. *Plant and Cell Physiology* **53**: 244–255.
- Genre A, Russo G. 2016.** Does a common pathway transduce symbiotic signals in plant-microbe interactions? *Frontiers in Plant Science* **7**: 1–8.
- Di Giacomo E, Laffont C, Sciarra F, Iannelli MA, Frugier F, Frugis G. 2016.** KNAT3/4/5-like class 2 KNOX transcription factors are involved in *Medicago truncatula* symbiotic nodule organ development. *New Phytologist*.
- Gleason C, Chaudhuri S, Yang T, Muñoz A, Poovaiah BW, Oldroyd GED, Mun A, Muñoz A, Poovaiah BW, Oldroyd GED. 2006.** Nodulation independent of rhizobia induced by a calcium-activated kinase lacking autoinhibition. *Nature* **441**: 1149–1152.
- Glebov OO, Bright NA, Nichols BJ. 2006.** Flotillin-1 defines a clathrin-independent endocytic pathway in mammalian cells. *Nat Cell Biol* **8**: 46–54.
- Gobbato E, Marsh JF, Vernié T, Wang E, Maillet F, Kim J, Miller JB, Sun J, Bano SA, Ratet P, et al. 2012.** A GRAS-type transcription factor with a specific function in mycorrhizal signaling. *Current Biology* **22**: 2236–2241.
- Gomez SK, Javot H, Deewatthanawong P, Torres-Jerez I, Tang Y, Blancaflor EB, Udvardi MK, Harrison MJ. 2009.** *Medicago truncatula* and *Glomus intraradices* gene expression in cortical cells harboring arbuscules in the arbuscular mycorrhizal symbiosis. *BMC plant biology* **9**: 10.
- Gonzalez-Rizzo S, Crespi M, Frugier F. 2006.** The *Medicago truncatula* CRE1 Cytokinin Receptor Regulates Lateral Root Development and Early Symbiotic Interaction with *Sinorhizobium meliloti*. *THE PLANT CELL ONLINE* **18**: 2680–2693.
- Groth M, Takeda N, Perry J, Uchida H, Dräxl S, Brachmann A, Sato S, Tabata S, Kawaguchi M, Wang TL, et al. 2010.** NENA, a *Lotus japonicus* homolog of Sec13, is required for rhizodermal infection by arbuscular mycorrhiza fungi and rhizobia but dispensable for cortical endosymbiotic development. *The Plant cell* **22**: 2509–2526.
- Gui J, Liu C, Shen J, Li L. 2014.** Grain setting defect 1, encoding a remorin protein, affects the grain setting in rice through regulating plasmodesmatal conductance. *Plant physiology* **166**: 1463–1478.
- Gui J, Zheng S, Liu C, Shen J, Li J, Li L. 2016.** OsREM4.1 Interacts with OsSERK1 to Coordinate the Interlinking between Abscisic Acid and Brassinosteroid Signaling in Rice. *Developmental Cell* **38**: 201–213.
- Gui J, Zheng S, Shen J, Li L. 2015.** Grain setting defect1 (GSD1) function in rice depends on S-acylation and interacts with actin 1 (OsACT1) at its C-terminal. *Frontiers in Plant Science* **6**: 1–11.
- Guillotin B, Couzigou J-M, Combier J-P. 2016.** NIN is involved in the regulation of Arbuscular Mycorrhizal symbiosis. *Frontiers in Plant Science*.
- Guinel FC. 2009.** Getting around the legume nodule: I. The structure of the peripheral zone in four nodule types. *Botany* **87**: 1117–1138.
- Guo Y, Han L, Hymes M, Denver R, Clark SE. 2010.** CLAVATA2 forms a distinct CLE-binding receptor complex regulating Arabidopsis stem cell specification. *Plant Journal* **63**: 889–900.
- Gutjahr C, Parniske M. 2013.** Cell and developmental biology of arbuscular mycorrhiza symbiosis. *Annual Review of Cell and Developmental Biology* **29**: 593–617.
- Handberg K, Stougaard J. 1992.** for Classical and Molecular Genetics. **2**: 487–496.
- Haney CH, Long SR. 2010.** Plant flotillins are required for infection by nitrogen-fixing bacteria. *Proceedings of the National Academy of Sciences of the United States of America* **107**: 478–483.

- Haney CH, Riely BK, Tricoli DM, Cook DR, Ehrhardt DW, Long SR, Figure S, Lyk T. 2011.** Symbiotic Rhizobia Bacteria Trigger a Change in Localization and Dynamics of the Medicago truncatula Receptor Kinase LYK3. *The Plant cell* **23**: 2774–2787.
- Harrison MJ. 2005.** SIGNALING IN THE ARBUSCULAR MYCORRHIZAL SYMBIOSIS. *Annual Review of Microbiology* **59**: 19–42.
- Harrison MJ. 2012.** Cellular programs for arbuscular mycorrhizal symbiosis. *Current Opinion in Plant Biology* **15**: 691–698.
- Harrison MJ, Dewbre GR, Liu JY. 2002.** A phosphate transporter from Medicago truncatula involved in the acquisition of phosphate released by arbuscular mycorrhizal fungi. *Plant Cell* **14**: 2413–2429.
- Hayashi T, Banba M, Shimoda Y, Kouchi H, Hayashi M, Imaizumi-Anraku H. 2010.** A dominant function of CCaMK in intracellular accommodation of bacterial and fungal endosymbionts. *Plant Journal* **63**: 141–154.
- Hayashi T, Shimoda Y, Sato S, Tabata S, Imaizumi-Anraku H, Hayashi M. 2014.** Rhizobial infection does not require cortical expression of upstream common symbiosis genes responsible for the induction of Ca²⁺ spiking. *Plant Journal* **77**: 146–159.
- He X, Zhang J. 2005.** Rapid subfunctionalization accompanied by prolonged and substantial neofunctionalization in duplicate gene evolution. *Genetics* **169**: 1157–1164.
- Heck C, Kuhn H, Heidt S, Walter S, Rieger N, Requena N. 2016.** Symbiotic Fungi Control Plant Root Cortex Development through the Novel GRAS Transcription Factor MIG1. *Current Biology*: 1–9.
- Heckmann AB, Sandal N, Bek AS, Madsen LH, Jurkiewicz A, Nielsen MW, Tirichine L, Stougaard J. 2011.** Cytokinin Induction of Root Nodule Primordia in Lotus japonicus Is Regulated by a Mechanism Operating in the Root Cortex. *Molecular Plant-Microbe Interactions* **24**: 1385–1395.
- Heidstra R, Nilsen G, Martinez-Abarca F, van Kammen A, Bisseling T. 1997.** Nod factor-induced expression of leghemoglobin to study the mechanism of NH₄NO₃ inhibition on root hair deformation. *Molecular plant-microbe interactions : MPMI* **10**: 215–20.
- Heijden M Van der, Klironomos J, Ursic M. 1998.** Mycorrhizal fungal diversity determines plant biodiversity, ecosystem variability and productivity. *Nature*.
- Held M, Hou H, Miri M, Huynh C, Ross L, Hossain MS, Sato S, Tabata S, Perry J, Wang TL, et al. 2014.** Lotus japonicus cytokinin receptors work partially redundantly to mediate nodule formation. *The Plant cell* **26**: 678–94.
- Hemsley PA. 2014.** Tansley review The importance of lipid modified proteins in plants.
- Hemsley P a. 2015.** The importance of lipid modified proteins in plants. *New Phytologist* **205**: 476–489.
- Hemsley P, Kemp A, Grierson C. 2005.** The TIP GROWTH DEFECTIVE1 S-acyl transferase regulates plant cell growth in Arabidopsis. *The Plant Cell*.
- Hemsley PA, Weimar T, Lilley KS, Dupree P, Grierson CS. 2013.** A proteomic approach identifies many novel palmitoylated proteins in Arabidopsis. *New Phytologist* **197**: 805–814.
- Den Herder G, Parniske M. 2009.** The unbearable naivety of legumes in symbiosis. *Current Opinion in Plant Biology* **12**: 491–499.
- Den Herder G, Yoshida S, Antolín-Llovera M, Ried MK, Parniske M, Antolín-Llovera M, Ried MK, Parniske M, Antolín-Llovera M, Ried MK, et al. 2012.**

- Lotus japonicus E3 Ligase SEVEN IN ABSENTIA4 Destabilizes the Symbiosis Receptor-Like Kinase SYMRK and Negatively Regulates Rhizobial Infection. *The Plant Cell* **24**: 1691–1707.
- Herendeen PS, Magallon-Puebla S, Lupia R, Crane PR, Kobylinska J. 1999.** A Preliminary Conspectus of the Allon Flora from the Late Cretaceous (Late Santonian) of Central Georgia, U.S.A. *Annals of the Missouri Botanical Garden* **86**: 407–471.
- Herrbach V, Remblière C, Gough C, Bensmihen S. 2014.** Lateral root formation and patterning in *Medicago truncatula*. *Journal of Plant Physiology* **171**: 301–310.
- Heyl A, Riefler M, Romanov GA, Schmülling T. 2012.** Properties, functions and evolution of cytokinin receptors. *European Journal of Cell Biology* **91**: 246–256.
- Hirsch AM. 2001.** What Makes the Rhizobia-Legume Symbiosis So Special? *PLANT PHYSIOLOGY* **127**: 1484–1492.
- Hirsch S, Kim J, Muñoz A, Heckmann AB, Downie JA, Oldroyd GED. 2009.** GRAS proteins form a DNA binding complex to induce gene expression during nodulation signaling in *Medicago truncatula*. *The Plant cell* **21**: 545–557.
- Hobe M, Müller R, Grünewald M, Brand U, Simon R. 2003.** Loss of CLE40, a protein functionally equivalent to the stem cell restricting signal CLV3, enhances root waving in *Arabidopsis*. *Development Genes and Evolution* **213**: 371–381.
- Høgslund N, Radutoiu S, Krusell L, Voroshilova V, Hannah M a., Goffard N, Sanchez DH, Lippold F, Ott T, Sato S, et al. 2009.** Dissection of symbiosis and organ development by integrated transcriptome analysis of *Lotus japonicus* mutant and wild-type plants. *PLoS ONE* **4**.
- Horváth B, Yeun LH, Domonkos Á, Halász G, Gobbato E, Ayaydin F, Miró K, Hirsch S, Sun J, Tadege M, et al. 2011.** *Medicago truncatula* IPD3 Is a Member of the Common Symbiotic Signaling Pathway Required for Rhizobial and Mycorrhizal Symbioses. *Molecular Plant-Microbe Interactions* **24**: 1345–1358.
- Huang K, Yanai A, Kang R, Arstikaitis P, Singaraja RR, Metzler M, Mullard A, Haigh B, Gauthier-Campbell C, Gutekunst CA, et al. 2004.** Huntingtin-interacting protein HIP14 is a palmitoyl transferase involved in palmitoylation and trafficking of multiple neuronal proteins. *Neuron* **44**: 977–986.
- Hudmon A, Schulman H. 2002.** Structure-function of the multifunctional Ca²⁺/calmodulin-dependent protein kinase II. *The Biochemical journal* **364**: 593–611.
- Humphreys CP, Franks PJ, Rees M, Bidartondo MI, Leake JR, Beerling DJ. 2010.** Mutualistic mycorrhiza-like symbiosis in the most ancient group of land plants. *Nature communications* **1**: 103.
- Ikonen E, Simons K. 1998.** Protein and lipid sorting from the trans-Golgi network to the plasma membrane in polarized cells. *Seminars in Cell & Developmental Biology* **9**: 503–509.
- Imaizumi-Anraku H, Takeda N, Charpentier M, Perry J, Miwa H, Umehara Y, Kouchi H, Murakami Y, Mulder L, Vickers K, et al. 2005.** Plastid proteins crucial for symbiotic fungal and bacterial entry into plant roots. *Nature* **433**: 527–531.
- Ivanov S, Fedorova EE, Limpens E, De Mita S, Genre a., Bonfante P, Bisseling T. 2012.** Rhizobium-legume symbiosis shares an exocytotic pathway required for arbuscule formation. *Proceedings of the National Academy of Sciences* **109**: 8316–8321.
- Jarsch IK, Konrad SS a, Stratil TF, Urbanus SL, Szymanski W, Braun P, Braun K-HH, Ott T. 2014.** Plasma Membranes Are Subcompartmentalized into a Plethora of Coexisting and Diverse Microdomains in *Arabidopsis* and *Nicotiana benthamiana*. *The Plant cell* **26**: 1698–1711.

- Javot H, Pumplin N, Harrison MJ. 2007.** Phosphate in the arbuscular mycorrhizal symbiosis: Transport properties and regulatory roles. *Plant, Cell and Environment* **30**: 310–322.
- Jin Y, Liu H, Luo D, Yu N, Dong W, Wang C, Zhang X, Dai H, Yang J, Wang E. 2016.** DELLA proteins are common components of symbiotic rhizobial and mycorrhizal signalling pathways. *Nature Communications* **7**: 12433.
- Juszczuk IM, Wiktorowska A, Malusá E, Rychter AM. 2004.** Changes in the concentration of phenolic compounds and exudation induced by phosphate deficiency in bean plants (*Phaseolus vulgaris* L.). *Plant and Soil* **267**: 41–49.
- Kanamori N, Madsen LH, Radutoiu S, Frantescu M, Quistgaard EMH, Miwa H, Downie JA, James EK, Felle HH, Haaning LL, et al. 2006.** A nucleoporin is required for induction of Ca²⁺ spiking in legume nodule development and essential for rhizobial and fungal symbiosis. *Proceedings of the National Academy of Sciences of the United States of America* **103**: 359–364.
- Kevei Z, Loughnon G, Mergaert P, Horváth G V, Kereszt A, Jayaraman D, Zaman N, Marcel F, Regulski K, Kiss GB, et al. 2007.** 3-hydroxy-3-methylglutaryl coenzyme a reductase 1 interacts with NORK and is crucial for nodulation in *Medicago truncatula*. *The Plant cell* **19**: 3974–3989.
- Kierszniowska S, Seiwert B, Schulze WX. 2009.** Definition of Arabidopsis sterol-rich membrane microdomains by differential treatment with methyl-beta-cyclodextrin and quantitative proteomics. *Molecular & cellular proteomics : MCP* **8**: 612–623.
- Kim H-S, Desveaux D, Singer AU, Patel P, Sondek J, Dangl JL. 2005.** The *Pseudomonas syringae* effector AvrRpt2 cleaves its C-terminally acylated target, RIN4, from *Arabidopsis* membranes to block RPM1 activation. *Proceedings of the National Academy of Sciences of the United States of America* **102**: 6496–501.
- Kistner C, Parniske M. 2002.** Evolution of signal transduction in intracellular symbiosis. *Trends in Plant Science* **7**: 511–518.
- Kistner C, Winzer T, Pitzschke A, Mulder L, Sato S, Kaneko T, Tabata S, Sandal N, Stougaard J, Webb KJ, et al. 2005.** Seven *Lotus japonicus* genes required for transcriptional reprogramming of the root during fungal and bacterial symbiosis. *The Plant cell* **17**: 2217–2229.
- Kleine-Vehn J, Wabnik K, Martinière A, Łangowski Ł, Willig K, Naramoto S, Leitner J, Tanaka H, Jakobs S, Robert S, et al. 2011.** Recycling, clustering, and endocytosis jointly maintain PIN auxin carrier polarity at the plasma membrane. *Molecular systems biology* **7**: 540.
- Koldsø H, Reddy T, Fowler PW, Duncan AL, Sansom MSP. 2016.** Membrane Compartmentalization Reducing the Mobility of Lipids and Proteins within a Model Plasma Membrane. *The Journal of Physical Chemistry B* **120**: 8873–8881.
- Konrad SS a. a, Ott T. 2015.** Molecular principles of membrane microdomain targeting in plants. *Trends in Plant Science* **20**: 351–361.
- Konrad SSA, Popp C, Stratil TF, Jarsch IK, Thallmair V, Folgmann J, Marín M, Ott T. 2014.** S-acylation anchors remorin proteins to the plasma membrane but does not primarily determine their localization in membrane microdomains. *New Phytologist* **203**: 758–769.
- Kosuta S, Hazledine S, Sun J, Miwa H, Morris RJ, Downie JA, Oldroyd GED. 2008.** Differential and chaotic calcium signatures in the symbiosis signaling pathway of legumes. *Proceedings of the National Academy of Sciences of the United States of America* **105**: 9823–9828.
- Kosuta S, Held M, Hossain MS, Morieri G, MacGillivray A, Johansen C, Antolín-Llovera M, Parniske M, Oldroyd GED, Downie AJ, et al. 2011.** *Lotus*

- japonicus symRK-14 uncouples the cortical and epidermal symbiotic program. *Plant Journal* **67**: 929–940.
- Krusell L, Madsen LH, Sato S, Aubert G, Genua A, Szczyglowski K, Duc G, Kaneko T, Tabata S, de Bruijn F, et al. 2002.** Shoot control of root development and nodulation is mediated by a receptor-like kinase. *Nature* **420**: 422–426.
- Krusell L, Sato N, Fukuhara I, Koch BE V, Grossmann C, Okamoto S, Oka-Kira E, Otsubo Y, Aubert G, Nakagawa T, et al. 2011.** The *Clavata2* genes of pea and lotus japonicus affect autoregulation of nodulation. *Plant Journal* **65**: 861–871.
- Kumar M, Wightman R, Atanassov I, Gupta A, Hurst CH, Hemsley PA, Turner S. 2016.** S-Acylation of the cellulose synthase complex is essential for its plasma membrane localization. *Science* **353**: 166–169.
- Küster H, Vieweg MF, Manthey K, Baier MC, Hohnjec N, Perlick AM. 2007.** Identification and expression regulation of symbiotically activated legume genes. *Phytochemistry* **68**: 8–18.
- Kusumi A, Fujiwara TK, Morone N, Yoshida KJ, Chadda R, Xie M, Kasai RS, Suzuki KGN. 2012.** Membrane mechanisms for signal transduction: The coupling of the meso-scale raft domains to membrane-skeleton-induced compartments and dynamic protein complexes. *Seminars in Cell & Developmental Biology* **23**: 126–144.
- Kusumi A, Nakada C, Ritchie K, Murase K, Suzuki K, Murakoshi H, Kasai RS, Kondo J, Fujiwara T. 2005.** PARADIGM SHIFT OF THE PLASMA MEMBRANE CONCEPT FROM THE TWO-DIMENSIONAL CONTINUUM FLUID TO THE PARTITIONED FLUID : High-Speed Single-Molecule Tracking of Membrane Molecules.
- Kwon C, Neu C, Pajonk S, Yun HS, Lipka U, Humphry M, Bau S, Straus M, Kwakitaal M, Rampelt H, et al. 2008.** Co-option of a default secretory pathway for plant immune responses. *Nature* **451**: 835–840.
- Laffont C, Rey T, André O, Novero M, Kazmierczak T, Debelle F, Bonfante P, Jacquet C, Frugier F. 2015.** The CRE1 cytokinin pathway is differentially recruited depending on *Medicago truncatula* root environments and negatively regulates resistance to a pathogen. *PLoS ONE* **10**: 1–19.
- Laplaze L, Benkova E, Casimiro I, Maes L, Vanneste S, Swarup R, Weijers D, Calvo V, Parizot B, Herrera-Rodriguez MB, et al. 2007.** Cytokinins act directly on lateral root founder cells to inhibit root initiation. *The Plant cell* **19**: 3889–3900.
- Laporte P, Lepage A, Fournier JJJ, Catrice O, Moreau S, Jardinaud MFFF, Mun JH, Larrainzar E, Cook DR, Gamas P, et al. 2014.** The CCAAT box-binding transcription factor NF-YA1 controls rhizobial infection. *Journal of Experimental Botany* **65**: 481–494.
- Lauressergues D, Delaux PM, Formey D, Lelandais-Brière C, Fort S, Cottaz S, Bécard G, Niebel A, Roux C, Combier JP. 2012.** The microRNA miR171h modulates arbuscular mycorrhizal colonization of *Medicago truncatula* by targeting NSP2. *Plant Journal* **72**: 512–522.
- Lefebvre B, Furt F, Hartmann M-A, Michaelson L V, Carde J-P, Sargueil-Boiron F, Rossignol M, Napier J a, Cullimore J, Bessoule J-J, et al. 2007.** Characterization of lipid rafts from *Medicago truncatula* root plasma membranes: a proteomic study reveals the presence of a raft-associated redox system. *Plant physiology* **144**: 402–418.
- Lefebvre B, Timmers T, Mbengue M, Moreau S, Hervé C, Tóth K, Bittencourt-Silvestre J, Klaus D, Deslandes L, Godiard L, et al. 2010.** A remorin protein interacts with symbiotic receptors and regulates bacterial infection. *Proceedings of the National Academy of Sciences of the United States of America* **107**: 2343–2348.

- Lenne P-F, Wawrezynieck L, Conchonaud F, Wurtz O, Boned A, Guo X-J, Rigneault H, He H-T, Marguet D. 2006.** Dynamic molecular confinement in the plasma membrane by microdomains and the cytoskeleton meshwork. *The EMBO journal* **25**: 3245–56.
- Lerouge P, Roche P, Faucher C, Maillet F, Truchet G, Promé JC, Dénarié J. 1990.** Symbiotic host-specificity of *Rhizobium meliloti* is determined by a sulphated and acylated glucosamine oligosaccharide signal. *Nature* **344**: 781–784.
- Levental I, Grzybek M, Simons K. 2010a.** Greasing Their Way: Lipid Modifications Determine Protein Association with Membrane Rafts. *Biochemistry* **49**: 6305–6316.
- Levental I, Lingwood D, Grzybek M. 2010b.** Palmitoylation regulates raft affinity for the majority of integral raft proteins. *Proceedings of the*
- Levy J, Bres C, Geurts R, Chalhoub B, Kulikova O, Duc G, Journet E-P, Ane J-M, Lauber E, Bisseling T, et al. 2004.** A Putative Ca²⁺ and Calmodulin-Dependent Protein Kinase Required for Bacterial and Fungal Symbioses. *Science* **303**: 1361–1364.
- Li-Beisson Y, Shorrosh B, Beisson F, Andersson MX, Arondel V, Bates PD, Baud S, Bird D, DeBono A, Durrett TP, et al. 2013.** Acyl-Lipid Metabolism. *The Arabidopsis Book* **11**: e0161.
- Liao J, Singh S, Hossain MS, Andersen SU, Ross L, Bonetta D, Zhou Y, Sato S, Tabata S, Stougaard J, et al. 2012.** Negative regulation of CCaMK is essential for symbiotic infection. *Plant Journal* **72**: 572–584.
- Li X, Wang X, Yang Y, Li R, He Q, Fang X, Luu D-T, Maurel C, Lin J. 2011.** Single-molecule analysis of PIP₂;1 dynamics and partitioning reveals multiple modes of *Arabidopsis* plasma membrane aquaporin regulation. *The Plant cell* **23**: 3780–97.
- Limpens E, Bisseling T. 2014.** CYCLOPS: A new vision on rhizobium-induced nodule organogenesis. *Cell Host and Microbe* **15**: 127–129.
- Limpens E, Franken C, Smit P, Willemse J, Bisseling T, Geurts R. 2003.** LysM domain receptor kinases regulating rhizobial Nod factor-induced infection. *Science (New York, N.Y.)* **302**: 630–633.
- Limpens E, Moling S, Hooiveld G, Pereira P a., Bisseling T, Becker JD, Küster H. 2013.** Cell- and Tissue-Specific Transcriptome Analyses of *Medicago truncatula* Root Nodules (I De Smet, Ed.). *PLoS ONE* **8**: e64377.
- Lingwood D, Simons K. 2010.** Lipid rafts as a membrane-organizing principle. *Science (New York, N.Y.)* **327**: 46–50.
- Liu C-W, Murray J. 2016.** The Role of Flavonoids in Nodulation Host-Range Specificity: An Update. *Plants* **5**: 33.
- Liu J, Zhong S, Guo X, Hao L, Wei X, Huang Q, Hou Y, Shi J, Wang C, Gu H, et al. 2013.** Membrane-bound RLCKs LIP1 and LIP2 are essential male factors controlling male-female attraction in *Arabidopsis*. *Current Biology* **23**: 993–998.
- Lohar DP, Sharopova N, Endre G, Peñuela S, Samac D, Town C, Silverstein K a T, VandenBosch K a. 2006.** Transcript analysis of early nodulation events in *Medicago truncatula*. *Plant physiology* **140**: 221–234.
- Lohmann GV, Shimoda Y, Nielsen MW, Jørgensen FG, Grossmann C, Sandal N, Sørensen K, Thirup S, Madsen LH, Tabata S, et al. 2010.** Evolution and regulation of the *Lotus japonicus* LysM receptor gene family. *Molecular plant-microbe interactions : MPMI* **23**: 510–521.
- Łotocka B, Kopcińska J, Skalniak M. 2012.** Review article: The meristem in indeterminate root nodules of Faboideae. *Symbiosis* **58**: 63–72.
- Lynch M, Conery J. 2000.** The evolutionary fate and consequences of duplicate

genes. *Science*.

Macasev D, Whelan J, Newbigin E, Silva-Filho MC, Mulhern TD, Lithgow T. 2004. Tom22', an 8-kDa trans-Site Receptor in Plants and Protozoans, Is a Conserved Feature of the TOM Complex That Appeared Early in the Evolution of Eukaryotes. *Molecular Biology and Evolution* **21**: 1557–1564.

Madsen EB, Antolín-Llovera M, Grossmann C, Ye J, Vieweg S, Broghammer A, Krusell L, Radutoiu S, Jensen ON, Stougaard J, et al. 2011. Autophosphorylation is essential for the in vivo function of the *Lotus japonicus* Nod factor receptor 1 and receptor-mediated signalling in cooperation with Nod factor receptor 5. *Plant Journal* **65**: 404–417.

Madsen EB, Madsen LH, Radutoiu S, Olbryt M, Rakwalska M, Szczyglowski K, Sato S, Kaneko T, Tabata S, Sandal N, et al. 2003. A receptor kinase gene of the LysM type is involved in legume perception of rhizobial signals. *Nature* **425**: 637–640.

Madsen LH, Tirichine L, Jurkiewicz A, Sullivan JT, Heckmann AB, Bek AS, Ronson CW, James EK, Stougaard J. 2010. The molecular network governing nodule organogenesis and infection in the model legume *Lotus japonicus*. *Nature communications* **1**: 10.

Maeda Y, Kinoshita T. 2011. Structural remodeling, trafficking and functions of glycosylphosphatidylinositol-anchored proteins. *Progress in Lipid Research* **50**: 411–424.

Magori S, Oka-Kira E, Shibata S, Umehara Y, Kouchi H, Hase Y, Tanaka A, Sato S, Tabata S, Kawaguchi M. 2009. Too much love, a root regulator associated with the long-distance control of nodulation in *Lotus japonicus*. *Molecular plant-microbe interactions : MPMI* **22**: 259–268.

Maillet F, Poinso V, André O, Puech-Pagès V, Haouy A, Gueunier M, Cromer L, Giraudet D, Formey D, Niebel A, et al. 2011. Fungal lipochitooligosaccharide symbiotic signals in arbuscular mycorrhiza. *Nature* **469**: 58–63.

Malinsky J, Opekarová M, Grossmann G, Tanner W. 2013. Membrane microdomains, rafts, and detergent-resistant membranes in plants and fungi. *Annual review of plant biology* **64**: 501–29.

Marín M, Ott T. 2012. Phosphorylation of intrinsically disordered regions in remorin proteins. *Frontiers in plant science* **3**: 86.

Marín M, Thallmair V, Ott T. 2012. The intrinsically disordered N-terminal region of AtREM1.3 remorin protein mediates protein-protein interactions. *The Journal of biological chemistry* **287**: 39982–39991.

Markmann K, Parniske M. 2009. Evolution of root endosymbiosis with bacteria: how novel are nodules? *Trends in Plant Science* **14**: 77–86.

Marsh JF, Rakocevic A, Mitra RM, Brocard L, Sun J, Eschstruth A, Long SR, Schultze M, Ratet P, Oldroyd GEDD. 2007. *Medicago truncatula* NIN is essential for rhizobial-independent nodule organogenesis induced by autoactive calcium/calmodulin-dependent protein kinase. *Plant physiology* **144**: 324–335.

Marsh JF, Schultze M. 2001. Analysis of arbuscular mycorrhizas using symbiosis-defective plant mutants. *New Phytologist* **150**: 525–532.

Martinière A, Lavagi I, Nageswaran G, Rolfe DJ, Maneta-Peyret L, Luu D-T, Botchway SW, Webb SED, Mongrand S, Maurel C, et al. 2012. Cell wall constrains lateral diffusion of plant plasma-membrane proteins. *Proceedings of the National Academy of Sciences of the United States of America* **109**: 12805–10.

Matsuzaki Y, Ogawa-Ohnishi M, Mori A, Matsubayashi Y. 2010. Secreted Peptide Signals Required for Maintenance of Root Stem Cell Niche in

- Arabidopsis *Science* **329**: 1065 LP-1067.
- Maxwell CA, Hartwig UA, Joseph CM, Phillips DA. 1989.** A Chalcone and Two Related Flavonoids Released from Alfalfa Roots Induce nod Genes of *Rhizobium meliloti*. *Plant physiology* **91**: 842–7.
- Mbengue M, Camut S, de Carvalho-Niebel F, Deslandes L, Froidure S, Klaus-Heisen D, Moreau S, Rivas S, Timmers T, Hervé C, et al. 2010.** The *Medicago truncatula* E3 ubiquitin ligase PUB1 interacts with the LYK3 symbiotic receptor and negatively regulates infection and nodulation. *The Plant cell* **22**: 3474–3488.
- McMahon HT, Gallop JL. 2005.** Membrane curvature and mechanisms of dynamic cell membrane remodelling. *Nature* **438**: 590–596.
- Meixner C, Vegvari G, Ludwig-Müller J, Gagnon H, Steinkellner S, Staehelin C, Gresshoff P, Vierheilig H. 2007.** Two defined alleles of the LRR receptor kinase GmNARK in supernodulating soybean govern differing autoregulation of mycorrhization. *Physiologia Plantarum* **130**: 261–270.
- Men S, Boutte Y, Ikeda Y, Li X, Palme K, Stierhof Y-D, Hartmann M-A, Moritz T, Grebe M. 2008.** Sterol-dependent endocytosis mediates post-cytokinetic acquisition of PIN2 auxin efflux carrier polarity. *Nat Cell Biol* **10**: 237–244.
- Meng L, Buchanan BB, Feldman LJ, Luan S. 2012.** CLE-like (CLEL) peptides control the pattern of root growth and lateral root development in *Arabidopsis*. *Proceedings of the National Academy of Sciences of the United States of America* **109**: 1760–5.
- Mergaert P, Uchiumi T, Alunni B, Evanno G, Cheron A, Catrice O, Mausset A-E, Barloy-Hubler F, Galibert F, Kondorosi A, et al. 2006.** Eukaryotic control on bacterial cell cycle and differentiation in the *Rhizobium*-legume symbiosis. *Proceedings of the National Academy of Sciences* **103**: 5230–5235.
- Messinese E, Mun J-HH, Yeun LH, Jayaraman D, Rougé P, Barre A, Loughon G, Schornack S, Bono J-JJ, Cook DR, et al. 2007.** A novel nuclear protein interacts with the symbiotic DMI3 calcium- and calmodulin-dependent protein kinase of *Medicago truncatula*. *Molecular plant-microbe interactions : MPMI* **20**: 912–921.
- Middleton PH, Jakab J, Penmetsa RV, Starker CG, Doll J, Kaló P, Prabhu R, Marsh JF, Mitra RM, Kereszt A, et al. 2007.** An ERF transcription factor in *Medicago truncatula* that is essential for Nod factor signal transduction. *The Plant cell* **19**: 1221–1234.
- Miller JB, Pratap A, Miyahara A, Zhou L, Bornemann S, Morris RJ, Oldroyd GED. 2013.** Calcium/Calmodulin-dependent protein kinase is negatively and positively regulated by calcium, providing a mechanism for decoding calcium responses during symbiosis signaling. *The Plant cell* **25**: 5053–66.
- De Mita S, Streng A, Bisseling T, Geurts R. 2014.** Evolution of a symbiotic receptor through gene duplications in the legume-rhizobium mutualism. *New Phytologist* **201**: 961–972.
- Mitra RM, Gleason C a, Edwards A, Hadfield J, Downie JA, Oldroyd GED, Long SR. 2004.** A Ca²⁺-calmodulin-dependent protein kinase required for symbiotic nodule development : Gene identification by transcript-based cloning. *Proceedings of the National Academy of Sciences of the United States of America* **101**: 4701–4705.
- Miwa H, Sun J, Oldroyd GED, Downie JA. 2006.** Analysis of Nod-Factor-Induced Calcium Signaling in Root Hairs of Symbiotically Defective Mutants of *Lotus japonicus*. *Molecular Plant-Microbe Interactions* **19**: 914–923.
- Miyata K, Kozaki T, Kouzai Y, Ozawa K, Ishii K, Asamizu E, Okabe Y, Umehara Y, Miyamoto A, Kobae Y, et al. 2014.** The bifunctional plant receptor,

- OsCERK1, regulates both chitin-triggered immunity and arbuscular mycorrhizal symbiosis in rice. *Plant and Cell Physiology* **55**: 1864–1872.
- Miyazawa H, Oka-Kira E, Sato N, Takahashi H, Wu G-J, Sato S, Hayashi M, Betsuyaku S, Nakazono M, Tabata S, et al. 2010.** The receptor-like kinase KLAVIER mediates systemic regulation of nodulation and non-symbiotic shoot development in *Lotus japonicus*. *Development (Cambridge, England)* **137**: 4317–25.
- Moling S, Pietraszewska-Bogiel a., Postma M, Fedorova E, Hink M a., Limpens E, Gadella TWJ, Bisseling T. 2014.** Nod Factor Receptors Form Heteromeric Complexes and Are Essential for Intracellular Infection in *Medicago* Nodules. *The Plant Cell* **26**: 4188–4199.
- Mongrand S, Morel J, Laroche J, Claverol S, Carde JP, Hartmann MA, Bonneau M, Simon-Plas F, Lessire R, Bessoule JJ. 2004.** Lipid rafts in higher plant cells: Purification and characterization of triton X-100-insoluble microdomains from tobacco plasma membrane. *Journal of Biological Chemistry* **279**: 36277–36286.
- Morandi D, Sagan M, Prado-Vivant E, Duc G. 2000.** Influence of genes determining supernodulation on root colonization by the mycorrhizal fungus *Glomus mosseae* in *Pisum sativum* and *Medicago truncatula* mutants. *Mycorrhiza* **10**: 37–42.
- Moreau S, Fromentin J, Vaillau F, Vernié T, Huguet SS, Balzergue S, Frugier F, Gamas P, Jardinaud MFF, Verni?? T, et al. 2014.** The symbiotic transcription factor MtEFD and cytokinins are positively acting in the *Medicago truncatula* and *Ralstonia solanacearum* pathogenic interaction. *New Phytologist* **201**: 1343–1357.
- Morel J. 2006.** Proteomics of Plant Detergent-resistant Membranes. *Molecular & Cellular Proteomics* **5**: 1396–1411.
- Morone N, Fujiwara T, Murase K, Kasai RS, Ike H, Yuasa S, Usukura J, Kusumi A. 2006.** Three-dimensional reconstruction of the membrane skeleton at the plasma membrane interface by electron tomography. *The Journal of cell biology* **174**: 851–62.
- Mortier V, Holsters M, Goormachtig S. 2012.** Never too many? How legumes control nodule numbers. *Plant, Cell and Environment* **35**: 245–258.
- Mortier V, Wasson A, Jaworek P, De Keyser A, Decroos M, Holsters M, Tarkowski P, Mathesius U, Goormachtig S. 2014.** Role of LONELY GUY genes in indeterminate nodulation on *Medicago truncatula*. *New Phytologist* **202**: 582–593.
- Mulligan JT, Long SR. 1985.** Induction of *Rhizobium meliloti* nodC expression by plant exudate requires nodD. *Proceedings of the National Academy of Sciences of the United States of America* **82**: 6609–13.
- Murray JD. 2011.** Invasion by invitation: rhizobial infection in legumes. *Molecular plant-microbe interactions : MPMI* **24**: 631–639.
- Murray JD, Cousins DR, Jackson KJ, Liu C. 2013.** Signaling at the root surface: The role of cutin monomers in mycorrhization. *Molecular Plant* **6**: 1381–1383.
- Murray J, Karas B, Ross L, Brachmann A, Wagg C, Geil R, Perry J, Nowakowski K, MacGillivray M, Held M, et al. 2006.** Genetic suppressors of the *Lotus japonicus* har1-1 hypernodulation phenotype. *Molecular plant-microbe interactions : MPMI* **19**: 1082–1091.
- Ng JLP, Hassan S, Truong TT, Hocart CH, Laffont C, Frugier F, Mathesius U. 2015.** Flavonoids and Auxin Transport Inhibitors Rescue Symbiotic Nodulation in the *Medicago truncatula* Cytokinin Perception Mutant cre1. *The Plant cell* **27**: 2210–2226.
- Nicolson GL. 2014.** The Fluid - Mosaic Model of Membrane Structure: Still relevant to understanding the structure, function and dynamics of biological membranes after more than 40 years. *Biochimica et Biophysica Acta - Biomembranes* **1838**: 1451–

1466.

- Nishimura R, Hayashi M, Wu G-J, Kouchi H, Imaizumi-Anraku H, Murakami Y, Kawasaki S, Akao S, Ohmori M, Nagasawa M, et al. 2002.** HAR1 mediates systemic regulation of symbiotic organ development. *Nature* **420**: 426–429.
- Oba H, Tawaray K, Wagatsuma T. 2001.** Arbuscular mycorrhizal colonization in Lupinus and related genera. *Soil Science and Plant Nutrition* **48**: 117–120.
- Okamoto S, Ohnishi E, Sato S, Takahashi H, Nakazono M, Tabata S, Kawaguchi M. 2009.** Nod factor/nitrate-induced CLE genes that drive HAR1-mediated systemic regulation of nodulation. *Plant and Cell Physiology* **50**: 67–77.
- Okamoto S, Shinohara H, Mori T, Matsubayashi Y, Kawaguchi M. 2013.** Root-derived CLE glycopeptides control nodulation by direct binding to HAR1 receptor kinase. *Nature Communications* **4**: 2191.
- Oldroyd GED. 2013.** Speak, friend, and enter: signalling systems that promote beneficial symbiotic associations in plants. *Nature reviews. Microbiology* **11**: 252–63.
- Oldroyd GED, Murray JD, Poole PS, Downie JA. 2011.** The Rules of Engagement in the Legume-Rhizobial Symbiosis. *Annual Review of Genetics* **45**: 119–144.
- Op den Camp RHM, De Mita S, Lillo A, Cao Q, Limpens E, Bisseling T, Geurts R. 2011a.** A Phylogenetic Strategy Based on a Legume-Specific Whole Genome Duplication Yields Symbiotic Cytokinin Type-A Response Regulators. *Plant Physiology* **157**: 2013–2022.
- Op den Camp R, Streng A, De Mita S, Cao Q, Polone E, Liu W, Ammiraju JSS, Kudrna D, Wing R, Untergasser A, et al. 2011b.** LysM-type mycorrhizal receptor recruited for rhizobium symbiosis in nonlegume Parasponia. *Science (New York, N.Y.)* **331**: 909–912.
- Ovchinnikova E, Journet E-P, Chabaud M, Cosson V, Ratet P, Duc G, Fedorova E, Liu W, den Camp RO, Zhukov V, et al. 2011.** IPD3 Controls the Formation of Nitrogen-Fixing Symbiosomes in Pea and *Medicago* Spp. *Molecular Plant-Microbe Interactions* **24**: 1333–1344.
- Padamsee M, Johansen RB, Stuckey SA, Williams SE, Hooker JE, Burns BR, Bellgard SE. 2016.** The arbuscular mycorrhizal fungi colonising roots and root nodules of New Zealand kauri *Agathis australis*. *Fungal Biology* **120**: 807–817.
- Pan J, Fujioka S, Peng J, Chen J, Li G, Chen R. 2009.** The E3 ubiquitin ligase SCFTIR1/AFB and membrane sterols play key roles in auxin regulation of endocytosis, recycling, and plasma membrane accumulation of the auxin efflux transporter PIN2 in *Arabidopsis thaliana*. *The Plant cell* **21**: 568–580.
- Park H-J, Floss DS, Levesque-Tremblay V, Bravo A, Harrison MJ. 2015.** Hyphal Branching during Arbuscule Development Requires Reduced Arbuscular Mycorrhizal. *Plant physiology* **169**: 2774–88.
- Parniske M. 2008.** Arbuscular mycorrhiza: the mother of plant root endosymbioses. *Nature reviews. Microbiology* **6**: 763–775.
- Penmetta R V, Frugoli JA, Smith LS, Long SR, Cook DR. 2003.** Dual genetic pathways controlling nodule number in *Medicago truncatula*. *Plant Physiol* **131**: 998–1008.
- Perraki A, Binaghi M, Mecchia M a., Gronnier J, German-Retana S, Mongrand S, Bayer E, Zelada AM, Germain V. 2014.** StRemorin1.3 hampers Potato virus X TGBp1 ability to increase plasmodesmata permeability, but does not interfere with its silencing suppressor activity. *FEBS Letters* **588**: 1699–1705.
- Perraki a., Cacas J-L, Crowet J-M, Lins L, Castroviejo M, German-Retana S, Mongrand S, Raffaele S. 2012.** Plasma Membrane Localization of *Solanum tuberosum* Remorin from Group 1, Homolog 3 Is Mediated by Conformational

- Changes in a Novel C-Terminal Anchor and Required for the Restriction of Potato Virus X Movement]. *Plant Physiology* **160**: 624–637.
- Perry JA. 2003.** A TILLING Reverse Genetics Tool and a Web-Accessible Collection of Mutants of the Legume *Lotus japonicus*. *PLANT PHYSIOLOGY* **131**: 866–871.
- Peters NK, Frost JW, Long SR. 1986.** A plant flavone, luteolin, induces expression of *Rhizobium meliloti* nodulation genes. *Science (New York, N.Y.)* **233**: 977–80.
- Pietraszewska-Bogiel A, Lefebvre B, Koini MA, Klaus-Heisen D, Takken FLW, Geurts R, Cullimore J V., Gadella TWJ. 2013.** Interaction of *Medicago truncatula* Lysin Motif Receptor-Like Kinases, NFP and LYK3, Produced in *Nicotiana benthamiana* Induces Defence-Like Responses. *PLoS ONE* **8**: 16–18.
- Pike LJ. 2006.** Rafts defined: a report on the Keystone Symposium on Lipid Rafts and Cell Function. *J Lipid Res* **47**: 1597–1598.
- Pike LJ. 2009.** The challenge of lipid rafts. *J Lipid Res* **50 Suppl**: S323–S328.
- Pimprikar P, Carbonnel S, Paries M, Katzer K, Klingl V, Bohmer MJJ, Karl L, Floss DSS, Harrison MJJ, Parniske M, et al. 2016.** A CCaMK-CYCLOPS-DELLA Complex Activates Transcription of RAM1 to Regulate Arbuscule Branching. *Current Biology* **26**: 1–12.
- Plet J, Wasson A, Ariel F, Le Signor C, Baker D, Mathesius U, Crespi M, Frugier F. 2011.** MtCRE1-dependent cytokinin signaling integrates bacterial and plant cues to coordinate symbiotic nodule organogenesis in *Medicago truncatula*. *Plant Journal* **65**: 622–633.
- Popp C, Ott T. 2011.** Regulation of signal transduction and bacterial infection during root nodule symbiosis. *Current Opinion in Plant Biology* **14**: 458–467.
- Radutoiu S, Madsen LH, Madsen EB, Felle HH, Umehara Y, Grønlund M, Sato S, Nakamura Y, Tabata S, Sandal N, et al. 2003.** Plant recognition of symbiotic bacteria requires two LysM receptor-like kinases. *Nature* **425**: 585–592.
- Raffaele S, Bayer E, Lafarge D, Cluzet S, German Retana S, Boubekour T, Leborgne-Castel N, Carde J-P, Lherminier J, Noirot E, et al. 2009.** Remorin, a solanaceae protein resident in membrane rafts and plasmodesmata, impairs potato virus X movement. *The Plant cell* **21**: 1541–1555.
- Raffaele S, Mongrand S, Gamas P, Niebel A, Ott T. 2007.** Genome-Wide Annotation of Remorins, a Plant-Specific Protein Family: Evolutionary and Functional Perspectives. *Plant Physiology* **145**: 593–600.
- Rasmussen SR, Füchtbauer W, Novero M, Volpe V, Malkov N, Genre A, Bonfante P, Stougaard J, Radutoiu S. 2016.** Intraradical colonization by arbuscular mycorrhizal fungi triggers induction of a lipochitooligosaccharide receptor. *Scientific reports* **6**: 29733.
- Redecker D, Kodner R, Graham LE. 2000.** Glomalean Fungi from the Ordovician. *Science* **289**: 1920 LP-1921.
- Reid DE, Ferguson BJ, Gresshoff PM. 2011.** Inoculation- and Nitrate-Induced CLE Peptides of Soybean Control NARK-Dependent Nodule Formation. *Molecular Plant-Microbe Interactions* **24**: 606–618.
- Reid DE, Li D, Ferguson BJ, Gresshoff PM. 2013.** Structure-function analysis of the GmRIC1 signal peptide and CLE domain required for nodulation control in soybean. *Journal of Experimental Botany* **64**: 1575–1585.
- Reymond P, Kunz B, Paul-Pletzer K, Grimm R, Eckerskorn C, Farmer EE. 1996.** Cloning of a cDNA encoding a plasma membrane-associated, uronide binding phosphoprotein with physical properties similar to viral movement proteins. *The Plant cell* **8**: 2265–2276.

- Ried MK, Antolín-Llovera M, Parniske M. 2014.** Spontaneous symbiotic reprogramming of plant roots triggered by receptor-like kinases. *eLife* **3**: 1–17.
- Riefler M, Novak O, Strnad M, Schmu T. 2006.** Arabidopsis Cytokinin Receptor Mutants Reveal Functions in Shoot Growth, Leaf Senescence, Seed Size, Germination, Root Development, and Cytokinin Metabolism. **18**: 40–54.
- Rival P, de Billy F, Bono J-J, Gough C, Rosenberg C, Bensmihen S. 2012.** Epidermal and cortical roles of NFP and DMI3 in coordinating early steps of nodulation in *Medicago truncatula*. *Development* **139**: 3383–3391.
- Roth AF, Feng Y, Chen L, Davis NG. 2002.** The yeast DHHC cysteine-rich domain protein Akr1p is a palmitoyl transferase. *Journal of Cell Biology* **159**: 23–28.
- Routray P, Miller JB, Du L, Oldroyd G, Poovaiah BW. 2013.** Phosphorylation of S344 in the calmodulin-binding domain negatively affects CCaMK function during bacterial and fungal symbioses. *Plant Journal* **76**: 287–296.
- Roux B, Rodde N, Jardinaud MF, Timmers T, Sauviac L, Cottret L, Carrère S, Sallet E, Courcelle E, Moreau S, et al. 2014.** An integrated analysis of plant and bacterial gene expression in symbiotic root nodules using laser-capture microdissection coupled to RNA sequencing. *Plant Journal* **77**: 817–837.
- De Ruijter NCA, Rook MB, Bisseling T, Mie A, Emons C. 1998.** Lipochito-oligosaccharides re-initiate root hair tip growth in *Vicia sativa* with high calcium and spectrin-like antigen at the tip. *The Plant Journal* **13**: 341–350.
- Running M, Lavy M, Sternberg H. 2004.** Enlarged meristems and delayed growth in *plp* mutants result from lack of CaaX prenyltransferases. *Proceedings of the*
- Saha S, Paul A, Herring L, Dutta A, Bhattacharya A, Samaddar S, Goshe MB, DasGupta M. 2016.** Gatekeeper Tyrosine phosphorylation of SYMRK is essential for synchronising the epidermal and cortical responses in root nodule symbiosis. *Plant Physiology*: pp.01962.2015.
- Saito K, Yoshikawa M, Yano K, Miwa H, Uchida H, Asamizu E, Sato S, Tabata S, Imaizumi-Anraku H, Umehara Y, et al. 2007.** NUCLEOPORIN85 is required for calcium spiking, fungal and bacterial symbioses, and seed production in *Lotus japonicus*. *The Plant cell* **19**: 610–624.
- Sanderfoot A. 2007.** Increases in the number of SNARE genes parallels the rise of multicellularity among the green plants. *Plant physiology* **144**: 6–17.
- Sasaki T, Suzaki T, Soyano T, Kojima M, Sakakibara H, Kawaguchi M. 2014.** Shoot-derived cytokinins systemically regulate root nodulation. *Nature Communications* **5**: 4983.
- Sathyanarayanan P V, Cremo CR, Poovaiah BW. 2000.** Plant chimeric Ca²⁺/Calmodulin-dependent protein kinase. Role of the neural visinin-like domain in regulating autophosphorylation and calmodulin affinity. *The Journal of biological chemistry* **275**: 30417–22.
- Sato S, Nakamura Y, Kaneko T, Asamizu E, Kato T, Nakao M, Sasamoto S, Watanabe A, Ono A, Kawashima K, et al. 2008.** Genome structure of the legume, *Lotus japonicus*. *DNA Research* **15**: 227–239.
- Saur IML, Oakes M, Djordjevic MA, Imin N. 2011.** Crosstalk between the nodulation signaling pathway and the autoregulation of nodulation in *Medicago truncatula*. *New Phytologist* **190**: 865–874.
- Saxton MJ. 1990.** Lateral diffusion in a mixture of mobile and immobile particles. A Monte Carlo study. *Biophysical journal* **58**: 1303–6.
- Schaarschmidt S, Gresshoff PM, Hause B. 2013.** Analyzing the soybean transcriptome during autoregulation of mycorrhization identifies the transcription factors GmNF-YA1a/b as positive regulators of arbuscular mycorrhization. *Genome*

- biology* **14**: R62.
- Schauser L, Roussis a, Stiller J, Stougaard J. 1999.** A plant regulator controlling development of symbiotic root nodules. *Nature* **402**: 191–195.
- Schnabel E, Journet EP, De Carvalho-Niebel F, Duc GGG, Frugoli J. 2005.** The *Medicago truncatula* SUNN gene encodes a CLV1-like leucine-rich repeat receptor kinase that regulates nodule number and root length. *Plant Molecular Biology* **58**: 809–822.
- Schnabel E, Karve A, Kassaw T, Mukherjee A, Zhou X, Hall T, Frugoli J. 2012.** The *M. truncatula* SUNN gene is expressed in vascular tissue, similarly to RDN1, consistent with the role of these nodulation regulation genes in long distance signaling. *Plant signaling & behavior* **7**: 4–6.
- Schubert KR. 1986.** Products of Biological Nitrogen Fixation in Higher Plants: Synthesis, Transport, and Metabolism. *Annual Review of Plant Physiology* **37**: 539–574.
- Schulte T, Paschke KA, Laessing U, Lottspeich F, Stuermer CA. 1997.** Reggie-1 and reggie-2, two cell surface proteins expressed by retinal ganglion cells during axon regeneration. *Development (Cambridge, England)* **124**: 577–87.
- Searle IR. 2003.** Long-Distance Signaling in Nodulation Directed by a CLAVATA1-Like Receptor Kinase. *Science* **299**: 109–112.
- Selosse M-A, Strullu-Derrien C, ;artin FM, Komoun S, Kenrick P. 2015.** Plants , fungi and oomycetes : a 400-million year affair that shapes the biosphere. : 501–506.
- Sherrier D, Prime T, Dupree P. 1999.** Glycosylphosphatidylinositol- anchored cell- surface proteins from Arabidopsis. *Electrophoresis*.
- Shimoda Y, Han L, Yamazaki T, Suzuki R, Hayashi M, Imaizumi-Anraku H. 2012.** Rhizobial and Fungal Symbioses Show Different Requirements for Calmodulin Binding to Calcium Calmodulin-Dependent Protein Kinase in *Lotus japonicus*. *The Plant Cell* **24**: 304–321.
- Sieberer BJ, Chabaud M, Fournier J, Timmers ACJ, Barker DG. 2012.** A switch in Ca²⁺ spiking signature is concomitant with endosymbiotic microbe entry into cortical root cells of *Medicago truncatula*. *Plant Journal* **69**: 822–830.
- Sieberer B, Emons AMC. 2000.** Cytoarchitecture and pattern of cytoplasmic streaming in root hairs of *Medicago truncatula* during development and deformation by nodulation factors. *Protoplasma* **214**: 118–127.
- Simons K, Gerl MJ. 2010.** Revitalizing membrane rafts: new tools and insights. *Nature reviews. Molecular cell biology* **11**: 688–699.
- Simons K, Ikonen E. 1997.** Functional rafts in cell membranes. *Nature* **387**: 569–572.
- Singer SJ, Nicolson GL. 1972.** The Fluid Mosaic Model of the Structure of Cell Membranes. *Science* **175**: 720 LP-731.
- Singh S, Katzer K, Lambert J, Cerri M, Parniske M. 2014.** CYCLOPS, A DNA-binding transcriptional activator, orchestrates symbiotic root nodule development. *Cell Host and Microbe* **15**: 139–152.
- Singh S, Parniske M. 2012.** Activation of calcium- and calmodulin-dependent protein kinase (CCaMK), the central regulator of plant root endosymbiosis. *Current Opinion in Plant Biology* **15**: 444–453.
- De Smet I, Vassileva V, De Rybel B, Levesque MP, Grunewald W, Van Damme D, Van Noorden G, Naudts M, Van Isterdael G, De Clercq R, et al. 2008.** Receptor-Like Kinase ACR4 Restricts Formative Cell Divisions in the Arabidopsis Root. *Science* **322**: 594–597.
- Smit G, Kijne JW, Lugtenberg BJ. 1987.** Involvement of both cellulose fibrils and a

- Ca²⁺-dependent adhesin in the attachment of *Rhizobium leguminosarum* to pea root hair tips. *Journal of bacteriology* **169**: 4294–301.
- Smit G, Logman TJ, Boerrigter ME, Kijne JW, Lugtenberg BJ. 1989.** Purification and partial characterization of the *Rhizobium leguminosarum* biovar *viciae* Ca²⁺-dependent adhesin, which mediates the first step in attachment of cells of the family Rhizobiaceae to plant root hair tips. *Journal of bacteriology* **171**: 4054–62.
- Smith SE, Read DJ. 2008.** *Mycorrhizal Symbiosis*. Academic Press.
- Smith SE, Smith FA. 2011.** Roles of Arbuscular Mycorrhizas in Plant Nutrition and Growth: New Paradigms from Cellular to Ecosystem Scales. *Annual Review of Plant Biology* **62**: 227–250.
- Smotrys JE, Linder ME. 2004.** Palmitoylation of Intracellular Signaling Proteins: Regulation and Function. *Annual Review of Biochemistry* **73**: 559–587.
- Soltis DE, Soltis PS, Chase MW, Mort ME, Albach DC, Zanis M, Savolainen V, Hahn WH, Hoot SB, Fay MF, et al. 2000.** Angiosperm phylogeny inferred from 18S rDNA, rbcL, and atpB sequences. *Bot. J. Linn. Soc.* **133**: 381–461.
- Soltis DE, Soltis PS, Morgant DR, Swensent SM, Mullin BC, Dowdi JM, Ii PGM. 1995.** Chloroplast gene sequence data suggest a single origin of the predisposition for symbiotic nitrogen fixation in angiosperms. **92**: 2647–2651.
- Sorek N, Bloch D, Yalovsky S. 2009.** Protein lipid modifications in signaling and subcellular targeting. *Current Opinion in Plant Biology* **12**: 714–720.
- Sorek N, Poraty L, Sternberg H, Bar E, Lewinsohn E, Yalovsky S. 2007.** Activation status-coupled transient S acylation determines membrane partitioning of a plant Rho-related GTPase. *Molecular and cellular biology* **27**: 2144–2154.
- Sorek N, Segev O, Gutman O, Bar E, Richter S, Poraty L, Hirsch JA, Henis YI, Lewinsohn E, Jürgens G, et al. 2010.** An S-Acylation Switch of Conserved G Domain Cysteines Is Required for Polarity Signaling by ROP GTPases. *Current Biology* **20**: 914–920.
- Soyano T, Hayashi M. 2014.** Transcriptional networks leading to symbiotic nodule organogenesis. *Current Opinion in Plant Biology* **20**: 146–154.
- Soyano T, Hirakawa H, Sato S, Hayashi M, Kawaguchi M, Shimoda Y, Hayashi M. 2014.** NODULE INCEPTION creates a long-distance negative feedback loop involved in homeostatic regulation of nodule organ production. *Proceedings of the National Academy of Sciences of the United States of America* **111**: 14607–14612.
- Soyano T, Kouchi H, Hirota A, Hayashi M. 2013.** NODULE INCEPTION Directly Targets NF-Y Subunit Genes to Regulate Essential Processes of Root Nodule Development in *Lotus japonicus*. *PLoS Genetics* **9**.
- Soyano T, Shimoda Y, Hayashi M. 2015.** NODULE INCEPTION antagonistically regulates gene expression with nitrate in *Lotus japonicus*. *Plant and Cell Physiology* **56**: 368–376.
- Spaink HP, Okker RJ, Wijffelman CA, Tak T, Goosen-de Roo L, Pees E, van Brussel AA, Lugtenberg BJ. 1989.** Symbiotic properties of rhizobia containing a flavonoid-independent hybrid nodD product. *Journal of bacteriology* **171**: 4045–53.
- Sprent JI. 2007.** Evolving ideas of legume evolution and diversity: A taxonomic perspective on the occurrence of nodulation: Tansley review. *New Phytologist* **174**: 11–25.
- Sprent JI. 2008.** 60Ma of legume nodulation. What's new? What's changing? *Journal of Experimental Botany* **59**: 1081–1084.
- Stahelin C, Xie Z-P, Illana A, Vierheilig H. 2011.** Long-distance transport of signals during symbiosis: are nodule formation and mycorrhization autoregulated in a similar way? *Plant signaling & behavior* **6**: 372–377.

- Stahl Y, Grabowski S, Bleckmann A, Kühnemuth R, Weidtkamp-Peters S, Pinto KG, Kirschner GK, Schmid JB, Wink RH, Hülsewede A, et al. 2013.** Moderation of arabidopsis root stemness by CLAVATA1 and ARABIDOPSIS CRINKLY4 receptor kinase complexes. *Current Biology* **23**: 362–371.
- Stahl Y, Wink RH, Ingram GC, Simon R. 2009.** A Signaling Module Controlling the Stem Cell Niche in Arabidopsis Root Meristems. *Current Biology* **19**: 909–914.
- Stougaard J. 2001.** Genetics and genomics of root symbiosis. *Current Opinion in Plant Biology* **4**: 328–335.
- Stracke S, Kistner C, Yoshida S, Mulder L, Sato S, Kaneko T, Tabata S, Sandal N, Stougaard J, Szczyglowski K, et al. 2002.** A plant receptor-like kinase required for both bacterial and fungal symbiosis. *Nature* **417**: 959–962.
- Strullu-Derrien C, Kenrick P, Pressel S, Duckett JG, Rioult J, Strullu-derrien C. 2014.** Fungal associations in Horneophyton ligneri from the Rhynie Chert (c . 407 million year old) closely resemble those in extant lower land plants : novel insights into ancestral plant – fungus symbioses. : 964–979.
- Suzaki T, Yano K, Ito M, Umehara Y, Suganuma N, Kawaguchi M. 2012.** Positive and negative regulation of cortical cell division during root nodule development in Lotus japonicus is accompanied by auxin response. *Development* **139**: 3997–4006.
- Suzuki K, Ritchie K, Kajikawa E, Fujiwara T, Kusumi A. 2005.** Rapid hop diffusion of a G-protein-coupled receptor in the plasma membrane as revealed by single-molecule techniques. *Biophysical journal* **88**: 3659–3680.
- Szczyglowski K, Kapranov P, Hamburger D, De Bruijn FJ. 1998.** The Lotus japonicus LjNOD70 nodulin gene encodes a protein with similarities to transporters. *Plant Molecular Biology* **37**: 651–661.
- Szymanski WG, Zauber H, Erban A, Gorka M, Wu XN, Schulze WX. 2015.** Cytoskeletal Components Define Protein Location to Membrane Microdomains. *Mol. Cell. Proteomics* **14**: 2493–2509.
- Tadege M, Ratet P, Mysore KS. 2005.** Insertional mutagenesis: a Swiss Army knife for functional genomics of Medicago truncatula. *Trends in Plant Science* **10**: 229–235.
- Tadege M, Wen J, He J, Tu H, Kwak Y, Eschstruth A, Cayrel A, Endre G, Zhao PX, Chabaud M, et al. 2008.** Large-scale insertional mutagenesis using the Tnt1 retrotransposon in the model legume Medicago truncatula. *Plant Journal* **54**: 335–347.
- Takahara M, Magori S, Soyano T, Okamoto S, Yoshida C, Yano K, Sato S, Tabata S, Yamaguchi K, Shigenobu S, et al. 2013.** TOO MUCH LOVE, a novel kelch repeat-containing F-box protein, functions in the long-distance regulation of the LEGUME-rhizobium symbiosis. *Plant and Cell Physiology* **54**: 433–447.
- Takeda N, Maekawa T, Hayashi M. 2012.** Nuclear-localized and deregulated calcium- and calmodulin-dependent protein kinase activates rhizobial and mycorrhizal responses in Lotus japonicus. *The Plant cell* **24**: 810–22.
- Takeda N, Tsuzuki S, Suzaki T, Parniske M, Kawaguchi M. 2013.** CERBERUS and NSP1 of lotus japonicus are common symbiosis genes that modulate arbuscular mycorrhiza development. *Plant and Cell Physiology* **54**: 1711–1723.
- Tanner W, Malinsky J, Opekarová M. 2011.** In Plant and Animal Cells, Detergent-Resistant Membranes Do Not Define Functional Membrane Rafts. *The Plant Cell Online* **23**: 1191–1193.
- Tapken W, Murphy AS. 2015.** Membrane nanodomains in plants: Capturing form, function, and movement. *Journal of Experimental Botany* **66**: 1573–1586.

- Taylor TN, Remy W, Hass H, Kerp H. 1995.** Fossil Arbuscular Mycorrhizae from the Early Devonian. *Mycologia* **87**: 560–573.
- Thaa B, Levental I, Herrmann A, Veit M. 2011.** Intrinsic membrane association of the cytoplasmic tail of influenza virus M2 protein and lateral membrane sorting regulated by cholesterol binding and palmitoylation. *The Biochemical journal* **437**: 389–397.
- Timmers a C, Auriac MC, Truchet G. 1999.** Refined analysis of early symbiotic steps of the Rhizobium-Medicago interaction in relationship with microtubular cytoskeleton rearrangements. *Development (Cambridge, England)* **126**: 3617–3628.
- Timmers ACJ, Soupène E, Auriac M-C, de Billy F, Vasse J, Boistard P, Truchet G. 2000.** Saprophytic Intracellular Rhizobia in Alfalfa Nodules. *Molecular Plant-Microbe Interactions* **13**: 1204–1213.
- Tirichine L, Imaizumi-Anraku H, Yoshida S, Murakami Y, Madsen LH, Miwa H, Nakagawa T, Sandal N, Albrektsen AS, Kawaguchi M, et al. 2006.** Dereglulation of a Ca²⁺/calmodulin-dependent kinase leads to spontaneous nodule development. *Nature* **441**: 1153–1156.
- Tirichine L, Sandal N, Madsen LH, Radutoiu S, Albrektsen AS, Sato S, Asamizu E, Tabata S, Stougaard J. 2007.** A Gain-of-Function Mutation in a Root Nodule Organogenesis. *Science (New York, N.Y.)* **2680**: 104–107.
- Tóth K, Stratil TF, Madsen EB, Ye J, Popp C, Antolín-Llovera M, Grossmann C, Jensen ON, Schüßler A, Parniske M, et al. 2012.** Functional domain analysis of the remorin protein LjSYMREM1 in lotus japonicus (RJ Morris, Ed.). *PLoS ONE* **7**: e30817.
- Traverso J, Micalella C, Martinez A, Brown S. 2013.** Roles of N-terminal fatty acid acylations in membrane compartment partitioning: Arabidopsis h-type thioredoxins as a case study. *The Plant*.
- Urbański DF, Malolepszy A, Stougaard J, Andersen SU. 2012.** Genome-wide LORE1 retrotransposon mutagenesis and high-throughput insertion detection in Lotus japonicus. *Plant Journal* **69**: 731–741.
- Valot B, Negroni L, Zivy M, Gianinazzi S, Dumas-Gaudot E. 2006.** A mass spectrometric approach to identify arbuscular mycorrhiza-related proteins in root plasma membrane fractions. *Proteomics* **6 Suppl 1**: S145-55.
- Vasse J, De Billy F, Camut S, Truchet G. 1990.** Correlation between ultrastructural differentiation of bacterioids and nitrogen fixation in alfalfa nodules. *Journal of Bacteriology* **172**: 4295–4306.
- Venkateshwaran M, Jayaraman D, Chabaud M, Genre A, Balloon AJ, Maeda J, Forshey K, den Os D, Kwiecien NW, Coon JJ, et al. 2015.** A role for the mevalonate pathway in early plant symbiotic signaling. *Proc Natl Acad Sci U S A* **112**: 9781–9786.
- Verdier J, Torres-Jerez I, Wang M, Andriankaja A, Allen SN, He J, Tang Y, Murray JD, Udvardi MK. 2013.** Establishment of the Lotus japonicus Gene Expression Atlas (LjGEA) and its use to explore legume seed maturation. *Plant Journal* **74**: 351–362.
- Vernié T, Camut S, Camps C, Rembliere C, de Carvalho-Niebel F, Mbengue M, Timmers T, Gascioli V, Thompson RD, Lesignor C, et al. 2016.** PUB1 interacts with the receptor kinase DMI2 and negatively regulates rhizobial and arbuscular mycorrhizal symbioses through its ubiquitination activity in Medicago truncatula. *Plant Physiology* **170**: pp.01694.2015.
- Vernié T, Kim J, Frances L, Ding Y, Sun J, Guan D, Niebel A, Gifford ML, de Carvalho-Niebel F, Oldroyd GED. 2015.** The NIN Transcription Factor Coordinates

- Diverse Nodulation Programs in Different Tissues of the *Medicago truncatula* Root. *The Plant Cell* **27**: tpc.15.00461.
- Vernié T, Moreau S, de Billy F, Plet J, Combier J-P, Rogers C, Oldroyd G, Frugier F, Niebel A, Gamas P. 2008.** EFD Is an ERF transcription factor involved in the control of nodule number and differentiation in *Medicago truncatula*. *The Plant cell* **20**: 2696–2713.
- Vierheilig H, Wyss U, Piche Y. 2000.** Systemic suppression of mycorrhizal colonization of barley roots already colonized by AM fungi. **32**: 589–595.
- Wang W, Esch JJ, Shiu S-H, Agula H, Binder BM, Chang C, Patterson SE, Bleecker AB. 2006.** Identification of Important Regions for Ethylene Binding and Signaling in the Transmembrane Domain of the ETR1 Ethylene Receptor of *Arabidopsis*. *THE PLANT CELL ONLINE* **18**: 3429–3442.
- Wang E, Schornack S, Marsh JF, Gobbato E, Schwessinger B, Eastmond P, Schultze M, Kamoun S, Oldroyd GED. 2012.** A common signaling process that promotes mycorrhizal and oomycete colonization of plants. *Current Biology* **22**: 2242–2246.
- Wang B, Yeun LH, Xue J, Liu Y, Ane J, Qiu Y. 2010.** Presence of three mycorrhizal genes in the common ancestor of land plants suggests a key role of mycorrhizas in the colonization of land by plants. : 514–525.
- Watson BS, Asirvatham VS, Wang L, Sumner LW. 2003.** Mapping the Proteome of Barrel Medic (*Medicago truncatula*). *PLANT PHYSIOLOGY* **131**: 1104–1123.
- Werner GD a, Cornwell WK, Sprent JI, Kattge J, Kiers ET. 2014.** A single evolutionary innovation drives the deep evolution of symbiotic N₂-fixation in angiosperms. *Nature communications* **5**: 4087.
- Wiśniewska J, Xu J, Seifertová D, Brewer PB, Růžička K, Blilou I, Rouquié D, Benková E, Scheres B, Friml J. 2006.** Polar PIN Localization Directs Auxin Flow in Plants. *Science* **312**.
- Wopereis J, Pajuelo E, Dazzo FB, Jiang Q, Gresshoff PM, De Bruijn FJ, Stougaard J, Szczyglowski K. 2000.** Short root mutant of *Lotus japonicus* with a dramatically altered symbiotic phenotype. *Plant Journal* **23**: 97–114.
- Xiao TT, Schilderink S, Moling S, Deinum EE, Kondorosi E, Franssen H, Kulikova O, Niebel A, Bisseling T. 2014.** Fate map of *Medicago truncatula* root nodules. *Development* **141**: 3517–3528.
- Xie ZP, Müller J, Wiemken A, Broughton WJ, Boller T. 1998.** Nod factors and triiodobenzoic acid stimulate mycorrhizal colonization and affect carbohydrate partitioning in mycorrhizal roots of *Lablab purpureus*. *New Phytologist* **139**: 361–366.
- Xie F, Murray JD, Kim J, Heckmann a. B, Edwards a., Oldroyd GED, Downie J a. 2012.** Legume pectate lyase required for root infection by rhizobia. *Proceedings of the National Academy of Sciences* **109**: 633–638.
- Xie ZP, Staehelin C, Vierheilig H, Wiemken a., Jabbouri S, Broughton WJ, Vogeli-Lange R, Boller T. 1995.** Rhizobial Nodulation Factors Stimulate Mycorrhizal Colonization of Nodulating and Nonnodulating Soybeans. *Plant Physiology* **108**: 1519–1525.
- Xue L, Cui H, Buer B, Vijayakumar V, Delaux P-M, Junkermann S, Bucher M. 2015.** Network of GRAS transcription factors involved in the control of arbuscule development in *Lotus japonicus*. *Plant physiology* **167**: 854–71.
- El Yahyaoui F. 2004.** Expression Profiling in *Medicago truncatula* Identifies More Than 750 Genes Differentially Expressed during Nodulation, Including Many Potential Regulators of the Symbiotic Program. *Plant Physiology* **136**: 3159–3176.
- Yang X, Claas C, Kraeft S-K, Chen LB, Wang Z, Kreidberg JA, Hemler ME.**

- 2002.** Palmitoylation of Tetraspanin Proteins: Modulation of CD151 Lateral Interactions, Subcellular Distribution, and Integrin-dependent Cell Morphology Xiuwei. *Molecular biology of the cell* **13**: 767–781.
- Yano K, Yoshida S, Müller J, Singh S, Banba M, Vickers K, Markmann K, White C, Schuller B, Sato S, et al. 2008.** CYCLOPS, a mediator of symbiotic intracellular accommodation. *Proceedings of the National Academy of Sciences of the United States of America* **105**: 20540–20545.
- Yoro E, Suzaki T, Toyokura K, Miyazawa H, Fukaki H, Kawaguchi M. 2014.** A positive regulator of nodule organogenesis, NODULE INCEPTION, acts as a negative regulator of rhizobial infection in *Lotus japonicus*. *PLANT PHYSIOLOGY* **165**: 747–758.
- Young ND, Debelle F, Oldroyd GED, Geurts R, Cannon SB, Udvardi MK, Benedito V a., Mayer KFX, Gouzy J, Schoof H, et al. 2011.** The Medicago genome provides insight into the evolution of rhizobial symbioses. *Nature* **480**: 520–524.
- Yu N, Luo D, Zhang X, Liu J, Wang W, Jin Y, Dong W, Liu J, Liu H, Yang W, et al. 2014.** A DELLA protein complex controls the arbuscular mycorrhizal symbiosis in plants. *Cell research* **24**: 130–3.
- Yue J, Li C, Liu Y, Yu J. 2014.** A remorin gene SiREM6, the target gene of SiARDP, from foxtail millet (*Setaria italica*) promotes high salt tolerance in transgenic Arabidopsis. *PLoS ONE* **9**: 1–10.
- Zakaria Solaiman M, Senoo K, Kawaguchi M, Imaizumi-Anraku H, Akao S, Tanaka A, Obata H. 2000.** Characterization of Mycorrhizas Formed by *Glomus* sp. on Roots of Hypernodulating Mutants of *Lotus japonicus*. *Journal of Plant Research* **113**: 443–448.
- De Zélicourt A, Diet A, Marion J, Laffont C, Ariel F, Moison MM, Zahaf O, Crespi M, Gruber VV, Frugier F, et al. 2012.** Dual involvement of a *Medicago truncatula* NAC transcription factor in root abiotic stress response and symbiotic nodule senescence. *Plant Journal* **70**: 220–230.
- Zhang X, Dong W, Sun J, Feng F, Deng Y, He Z, Oldroyd GED, Wang E. 2015.** The receptor kinase CERK1 has dual functions in symbiosis and immunity signalling. *The Plant Journal* **81**: 258–267.
- Zhu Y, Wang Y, Li R, Song X, Wang Q, Huang S, Jin JB, Liu CM, Lin J. 2010.** Analysis of interactions among the CLAVATA3 receptors reveals a direct interaction between CLAVATA2 and CORYNE in Arabidopsis. *Plant Journal* **61**: 223–233.

Curriculum Vitae

Claudia Popp

geb. Zimmermann

Education

June 2003

Abitur, Goethe-Gymnasium Emmendingen

October 2003-June 2009

Biology (**Diploma**), (Major subject: Plant Physiology; Minor subjects: Microbiology, Biochemistry, and Theology),
University of Freiburg

February 2006-June 2006

Erasmus Exchange Programme; Bachelor project
`Caspase-3-like proteases are required for
programmed cell death on *Arabidopsis thaliana*`;
Supervisor: Dr. Patrick Gallois,
University of Manchester

September 2008- June 2009

Diploma Thesis at the Faculty of Biology
(Department of Plant Physiology) `Analysis of
Phytochrome Transport in the cell-free *Acetabularia*-
System`, in the laboratory of Prof. Dr. Eberhard
Schäfer; Supervisor: Dr. Thomas Kunkel
University of Freiburg

October 2009-April 2017

Doctoral student at the LSM graduate school,
PhD research project `Analysis of the membrane
binding mechanism of Remorins and their role in
beneficial endosymbioses` in the group of Prof.
Thomas Ott (now University of Freiburg), Genetics,
LMU Munich

Employment

July 2009-September 2009	Research Assistant in the group of Prof. Dr. Eberhard Schäfer at the University of Freiburg
October 2009-December 2016	Research Assistant in the group of Prof Dr. Thomas Ott at the LMU Munich
December 2011-November 2012	Maternity leave
October 2014-May 2015	Maternity leave

Danksagung

Zunächst möchte ich Prof. Dr. Thomas Ott dafür danken, dass ich in seiner Arbeitgruppe diese Arbeit anfertigen durfte. Danke Thomas, dass Du mir vor all den Jahren Dein Vertrauen geschenkt hast und mich für die Remorine begeistert hast! Vielen Dank für Deine Unterstützung (auch außerhalb des Labors), Deine motivierende Art und Deine offene Tür für alle großen und kleine Probleme. Es war eine intensive und lehrreiche Zeit, mit vielen Umbrüchen und Neuanfängen, die ich nicht missen möchte. Danke!

Außerdem möchte ich Prof. Dr. Wolfgang Frank für die Erstellung des Zweitgutachtens danken, sowie allen weiteren Mitgliedern der Prüfungskommission.

Ein herzliches Dank geht an all meine wunderbaren Arbeitskollegen, die ich in diesen Jahren kennenlernen durfte. Dank Ihnen war es immer eine Freude ins Labor zugehen. Danke Karl-Heinz, Joana, Iris und Katalin, dass ihr mir den Start in München so einfach gemacht habt. Danke, Susan, für die schönen “Wolf und Schaf” Geschichten. Danke Basti, dass Du in das Ankerprojekt eingestiegen bist und Du den Laden mit Deinen Scherzen aufgemischt hast. Meinem langjährigen Laborbank- und Büronachbar Tom möchte ich dafür danken, dass er es so lange mit mir ausgehalten hat, obwohl ich von Fußball so gar keine Ahnung habe – ich habe gerne über deine Scherze gelacht. Danke, Macarena, für dein kritisches und konstruktives Nachfragen, Deine Ratschläge und Deine “happy bubble”. Besonderen Dank geht an Corinna, mit der ich viele Erfahrungen teilen durfte, ich immer wieder über alles diskutieren konnte und die eine wunderbare Weggefährtin war.

Vielen, lieben Dank, Jessica! Ohne Dich wäre ich das eine oder andere Mal verloren gewesen. Danke für Deine zuverlässige Hilfe in allen Lebenslagen.

Ich möchte diesen Ort auch noch einmal nutzen, um allen Kollegen der AG Ott von Herzen zu danken, dass sie mir vor und während Vitus und Clara immer geholfen haben egal, um was es ging.

Danke, Sarah, dass Du ein Teil unserer Familie geworden bist! Ich kann mich immer noch sehr gut an Deine erste Vitus-Muskeltraining Stunde erinnern

Meinen Eltern möchte ich für ihre immerwährende Unterstützung danken, für ihren Glauben an meinen Lebensweg und den Freiraum und den Respekt, den sie meinen Entscheidungen entgegengebracht haben. Danke. Meinen Brüdern möchte ich dafür danken, dass sie immer ein beschützendes Auge auf mich hatten.

Während der Zeit der Doktorarbeit durfte ich zweimal das Gefühl purer Freude erleben: Vitus und Clara. Diese zwei kleinen Menschen haben mein Leben auf den Kopf gestellt und mischen es immer noch ziemlich auf und dafür liebe ich sie.

Felix, danke für deine unendliche Unterstützung, für deine Begabung mich für neue Dinge zu begeistern und dein Talent mich immer wieder an meine Grenzen zu bringen, damit ich sie erfolgreich überschreiten kann! Ohne dich wäre ich nicht bis hierher gekommen.